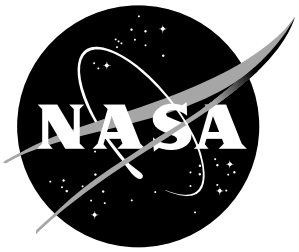

NASA Technical Memorandum 108541

International Space Station Program Phase III Integrated Atmosphere Revitalization Subsystem Test Final Report

J.L. Perry, G.D. Franks, and J.C. Knox

August 1997

NASA Technical Memorandum 108541

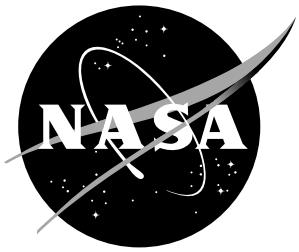

International Space Station Program Phase III Integrated Atmosphere Revitalization Subsystem Test Final Report

J.L. Perry, G.D. Franks, and J.C. Knox
Marshall Space Flight Center • MSFC, Alabama

National Aeronautics and Space Administration
Marshall Space Flight Center • MSFC, Alabama 35812

August 1997

ACKNOWLEDGMENTS

The author wishes to acknowledge several individuals who made significant contributions to the Integrated Atmosphere Revitalization Test (IART) and the subsequent test data analysis and reporting effort. Data reduction and data plot preparation are central to evaluating any test report. I greatly appreciate Jim Tatara, Silvia Minton-Summers, Charles Martin, and Charles Chiu of Ion Electronics for their dedication in handling all of the test data. Very significant contributions to the test were also made by the expert analyses conducted by Charles Martin on metabolic simulation and oxygen partial pressure control. Debra Terrell of Sverdrup Technology, Inc., made valuable contributions by tracking the gas sampling schedules and ensuring that all the major gas analyzers were operating properly. Thanks also go to Lee Miller of Sverdrup for all his troubleshooting efforts before and during the test. Jacqueline Roberts of Boeing played a key role in setting up and operating the on-line gas chromatograph, in addition to collecting and analyzing gas samples off-line during the test. Many civil service employees of the Development and Environmental Test Branch made the test possible. I thank you all.

TABLE OF CONTENTS

LIST OF FIGURES

LIST OF TABLES

ABBREVIATIONS AND ACRONYMS

acpp	carbon dioxide partial pressure, torr
aopp	oxygen partial pressure, torr
APM	Attached Pressurized Module (European Space Agency)
ARS	Atmosphere Revitalization Subsystem
awpp	water partial pressure, torr
CDA	Carbon Dioxide Analyzer
CDRA	Carbon Dioxide Removal Assembly
CDReA	Carbon Dioxide Reduction Assembly
CHX	condensing heat exchanger
CMIF	Core Module Integration Facility
CMS	Core Module Simulator
COA	Carbon Monoxide Analyzer
ECLSS	Environmental Control and Life Support System
EEF	End-Use Equipment Facility
FCA	Fluid Control Assembly
GC	gas chromatograph
Hab	(U.S.) Habitation Module
IART	Integrated Atmosphere Revitalization Test
IMV	intermodule ventilation
ISS	*International Space Station*
JEM	Japanese Experiment Module
Lab	(U.S.) Laboratory Module
LiOH	lithium hydroxide
LSM	Life Support Module
MCA	Major Constituent Analyzer
mdns	CDRA mode day/night status
mmod	CDRA mode indication
MSFC	Marshall Space Flight Center

N/A	not applicable
ND	not detected
NR	not reported
OGA	Oxygen Generator Assembly
p.	page
P/L	payload
par.	paragraph
PCA	Pressure Control Assembly
PCM	Particulate Counting Monitor
Pd	palladium
PID	Prime Item Development
POST	Predevelopment Operational Systems Test
ppm	parts per million
pp.	pages
RSA	Russian Space Agency
SDS	Sample Delivery System
SFWE	static feed water electrolyzer
SIT	simplified integrated test
sh	sheet
SM	Service Module
TCA	Thermal Control Assembly
TCCS	Trace Contaminant Control Subassembly
TCM	Trace Contaminant Monitor
THCS	Temperature and Humidity Control System
4BMS	Four-Bed Molecular Sieve

TECHNICAL MEMORANDUM

INTERNATIONAL SPACE STATION PROGRAM PHASE III INTEGRATED ATMOSPHERE REVITALIZATION SUBSYSTEM TEST FINAL REPORT

INTRODUCTION

Testing of the *International Space Station* (*ISS*) U.S. Segment baseline configuration of the Atmosphere Revitalization Subsystem (ARS) by NASA's Marshall Space Flight Center (MSFC) was conducted as part of the Environmental Control and Life Support System (ECLSS) design and development program. This testing was designed to answer specific questions regarding the control and performance of the baseline ARS subassemblies in the *ISS* U.S. Segment configuration. These questions resulted from the continued maturation of the *ISS* ECLSS configuration and design requirement changes since 1992.

The test used pressurized oxygen injection, a mass spectrometric major constituent analyzer (MCA), a Four-Bed Molecular Sieve (4BMS) Carbon Dioxide Removal Assembly (CDRA), and a Trace Contaminant Control Subassembly (TCCS) to maintain the atmospheric composition in a sealed chamber at *ISS* specifications for 30 days. Human metabolic processes for a crew of four were simulated according to projected *ISS* mission time lines. The performance of a static feed water electrolysis (SFWE) Oxygen Generator Assembly (OGA) was investigated during the test preparation phases; however, technical difficulties prevented its use during the integrated test.

The Integrated ARS Test (IART) program built upon previous closed-door and open-door integrated testing conducted at MSFC between 1987 and 1992. It is the most advanced test of an integrated ARS conducted by NASA to demonstrate its end-to-end control and overall performance. IART test objectives, facility design, pretest analyses, test and control requirements, and test results are presented.

BACKGROUND

Past Space Station ARS Testing

Testing of ECLSS subsystems and subassemblies for the *ISS* has been ongoing at NASA's MSFC since 1987. ECLSS development testing has followed a multiphased program that has gradually increased in complexity as the ECLSS design has matured. Each phase accounts for the various redesign and restructuring activities that have occurred during the *ISS* development.

Phase I of the development program, which began in 1987, includes subassembly demonstration, comparative testing, and long-duration testing. Phase I is designed to provide the necessary information to demonstrate basic subassembly performance, select the baseline subassemblies to be used on board the *ISS,* and assess their long-duration performance and maintainability. Primary products of Phase I are:

(1) Basic subassembly performance data that can be used for ECLSS design and modeling purposes.

(2) Selection of subassemblies for the *ISS* ECLSS baseline.[1]

(3) Long duration operational data that are necessary for determining the useful life and maintainability requirements for the ECLSS subassemblies.[2–4]

In parallel with Phase I, early integrated ARS testing was conducted under Phases II and III of the development program. Much experience was gained by NASA with the candidate subassemblies and their integrated operation during these tests. Phase II testing included a simplified integrated test (SIT) that was conducted in June 1987 to check out the predevelopment ECLSS system and an extended-duration metabolic control test that was conducted in November 1987. Hardware tested during Phase II included a 4BMS CDRA, a TCCS, a SFWE OGA, and a Sabatier Carbon Dioxide Reduction Assembly (CDReA).[5–8]

Phase III simplified integrated testing was conducted in August 1989 to prepare for fully integrated ARS and water recovery tests. The primary difference between the Phase II and Phase III integrated tests was the use of the Bosch CDReA in place of the Sabatier process.[9–11] The Bosch process had been selected as the initial station baseline process; however, at the conclusion of Phase I comparative testing, the Sabatier process was the final baseline selection. Hardware used during Phase III was of higher maturity than that of Phase II.

Additional integrated testing was conducted by Boeing at MSFC facilities under Phase IV. The Predevelopment Operational Systems Test (POST) built upon the knowledge obtained during NASA's tests. This testing was conducted during February through April 1992 using a SFWE OGA, 4BMS CDRA, Sabatier CDReA, and TCCS. All subassemblies were at prototype maturity levels. The primary objectives of this testing were to evaluate subassembly operating characteristics, demonstrate software and control functionality, and demonstrate remote control of the ARS.[12, 13]

Other integrated ARS testing conducted by NASA before 1996 was a part of the Early Human Test Initiative Phase II program. This testing, conducted at NASA's Johnson Space Center, was similar in scope to the *ISS* Phase II test conducted at MSFC in 1987. Although this test served to reinforce the results obtained during MSFC's testing program, no *ISS*-related issues were addressed during the test. Neither hardware maturity nor test system architecture was representative of the *ISS* configuration.[14]

ISS ARS Testing

Upon completing the redesign of the space station and its transition to the *ISS* Program in 1994, changes to the ARS design and its operation were identified that required additional testing to validate. To address these issues and to advance the ARS maturity to its next step, Phase III integrated testing was extended to the *ISS* Program. The IART was defined in January 1994 as part of the *ISS* development program and conducted beginning in March 1996. The Phase III IART draws upon the experience and knowledge gained during all previous ARS tests and uses the most mature ARS subassemblies available. It is a direct follow-on to the Phase III SIT and Phase IV POST with respect to its complexity and overall control approach.

The 4BMS CDRA, SFWE OGA, and TCCS were the primary subassemblies investigated. They were supplemented by a mass spectrometric MCA. This hardware complement represents the ARS configuration to be deployed on board the *ISS* U.S. Habitation Module. Scars are included in the test to accommodate carbon dioxide reduction. The primary purpose of the test was to provide the data necessary to assess the ARS's capability to control oxygen and carbon dioxide partial pressures within *ISS* specifications at operational conditions representative of *ISS* crew metabolic profiles and cyclic operation to minimize power consumption.[15, 16]

The test hardware used during the IART is, in most cases, the same hardware used during the Phase IV POST. The MCA, CDRA, and OGA were all used during the Phase IV POST; however, improvements and modifications were made to these subassemblies in order to reflect the most up-to-date design. The TCCS used during IART is the same that has been used during the earlier Phases II and III testing. It was also used for high temperature catalyst life testing. This unit was built by Lockheed in the mid-1970's; however, it is more advanced than the unit used during Phase IV POST and is considered to be the most advanced ground-test TCCS available to NASA. More details on each subassembly and improvements made as part of the IART are provided in the test configuration discussion.

ISS REQUIREMENTS

The *ISS* ARS must control the station cabin atmospheric pressure and composition within specified limits. These limits are based upon crew health considerations and are designed to provide a comfortable living and working environment. Specific details of these requirements are the following:

(1) Atmospheric pressure must be maintained between 92.9 kPa (14.2 psia) and 102.7 kPa (14.9 psia), with a minimum allowable pressure of 95.8 kPa (13.9 psia).

(2) Nitrogen partial pressure must be maintained below 80 kPa (11.6 psia).

(3) Oxygen partial pressure must be maintained between 19.5 kPa (2.83 psia) and 23.1 kPa (3.35 psia).

(4) Carbon dioxide partial pressure must be maintained below a daily average partial pressure of 706.6 Pa (5.3 mmHg), with the peak partial pressure not exceeding 1,013 Pa (7.6 mmHg).

(5) Trace chemical contaminants must be maintained below their spacecraft maximum allowable concentration.

The carbon dioxide and oxygen production rates necessary to meet these requirements are based upon a total *ISS* crew of six, with each person generating 1 kg (2.2 lb) of carbon dioxide per day and consuming 0.83 kg (1.84 lb) of oxygen per day. Trace contaminant removal must be capable of supporting an offgassing load from spacecraft hardware and metabolic production from six crew members. This load is split between the U.S. and Russian on-orbit segments of the *ISS*. The U.S. Segment ARS must be capable of supporting four crew members while the Russian Segment must be capable of supporting three. These control levels must also be maintained during crew exchanges. Loads from animals used in biological experimentation must also be accommodated by the U.S. Segment at a rate of 1.2 kg (2.7 lb) of carbon dioxide per day and 1.08 kg (2.38 lb) of oxygen per day. To achieve this, the U.S. Segment ARS must be able to remove the carbon dioxide load and provide oxygen for up to 5.29 crew members under normal conditions.[17, 18] The U.S. Segment TCCS design must be capable of handling the offgassing load for 75,000 kg (34,019 lb) of spacecraft hardware and the metabolic load from 5.25 crew members.

All of the *ISS* requirements pertaining to the capabilities that the ARS provides must be achieved with a limited amount of the resources available on board the *ISS*. Primary resources include electrical power and crew time for maintenance. To minimize power requirements during the dark portions of the orbit, some ARS subassemblies are required to transition to a standby mode. This approach adds control complexity and challenges the capabilities of the hardware. By implementing an optimized control scheme, electrical power and maintenance time may be minimized while achieving the specified atmospheric control requirements. Such a control scheme must be demonstrated. The Phase III IART objectives are designed to provide this demonstration and to ensure that the ARS can meet the *ISS* atmospheric composition control and revitalization requirements.

TEST OBJECTIVES

To determine whether the U.S. Segment ARS can adequately achieve *ISS* requirements, the primary Phase III IART test objectives were the following:

(1) Demonstrate integrated ARS operation under remote automatic control.

(2) Provide performance data on oxygen and carbon dioxide partial pressure control for crew of four.

(3) Demonstrate automated oxygen partial pressure control using the MCA signal as control input to the OGA.

(4) Demonstrate cyclic operation of the OGA and CDRA on a day/night orbital cycle to accommodate *ISS* power allocations.

(5) Demonstrate OGA performance using reclaimed water from *ISS* water processor testing.

(6) Determine the MCA water vapor measurement accuracy through a remote sample delivery system.

These objectives are designed to address specific issues associated with the operation and control of the baseline U.S. Segment ARS configuration and its capability to achieve *ISS* program requirements.

It should be noted that these objectives do not include an investigation of trace chemical contaminant control. Based upon the complexity of such a test, it has been defined as a follow-up to the IART. Objectives for the contaminant injection test include investigating the effects of humidity, temperature, and the control assist provided by the CDRA and the temperature and humidity control system.

An additional note is that during independent testing to address objectives 4 and 5, the OGA encountered technical difficulties.[19] Although the OGA successfully demonstrated its ability to operate in a cyclic power-saving mode using reclaimed water from the *ISS* water processor, it could not be repaired in a timely manner to allow it to participate in the integrated test. For this reason, oxygen injection from a pressurized source was used during the IART in place of the OGA.

Specific *ISS* Program concerns drove objective 6. Orbital Sciences Corporation, the subcontractor responsible for building the MCA, has expressed a concern to the *ISS* developer, Boeing, regarding whether the MCA would be able to measure the water vapor percentage in the cabin due to the long tubing lengths found in interfacing with the Sample Delivery System (SDS). The SDS is made of stainless steel, which has an affinity for water. To investigate and document the extent to which the SDS impacts the accuracy of the water vapor measurement, a simulation of sampling among the various

lengths possible through the SDS was added to the IART. This simulation was conducted in 7.6-m (25-ft) increments, with dewpoint sensors placed at each increment to compare to the MCA water reading. Originally, Teflon™ tubing was considered for the SDS due to this problem with the water reading, but the increased offgassing from Teflon™ would have had a greater impact on readings for the Trace Contaminant Monitor (TCM), which was also to use the sample lines.

TEST CONFIGURATION

Test Facility Description

The Phase III IART was conducted in the Core Module Simulator (CMS), a 175-m^3 (6,180-ft^3) sealed chamber that provides a closed working volume and connections to facility power and consumable resources. Test control, data acquisition and management, and process monitoring capabilities are also provided by the facility. The entire test facility, called the Core Module Integration Facility (CMIF), includes the CMS, resource distribution network, and control room. Bench test stands that support ongoing Phase I testing, the End-Use Equipment Facility (EEF), and Water Processor Test facility are located near the CMIF. Figure 1 depicts the CMIF floor plan.

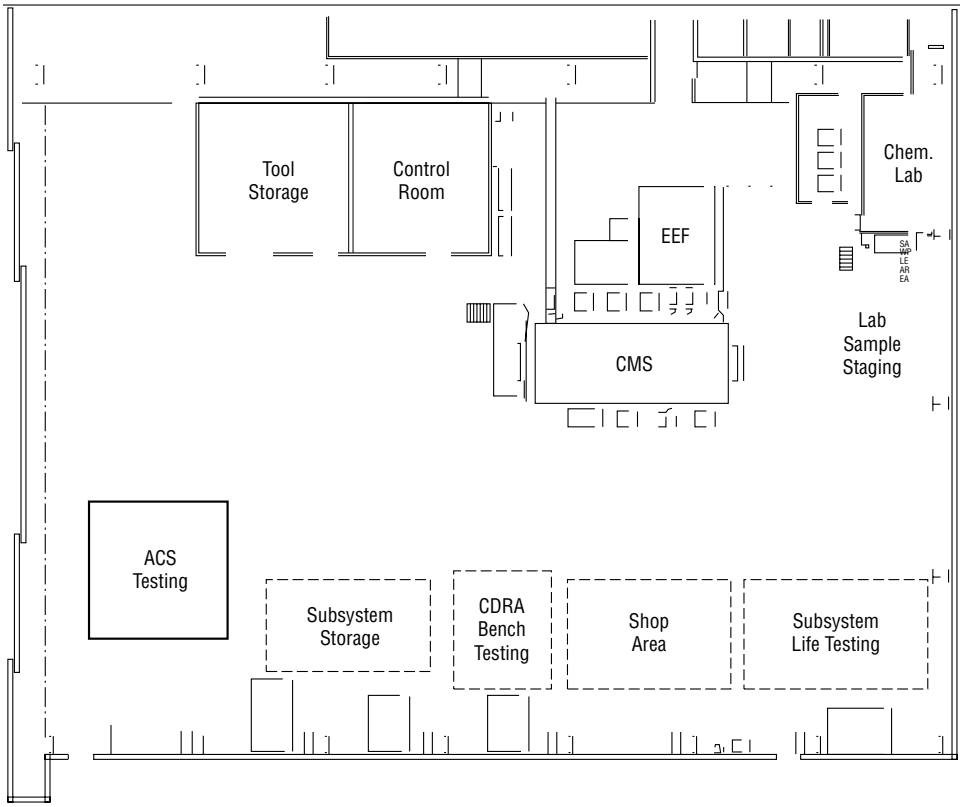

FIGURE 1.—Simplified CMIF layout.

Facility support hardware is provided to simulate human metabolic production of water vapor and carbon dioxide, human metabolic consumption of oxygen, and space vacuum. Facility temperature and humidity control are provided in the CMS to maintain the temperature and humidity conditions inside the CMS within *ISS* specifications. Additional facility gas analysis capability is provided by a gas

chromatograph (GC) and an infrared Carbon Dioxide Analyzer (CDA). These instruments are designed to not only provide a continuing verification for MCA results, but also to study the CDRA process in detail.

The ARS hardware is mounted inside the CMS, with control and data acquisition provided from remote workstations located in the control room. The MCA, gas chromatograph, and infrared CDA are mounted externally to the CMS. Figure 2 shows the arrangement of the IART hardware.

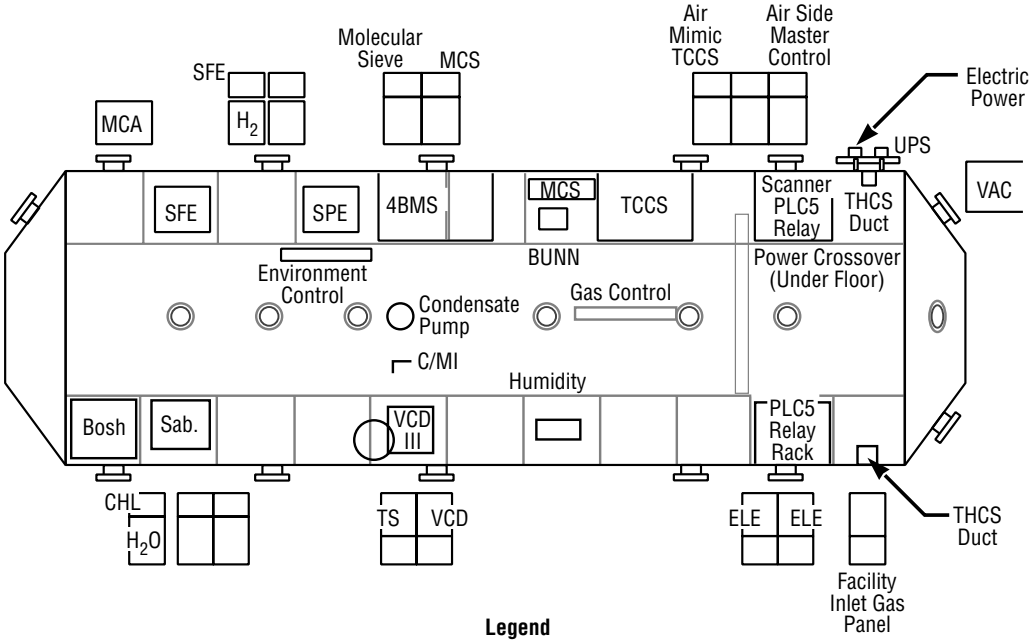

Legend

BOSCH	Bosch CO_2 Reduction Assembly
BUNN	MCS O_2 Removal
MCA	Major Constituent Analyzer
MCS	Metabolic Control Simulator
PLC	Programmable Logic Controller
Sab.	Sabatier CO_2 Reduction Assembly
SFE	Static Feed Electrolyzer
SPE	Solid Polymer Electrolyzer
TCCS	Trace Contaminant Control Subassembly
THCS	Temperature and Humidity Control System
UPS	Uninterruptable Power Supply
VCD	Vapor Compression Distillation Assembly
4BMS	Four-Bed Molecular Sieve CO_2 Removal Assembly

FIGURE 2.—Simplified CMS hardware layout.

ECLSS Subassembly Description

The IART is designed to test the *ISS* ARS configuration planned for the U.S. Habitation Module (Hab). This hardware complement includes an OGA, CDRA, TCCS, and MCA. Allowance is made for the addition of a Sabatier carbon dioxide reduction assembly as specified by the *ISS* design. The ARS configuration tested is shown schematically by figure 3.[20] A more detailed IART process and instrumentation diagram for the IART is provided by figure 4. Although pressurized oxygen injection was used during the test, both the OGA and pressurized oxygen injection are shown to emphasize the facility's capabilities.

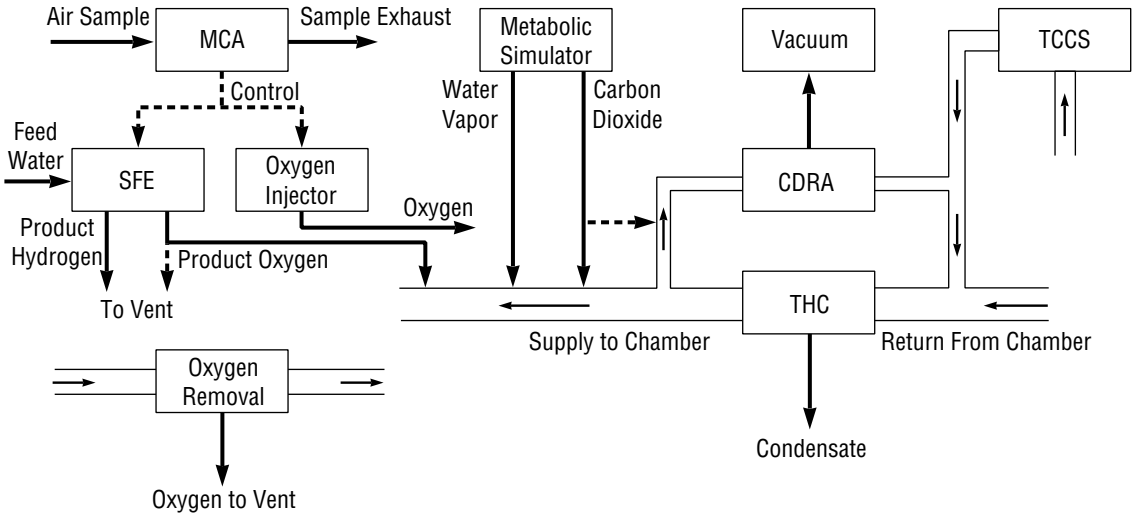

FIGURE 3.—Simplified IART process flow diagram.

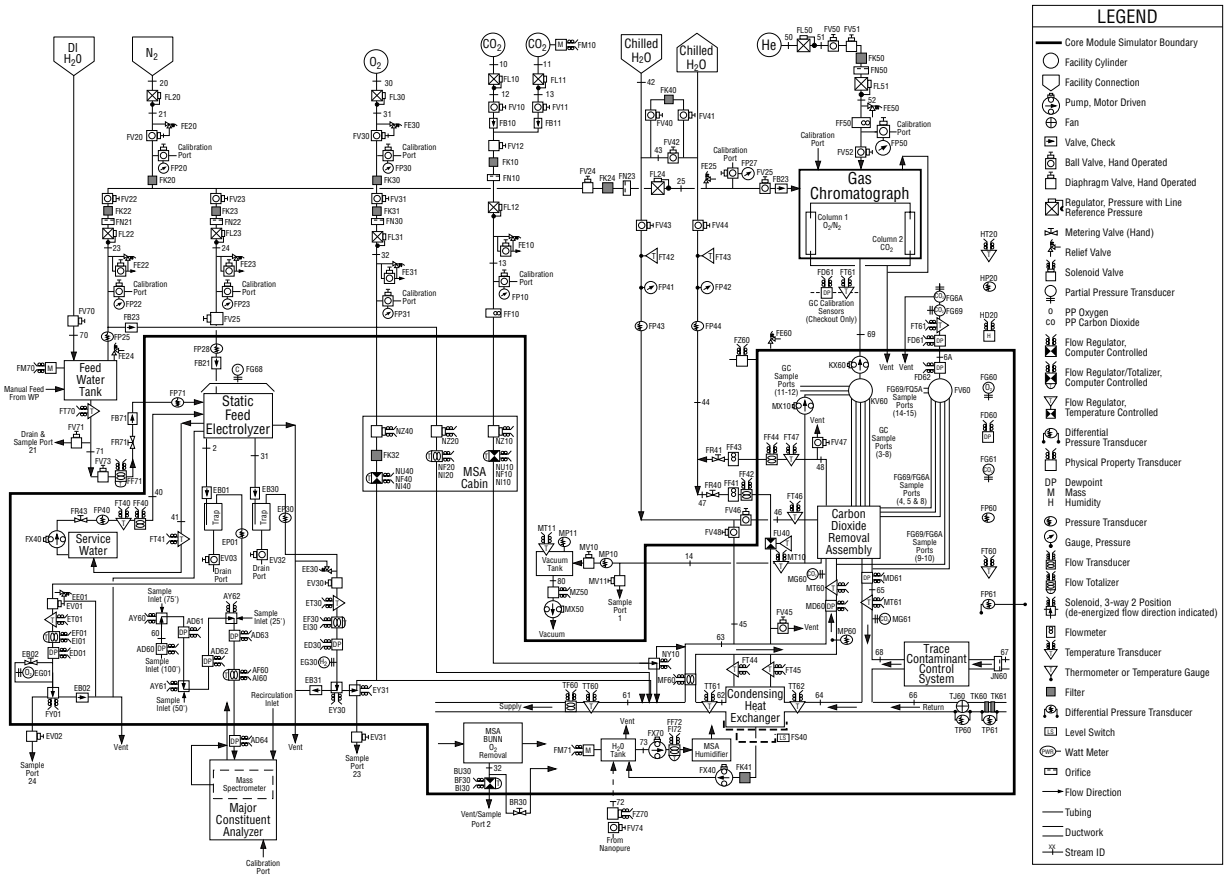

FIGURE 4.—Detailed IART process and instrumentation diagram.

Carbon Dioxide Removal Assembly

The CDRA utilizes silica gel, zeolite 13X, and zeolite 5A to dry the inlet air to the system and then remove carbon dioxide. Air enters the system and passes through one of two beds containing silica gel and zeolite 13X. These adsorbents remove water vapor that can inhibit the removal of carbon dioxide. Next, the air is cooled and passes through one of two beds filled with zeolite 5A to remove carbon dioxide. On a regular cycle, the zeolite 5A bed is isolated, heated, and exposed to vacuum to regenerate it. During this time, the second zeolite 5A bed is adsorbing carbon dioxide. The processed air flows out of the adsorbing zeolite 5A bed through the second bed filled with silica gel and zeolite 13X. Water is desorbed from the second bed by the exiting air. The CDRA process is shown schematically by figure 5.

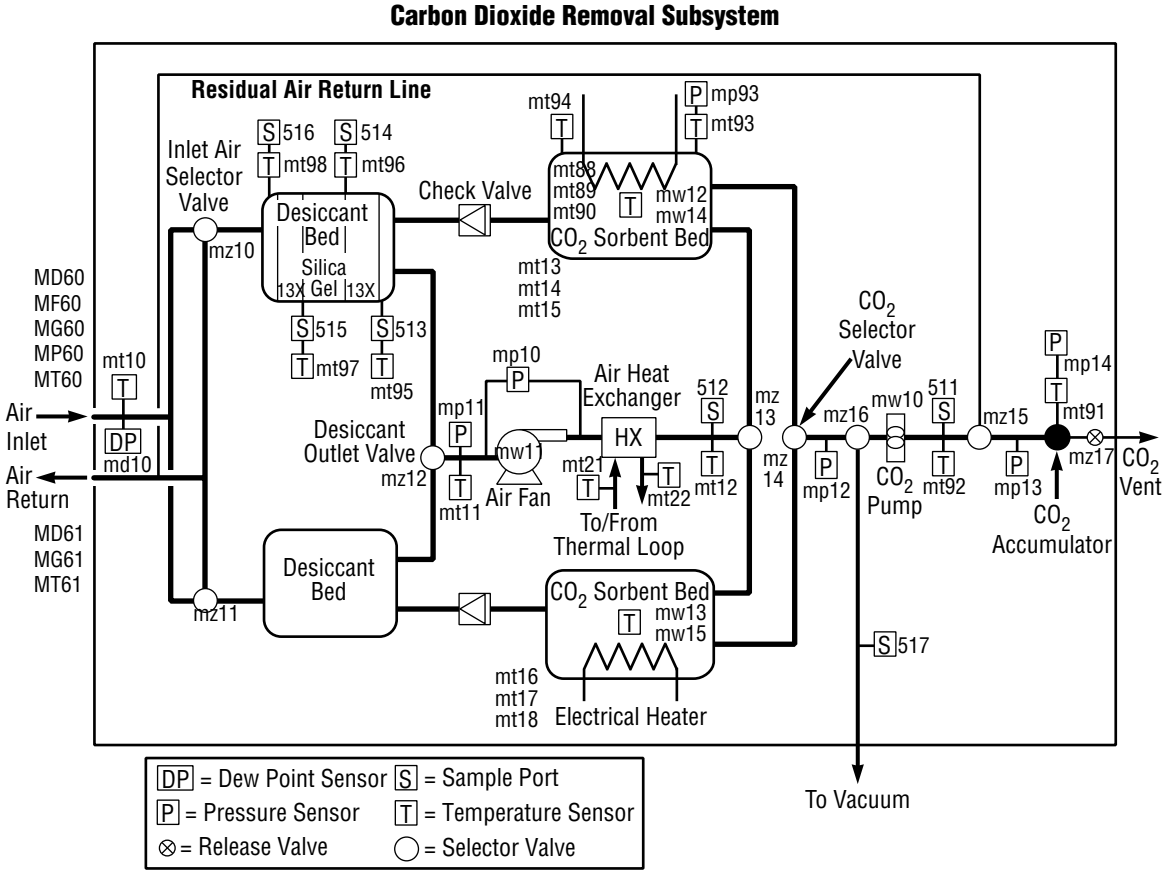

FIGURE 5.—4BMS CDRA.

The CDRA used during the IART was the same unit tested during the Phase IV POST. Several modifications were made to the CDRA before its use in the IART. These modifications included repacking the desiccant beds, installing instrumentation in one desiccant bed and one sorbent bed, removing excess 5A zeolite material from both sorbent beds and replacing the material with glass beads, installing new sorbent bed material containment screens and frames, and installing thermocouples into the sorbent beds to allow for temperature control from an internal reference point rather than an external reference point. Modifications to the packing of all beds provided the same volumetric quantity of silica gel,

13X zeolite, and 5A zeolite as the flight CDRA. In addition, the silica gel and 13X zeolite used were from the same production lot as the flight CDRA materials. Control software modifications were also made to allow the CDRA to be operated in a day/night mode. Final software modifications were made in the CDRA flowrate, sorbent bed operating temperature setpoint, and half-cycle time before integrated testing.

Oxygen Generator Assembly

The OGA consists of an electrolysis module, a fluids control assembly, a pressure control assembly, and a thermal control assembly. Electrolysis of water processed during *ISS* water processor testing occurs in the electrolysis module, which consists of 24 cells. Each cell contains a water feed compartment, an oxygen compartment, and a hydrogen compartment. The water and hydrogen compartments are separated by a selectively permeable membrane, and the two gas compartments are separated by an aqueous potassium hydroxide and electrode assembly. The electrolysis process produces a water deficiency in the electrolyte that causes water to diffuse from the water feed compartment through the hydrogen compartment into the electrolyte. Water is replenished in the feed compartment by maintaining a static pressure at the feed tank. This process occurs as long as power is supplied to the cell stack. Figure 6 shows a schematic of the OGA.

Modifications to both software and hardware were made to the OGA before testing. Software additions were made to allow for day/night cyclic operations, a higher operating temperature setpoint to prevent condensation in gas passages, and an increased current level to allow for the lag time during the transition between standby and normal operating modes. These changes were necessary to provide for smooth operations using a 53-min daylight and 37-min night cycle, using a nitrogen supply interface pressure of 689 ± 69 kPa (100 ± 10 psia). Hardware modifications were made to the electrochemical module, the Pressure Control Assembly (PCA), the Fluids Control Assembly (FCA), and the Thermal Control Assembly (TCA). The electrochemical module modifications included the addition of filter/barrier cells with heaters, temperature sensors, and thermostat; the addition of an extra nonoperating cell for thermal control; the relocation of pressure taps directly into the module; the addition of two pressure switches in the product gas streams; and the elimination of unneeded passages in the fluids insulation plate and structural insulation plate. The PCA was modified by changing the regulator poppets from a spherical to a conical geometry and using a steep conical sealing surface rather than a shallow conical surface. Two check valves, a filter, and an orifice were eliminated from the FCA, and four solenoid valves, two pressure sensors, and two nitrogen holding tanks were added. The TCA was modified by eliminating a diverter valve, a solenoid valve, and a check valve, and adding one three-way solenoid valve. The heat exchanger and pump were also relocated to the exterior of the TCA body. The TCA pump was replaced with a commercial gear pump using Teflon^{TM} gears and bushings. The entire system was retrofit with two low-pressure relief valves, a deiodinator, a deionizer, two fill-and-drain valves, and a conductivity sensor.

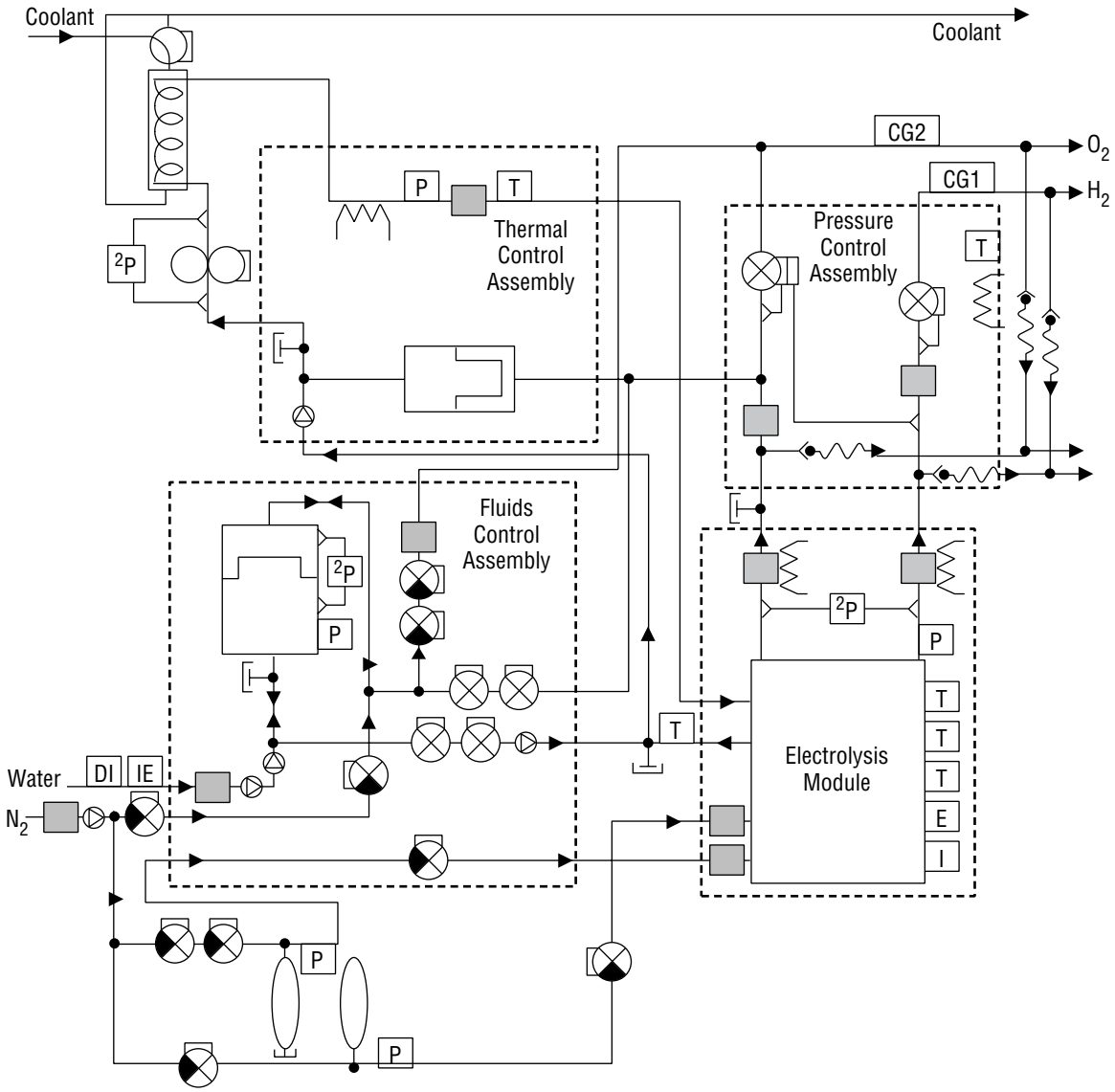

FIGURE 6.—Static feed electrolysis OGA.

Trace Contaminant Control Subassembly

The TCCS utilizes activated charcoal adsorption, high temperature catalytic oxidation, and lithium hydroxide (LiOH) chemisorption to remove trace chemical contaminants and acidic oxidation products from the chamber atmosphere. In this process, air enters the activated charcoal bed to remove high molecular weight contaminants. After the charcoal bed, the process stream splits, with approximately one-third of the flow passing through a recuperative heat exchanger, catalytic reactor, and postsorbent bed. The catalytic reactor is packed with 0.5 percent palladium (Pd) catalyst supported on cylindrical alumina pellets. The postsorbent bed is filled with granular LiOH. Total airflow through the TCCS is 15.29 m^3/hr (9 ft^3/min) with 4.59 m^3/hr (2.7 ft^3/min) airflow through the high-temperature oxidizer. Figure 7 shows a schematic of the flight TCCS process.

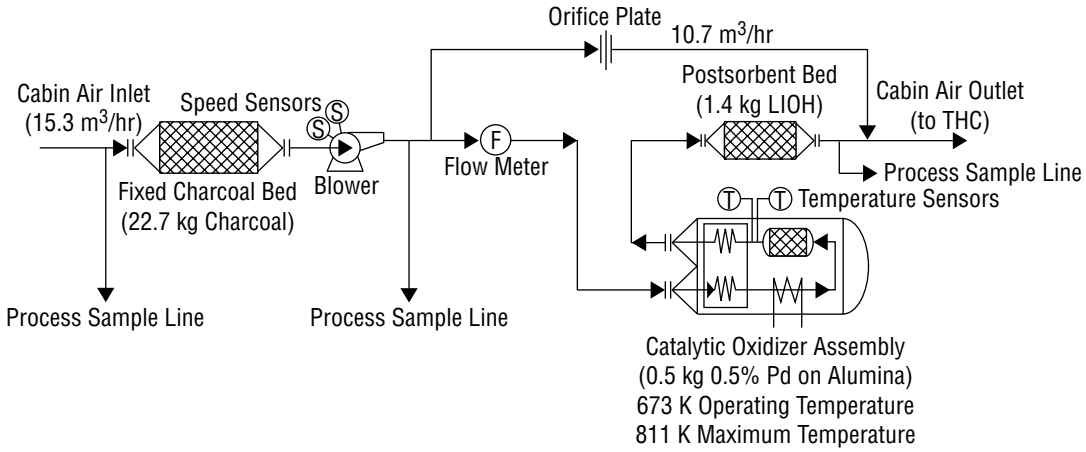

FIGURE 7.—Flight TCCS process flow diagram.

It should be noted that the TCCS hardware used in the IART has several differences from the flight TCCS. As can be seen in figure 8, these differences include the use of two blowers rather than one and the existence of a regenerable charcoal bed and a LiOH presorbent bed. Also, the charcoal bed contains 21.8 kg (48 lb) as compared to the 22.7 kg (50 lb) provided by the flight unit. In order for the TCCS tested to provide the same function as the flight unit, the regenerable charcoal bed does not have any packing and serves only as a duct. The LiOH presorbent bed functions only to remove sulfide compounds that are produced in a spacecraft cabin at extremely low levels. As a result, the presence of the LiOH presorbent bed is considered insignificant. For the scope of the test, the lower charcoal weight is also an insignificant factor; however, it will have to be addressed for future contaminant injection testing. The test unit is also capable of providing up to a 59.5 m^3/hr (35 ft^3/min) flowrate. However, the flight TCCS design has only a 15.3 m^3/hr (9 ft^3/min) inlet flowrate. An orifice was added to the TCCS inlet to provide the proper inlet flowrate. Functionally, the TCCS tested is an exceptionally high-fidelity unit capable of providing the full range of *ISS* contamination control capability.

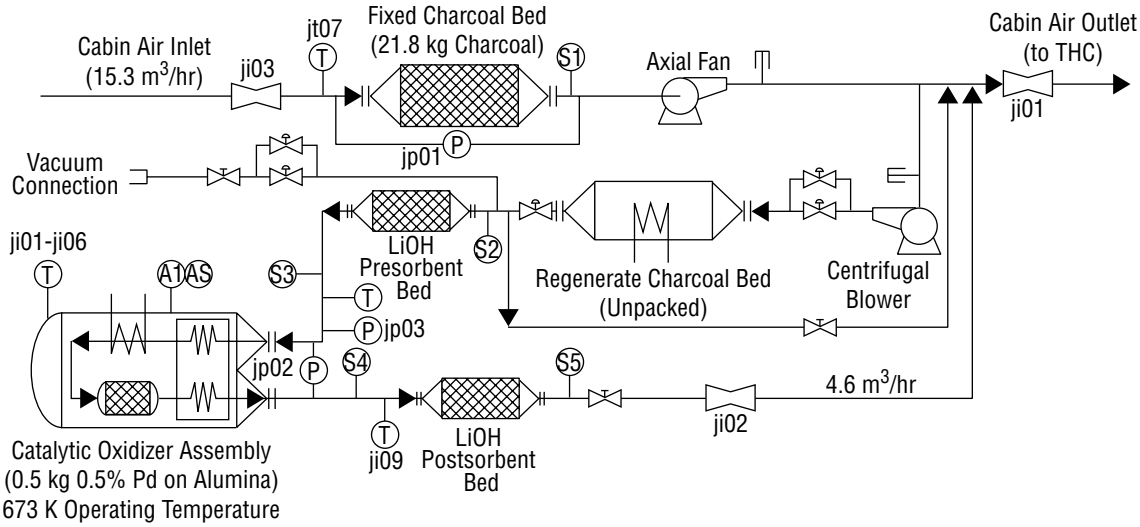

FIGURE 8.—IART TCCS process and instrumentation diagram.

Major Constituent Analyzer

The MCA utilizes a single-focusing, fixed-magnet scanning mass spectrometer to analyze the chamber atmosphere for nitrogen, oxygen, carbon dioxide, methane, hydrogen, and water vapor. Samples are pumped from remote locations in the chamber to the MCA via a sample distribution system. The MCA sample pump first purges the sample line and then introduces a very small portion of the sample into the mass spectrometer via an inlet leak. The sample gas is ionized by an electron beam and the resulting positively charged ions are directed into a magnetic field where they are separated according to their mass-to-charge ratios. The separated ion beams are focused through resolving slits along a focal plane into Faraday current collectors. The number of molecules admitted in the gas sample is directly proportional to the collected current. This current is processed and utilized for controlling atmospheric composition in the test chamber. The mass spectrometer vacuum is maintained by an ion pump, while initial roughing vacuum is provided by a facility vacuum system. Sample and bypass streams exhaust into the CMS to minimize gas losses. Data collected by the MCA are processed and relayed to the OGA to regulate the rate of oxygen production. Figure 9 shows a pneumatic schematic of the MCA, while figure 10 shows a more detailed diagram of the mass spectrometer.[21, 22]

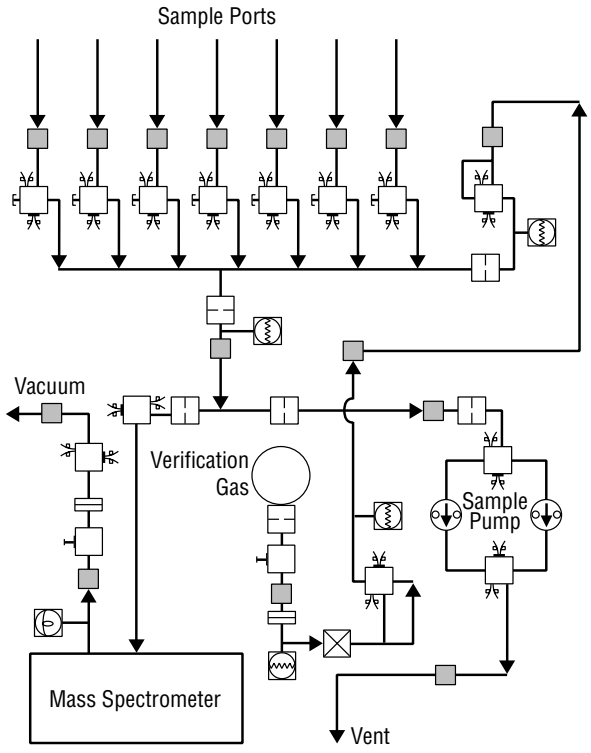

FIGURE 9.—Simplified MCA pneumatic diagram.

For the IART, the sample distribution system consisted of a single 30.6-m (100-ft) long, 3.2-mm (0.125-in) diameter sample line. This line had dewpoint sensors located at 30.6 m (100 ft), 22.9 m (75 ft), 15.3 m (50 ft), and 7.6 m (25 ft) away from the MCA inlet. A dewpoint sensor was also located adjacent to the MCA sample inlet. Samples were taken using the various sample line lengths during the IART.

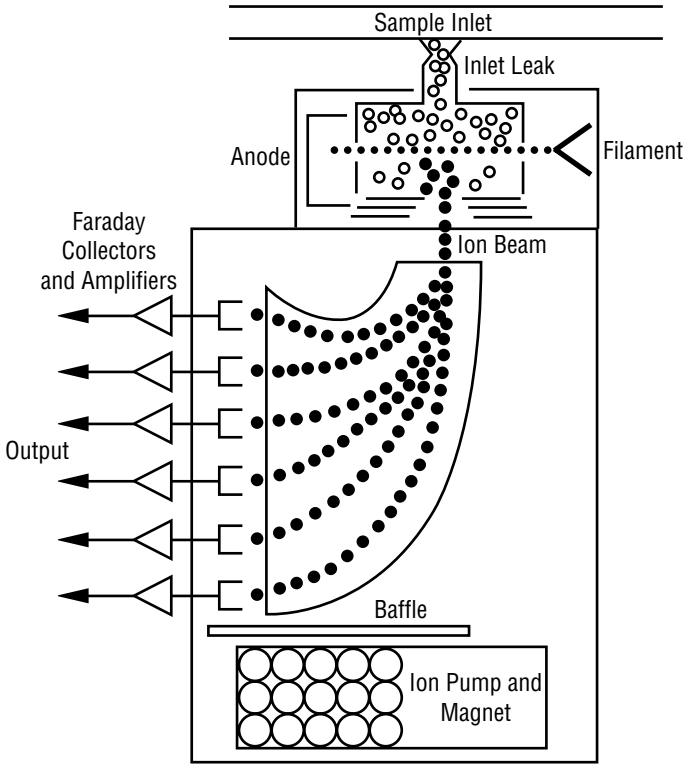

FIGURE 10.—Simplified mass spectrometer schematic.

The MCA used for the IART was also used during Phase IV POST. It is included in a package of instruments designed to monitor different analytes of the *ISS* cabin atmosphere. This package includes a carbon monoxide analyzer (COA) and a TCM in addition to the MCA. A particulate counting monitor (PCM) was also included earlier. Together, these instruments comprised the Atmosphere Composition Monitor Assembly. During the space station redesign, the MCA was the only instrument retained for monitoring the cabin atmosphere. Therefore, the COA, TCM, and PCM were not used during the IART, and the unit was configured to use only the MCA.

Integrated ARS Description

The CDRA, OGA, TCCS, and MCA were integrated with the CMS as shown previously by figures 3 and 4. During the test, a facility-provided condensing heat exchanger (CHX) removed water vapor from the CMS atmosphere and controlled its temperature. To approximate the metabolic contribution of four crew members, water vapor was injected into the central part of the chamber volume as a mist, while carbon dioxide was injected into the Temperature and Humidity Control System (THCS) air circulation duct according to rates projected by *ISS* crew activity time lines. Oxygen consumption by the crew was simulated by a facility-provided oxygen concentrator. This concentrator adsorbed oxygen from the chamber atmosphere and vented it outside the facility according to the same projected crew activity time line. Metabolic simulation was controlled by the facility host computer.

The CDRA inlet interfaced with the facility-provided THCS downstream of the CHX, and air processed by the CDRA exhausted into the THCS upstream of the CHX. The TCCS inlet interfaced directly with the CMS atmosphere, and its exhaust combined with the CDRA exhaust before it was

returned to the THCS. The inlet to the TCCS had a facility-provided orifice installed to control its inlet flowrate to the *ISS* design. The MCA was located outside the CMS because of its size. Air samples were pumped to the MCA and exhausted back into the CMS to minimize gas losses. During OGA operations, feed water collected from *ISS* water processor tests was pumped from an externally mounted tank, and the oxygen product was vented to the THCS while the hydrogen product was vented out of the facility. In the event that the OGA was not available for testing, the facility host computer was also capable of conditioning the MCA oxygen partial pressure signal and sending commands to a solenoid valve to allow oxygen injection from a pressurized source. Normally, the MCA oxygen partial pressure signal would be used by the host computer to command the OGA to operate at 90, 100, or 110 percent of its rated capacity. Humidity condensate was collected in a drip pan located beneath the CHX and recycled into the metabolic simulator. Facility-provided nitrogen was used to help maintain the chamber total pressure slightly above the prevailing ambient barometric pressure. This approach precluded the potential for diluting the carbon dioxide partial pressure in the chamber with ambient air.

Test Control Description

Test facility control was provided by both remote and local process controllers. Although flight software was not used for the test, the control scheme mimicked the command-and-control architecture of the *ISS* as closely as possible. The facility provided for subassembly control setpoint designation, metabolic simulation, day/night cycling, and overall system-level control.

Day/Night Power Cycling Control

Pretest analysis of the planned *ISS* orbit established a worst case day/night cycle of 53 min of daylight operation and 37 min of nighttime operations. The day/night control signal was initiated by the facility host computer. This signal instructed the CDRA and OGA to initiate their power-saving mode during the nighttime portion of the cycle and resume normal operations during the daylight portion of the cycle.

Metabolic Simulation Control

Simulation of the principal metabolic functions of four crew members was provided by facility-supplied hardware and software. Respiration was the primary metabolic function simulated. This simulation, controlled by the facility host computer, involved injecting carbon dioxide and water vapor, while removing oxygen at rates that mimicked a representative *ISS* crew activity timeline. Carbon dioxide was injected from a facility-provided pressurized bottle, while makeup water was provided from the facility's deionized water system. The water was injected into the CMS as a mist after being mixed with condensate water from the THCS. Oxygen removal was provided by a regenerable adsorption system located inside the CMS. The metabolic simulation duration was 24 hr and was repeated on a daily cycle.

Chamber Total Pressure Control

Total pressure control was maintained between 0.40 and 0.93 kPa (3 and 7 mmHg) above the prevailing barometric pressure (gauge pressure). Chamber venting occurred if the pressure reached 1.6-kPa (12-mmHg) gauge pressure. At less than 0.40-kPa gauge pressure, nitrogen injection was

initiated. Injection stopped at 0.93-kPa gauge pressure. This control approach ensured that no dilution from the ambient atmosphere occurred and that the atmospheric composition inside the test chamber was purely the result of ARS subassembly operations. Figure 11 summarizes the CMS total pressure control logic.

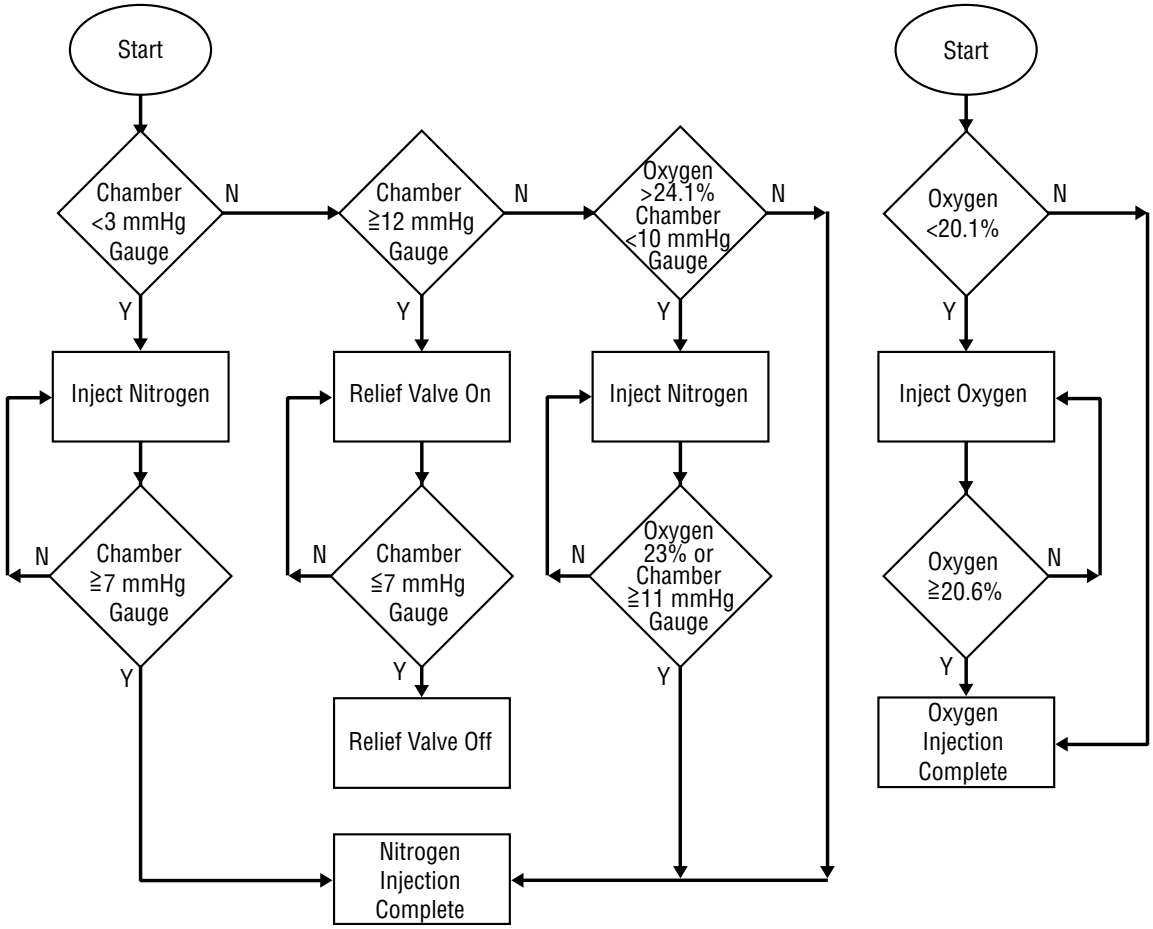

FIGURE 11.—CMS total pressure and oxygen partial pressure control logic.

Oxygen Partial Pressure Control

The oxygen partial pressure control range was set between 20.3 and 20.9 kPa (2.95 and 3.03 psia). To achieve this control, the oxygen partial pressure signal from the MCA was conditioned by the host computer and used to open and close a facility-provided valve that allowed oxygen to flow into the chamber at 0.0454 to 0.0907 kg/min (0.1 to 0.2 lb/min). Oxygen partial pressure could also be regulated by using this same conditioned MCA oxygen partial pressure signal to control the OGA oxygen production rate; however, technical difficulties prevented the OGA from being used in the test. In the event that oxygen partial pressure became too high, additional nitrogen would be injected into the chamber to dilute it. This approach is shown schematically by figure 11.

Subassembly Control

Subassembly control was provided by dedicated personal computers with a system interface to a host computer. The host computer provided the means for changing control setpoints and provided the signals for daytime and nighttime operating mode initiation and termination. All facility and subsystem-level control was provided by the host computer. For example, the CDRA was controlled by its own computer with input from the host computer for daytime and nighttime cycling. The MCA and TCCS operated continuously according to the current *ISS* operational approach. Although the IART did not use flight software, the overall control approach used during the IART was consistent with that to be used on board the *ISS* in that high-level commands are initiated from a central control console, while detailed subassembly control is provided at the rack level.

Data Acquisition

Data acquisition was provided by the facility. Data from both facility sensors and each individual subassembly were collected by Systems and Components Automated Test System (SCATS) and stored in files on a mainframe computer. These data file names were logged into the master SCATS log for reference. Upon completing a data file, it was transmitted electronically to be loaded into the Functional ECLSS Data System, the ECLSS test database. These data were then accessed, reduced, and analyzed.

PRETEST ANALYSIS SUMMARY

Day/Night Cycle Duration

An assessment was conducted to determine the daylight and nighttime period duration for the *ISS* orbit. This assessment considered the effects of parameters such as orbital altitude and beta angle. The beta angle is the angle of the orbital plane relative to the Earth-Sun line. The minimum *ISS* altitude will be approximately 175±5 nautical miles. This accounts for reboost and subsequent orbital decay. Once reboost occurs, however, it is estimated that the *ISS* will remain in its higher orbit for approximately 1 yr. The beta angle for the *ISS* orbit ranges between zero and ±27° for more than 2 wk each month. During that time, the nighttime period of the orbit varies by only about 1.5 min for any altitude. Given these parameters, the duration of the nighttime period of the orbit accounts for approximately 41 percent of the orbit duration. With a 90-min orbit, the nighttime period duration was determined to be 37 min, while the daylight period duration was 53 min. This cycle was used as the basis for the IART.[23]

Oxygen Partial Pressure Control

With the use of an OGA for oxygen partial pressure control, it was necessary to investigate the CMS response while considering atmospheric leakage and OGA operating capacity. This assessment was necessary to determine whether the CMS atmosphere would need to be conditioned to within the specified control band before starting the OGA. Late in the preparation for the IART, it became apparent that technical difficulties would prevent the OGA from being used for the test. As a result, an additional analysis was conducted to investigate oxygen partial pressure control via a pressurized source. The need for preconditioning the CMS atmosphere also had be to reassessed. The results from these analyses are summarized by the following discussion.[24]

Oxygen Partial Pressure Control Using the OGA

During initial test planning, the OGA was to be used to supply oxygen by electrolyzing water. Given that the OGA was limited to producing oxygen at a four-human metabolic equivalent rate and that it would be in normal operations for 59 percent of the time, it became apparent that CMS leakage would be important to maintaining the chamber oxygen partial pressure within specified limits. Oxygen production rate and removal rate would also work together to provide the resulting test system response time. An analysis was conducted that investigated the ability of the OGA to maintain the oxygen partial pressure within the CMS at various leakage rates and also determine the response time for the CMS to reach steady-state oxygen partial pressure control at various leakage rates.

The nominal metabolic simulation profile for oxygen consumption to be used in the test was employed for the analysis. Also considered was the ability of the OGA to produce oxygen at a four-human-metabolic equivalent plus or minus 10 percent. For nominal OGA operation at 100-percent capacity, the analysis found that the CMS response would be slow. More than 14 days would be required before the control band would be reached. This response was not acceptable since the total test duration was scheduled for 30 days.

Other means for more rapidly reaching the oxygen partial pressure control range were investigated. By operating the OGA at 90-percent capacity, the control band could be reached within 7 days at 0.91 kg/day (2 lb/day) leakage and within 5 days for 1.81 kg/day (4 lb/day) leakage. The projected average oxygen partial pressure control level for 90-percent OGA operating capacity was 19.96 kPa (2.895 psia) with a lower bound of approximately 19.89 kPa (2.885 psia), which is within the allowable *ISS* operational range of 19.5 to 23.1 kPa (2.83 to 3.35 psia).

As a result of this study, it was recommended that the CMS atmosphere be preconditioned to the predicted control band before initiating OGA operations. Such an approach reduced the time to achieve oxygen partial pressure control to less than 48 hr.

As an extension of this analysis, two additional cases were investigated to assess the effects of higher leakage rates on steady-state oxygen partial pressure. First, at 110-percent OGA operating capacity, the average projected oxygen partial pressure was found to be approximately 15.5 kPa (2.25 psia) for a 2.27 kg/day (5 lb/day) leakage rate. This level is well below the allowable *ISS* range and indicates that for the OGA to be used for the IART, leakage greater than about 1.81 kg/day (4 lb/day) was not acceptable. Fortunately, static leakage tests of the CMS determined the leakage to be approximately 0.69 kg/day (1.52 lb/day). Second, a case was investigated to project the response for a six-human metabolic equivalent loading with oxygen production also at a six-person rate. This case showed that at 100-percent capacity, the OGA would be able to maintain oxygen partial pressure between 20.28 and 20.32 kPa (2.942 and 2.948 psia) for 0.45- and 2.72-kg/day (1.0- and 6.0-lb/day) leakage rates, respectively. This result demonstrated that the OGA, when operating in a day/night power-saving mode, most likely is capable of maintaining the oxygen partial pressure of the *ISS* cabin within the required 19.5-kPa (2.83-psia) to 23.1-kPa (3.35-psia) range even with up to 0.45-kg/day (1.0-lb/day) leakage from each U.S. Segment module. These results reinforce the approach of sizing the nominal *ISS* oxygen generation capacity to accommodate the impacts from leakage.

Oxygen Partial Pressure Control Using Pressurized Injection

After it became apparent that technical difficulties with the OGA would prevent it from being used during the IART, pressurized injection became the primary means for oxygen partial pressure control. This configuration approximated that of the U.S. Laboratory (USL) in which oxygen is injected at a rate of 0.0454 to 0.0907 kg/min (0.1 to 0.2 lb/min). A valve in the USL pressure control assembly is opened to allow oxygen flow when the lower bound of the oxygen partial pressure control band is reached. To understand the CMS response to this approach to oxygen partial pressure control, an additional analysis was conducted using an injection flowrate of 0.068 kg/min (0.15 lb/min). Oxygen flow was initiated at an oxygen partial pressure of 20.34 kPa (2.95 psia) and stopped at 20.68 kPa (3.00 psia). Leakage for the analysis was set at 0.69 kg/day (1.52 lb/day) based upon CMS static leakage tests. The resulting response, shown by figure 12, indicated that oxygen partial pressure control would be maintained very close to 20.68 kPa (3.00 psia) with little difficulty. Essentially no time lag was observed, which indicated that the CMS oxygen partial pressure would not need to be conditioned upon test startup.

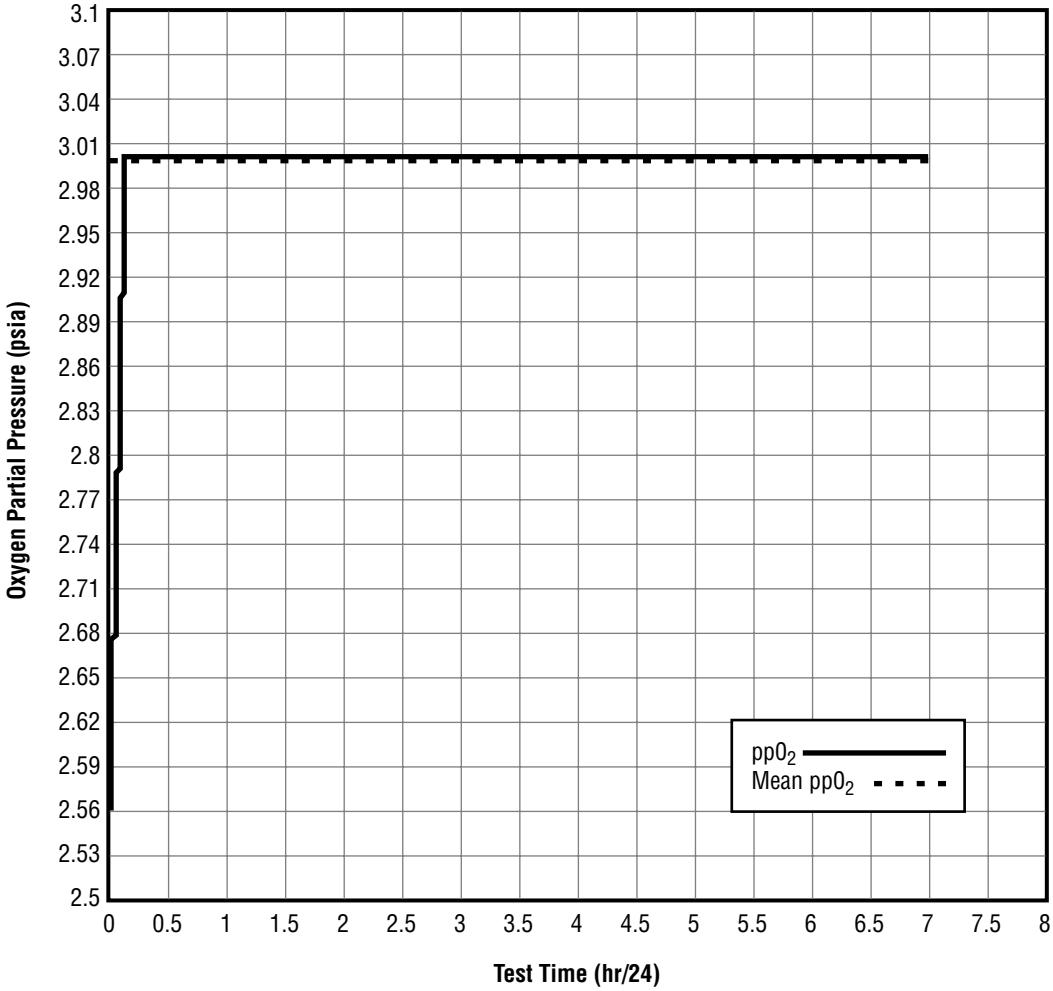

FIGURE 12.—Predicted oxygen partial pressure control using pressurized injection.

Metabolic Simulation

Metabolic simulation parameters were derived from a representative daily crew activity time line for the *ISS* configuration at assembly flight 14A. This time line, shown by figure 13, tracks the activities of six crew members through a 24-hr day according to their major activities and location within the *ISS* cabin. Crew member movement throughout the *ISS* and the effects of intermodule ventilation (IMV) and IMV short-circuiting are important to the metabolic simulation. The effects of Russian carbon dioxide removal equipment are also important and were approximated in the simulations of crew member metabolic activity. As the crew members' activity levels change during the day and they move through the *ISS* cabin between various workstations, the atmospheric composition in the USL will change. Since the ARS will use the local conditions within the USL to control the atmospheric composition in the *ISS* cabin, the metabolic input to the USL as a function of the crew activity time line was needed.

To obtain a representative USL metabolic input profile, a carbon dioxide mass balance simulation of the entire assembly flight 14A configuration was conducted.[25] This simulation used the metabolic

carbon dioxide production of six crew members according to the activity time line shown by figure 13. An analysis was conducted that also considered the metabolic contribution of experimental animals. The carbon dioxide mass influx to U.S. modules for the two cases are shown by figures 14 and 15.

For the IART, the USL mass influx profile with animal contribution served as the basis for the metabolic simulation. This profile was approximated as a series of step increases and decreases relative to the 24-hr average loading for the USL. This loading was scaled from the level of six crew members plus research animals to four crew members plus 1.23 metabolic equivalents for research animals to more adequately address the program requirements placed upon the U.S. ARS system. Figure 16 shows the profile schematically while table 1 lists the percentage deviation from the mean for each phase of the profile.[26, 27]

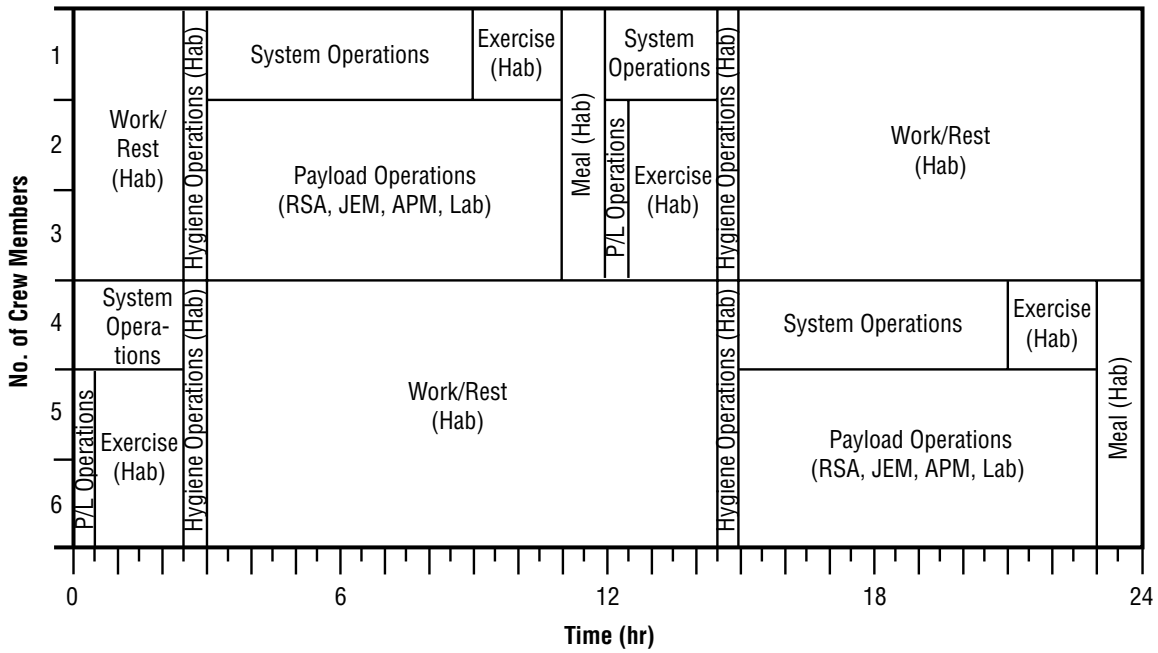

APM Attached Pressurized Module (European Space Agency)
JEM Japanese Experiment Module
RSA Russian Space Agency
P/L Payload

FIGURE 13.—Mission 14A crew activity time line.

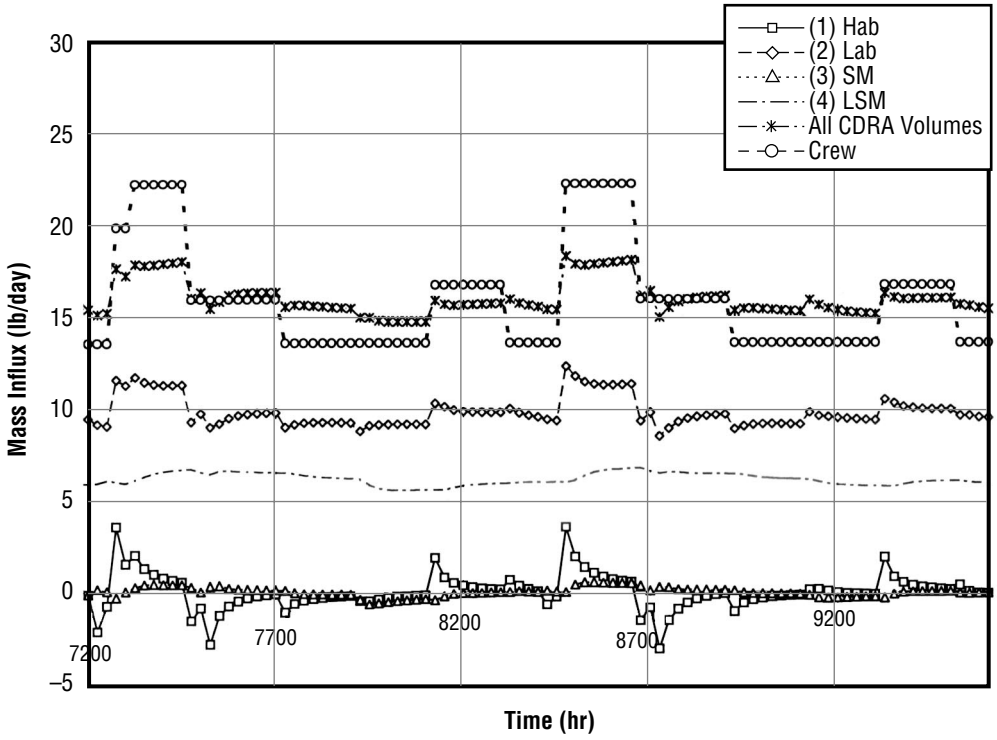

FIGURE 14.—U.S. Segment carbon dioxide mass influx with animals.

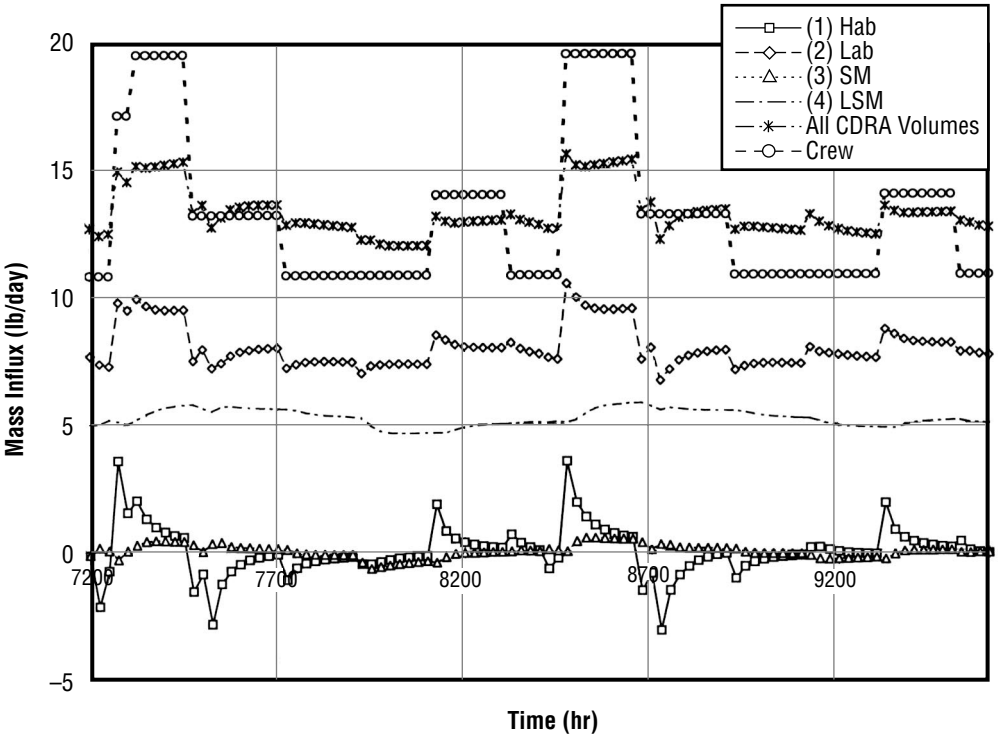

FIGURE 15.—U.S. Segment carbon dioxide mass influx without animals.

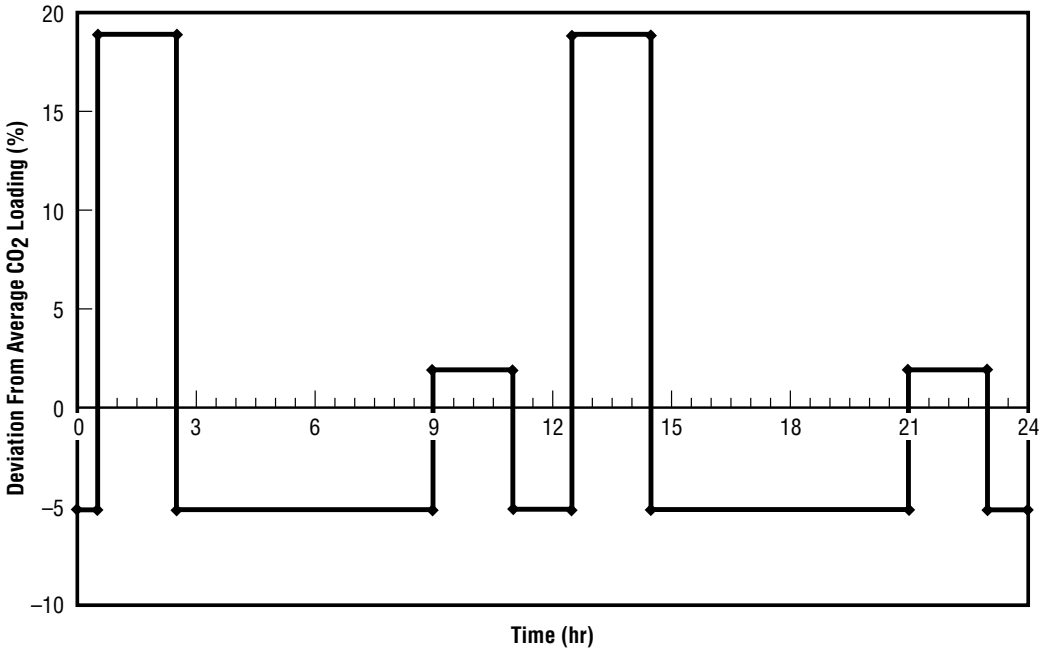

FIGURE 16.—Carbon dioxide loading profile.

TABLE 1.—*Deviation from 24-hr average carbon dioxide loading.*

Time (hr)	Deviation, σ (%)
0.0	–5.30
0.5	18.96
2.5	–5.30
9.0	1.94
11.0	–5.30
12.5	18.96
14.5	–5.30
21.0	1.94
23.0	–5.30

A scaling factor, ε, equal to 2.243, was used to vary the amplitude of the steps without changing the average flowrate over the 24-hr period. This factor accounted for the difference in volume of the CMS relative to the USL. Originally, the profile in figure 16 was used to approximate the metabolic loading from four crew members and 1.23 human metabolic equivalents for research animals as defined by equation (1).

$$\dot{m}_{CO_2} = \frac{(100 + \varepsilon\sigma)}{100}(5.23)\frac{2.2\ \text{lb}}{24\ \text{hr}} \quad . \tag{1}$$

However, since the OGA to be used for IART was sized to accommodate a metabolic loading for only four crew members, equation (1) was adjusted to remove the contribution from research animals. Equation (2) shows the final form for the carbon dioxide mass loading equation.

$$\dot{m}_{CO_2} = \frac{\left(100 + \frac{5.23}{4}\varepsilon\sigma\right)}{100}(4.0)\,\frac{2.2\ \text{lb}}{24\ \text{hr}}\ . \tag{2}$$

Both water vapor and oxygen removal rates can be correlated to the carbon dioxide production rate.[28] The resulting equation for water vapor loading is shown by equation (3), with further definition provided by equations (4) and (5).

$$\dot{m}_{H_2O} = \frac{XLHEAT}{1{,}056.7}\,\frac{\text{lb}}{\text{hr}}, \tag{3}$$

$$XLHEAT = TMET - 430 + \left(\frac{TMET}{1{,}000} + 10\right)(T_{CMS} - 60), \tag{4}$$

$$TMET = \frac{11{,}200}{2.2}\,\dot{m}_{CO_2}\,\frac{\text{BTU}}{\text{hr}}\ . \tag{5}$$

Again, since the OGA was not capable of supporting more than the nominal four crew members, the carbon dioxide loading used to calculate the oxygen removal was modified to remove the research animal load. The resulting equation for oxygen removal rate is shown by equation (6).

$$\dot{m}_{O_2} = \frac{\left(100 + \frac{5.23}{4}\varepsilon\sigma\right)}{100} \cdot 4 \cdot \frac{11{,}200 \cdot 0.000163}{24}\,\frac{\text{lb}}{\text{hr}}\ . \tag{6}$$

Applying these equations, using a scaling factor of 2.243, to the normal CMS operating conditions of 22 °C (72 °F) and 99.97 kPa (14.5 psia), the injection rates for carbon dioxide and water and removal rates for oxygen were derived. These rates are listed in table 2.

TABLE 2.—*Metabolic simulation injection rates.*

Time (hr)	CO_2 Injection Rate (kg/hr)	O_2 Removal Rate (kg/hr)	H_2O Injection Rate (kg/hr)
0.0–0.5	0.14	0.12	0.55
0.5–2.5	0.26	0.21	1.13
2.5–9.0	0.14	0.12	0.55
9.0–11.0	0.18	0.15	0.72
11.0–12.5	0.14	0.12	0.55
12.5–14.5	0.26	0.21	1.13
14.5–21.0	0.14	0.12	0.55
21.0–23.0	0.18	0.15	0.72
23.0–24.0	0.14	0.12	0.55

FACILITY AND SUBASSEMBLY PRETEST SUMMARY

Chamber Leakage Test

Static leakage tests of the CMS were conducted as part of the overall system checkout. Pretest analysis had indicated that up to 1.81 kg/day (4 lb/day) of leakage could be tolerated before chamber atmospheric composition control would be compromised. As shown by pretest analysis, when leakage approaches greater than 2.27 kg/day (5 lb/day), the OGA could maintain only a steady-state oxygen partial pressure of 15.6 volume percent.[29] The static leakage test results showed that the chamber leakage of 0.69 kg/day (1.53 lb/day) was well within the allowable limit. This rate was obtained by analyzing the pressure and temperature conditions between 11.3 and 17.3 hr of the leakage test.[30] Figure 17 shows the leakage and temperature profiles for the chamber static leakage test. The major leakage path for the test facility was determined to be the MCA. Leakage from the MCA was difficult to eliminate because of its overall complexity, the large number of tubing connections and valves used in its design, and the fact that it was located outside the test chamber.

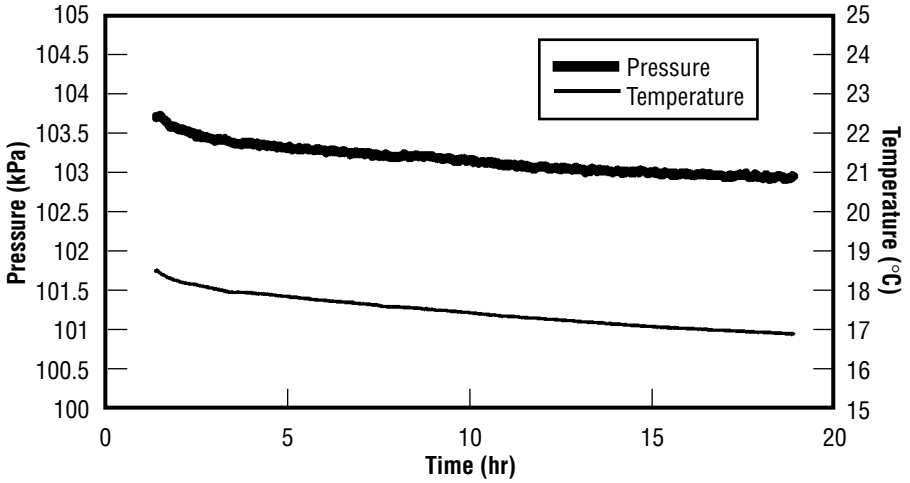

FIGURE 17.—Test chamber leakage.

Carbon Dioxide Removal Assembly

Baseline CDRA operations were demonstrated using several operational modes before the test to ensure acceptable performance with new operating conditions and to compare the performance of the recently modified CDRA to its past performance. These tests ensured that the CDRA performance had not degraded as a result of any refurbishment work conducted and provided preliminary information on its performance using two different power-saving operational modes. Test conditions are summarized by tables 3, 4, 5, and 6.

TABLE 3.—*CDRA baseline test 1 conditions and performance summary.*

4BMS Baseline Test 1 Summary Start Time: 10:05 Start Date: 02/09/96
End Time: 24:00 End Date: 02/11/96

Purpose:

Verify that the continuous operation of two heaters during desorb and half-cycle time of 160 min will provide greater than the *ISS* required level of performance. This test will determine if the CDRA satisfies the first part (continuous heater operation) of para. 3.2.1.1 of the *ISS* CDRA Envelope Drawing (683–10009, Rev. G)

Operation:

			Power Usage	Average	Peak
Mode:	Day/Night With Cont. Day		Total	**774**	1,299 W
Half Cycle:	160 min		Heaters	642	990 W
Heater Setting:	390 to 400 °F		Blower	104	111 W
Heater Power:	500 W	Primary	Vacuum Pump	28	379 W
	500 W	Secondary			

Using the *ISS* CDRA Envelope Drawing (683–10009, Rev. G):

Air Inlet Conditions

	Range	Target	Actual		Error (%)	Reference
			Raw Data	Calibrated		
Temperature	40 to 50 °F	50	52.27		4.5	Table II, sh 15
Dewpoint	40 to 50 °F	50	48.40		–3.2	Table II, sh 15
Inlet $ppCO_2$	0.4 to 0.5%	#N/A	0.711	0.507	#N/A	Fig. 3, sh 17
Flowrate	20 ft^3/min	20	20.16		0.8	N/A

Precooler Coolant Water

	Range	Target	Actual	Error (%)	Reference
Temperature	38 to 42 °F	42	46.34	10.3	Par. 3.2.1.5, sh 18
Flowrate	0.5 to 0.54 gal/min	0.5	0.4916	–1.7	Par. 3.2.1.5, sh 18

CO_2 Removal Calculations (Bold type denotes data points plotted in figs. 18 and 19.)

	Range	Target	Actual		Error (%)	Reference
			Raw Data	Calibrated		
Calculated From Inlet and Outlet to 4BMS:						
Inlet $ppCO_2$	2 to 4 mmHg	#N/A	5.288	**3.771**	#N/A	Fig. 3, sh 17
CO_2 Removal	0.28 to 0.58 lb/hr	0.561		**0.614**	**9.4**	Fig. 3, sh 17
Efficiency				87.8%		
Calculated With CO_2 Injection and Module CO_2 Level:						
Module $ppCO_2$	2 to 4 mmHg	#N/A	5.03	**4.013**	**#N/A**	Lab PID fig. 65, p. 100
CO_2 Injection	0.28 to 0.58 lb/hr	0.562		**0.547**	–2.7	Lab PID fig. 65, p. 100

Period Used for Calculations

From	1.67	to	6.99 hr	Starting on Julian Day	42
Total Time of	5.33 hr	or	320 min		

TABLE 4.—*CDRA baseline test 2 conditions and performance summary.*

4BMS Baseline Test 2 Summary

Start Time: 14:00 Start Date: 02/22/96
End Time: 24:00 End Date: 02/24/96

Purpose:

Verify that the operation of two heaters during desorb and half-cycle time of 160 min will provide greater than the *ISS* required level of performance. This test will determine if the CDRA satisfies the second part (day/night heater operation) of par. 3.2.1.1 of the *ISS* CDRA Envelope Drawing (683–10009, Rev. G)

Operation:

			Power Usage	Average	Peak
Mode:	Day/Night		Total	**636**	1,434 W
Half cycle:	160 min		Heaters	506	957 W
Heater Setting:	390 to 400 °F		Blower	102	106 W
Heater Power:	460 W	Primary	Vacuum Pump	28	389 W
	500 W	Secondary			

Using the *ISS* CDRA Envelope Drawing (683–10009, Rev. G):

Air Inlet Conditions

	Range	Target	Actual		Error (%)	Reference
			Raw Data	Calibrated		
Temperature	40 to 50 °F	50	53.74		7.5	Table II, sh 15
Dewpoint	40 to 50 °F	50	49.67		–0.7	Table II, sh 15
Inlet $ppCO_2$	0.4 to 0.5%	#N/A	0.576	0.365	#N/A	Fig. 3, sh 17
Flowrate	20 ft^3/min	20	20.65		3.2	N/A

Precooler Coolant Water

	Range	Target	Actual	Error (%)	Reference
Temperature	38 to 42 °F	42	47.31	12.6	Par. 3.2.1.5, sh 18
Flowrate	0.5 to 0.54 gal/min	0.5	0.4744	–5.1	Par. 3.2.1.5, sh 18

CO_2 Removal Calculations (Bold type denotes data points plotted in figs. 18 and 19.)

	Range	Target	Actual		Error (%)	Reference
			Raw Data	Calibrated		
Calculated From Inlet and Outlet to 4BMS:						
Inlet $ppCO_2$	2 to 4 mmHg	#N/A	4.294	**2.720**	#N/A	Fig. 3, sh 17
CO_2 Removal	0.28 to 0.58 lb/hr	0.395		**0.447**	**13.3**	Fig. 3, sh 17
Efficiency				86.7%		
Calculated With CO_2 Injection and Module CO_2 Level:						
Module $ppCO_2$	2 to 4 mmHg	2.762	3.60	**2.933**	**–6.2**	Lab PID fig. 65, p. 100
CO_2 Injection	0.28 to 0.58 lb/hr	0.367		**0.365**	–0.5	Lab PID fig. 65, p. 100

Period Used for Calculations

From	17.01	to	40.99 hr	Starting on Julian Day	54
Total Time of	24.00 hr	or	1,440 min		

TABLE 5.—*CDRA baseline test 3A conditions and performance summary.*

4BMS Baseline Test 3A Summary

Start Time:	15:25	Start Date:	03/01/96
End Time:	13:00	End Date:	03/04/96

Purpose:

Verify that the "power-save" operation of two heaters during desorb and half-cycle time of 144 min will provide greater than the *ISS* required level of performance. This test will determine if the CDRA satisfies the second part (day/night cycle heater operation) of par. 3.2.1.1 of the *ISS* CDRA Envelope Drawing (683–10009, Rev. G)

Operation:

			Power Usage	Average	Peak
Mode:	Day/Night		Total	**449**	1,141 W
Half Cycle:	144 min		Heaters	307	961 W
Heater Setting:	225–260 °F		Blower	110	115 W
Heater Power:	480 W	primary	Vac. Pump	31	392 W
	480 W	secondary			

Using the *ISS* CDRA Envelope Drawing (683–10009, Rev. G):

Air Inlet Conditions

	Range	Target	Actual		Error (%)	Reference
			Raw Data	Calibrated		
Temperature	40 to 50 °F	50	50.07		0.1	Table II, sh 15
Dewpoint	40 to 50 °F	50	43.88		–12.2	Table II, sh 15
Inlet $ppCO_2$	0.4 to 0.5%	#N/A	0.559	0.349	#N/A	Fig. 3, sh 17
Flowrate	22.2 ft^3/min	22.2	23.73		6.9%	N/A

Precooler Coolant Water

	Range	Target	Actual	Error (%)	Reference
Temperature	38 to 42 °F	42	42.56	1.3	Par. 3.2.1.5, sh 18
Flowrate	0.5 to 0.54 gal/min	0.5	0.4677	–6.5	Par. 3.2.1.5, sh 18

CO_2 Removal Calculations (Bold type denotes data points plotted in figs. 18 and 19.)

	Range	Target	Actual		Error (%)	Reference
			Raw Data	Calibrated		
Calculated From Inlet and Outlet to 4BMS:						
Inlet $ppCO_2$	2 to 4 mmHg	#N/A	4.151	**2.589**	#N/A	Fig. 3, sh 17
CO_2 Removal	0.28 to 0.58 lb/hr	0.374		**0.432**	**15.5**	Fig. 3, sh 17
Efficiency				79.0%		
Calculated With CO_2 Injection and Module CO_2 Level:						
Module $ppCO_2$	2 to 4 mmHg	2.762	3.39	**2.749**	**0.5**	Lab PID fig. 65, p. 100
CO_2 Injection	0.28 to 0.58 lb/hr	0.367		**0.365**	–0.5	Lab PID fig. 65, p. 100

Period Used for Calculations

From	1.91	to	13.89 hr	Starting on Julian Day	62
Total time of	12.00 hr	or	720 min		

TABLE 6.—*CDRA baseline test 3B conditions and performance summary.*

4BMS Baseline Test 3B Summary

Start Time:	14:37	Start Date:	03/08/96
End Time:	08:00	End Date:	03/11/96

Purpose:

Verify that the "power-save" operation of two heaters during desorb and half-cycle time of 144 min will provide greater than the *ISS* required level of performance. This test will determine if the CDRA satisfies the second part (day/night cycle heater operation) of par. 3.2.1.1 of the *ISS* CDRA Envelope Drawing (683–10009, Rev. G)

Operation:

			Power Usage	Average	Peak
Mode:	Day/Night		Total	**544.18**	W
Half Cycle:	144 min		Heaters		W
Heater Setting:	225–260 °F		Blower		W
Heater Power:	480 W	Primary	Vacuum Pump		W
	480 W	Secondary			

Using the *ISS* CDRA Envelope Drawing (683–10009, Rev. G):

Air Inlet Conditions

	Range	Target	Actual		Error (%)	Reference
			Raw Data	Calibrated		
Temperature	40 to 50 °F	50	50.51		1.1	Table II, sh 15
Dewpoint	40 to 50 °F	50	47.26		–5.5	Table II, sh 15
Inlet $ppCO_2$	0.4 to 0.5%	#N/A	0.554	0.409	#N/A	Fig. 3, sh 17
Flowrate	22.2 ft^3/min	22.2	23.57		6.2	N/A

Precooler Coolant Water

	Range	Target	Actual	Error (%)	Reference
Temperature	38 to 42 °F	42	42.24	0.6	Par. 3.2.1.5, sh 18
Flowrate	0.5 to 0.54 gal/min	0.5	0.4879	–2.4	Par. 3.2.1.5, sh 18

CO_2 Removal Calculations (Bold type denotes data points plotted in figs. 18 and 19.)

	Range	Target	Actual		Error (%)	Reference
			Raw Data	Calibrated		
Calculated From Inlet and Outlet to 4BMS:						
Inlet $ppCO_2$	2 to 4 mmHg	#N/A	4.214	**3.115**	#N/A	Fig. 3, sh 17
CO_2 Removal	0.28 to 0.58 lb/hr	0.457		**0.537**	**17.5**	Fig. 3, sh 17
Efficiency				82.7%		
Calculated With CO_2 Injection and Module CO_2 Level:						
Module $ppCO_2$	2 to 4 mmHg	#N/A	0.84	**0.770**	**#N/A**	Lab PID fig. 65, p. 100
CO_2 Injection	0.28 to 0.58 lb/hr	0.458		**0.456**	–0.5	Lab PID fig. 65, p. 100

Period Used for Calculations

From	0.01	to	23.99 hr	Starting on Julian Day	70
Total time of	24.00 hr	or	1,440 min		

As part of the IART, new control software was provided for the CDRA to allow it to operate in a power-saving day/night cycling mode. In this mode, airflow is maintained through the CDRA but the heaters used during the desorption cycle are shut off. Baseline performance runs were conducted in the closed chamber to assess the CDRA performance for continuous operation and two power-saving modes. The first power-saving mode cycled the adsorbent bed heaters on and off according to facility day/night power cycling commands using a desorption temperature setpoint of 204 °C (400 °F), a half cycle time of 160 min, and an air flowrate of 40.8 kg/hr (90 lb/hr). The second used a similar approach but with a temperature setpoint of 121 °C (250 °F), a half cycle time of 144 min, and an air flowrate of 45.5 kg/hr (100 lb/hr). The second day/night power-saving mode proved to be most efficient while still meeting the *ISS* carbon dioxide removal system performance specification. The first power-saving operational mode realized a savings of approximately 138 W over the continuous operation mode's 774.5 W. Up to an additional 92 W of power savings were observed for the second power-saving mode. Overall, the 121 °C temperature setpoint and 144-min half cycle time provides a total power savings of approximately 230 W over the continuous operation mode using the 204 °C setpoint and 160-min half cycle. As a result, the 121 °C temperature setpoint and 144-min half cycle was selected for the integrated test. Figures 18 and 19 summarize the CDRA performance for the various baseline runs compared to *ISS* carbon dioxide removal specifications. In figures 18 and 19, baseline run 1 corresponds to operating the CDRA with no power-saving mode, baseline 2 corresponds to the first power-saving mode, and baselines 3A and 3B correspond to the power-saving mode used during the IART. More detailed information summarizing the performance observed during these pretest runs is presented in appendix A.

It was noted during this testing that the 121 °C heater setpoint and 144-min half cycle may not allow recovery from conditions in which the CDRA accumulates large quantities of water in the desiccant beds. Normal water loading can be accommodated; however, recovery from high-water loading that could result from prolonged periods between CDRA operation may require the use of the 204 °C desorption temperature setpoint and 144-min half-cycle time.

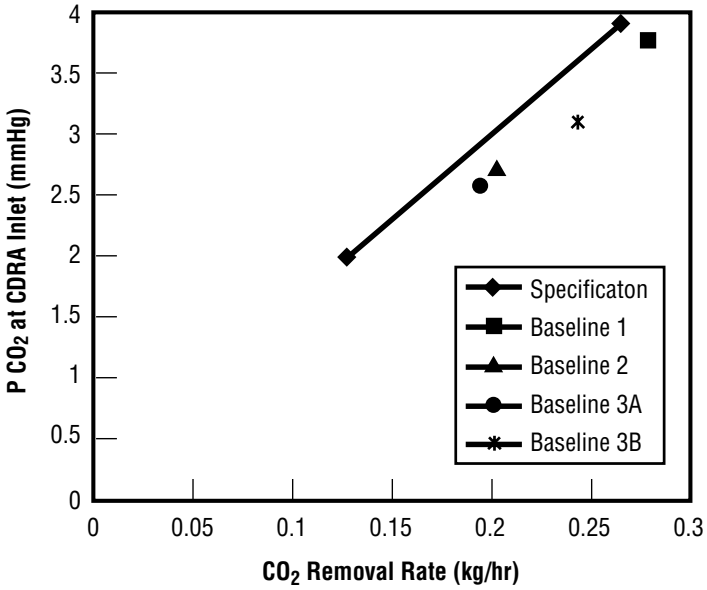

FIGURE 18.—CDRA performance at inlet condition.

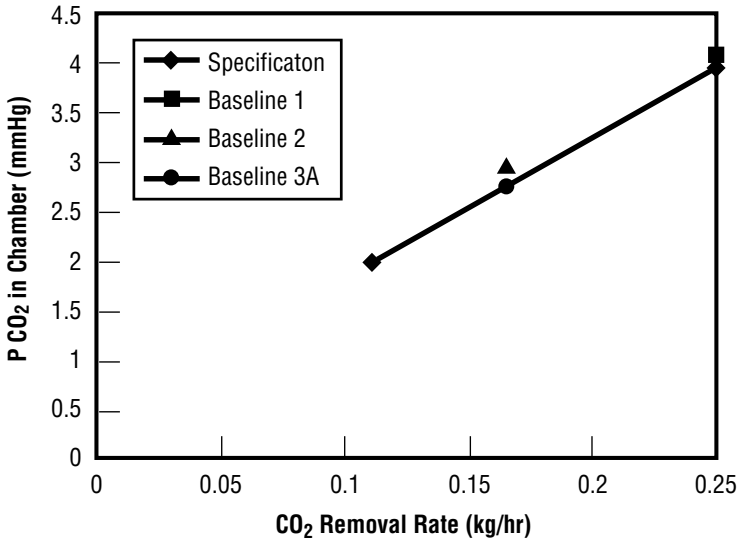

FIGURE 19.—CDRA performance at chamber condition.

Oxygen Generator Assembly

The SFWE OGA was operated independently from June 21, 1995, to November 29, 1995, to determine whether it could produce oxygen at the required rate under *ISS* operating conditions. These conditions included day/night power cycling in which the OGA was placed into a standby mode during the dark portion of the orbital cycle and used feedwater produced by the *ISS* water processor. The new *ISS* nitrogen interface pressure of 620 kPa (90 psia) to 758 kPa (110 psia) was also tested. During the test period, 26 days of testing were accumulated with one period of uninterrupted operation from August 12–18, 1995, and a second period from September 29 to October 14. Command and control signals to change OGA operational modes between day and night cycles were successfully demonstrated, and it was capable of producing oxygen using feedwater obtained from previous *ISS* water processor testing. Also, control signals to change oxygen production rate from 90 to 110 percent of nominal were sent to the OGA via the facility control console. These control tests were a precursor to integrating the OGA with the MCA oxygen partial pressure signal to control the oxygen production rate. At the conclusion of independent testing, problems with the OGA PCA were investigated from November 1995 through January 1996. Before integrated testing began, however, it was determined that the technical problems could not be solved to allow the IART to be conducted in a timely manner. This prevented its participation in the test; however, the majority of the IART test objectives regarding the OGA were satisfactorily addressed during the checkout testing phase.[31]

INTEGRATED TESTING SUMMARY

Integrated testing began on March 12, 1996, and continued until April 18. During this time, a cumulative total of 30 days of operation with two periods of uninterrupted operation were obtained. The first uninterrupted period lasted 7 days (March 22 through 29) while the second period continued for a 12-day duration (March 30 through April 12). An additional 4 days of testing was conducted on the MCA to investigate its response to transient humidity changes in the chamber. All testing was completed on April 18.

Test Condition Summary

Chamber Total Pressure and Temperature

Test chamber total pressure was maintained greater than 0.40 kPa (3 mmHg) above ambient pressure (gauge pressure) and did not exceed 1.6 kPa (12 mmHg) gauge pressure except on March 30 after the metabolic simulation program had malfunctioned. The excess pressure was vented. After this event, the total pressure was maintained within the specified range of 0.40 to 0.93 kPa (3 to 7 mmHg) gauge pressure. The test chamber temperature was maintained between 21 and 22 °C (70 and 72 °F) during the entire test. Figures 20 and 21 show representative total pressure and temperature profiles during the uninterrupted test segments. More extensive data plots may be found in appendix B.

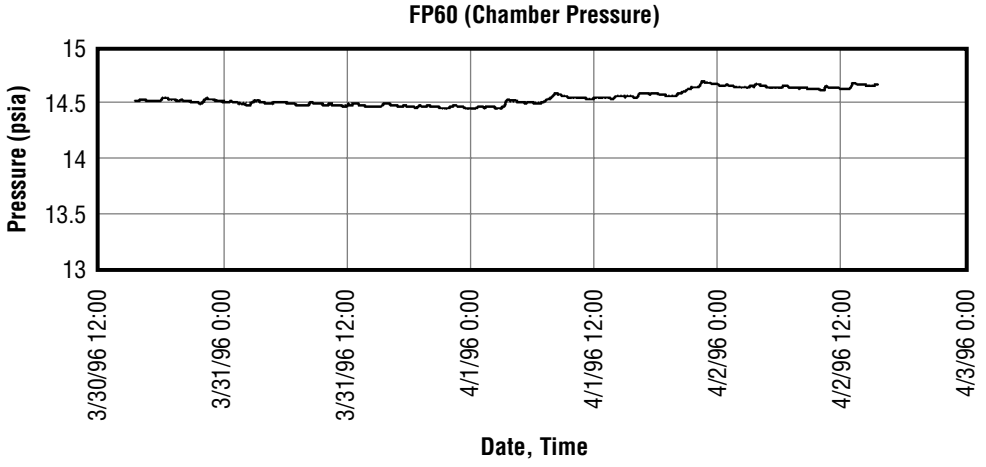

FIGURE 20.—Representative CMS total pressure profile.

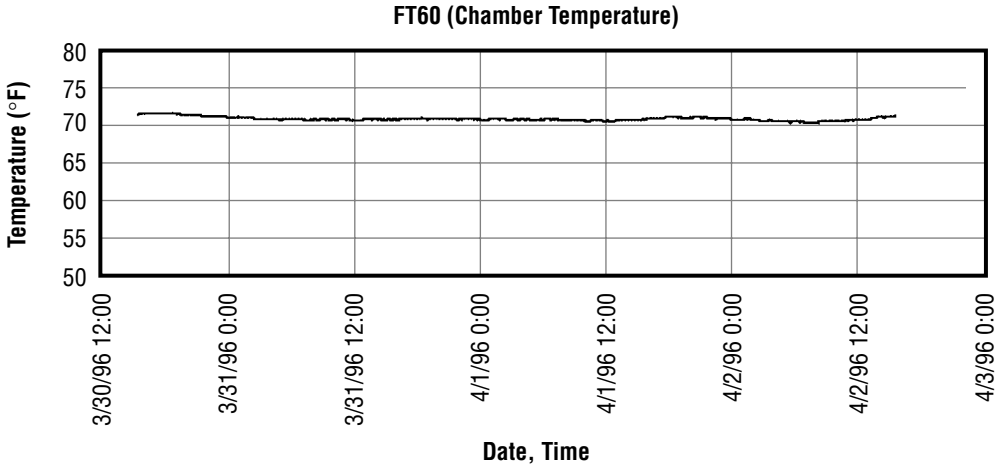

FIGURE 21.—Representative CMS temperature profile.

Chamber Atmospheric Composition

During the entire test, the CMS atmospheric composition was monitored by several means. These included measurements from the MCA, an in-line gas chromatograph (GC), an in-line infrared CDA, and several facility-provided single gas sensors mounted inside the CMS. A comparison of data gathered by the various instruments used during the IART is provided in appendix C.

Because the MCA, GC, and infrared CDA's operated at different sampling frequencies, a complete set of samples was not collected at the same time using all of the instruments. The MCA and GC samples were generally collected within a few minutes of each other because the MCA collected a sample once per minute. Internally mounted oxygen and carbon dioxide monitors recorded gas concentrations every 15 sec. In general, the internally mounted sensor measurements reported are within a few minutes of the time grab samples were taken. Statistical analysis of the data provided in appendix C indicates consistently close atmospheric composition monitoring results as seen by the relatively small standard deviation from the mean. A more detailed discussion of these results is provided as part of the MCA performance summary.

In addition, grab samples were collected for independent laboratory analysis. A summary of these grab sample data is provided in appendix D. Analysis of the grab sample results shows that the CMS atmosphere averaged 78 percent nitrogen, 21.1 percent oxygen, and 0.35 percent carbon dioxide for the IART.

Samples were also collected and analyzed for nitrogen dioxide and ozone. These compounds were monitored because there was concern that they could be produced by the electrical systems (such as electric motors) and the TCCS. Ozone can be produced from arcing when operating electrical systems. Nitrogen dioxide may result from the oxidation of nitrogen in the atmosphere in the TCCS high-temperature oxidizer. Although a previous bench-scale test of the TCCS high-temperature catalyst's ability to oxidize nitrogen in the atmosphere showed no production of nitrogen oxides, a system-level analysis was conducted to confirm the results.[32] As seen in appendix E, the ozone concentration in the CMS was typically comparable to or lower than ambient levels, and no nitrogen dioxide was

produced.[33] This latter result confirmed the results of the earlier study. The methods used to analyze both ozone and nitrogen dioxide had detection limits of 0.05 parts per million (ppm). Results within the CMS were below the detection limit during all samples.

Subassembly Operations Summary

Overall, the ARS operated smoothly with no major subassembly anomalies. Three subassembly anomalies were experienced during the course of the test, with two leading to temporary shutdowns of the CDRA and MCA. Details on these anomalies and their resolution are summarized by reference 33. Summaries for these shutdowns are provided by the following discussion. The TCCS did not experience any anomalies.

The MCA experienced a single shutdown on March 21 due to a high electrical current to its ion pump. This shutdown was traced to a failed delay circuit that was not flight-like and, therefore, not necessary for conducting the test. The circuit was bypassed and the MCA operated with no problems for the remainder of the test.

The CDRA experienced two anomalies. The first occurred on March 21 and caused the unit to shut down. The cause for the shutdown was traced to an airflow selector valve that was not in the proper position. The CDRA was restarted and the problem did not repeat during the remainder of the test. It is thought that a facility power surge or voltage decay may have caused an inadequate current to the valve resulting in its improper positioning. The second anomaly occurred on April 3 when one of the sorbent bed heaters did not receive electrical power for approximately 3 hr. This problem corrected itself and no explanation could be found. The CDRA sorbent beds are to be refurbished following the test, and attention will be given to possible electrical shorts and other potential causes for this problem.

Facility Operations Summary

Facility anomalies accounted for several problems encountered during the test. Details on test problems and their resolution are provided by reference 34. Most facility-related anomalies were minor and were corrected quickly. A summary of the test facility operations is provided by the following discussion.

The first anomaly occurred on March 16 when the facility electrical power failed. This caused the entire test facility to shut down temporarily. Approximately 1.5 hr of processing time were lost before the test could be restarted. The power failure also resulted in CDRA operation to reset to local control. This caused the CDRA to ignore the day/night commands from the host computer. This problem was discovered and corrected on March 20; however, the test days between March 16 and 20 did not meet the IART requirements for day/night cyclic operations.

Facility-provided gas monitors were responsible for several interruptions in the metabolic simulation program. During calibration of the gas chromatograph, communication errors with the host computer caused the metabolic simulation program to shut down. These shutdowns had no impact to the test

other than a brief interruption of the metabolic simulation. The program was quickly restarted in each case. On one occasion, however, this problem caused the water injection tank to completely empty. As a result, the test chamber had to be opened on March 30 to prime the injection pump. This caused an interruption in the consecutive uninterrupted test days; however, it could be argued that entering the chamber was of no greater impact to the test than a pressure relief event since the oxygen and carbon dioxide partial pressure control was not affected.

The test chamber was also opened on March 13 and March 16 to make other repairs to the water injection system. On March 13, the water injection system failed. It was found that a metering valve was set too tightly and became blocked with debris. The valve was opened wider and control parameters were reset. After the facility power failure on March 16, water injection system setpoints for the injection tank scale had to be reset. The test chamber was entered to reset the scale setpoints and connect it to an uninterruptable power supply to prevent a recurrence. In both instances, oxygen and carbon dioxide partial pressure control was not affected.

The final test facility anomaly occurred on April 8 when the daily rate of oxygen injection into the chamber began to decline from its normal 3 to 4 kg/day (7 to 9 lb/day) to 0.7 kg/day (1.5 lb/day). At the same time, the nitrogen injection rate increased. Analysis of the test data indicated that total pressure control had lost its assist from the oxygen injection system. A possible cause for this was oxygen removal subassembly failure. The gas removal rate for the oxygen removal subassembly did not change; however, an analysis of the gas composition from the subassembly showed a composition of 73.6-percent nitrogen and 25.1-percent oxygen. The normal outlet gas composition for this device is 99-percent oxygen and 1-percent nitrogen; therefore, it was confirmed that the unit had failed. Since the oxygen removal unit failure occurred near the end of the test and it did not affect the operations of the MCA, the test was not shut down to repair it.

Overall Test Operations Assessment

The IART had the fewest problems of any integrated test conducted. With very few exceptions, the test facility operated flawlessly, allowing a very accurate assessment of the integrated USL ARS and atmosphere control and supply (ACS) functions under automated control. Day/night cyclic operations for both the CDRA and OGA were demonstrated during the course of independent subassembly and integrated subsystem testing.

DISCUSSION OF RESULTS

CDRA Performance Results

The CDRA operated during the test with only the two previously mentioned anomalies. The first involved a valve position error, while the second was a loss of power to a carbon dioxide adsorbent bed heater. As noted earlier, these anomalies were short-lived and did not recur. During the test, the partial pressure of carbon dioxide within the chamber was maintained between 333.3 and 400 Pa (2.5 and 3 mmHg). This was well below the *ISS* maximum allowable of 706.6 Pa (5.3 mmHg).

Since very little variation in the chamber carbon dioxide partial pressure was experienced, 3 days of CDRA operations were analyzed to assess its performance. Twenty-four-hr periods on March 14–15, March 27, and April 11 were considered to investigate performance early in the test, midway through the test, and at the end of the test, respectively. Tables 7, 8, and 9 summarize the conditions under which the CDRA was operating during these three periods and how closely they comply with *ISS* CDRA design specifications. As can be seen by examining the test conditions, very little change was observed and good agreement with *ISS* design specifications was obtained. Coolant water flowrate experienced the highest deviation; however, the CDRA precooler design is not highly sensitive to flowrate. The coolant temperature was maintained very well, but was near the upper range of acceptability. The CDRA performance is more sensitive to this temperature and the test results were, therefore, obtained under a worst-case condition for coolant temperature.

Average power required by the CDRA ranged from a high of 550.09 W to a low of 532.12 W, with an average of 540.6 W for the three periods assessed. This compares with the observed 544.2 W from pretesting. Compared to the 774.5 W required for the continuous operation baseline with no day/night power cycling, the observed test results represent a savings of approximately 203.9 W.

Carbon dioxide removal rate was assessed at both the CDRA inlet and chamber-level conditions. Performance based upon the CDRA inlet conditions exceeded the *ISS* specification requirements at the three periods for which data were analyzed, as shown by figure 22. An average of 0.198 kg/hr (0.437 lb/hr) at an average CDRA inlet concentration of 349.8 Pa (2.624 mmHg) was observed. Performance based upon module-level conditions was very close to the *ISS* requirement, as shown by figure 23. At the module level, the CDRA removed an average of 0.166 kg/hr (0.365 lb/hr) of carbon dioxide at an average chamber partial pressure of 371.7 Pa (2.788 mmHg). Since the chamber conditions were maintained with very little fluctuation during the remainder of the test, it can be concluded that the CDRA's performance consistently met or exceeded *ISS* requirements. Supporting data on the CDRA's performance during these three periods is provided in appendix F.

As noted during CDRA baseline testing, concern existed with respect to possible desiccant bed breakthrough by water vapor. Because the carbon dioxide bed regeneration temperature was significantly lower than any previously tested and the day/night power cycling could result in incomplete

desiccant bed regeneration, possible water vapor breakthrough and subsequent sorbent bed poisoning was anticipated. Although significant sorbent bed poisoning was not indicated by a decrease in carbon dioxide removal efficiency (it actually increased), the increasing water breakthrough in desiccant beds 1 and 2 was observed as the test progressed. Although these figures show data for a single half-cycle, the trends and magnitudes are representative for the indicated time periods.

As the test progressed, it was observed that the baseline outlet dewpoint increased by a magnitude of 2.2 to 2.8 °C (4 to 5 °F). The exact baseline dewpoint could not be determined because of a small leak in the CDRA that was discovered at the conclusion of the test. Although the leak did not affect overall performance, it is possible that the baseline dewpoint measurement could have been affected slightly. Therefore, its actual magnitude could not be accurately determined. Even with this small leak, the accompanying occurrence of progressively greater water breakthrough establishes that water retention gradually increased with the lower heater setpoint temperature of 121 °C (250 °F). For this reason, it is desirable to retain the capability for sorbent bed regeneration at 204 °C (400 °F) as a means to periodically regenerate the beds more completely.

TABLE 7.—*CDRA operating conditions early during integrated testing.*

IART Early Phase

Start Time:	06:00	Start Date:	03/14/96
End Time:	06:00	End Date:	03/15/96

Purpose:

Verify that the "power-save" operation of the CDRA with metabolic simulation and day/night operation will provide greater than the *ISS* required level of performance. This testing will determine if the CDRA satisfies the second part (day/night cycle heater operation) of par. 3.2.1.1 of the *ISS* CDRA Envelope Drawing (683–10009, Rev. G)

Operation:

			Power Usage	Average	Peak
Mode:	Day/Night		Total	**550**	1,768 W
Half Cycle:	144 min		Heaters	403	983 W
Heater Setting:	225–260 °F		Blower	108	111 W
Heater Power:	480 W	Primary	Vacuum Pump	39	417 W
	480 W	Secondary			

Using the *ISS* CDRA Envelope Drawing (683–10009, Rev. G):

Air Inlet Conditions

	Range	Target	Actual		Error (%)	Reference
			Raw Data	Calibrated		
Temperature	40 to 50 °F	50	50.65		1.3	Table II, sh 15
Dewpoint	40 to 50 °F	50	49.27		–1.5	Table II, sh 15
Inlet $ppCO_2$	0.4 to 0.5%	#N/A	0.528	0.355	#N/A	Fig. 3, sh 17
Flow Rate	22.2 ft^3/min	22.2	21.99		–1.0	N/A

Precooler Coolant Water

	Range	Target	Actual	Error (%)	Reference
Temperature	38 to 42 °F	42	42.31	0.7	Par. 3.2.1.5, sh 18
Flowrate	0.5 to 0.54 gal/min	0.5	0.6536	30.7	Par. 3.2.1.5, sh 18

CO_2 Removal Calculations (Bold type denotes data points plotted in figs. 22 and 23.)

	Range	Target	Actual		Error (%)	Reference
			Raw Data	Calibrated		
Calculated From Inlet and Outlet to 4BMS:						
Inlet $ppCO_2$	2 to 4 mmHg	#N/A	3.989	**2.685**	#N/A	Fig. 3, sh 17
CO_2 Removal	0.28 to 0.58 lb/hr	0.389		**0.428**	**10.1**	Fig. 3, sh 17
Efficiency				81.5%		
Calculated With CO_2 Injection and Module CO_2 Level:						
Module $ppCO_2$	2 to 4 mmHg	2.761	3.21	**2.840**	**–2.8**	Lab PID fig. 65, p. 100
CO_2 Injection	0.28 to 0.58 lb/hr	0.367		**0.365**	–0.6	Lab PID fig. 65, p. 100

Period Used for Calculations

From	6.02	to	29.98 hr	Starting on Julian Day	74
Total Time of	24.00 hr	or	1,440 min		

TABLE 8.—*CDRA operating conditions midway through integrated testing.*

IART Mid-Test Phase

Start Time:	00:00	Start Date:	03/27/96
End Time:	24:00	End Date:	03/27/96

Purpose:

Verify that the "power-save" operation of the CDRA with metabolic simulation and day/night operation will provide greater than the *ISS* required level of performance. This testing will determine if the CDRA satisfies the second part (day/night cycle heater operation) of par. 3.2.1.1 of the *ISS* CDRA Envelope Drawing (683–10009, Rev. G)

Operation:

			Power Usage	**Average**	**Peak**
Mode:	Day/Night		Total	**532**	1,689 W
Half Cycle:	144 min		Heaters	387	975 W
Heater Setting:	225–260 °F		Blower	109	113 W
Heater Power:	480 W	Primary	Vacuum Pump	36	415 W
	480 W	Secondary			

Using the *ISS* CDRA Envelope Drawing (683–10009, Rev. G):

Air Inlet Conditions

	Range	**Target**	**Actual**		**Error (%)**	**Reference**
			Raw Data	**Calibrated**		
Temperature	40 to 50 °F	50	51.60		3.2	Table II, sh 15
Dewpoint	40 to 50 °F	50	50.05		0.1	Table II, sh 15
Inlet $ppCO_2$	0.4 to 0.5%	#N/A	0.509	0.338	#N/A	Fig. 3, sh 17
Flowrate	22.2 ft^3/min	22.2	21.93		–1.2	N/A

Precooler Coolant Water

	Range	**Target**	**Actual**	**Error (%)**	**Reference**
Temperature	38 to 42 °F	42	43.27	3.0	Par. 3.2.1.5, sh 18
Flowrate	0.5 to 0.54 gal/min	0.5	0.5612	12.2	Par. 3.2.1.5, sh 18

CO_2 Removal Calculations (Bold type denotes data points plotted in figs. 22 and 23.)

	Range	Target	Actual		Error (%)	Reference
			Raw Data	Calibrated		
Calculated From Inlet and Outlet to 4BMS:						
Inlet $ppCO_2$	2 to 4 mmHg	#N/A	3.874	**2.567**	#N/A	Fig. 3, sh 17
CO_2 Removal	0.28 to 0.58 lb/hr	0.371		**0.435**	**17.3**	Fig. 3, sh 17
Efficiency				86.6%		
Calculated With CO_2 Injection and Module CO_2 Level:						
Module $ppCO_2$	2 to 4 mmHg	2.762	3.09	**2.746**	**0.6**	LAB PID fig. 65, pg 100
CO_2 Injection	0.28 to 0.58 lb/hr	0.367		**0.365**	–0.5	LAB PID fig. 65, pg 100

Period Used for Calculations

From	0.02	to	23.98 hr	Starting on Julian Day	87
Total time of	24.00 hr	or	1,440 min		

TABLE 9.—*CDRA operating conditions at the end of integrated testing.*

IART Late Test Phase Start Time: 0:00 Start Date: 04/11/96
End Time: 24:00 End Date: 04/12/96

Purpose:

Verify that the "power-save" operation of the CDRA with metabolic simulation and day/night operation will provide greater than the *ISS* required level of performance. This testing will determine if the CDRA satisfies the second part (day/night cycle heater operation) of par. 3.2.1.1 of the *ISS* CDRA Envelope Drawing (683–10009, Rev. G)

Operation:

			Power Usage	Average	Peak
Mode:	Day/Night		Total	**539**	1,315 W
Half Cycle:	144 min		Heaters	396	985 W
Heater Setting:	225–260 °F		Blower	107	111 W
Heater Power:	480 W	Primary	Vacuum Pump	36	393 W
	480 W	Secondary			

Using the *ISS* CDRA Envelope Drawing (683–10009, Rev. G):

Air Inlet Conditions

	Range	Target	Actual		Error (%)	Reference
			Raw Data	Calibrated		
Temperature	40 to 50 °F	50	52.34		4.7	Table II, sh 15
Dewpoint	40 to 50 °F	50	50.42		0.8	Table II, sh 15
Inlet $ppCO_2$	0.4 to 0.5%	#N/A	0.510	0.346	#N/A	Fig. 3, sh 17
Flowrate	22.2 ft^3/min	22.2	21.62		–2.6	N/A

Precooler Coolant Water

	Range	Target	Actual	Error (%)	Reference
Temperature	38 to 42 °F	42	43.12	2.7	Par. 3.2.1.5, sh 18
Flowrate	0.5 to 0.54 gal/min	0.5	0.4947	–1.1	Par. 3.2.1.5, sh 18

CO_2 Removal Calculations (Bold type denotes data points plotted in figs. 22 and 23.)

	Range	Target	Actual		Error (%)	Reference
			Raw Data	Calibrated		
Calculated From Inlet and Outlet to 4BMS:						
Inlet $ppCO_2$	2 to 4 mmHg	#N/A	3.858	**2.620**	#N/A	Fig. 3, sh 17
CO_2 Removal	0.28 to 0.58 lb/hr	0.379		**0.448**	**18.2**	Fig. 3, sh 17
Efficiency				88.0%		
Calculated With CO_2 Injection and Module CO_2 Level:						
Module $ppCO_2$	2 to 4 mmHg	2.761	3.11	**2.777**	**–0.6**	Lab PID fig. 65, p. 100
CO_2 Injection	0.28 to 0.58 lb/hr	0.367		**0.364**	–0.6	Lab PID fig. 65, p. 100

Period Used for Calculations

From	0.02	to	23.98 hr	Starting on Julian Day	102
Total time of	24.00 hr	or	1,440 min		

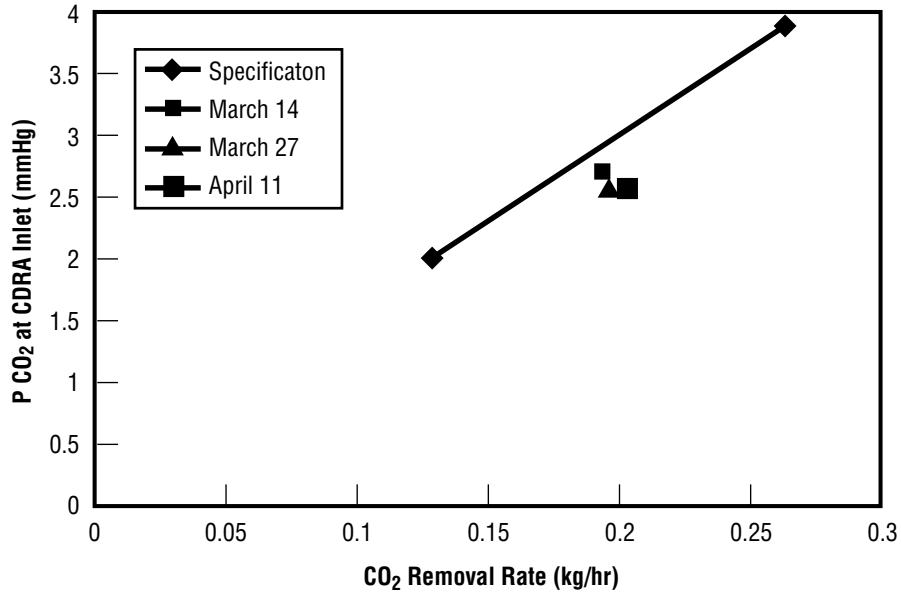

FIGURE 22.—CDRA performance relative to inlet specification.

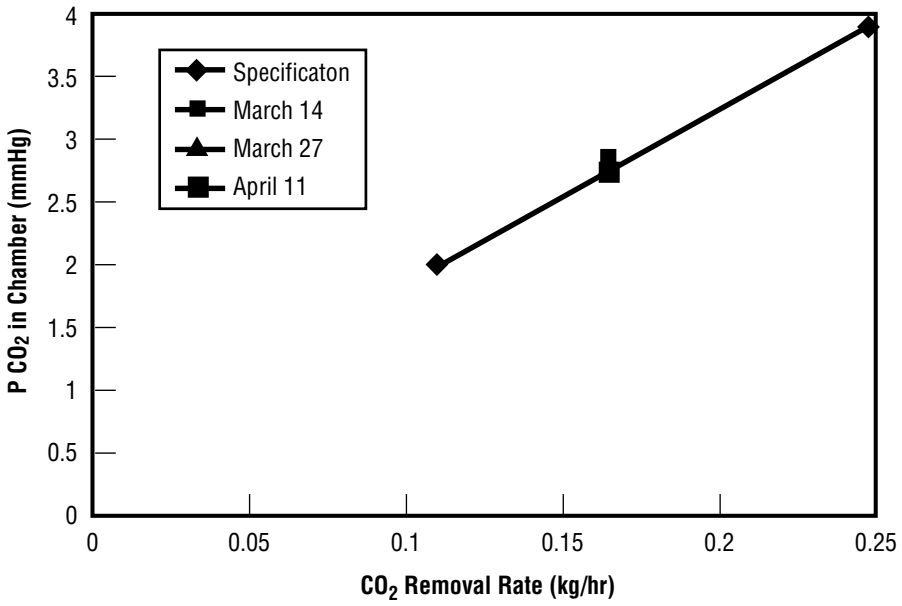

FIGURE 23.—CDRA performance with respect to module specification.

As noted above, despite increased water breakthrough, the carbon dioxide removal efficiency increased over the test, from 81.5 to 86.6 to 88 percent on March 14, March 27, and April 11, respectively. A possible cause is that increased water saturation decreases carbon dioxide adsorption capacity of the desiccant beds. Any carbon dioxide stored on the desiccant beds is returned to the cabin on the subsequent cycle, decreasing overall efficiency. Since the carbon dioxide sorbent beds are not saturated with carbon dioxide for this mode of operation, the small amount of water passing through the desiccant beds during this test did not affect overall performance. However, if this test had continued, desiccant breakthrough would likely continue to increase, and the carbon dioxide sorbent bed water poisoning

would eventually adversely affect overall performance. Based on the reasoning above, an ideal cycle might allow a very slight water breakthrough without a progressive increase in the desiccant bed water retention. High-temperature regeneration would still be required for periodic dryout of the carbon dioxide sorbent bed.

MCA Performance Results

The MCA performed nominally throughout the entire test, with the only exception being the shutdown experienced on March 21 due to a high electrical current to the ion pump. As previously related, this shutdown was traced to a failed delay circuit that was not flight-like and, therefore, not necessary for conducting the test. The circuit was bypassed and the MCA operated with no problems for the remainder of the test.

The MCA performance was verified by comparison to other in-line instruments mounted both inside and outside the test chamber. Periodic grab samples were also analyzed off-line by the Boeing Analytical Services laboratory. Overall results of these analyses are summarized in the following discussion, and a tabular comparison of results from the different analytical methods for each individual gas is provided by appendix C. Overall the MCA readings correlated very well with those from all of the other sensors. The low standard deviation for the readings from all the sensors used indicate a high degree of accuracy and measurement reliability during the test.

CMS Oxygen Partial Pressure Monitoring and Control

The oxygen partial pressure was monitored by the MCA, an in-line GC, daily grab samples, and an internally mounted dumbbell-type paramagnetic oxygen monitor. Chamber oxygen levels averaged 20.6 percent from all sources of data, with a standard deviation of 0.64. A comparative listing of oxygen analytical results is provided in appendix C. Figure 24 compares the MCA oxygen composition reading to that from the in-line paramagnetic monitor. It was observed that the MCA tracks the trends from the in-line monitor very well.

Real-time assessment of the response of the various sensors for oxygen is provided by figure 25. In this figure, the MCA output converted to percent is compared with the response of the facility oxygen sensor and discrete data points obtained via the on-line GC. The data tabulated in appendix C were taken from readings from all three instruments at the time GC measurements were made. As seen by figures 24 and 25, the MCA output has considerable scatter but tracks the atmospheric composition trends very well. MCA results were typically lower than those obtained via the GC but much closer to those obtained from the facility sensor. The median oxygen percentage for the results shown by figure 25 are 20.78, 20.59, and 21.29 percent for the facility sensor, MCA, and on-line GC, respectively.

Oxygen was controlled to an average partial pressure of 20.6 kPa (3 psia or 155 mmHg). Peaks in oxygen partial pressure were observed during every injection sequence as shown by figure 26. Likewise, decreases in partial pressure were observed as a function of the metabolic oxygen consumption profile. As shown by figure 27, the rate of oxygen partial pressure decrease is most steep during the high metabolic loading period and less severe during the lowest loading period, as would be expected. The stable system response shown by figure 24 demonstrated that using the MCA oxygen partial pressure

signal for maintaining control works very well. Similar results provided by appendix G were obtained during the entire test.

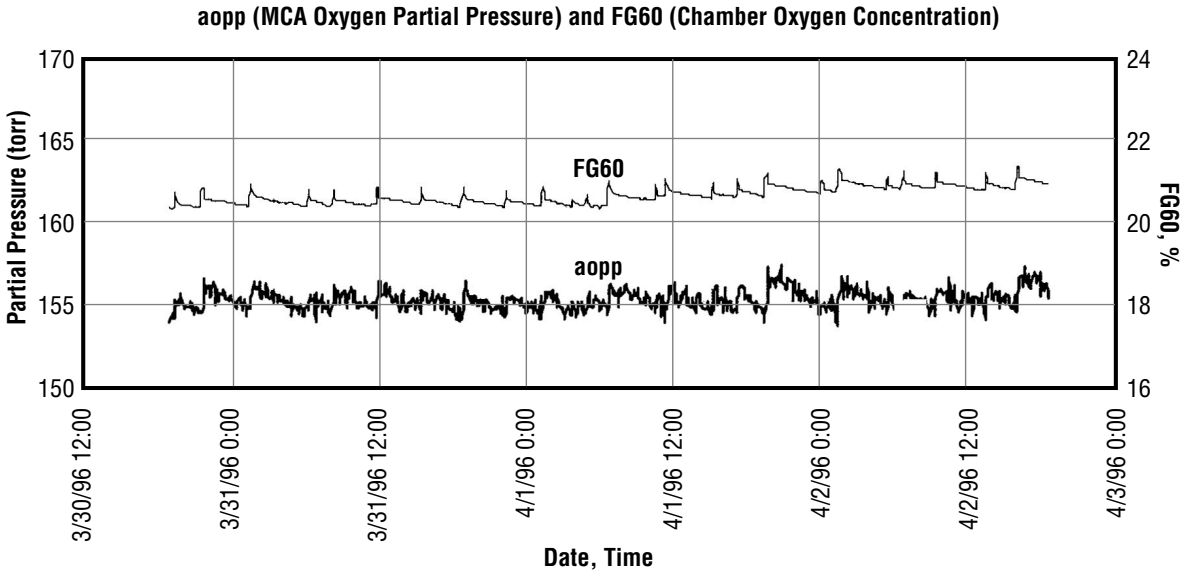

FIGURE 24.—Typical MCA oxygen partial pressure response.

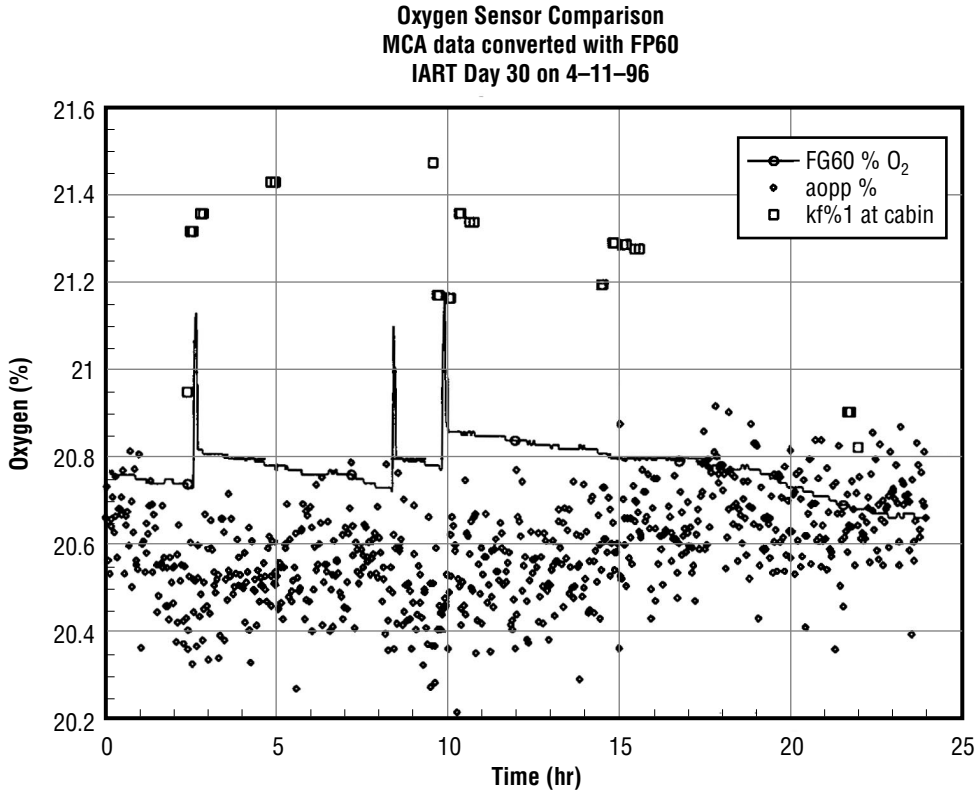

FIGURE 25.—IART oxygen sensor comparison.

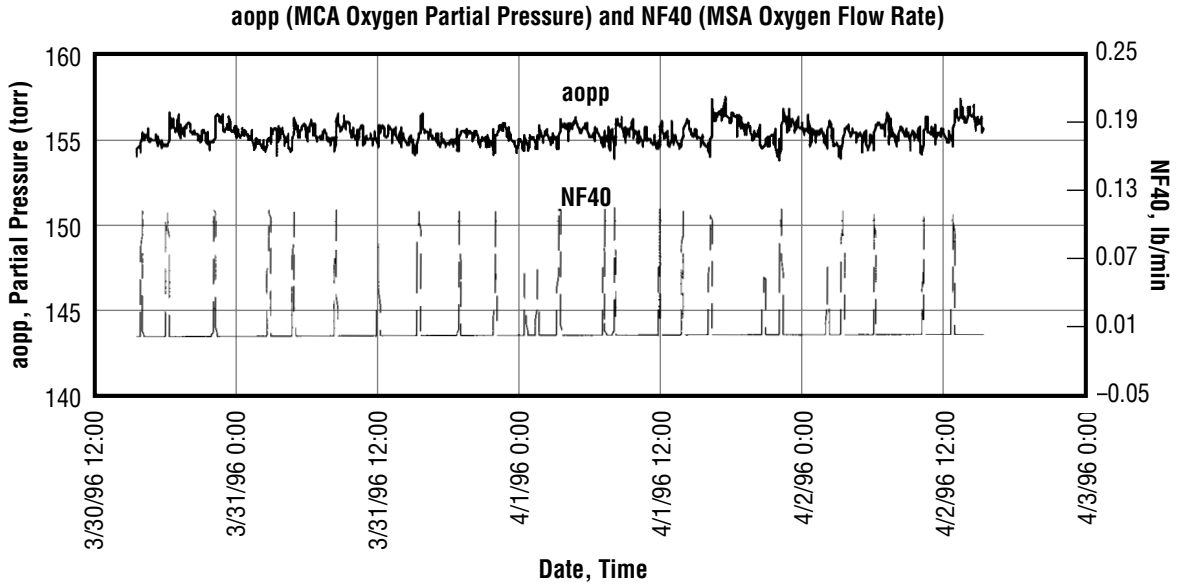

FIGURE 26.—Effects of oxygen injection on CMS oxygen partial pressure.

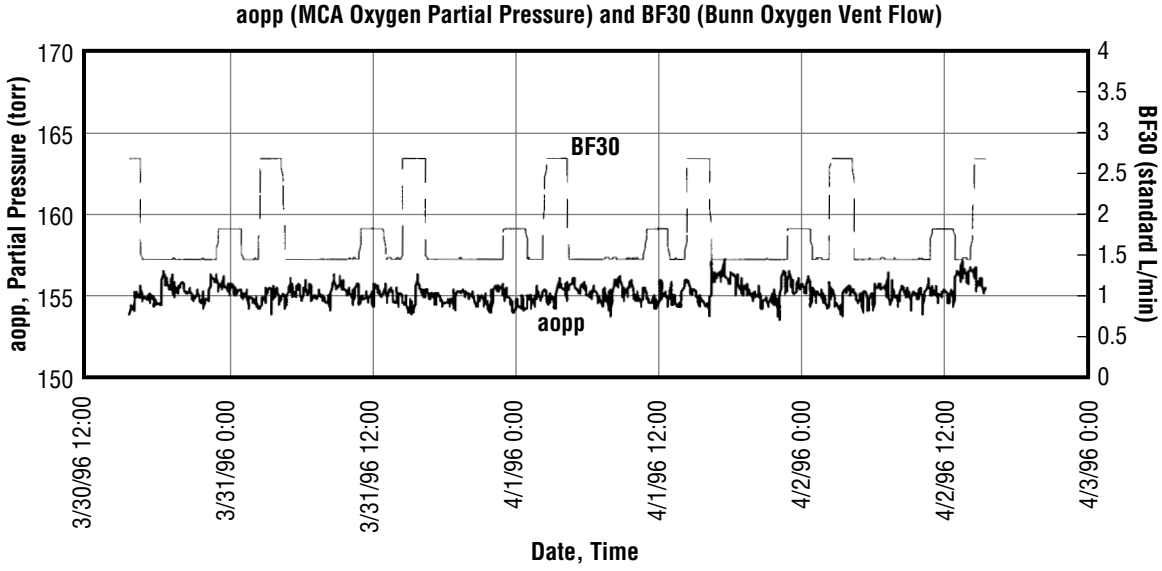

FIGURE 27.—Effects of metabolic consumption on CMS oxygen partial pressure.

CMS Nitrogen Partial Pressure Monitoring and Control

The nitrogen level in the test chamber was analyzed by the MCA, the in-line GC, and daily grab samples. The average nitrogen concentration from the three different analyzers was 78.7 percent, with a standard deviation of 1.9. A comparative listing of these results is provided in appendix C.

Nitrogen partial pressure control was provided by periodic injection. This injection also affected the chamber total pressure. An example of these effects is provided by figure 28. The total nitrogen

partial pressure and chamber total pressure were also affected by oxygen injection. By comparing figure 28 with figure 26, it can be seen that the total pressure peaks correspond directly to oxygen injection events; therefore, the oxygen injection tended to produce the most dynamic variability in chamber atmospheric composition and total pressure over time. Similar results were observed throughout the test as can be seen by data plots provided in appendix H.

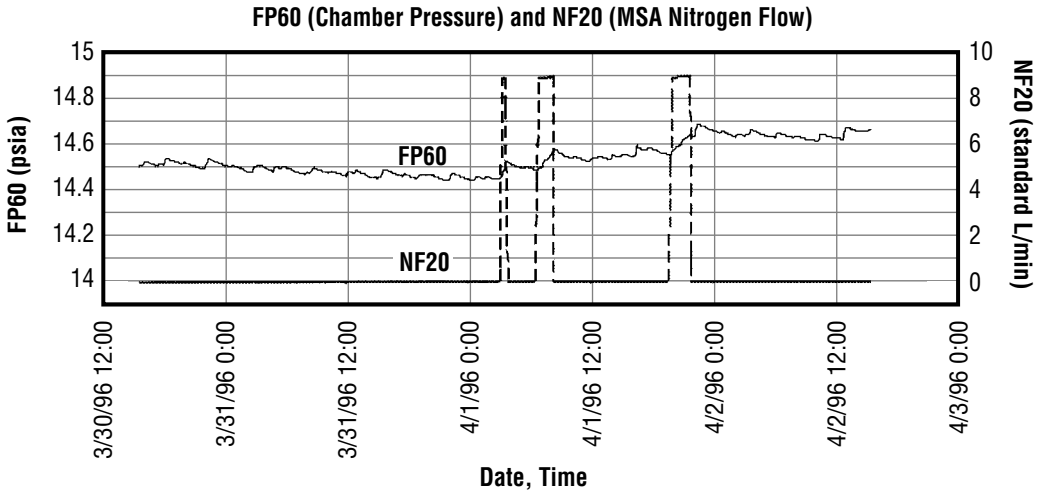

FIGURE 28.—Effects of nitrogen injection on CMS total pressure.

CMS Carbon Dioxide Partial Pressure Monitoring.

Overall, the CMS carbon dioxide response was stable, as seen by figure 29. This allowed a comparison between carbon dioxide sensors to be made with good reliability. The MCA carbon dioxide response was very similar to that of the internally mounted nondispersive infrared sensor and tracked chamber profiles well. As can be seen by figure 30, the chamber carbon dioxide partial pressure was sensitive to the metabolic input. However, little variability was observed as a result of the day/night cycle and CDRA operating mode as shown by figures 31 and 32, respectively. Similar results were observed for the entire test for carbon dioxide partial pressure. Additional data plots for the CMS carbon dioxide response and effects of metabolic simulation on carbon dioxide partial pressure are provided in appendix I.

Since carbon dioxide level is a significant design factor for *ISS* ECLSS performance, its level was monitored by several instruments. Some of these instruments had been installed to gather more detailed data for improved CDRA modeling and performance enhancement studies, but since they were currently available they were utilized in this testing also. The carbon dioxide was monitored by the MCA, the in-line GC, daily grab samples, internally mounted nondispersive infrared carbon dioxide monitors, and the external Horiba carbon dioxide analyzer. Results of analyses conducted by each method are tabulated in appendix C. These results reflect readings taken at various times during the test very close to the time that in-line GC measurements were taken. The average value for carbon dioxide from all analyzers for these tabulated values was 0.37 percent, with a standard deviation of 0.03. Carbon dioxide levels reported by the internally mounted monitor were almost always the highest value, with an individual sensor average of 0.41 percent.

A real-time comparison of carbon dioxide results for the MCA, two facility-provided sensors, and the in-line GC is provided by figure 33. These results are normalized around facility sensor FG69 as shown by figure 34. As seen by these results, the tabular listing of appendix C is confirmed. The MCA results were consistently lower than those obtained from the on-line GC and facility-provided sensors. Median values for the real-time data presented by figure 33 are 0.33, 0.40, 0.36, and 0.39 percent for the MCA, FG61 facility sensor, FG69 facility sensor, and in-line GC, respectively.

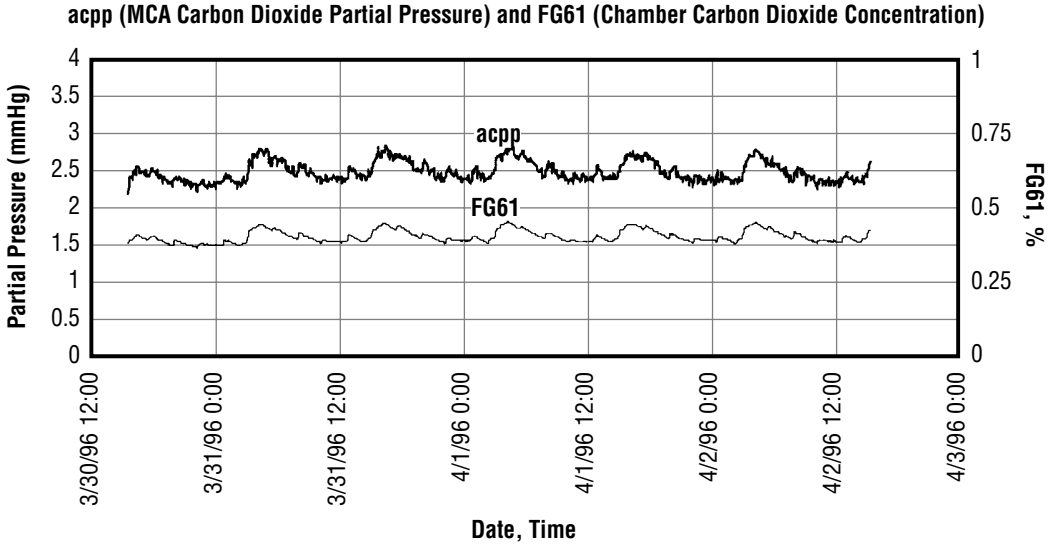

FIGURE 29.—Typical MCA carbon dioxide partial pressure response.

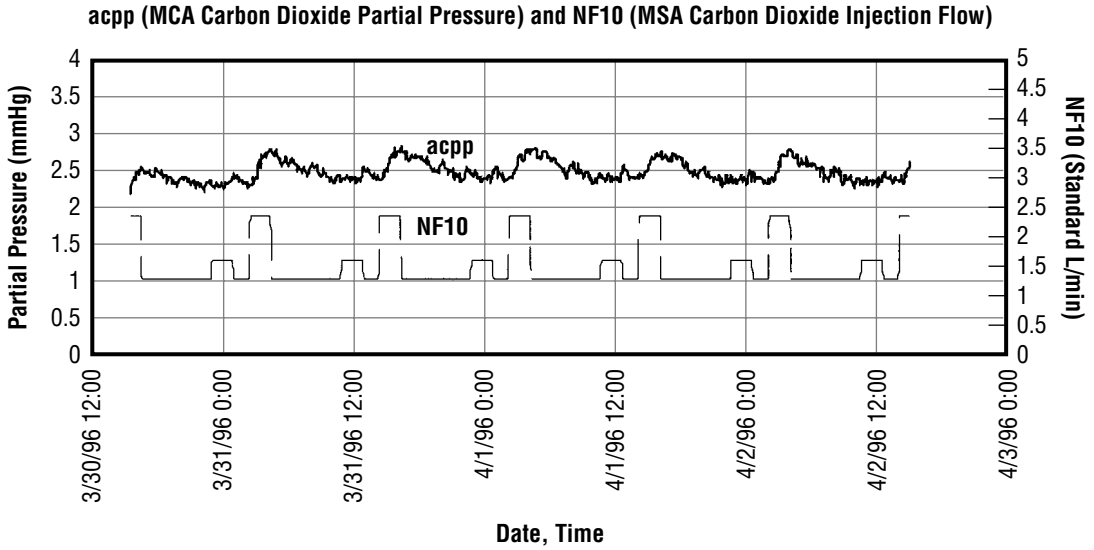

FIGURE 30.—Effects of metabolic input on CMS carbon dioxide partial pressure.

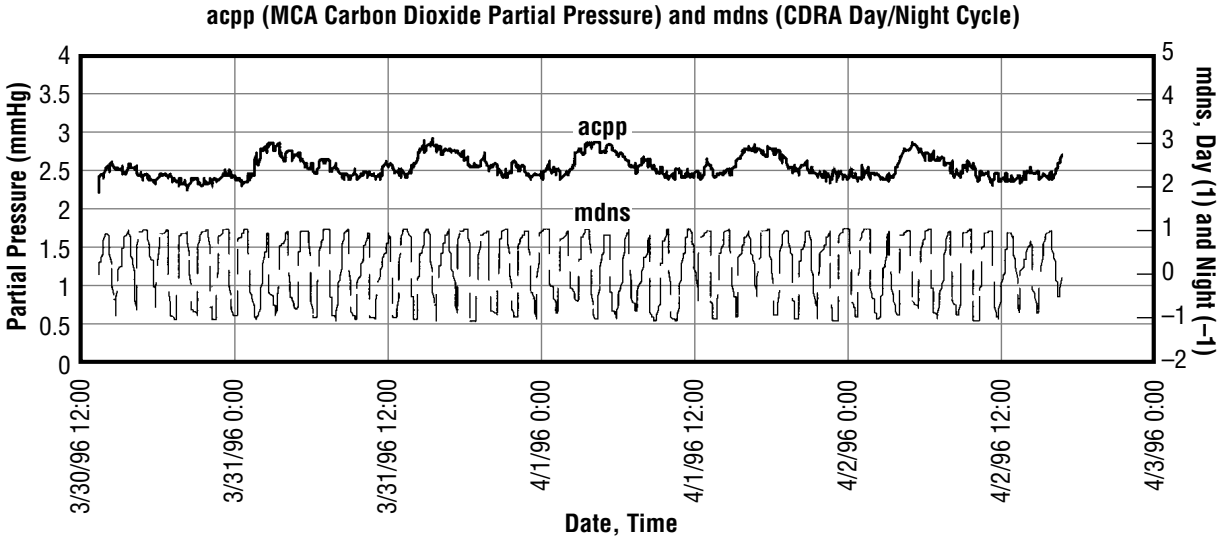

FIGURE 31.—Effects of day/night CDRA cycling on CMS carbon dioxide partial pressure.

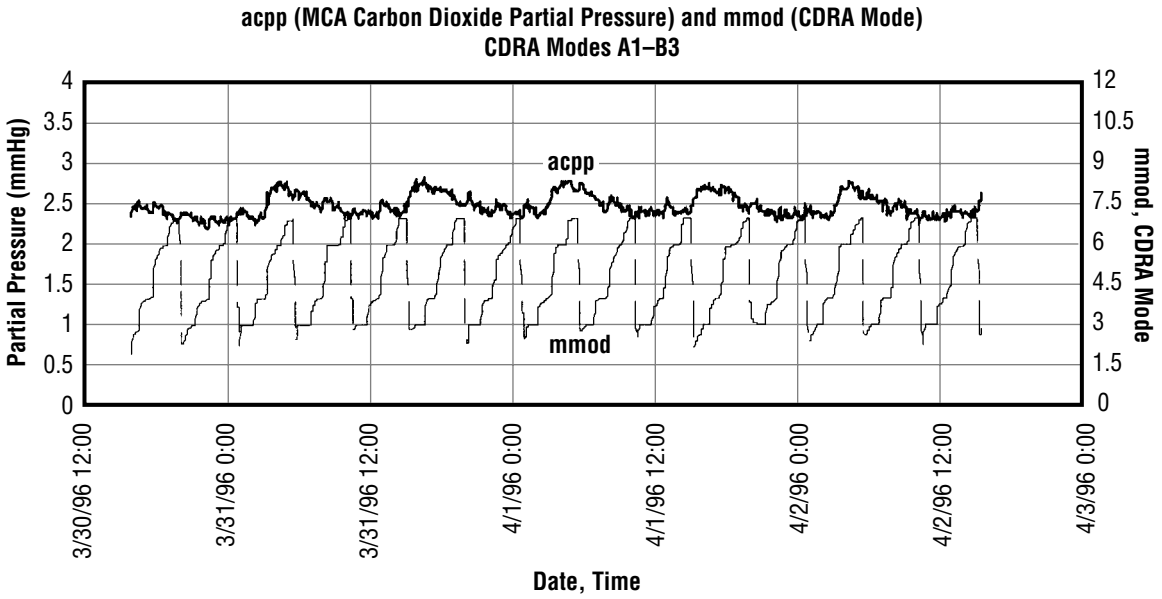

FIGURE 32.—Effects of CDRA operational mode on CMS carbon dioxide partial pressure.

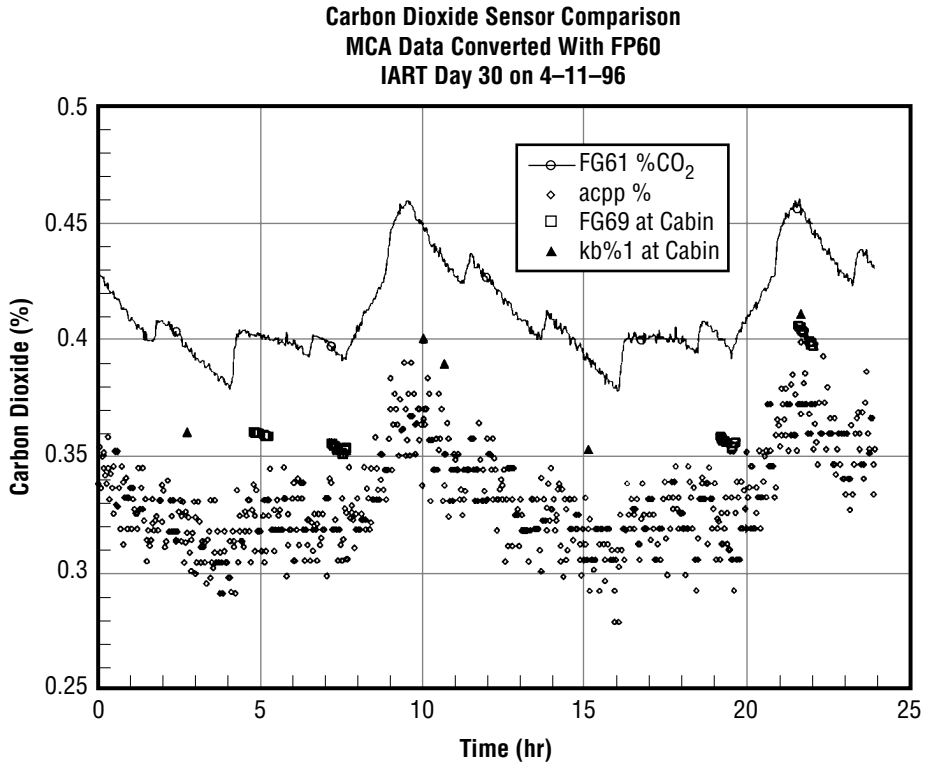

FIGURE 33.—IART carbon dioxide sensor comparison.

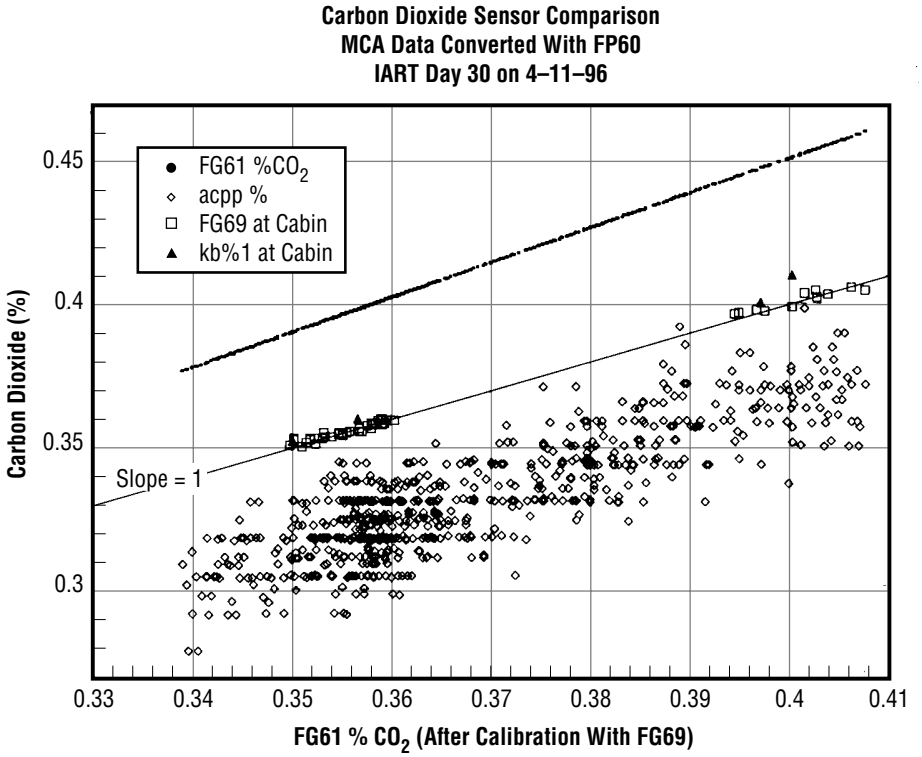

FIGURE 34.—Normalized IART carbon dioxide sensor comparison.

CMS Water Vapor Monitoring

Water vapor was analyzed by the MCA, the in-line GC, and by dewpoint sensors located in the test chamber and at various points in the SDS lines. Only the MCA and GC data were correlated since the dewpoint sensors actually measure in terms of dewpoints, not percentages as do the MCA and GC. A comparative listing of MCA and GC water vapor measurements is provided in appendix C. The average water vapor concentration for both of these instruments was 1.24 percent, with a standard deviation of 0.21. However, it should be noted that water vapor concentrations varied throughout the test based on metabolic simulation loads. This variation was increased during the off-nominal humidity test that followed the initial IART to demonstrate the quickness of the MCA response to off-nominal conditions.

Since the chamber response to water vapor loading was shown to be stable throughout the test, further real-time comparison of water vapor results from the MCA, GC, and a facility-provided dewpoint sensor was possible. Figure 35 shows this comparison with all readings converted to dewpoint. In this comparison, the MCA and in-line GC results agree very well, while the facility-provided sensor has an offset of about 1.1 °C (34.98 °F). The median dewpoint responses for the instruments compared during this 24-hr period are 11.13 °C (52.03 °F), 11.36 °C (52.44 °F), and 9.84 °C (49.71 °F) for the MCA, in-line GC, and facility dewpoint sensor, respectively.

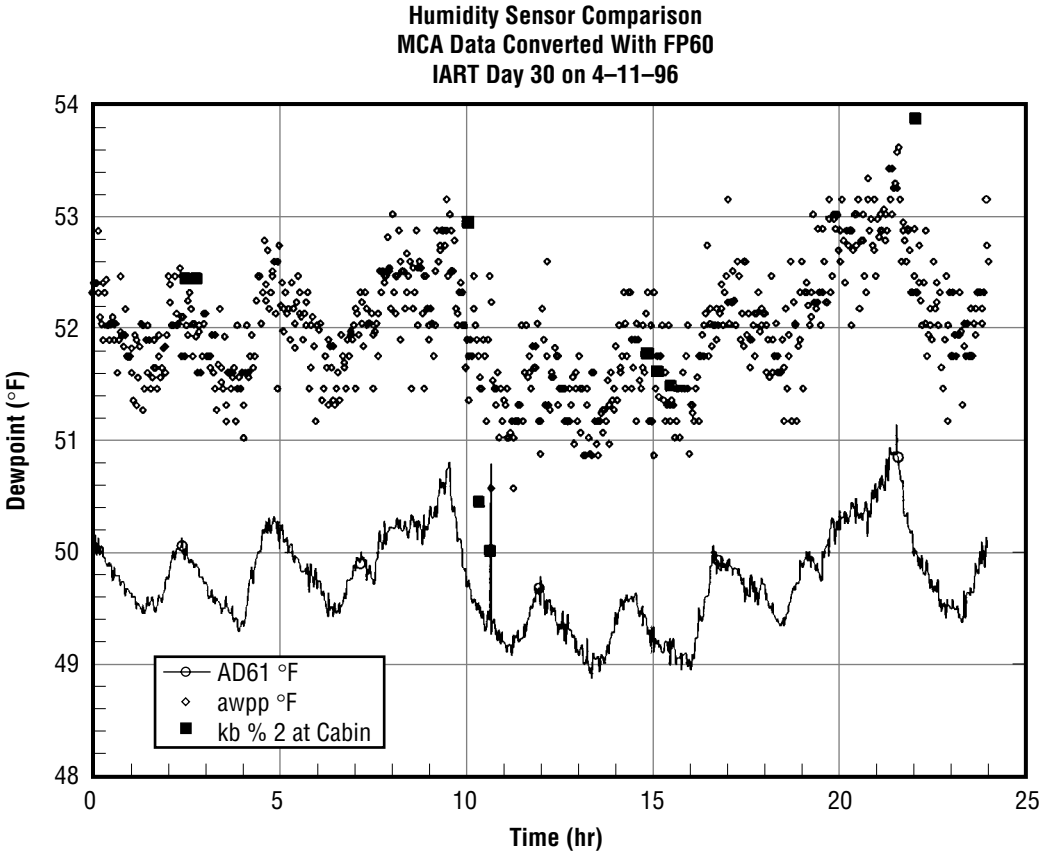

FIGURE 35.—IART water vapor sensor comparison.

Effects of Sample Delivery System on MCA Water Vapor Measurement

The investigation of SDS line lengths was conducted in two parts. First, the water reading was monitored during the nominal part of the test. Sample line lengths were changed at strategic times during that portion of the testing. Second, follow-on testing was conducted to monitor the cabin humidity as it was varied among the extremes possible in the test-bed.

According to every aspect of *ISS* operations that was simulated, the SDS does not have an appreciable effect on the accuracy of the water vapor measurement. During the nominal portion of the test, the sample line length was varied among the four possible configurations. In each of these settings, the MCA reading tracked exactly what was happening inside the module, whether it was the injection of metabolic water, the regeneration of the CDRA desiccant beds, or a combination of both. Any lag in the readings was only a matter of seconds.

A systematic effect on the dewpoint measurements made at various points in the SDS was observed. The measured dewpoint was perceived to decrease slightly as the sample flowed through the SDS. This effect, illustrated by figure 36, was fully systematic in origin and resulted from the pressure dependence of the dewpoint measurement. Since a pressure drop was experienced as the sample was pumped through the line, a corresponding perceived decrease in dewpoint was observed. The MCA, however, does not measure dewpoint, but the volume percentage of water. This effect can be compensated for by adjusting the MCA water reading to match the actual cabin pressure. The calculated dewpoint from the MCA partial pressure reading and cabin pressure consistently agreed with cabin dewpoint measurements. Appropriate pressure adjustments also reduced the perceived discrepancies in the SDS dewpoint readings to within instrument accuracy ranges.

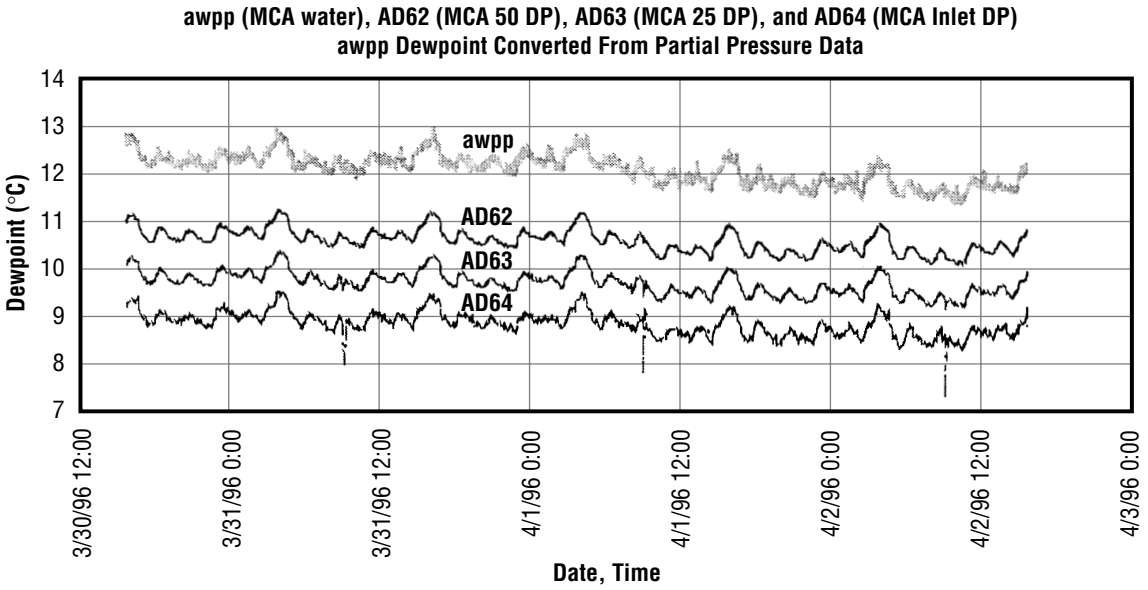

FIGURE 36.—Effects of sample line length on dewpoint measurements.

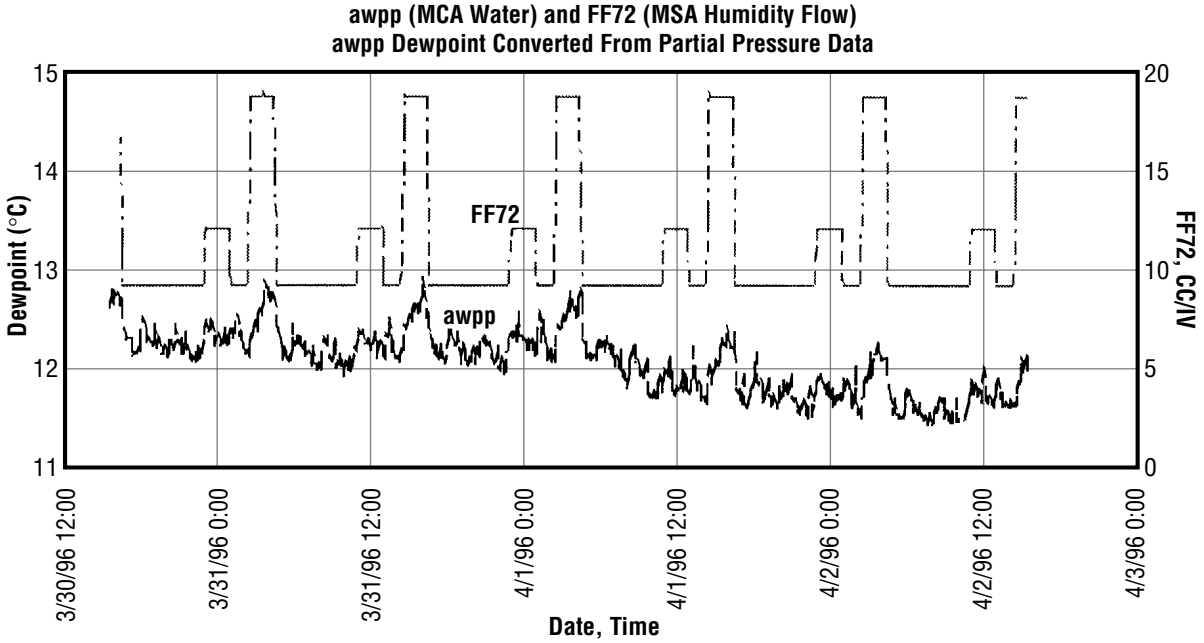

FIGURE 37.—Effects of metabolic water input on CMS dewpoint.

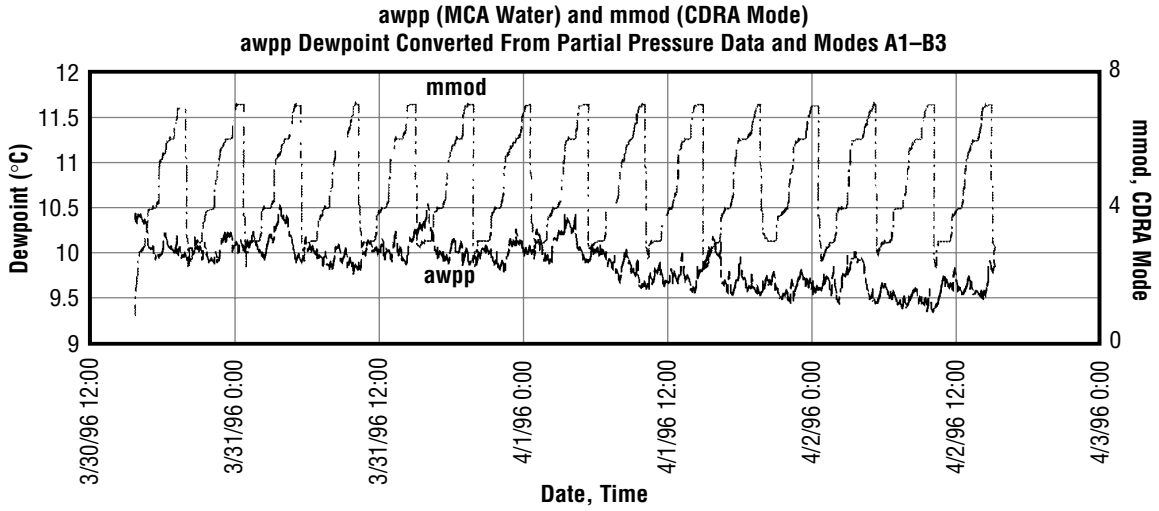

FIGURE 38.—Effects of CDRA operating mode on CMS dewpoint.

MCA Response to Humidity Fluctuations

During the follow-on testing, the humidity levels in the cabin were varied among the extremes possible within the test chamber—from approximately 45-percent relative humidity at the low end to 80 percent at the high end of the range. During this testing, the humidity was reduced to the lowest achievable level within the CMS; then the coolant flow to the CHX was shut off. This approach was used because the ability to detect loss of humidity removal was considered to be the most likely failure that the MCA should be required to recognize. A typical MCA response to several humidity swings is shown by figure 39. As the humidity level rose, the MCA reading followed it within a matter of seconds.

Figures 40, 41, and 42 isolate the first of the second set of dewpoint peaks to allow a better assessment of the MCA's response time. As can be seen by these figures, the MCA response lags the chamber sample system inlet dewpoint by approximately 30 to 60 sec. Based on these data and the baseline gathered during the nominal portion of the test, it can be concluded that the MCA will perform reliably onboard the *ISS*, and its water reading will be accurate and reliable for determining water removal failure of THCS. Additional data plots are provided in appendix K.

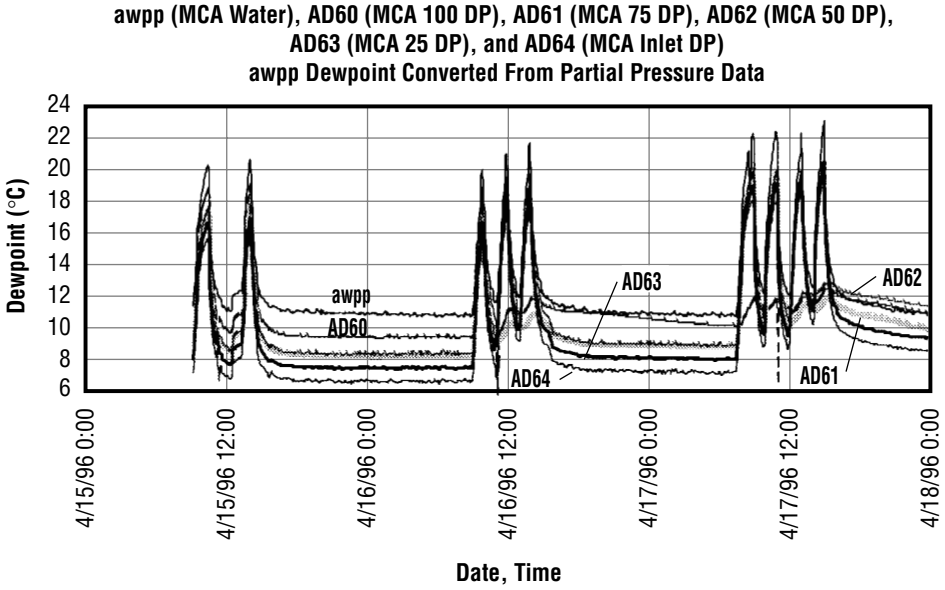

FIGURE 39.—Typical MCA response to CMS humidity swings.

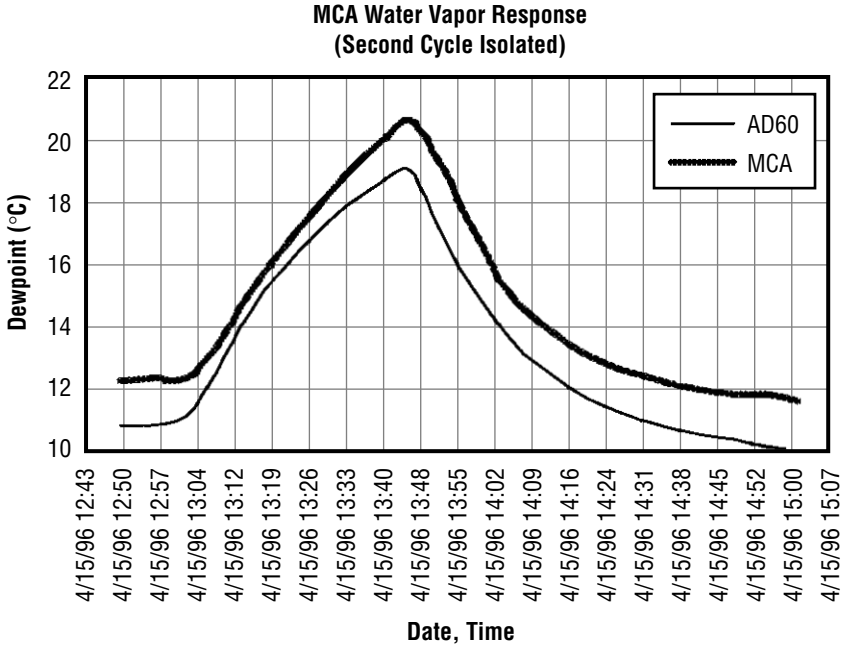

FIGURE 40.—MCA response during a single humidity cycle.

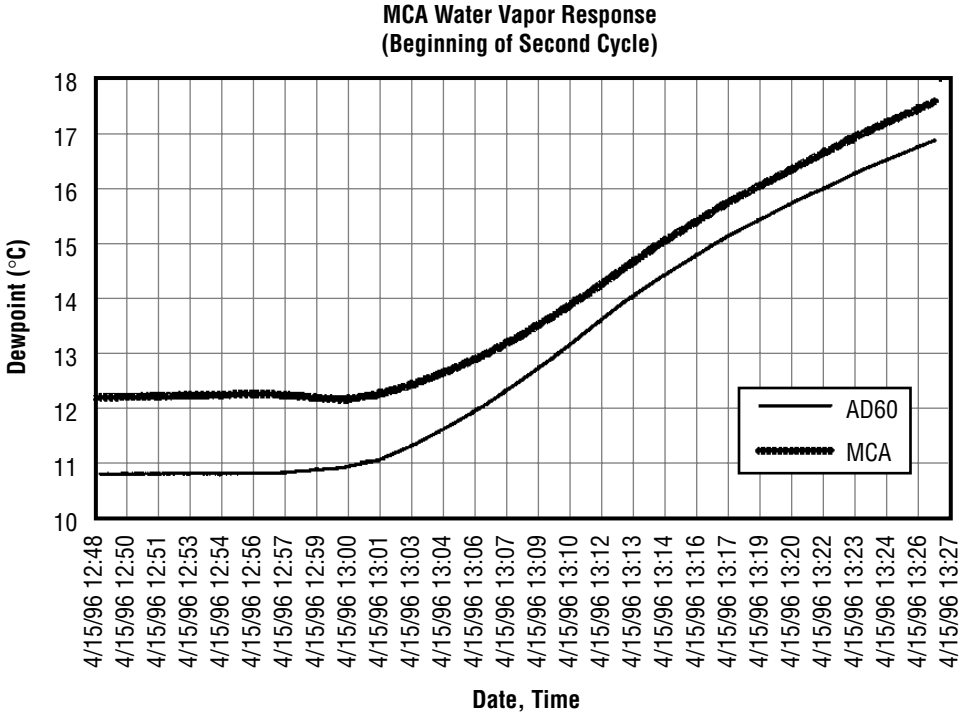

FIGURE 41.—MCA response to a sudden humidity increase.

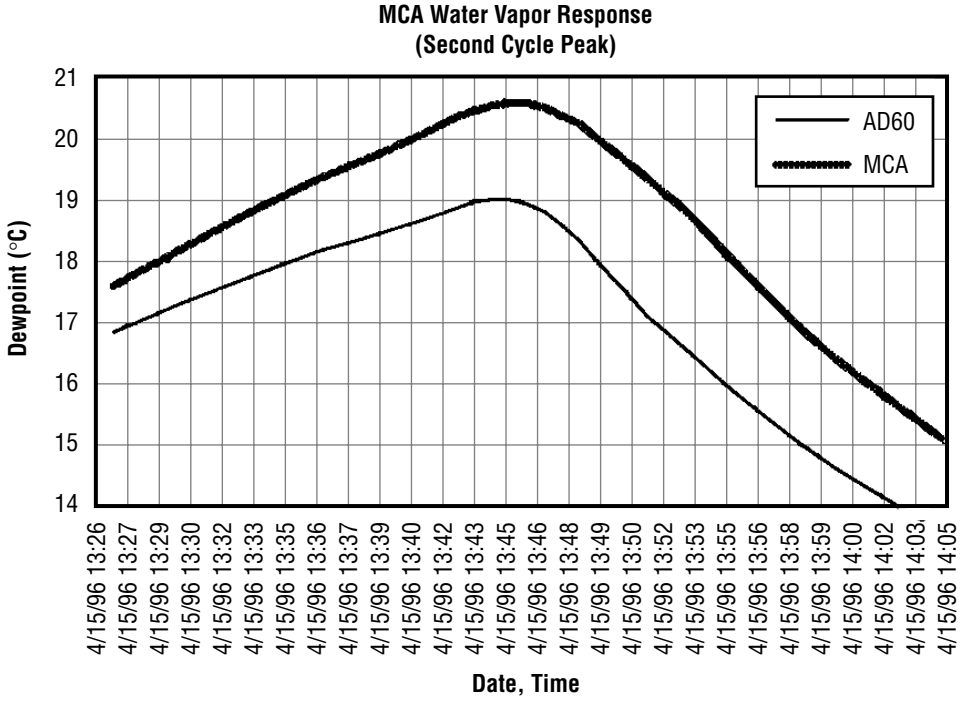

FIGURE 42.—MCA water vapor response to a sudden humidity decrease.

TCCS Performance Results

The TCCS operated with no problems during the test. Its flowrates were stable at approximately 15.3 m^3/hr (9 ft^3/min) through the charcoal bed and 4.6 m^3/hr (2.7 ft^3/min) through the catalytic oxidizer. The catalytic oxidizer, however, operated at cooler conditions than during previous extended-duration TCCS testing. The temperatures at points located just before the heating element (jt03), the midpoint of the catalyst bed (jt04), and the exit of the catalyst bed (jt05) averaged 653.1 K (715.8 °F), 671.2 K (748.5 °F), and 672.8 K (751.4 °F), respectively, during previous testing.[35] However, during the IART, temperatures at these points averaged 648.2 K (707 °F), 665.4 K (738 °F), and 667.6 K (742 °F) as shown by figure 43.

Appendix L documents an energy balance analysis of the catalytic oxidizer that shows that the heat of reaction of 60 mg/m^3 (90 ppm) of methane can account for up to a 2.3-K (4.2-°F) temperature rise in the reactor. In other words, the catalytic oxidizer would operate 2.3 K cooler if no methane oxidation occurred. Since no methane was injected into the CMS and the energy input of the heater power was the same as was used previously, the entire reactor operated at the observed cooler condition. An energy balance of the IART conditions shows that the observed temperatures result from the lack of methane injection. This analysis is also provided in appendix L.

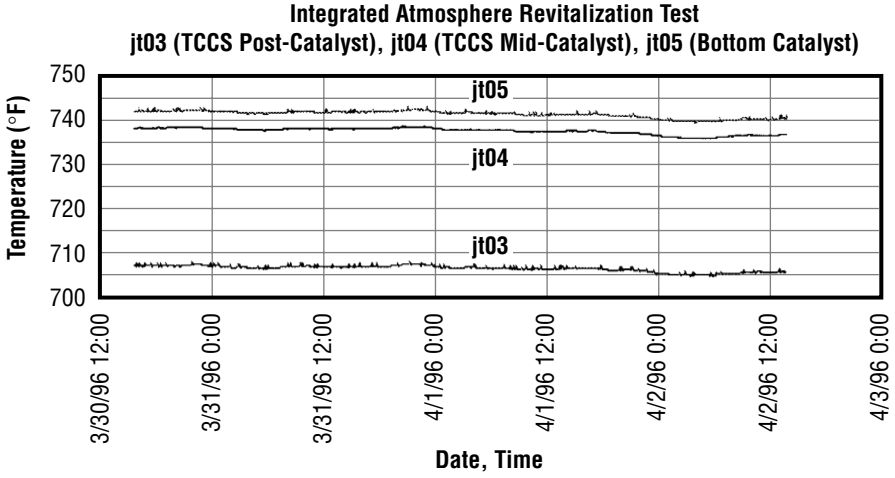

FIGURE 43.—Typical TCCS temperature conditions.

CONCLUSIONS

Based upon the results obtained during subassembly pretests and 30 days of integrated, closed-door subsystem testing, the following conclusions are drawn:

(1) The OGA is capable of producing oxygen at a four-crew person metabolic rate while operating in a day/night power cycling mode and using feedwater from the *ISS* water processor.

(2) The CDRA is capable of operating in a day/night power cycling mode while meeting *ISS* carbon dioxide removal specifications for a four-crew person metabolic rate.

(3) The MCA can be used in a feedback control loop for oxygen partial pressure control.

(4) The MCA water vapor signal is stable and is not affected by sample delivery system line length.

(5) The MCA is capable of responding rapidly to humidity changes in the cabin.

(6) The MCA response to carbon dioxide and oxygen are stable and track atmospheric trends well.

(7) Methane and other hydrocarbon oxidation in the TCCS high-temperature oxidizer contribute significantly to the oxidizer operating temperature.

(8) No ozone or oxides of nitrogen are produced by the ARS subassemblies during normal operations.

RECOMMENDATIONS

Although the IART successfully addressed the general system-level and specific subassembly-level operational and performance issues facing the *ISS* ARS design, some issues were raised by the testing. Recommendations concerning these issues are the following:

(1) Operating the CDRA at a lower temperature and shorter one-half-cycle time contributes to desiccant bed breakthrough. The CDRA operation on board the *ISS* should allow for the capability to operate at higher bed temperatures when necessary to periodically dry the desiccant beds more thoroughly.

(2) Although the technical difficulties with the OGA prevented its use in the integrated test, its ability to operate using power cycling and feedwater quality conditions similar to those expected on board the *ISS* was demonstrated. It is recommended, however, that additional testing be conducted to verify that the OGA oxygen production rate can be controlled using conditioned signals from the MCA. The ability of the OGA to operate in this manner to successfully control cabin oxygen partial pressure in an integrated test must be demonstrated.

REFERENCES

1. Carrasquillo, R.L.; Carter, D.L.; Holder, D.W.; McGriff, C.F.; and Ogle, K.Y.: "Space Station *Freedom* Environmental Control and Life Support System Regenerative Subsystem Selection." NASA TM–4340, February 1992.

2. Perry, J.L., and Roman, M.C.: "Environmental Control and Life Support System Life Testing Program." Attachment to NASA/MSFC Internal Memorandum ED62(44–94). Marshall Space Flight Center, September 29, 1994.

3. Tatara, J.D., and Perry, J.L.: "International Space Station Alpha Trace Contaminant Control Subassembly Life Test Final Report." NASA TM–108488, March 1995.

4. Chiu, C.Y.; Perry, J.L.; Salyer, B.H.; and Tatara, J.D.: "Preliminary Results of NASA ECLSS Life Testing." SAE 941463. 24th International Conference on Environmental Systems, Friedrichshafen, Germany, June 20–23, 1994.

5. Schunk, R.G.; Bagdigian, R.M.; Carrasquillo, R.L.; Ogle, K.Y.; and Wieland, P.O.: "Space Station ECLSS Simplified Integrated Test Final Report." NASA TM–100363, March 1989.

6. Schunk, R.G.; Bagdigian, R.M.; Carrasquillo, R.L.; Ogle, K.Y.; and Wieland, P.O.: "Space Station CMIF Extended Duration Metabolic Control Test Final Report." NASA TM–100362, March 1989.

7. Schunk, R.G.; Carrasquillo, R.L.; Ogle, K.Y.; Wieland, P.O.; and Bagdigian, R.M.: "CMIF ECLS System Test Findings." SAE 891552. 19th Intersociety Conference on Environmental Systems, San Diego, CA, July 24–26, 1989.

8. Schunk, R.G., and Humphries, W.R.: "Environmental Control and Life Support Testing at the Marshall Space Flight Center." SAE 871453, 17th Intersociety Conference on Environmental Systems, Seattle, WA, July 13–15, 1987.

9. Roberts, B.C.; Carrasquillo, R.L.; DuBiel, M.Y.; Ogle, K.Y.; Perry, J.L.; and Whitley, K.M.: "Space Station *Freedom* Environmental Control and Life Support System Phase III Simplified Integrated Test Detailed Report." NASA TM–4204, May 1990.

10. Perry, J.L.: "Space Station *Freedom* Environmental Control and Life Support System (ECLSS) Phase III Simplified Integrated Test Trace Contaminant Control Subsystem Performance." NASA TM–4202, October 1990.

11. Roberts, B.C.; Carrasquillo, R.L.; DuBiel, M.Y.; Ogle, K.Y.; Perry, J.L.; and Whitley, K.M.: "Phase III Simplified Integrated Test (SIT) Results: Space Station ECLSS Testing." SAE 901252. 20th Intersociety Conference on Environmental Systems, Williamsburg, VA, July 9–12, 1990.

12. Graves, J.; Joiner, C.; Peterson, B.; and Underwood S.: “Atmosphere Revitalization Predevelopment Operational Systems Test (POST) Report.” T683–80026–1, Boeing Defense and Space Group, Huntsville, AL, June 12, 1992.

13. Kidd, G.R.: “Analysis Report for the Atmosphere Revitalization System Predevelopment Operational System.” D683-10311-11, Boeing Defense and Space Group, Huntsville, AL, February 9, 1994.

14. Foerg, S.L.; Kallberg, M.R.; Dall-Bauman, L.; and Sharpe, T.J.: “Testing of an Integrated Air Revitalization System.” SAE 951661, 25th International Conference on Environmental Systems, San Diego, CA, July 10–13, 1995.

15. Carrasquillo, R.L.: “Requirements for Space Station Environmental Control and Life Support System Integrated Atmosphere Revitalization Test, Revision A.” Attachment to NASA MSFC Memo ED62(06–94).

16. Carrasquillo, R.L.: “Requirements for Space Station Environmental Control and Life Support System Integrated Atmosphere Revitalization Test, Revision B.” Attachment to NASA MSFC Memo ED62(59–94).

17. “System Specification for the *International Space Station Alpha*, SSP 41000B.” Boeing Defense and Space Group, Houston, TX, November 1, 1994, pp. 14, 18, 233.

18. “Segment Specification for the United States On-Orbit Segment, SSP 41162B.” Boeing Defense and Space Group, Houston, TX, March 28, 1995, pp. 26–27, 49–51.

19. Parrish, K.J.: “*International Space Station* Phase III Atmosphere Revitalization System Static Feed Electrolyzer Oxygen Generation Assembly Test Report.” ECLSS/TECH/EL96–002, NASA MSFC, Systems Analysis and Integration Laboratory, March 1996.

20. Carrasquillo, R.L.: “Requirements for Space Station Environmental Control and Life Support System Integrated Atmosphere Revitalization Test, Revision B.” Attachment to NASA MSFC Memo ED62(59–94), p. 3.

21. “Atmosphere Revitalization Subsystem Description MTC Configuration, Rev. A.” Boeing Defense and Space Group (NAS8–50000) D683–15003–1, February 26, 1993, pp. 5–5 to 5–7.

22. Torres, D.; Dencker, W.; and Bedard, T.: “Space Station ECLSS Major Constituent Analyzer Development Unit Test Results.” SAE 951468, 25th International Conference on Environmental Systems, San Diego, CA, July 10–13, 1995, p. 3.

23. Carrasquillo, R.L.: “Space Station Day/Night Times for Cyclic Operation.” NASA MSFC Memo, April 11, 1994.

24. Martin, C.E.: “Integrated Atmosphere Revitalization Test Core Module Simulator (CMS) Oxygen Response and Revised Test Conditions.” Ion Electronics, Huntsville, AL, February 1996.

25. Franks, G.D.: “Integrated Air Revitalization Test Carbon Dioxide Removal Analysis.” NASA MSFC Memo ED62(NO4–95).

26. Garr, J.: “Integrated Air Revitalization Test System Control and Response Simulation and Analysis.” Ion Electronics, Huntsville, AL, July 1995.

27. Martin C.E.: “Core Module Simulator (CMS) Metabolic Loading for System Checkout.” Ion Electronics, Huntsville, AL, November 21, 1995.

28. Knox, J.C.: CASE/A SETCREW FORTRAN Routine. NASA, Marshall Space Flight Center, AL, April 1992.

29. Martin, C.E.: “Integrated Atmosphere Revitalization Test Core Module Simulator (CMS) Oxygen Response and Revised Test Conditions.” Ion Electronics, Huntsville, AL, February 1996.

30. Martin, C.E.: “CMS Pressure Leak Data.” Ion Electronics, Huntsville, AL, April 11, 1996.

31. Parrish, K.J.: “*International Space Station* Phase III Atmosphere Revitalization System Static Feed Electrolyzer Oxygen Generation Assembly Test Report.” NASA/MSFC Test Report ECLSS/TECH/EL96–002, March 1996.

32. Wright, J.D.; Chen, B.; and Wang, C.M.: “Trace Contaminant Oxidation Catalyst Poisoning Investigation.” (NAS8–38250–15) for Ion Electronics by TDA Research, Inc., Wheat Ridge, CA, March 22, 1996, p. 60.

33. Terrell, D.: “Ozone, Nitrogen Dioxide, and Oxygen Removal Samples Integrated Atmosphere Revitalization Test.” Sverdrup Technology, Inc., Memo 96–222–006–003, April 25, 1996.

34. Parrish, K.J.: “*International Space Station*, Phase III Atmosphere Revitalization System, Integrated Atmosphere Revitalization Test Report.” ECLSS/TECH/EL96–004, NASA MSFC, Systems Analysis and Integration Laboratory, July 1996.

35. Tatara, J.D., and Perry, J.L.: “*International Space Station Alpha* Trace Contaminant Control Subassembly Life Test Final Report.” NASA TM–108488, March 1995.

APPENDIX A—
CDRA PRETEST SUPPORTING DATA

Pretest Baseline 1—Continuous Operations
(160-min half cycle, 204 °C regeneration temperature)

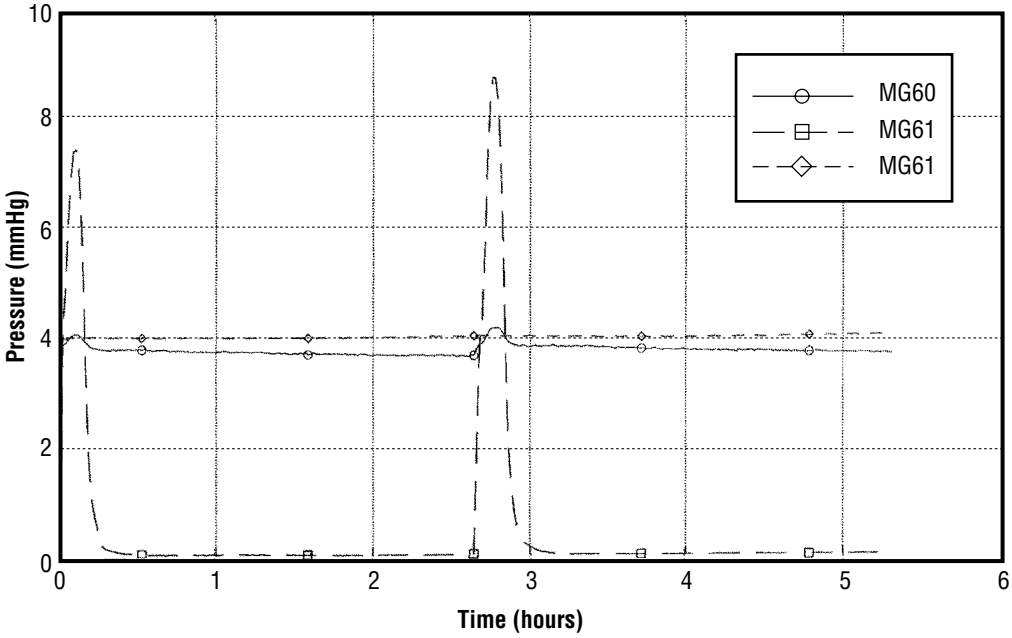

FIGURE A–1.—Plot 1: Carbon dioxide partial pressure 4BMS baseline 1 testing—day/night mode, continuous day elapsed time from 2–11–96, 01:40:00.

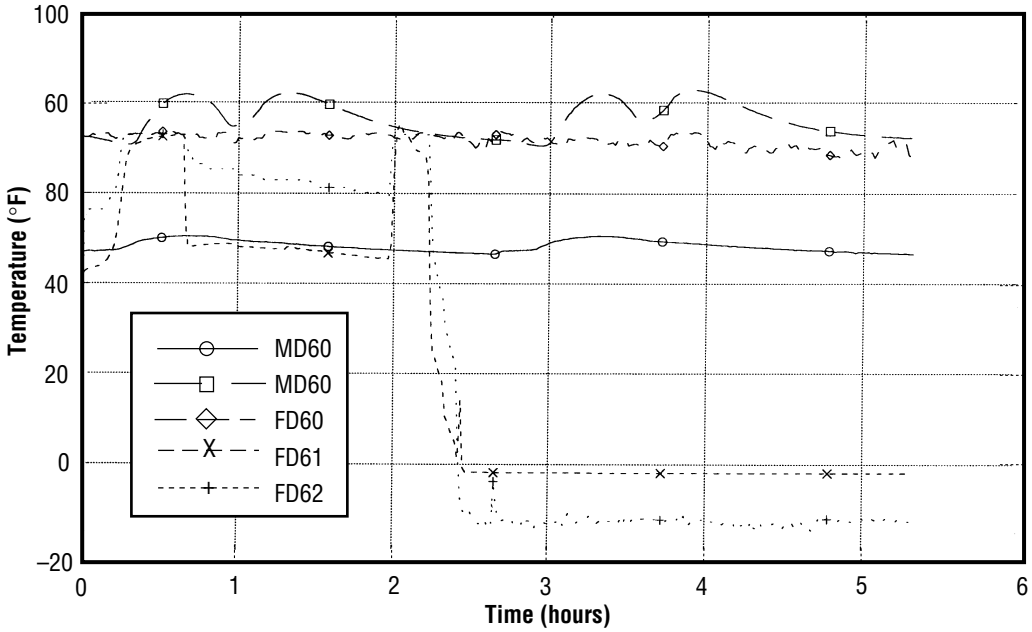

FIGURE A–2.—Plot 2: Dewpoint temperatures 4BMS baseline 1 testing—day/night mode, continuous day elapsed time from 2–11–96, 01:40:00.

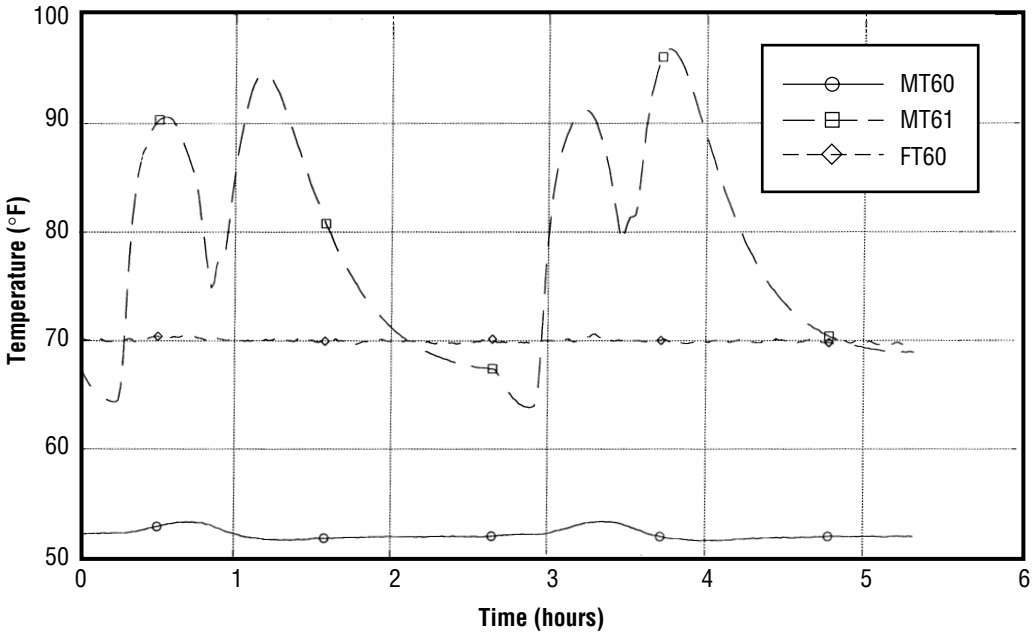

FIGURE A–3.—Plot 3: Inlet/outlet/module temperatures 1BMS baseline 1 testing—day/night mode, continuous day elapsed time from 2–11–96, 01:40:00.

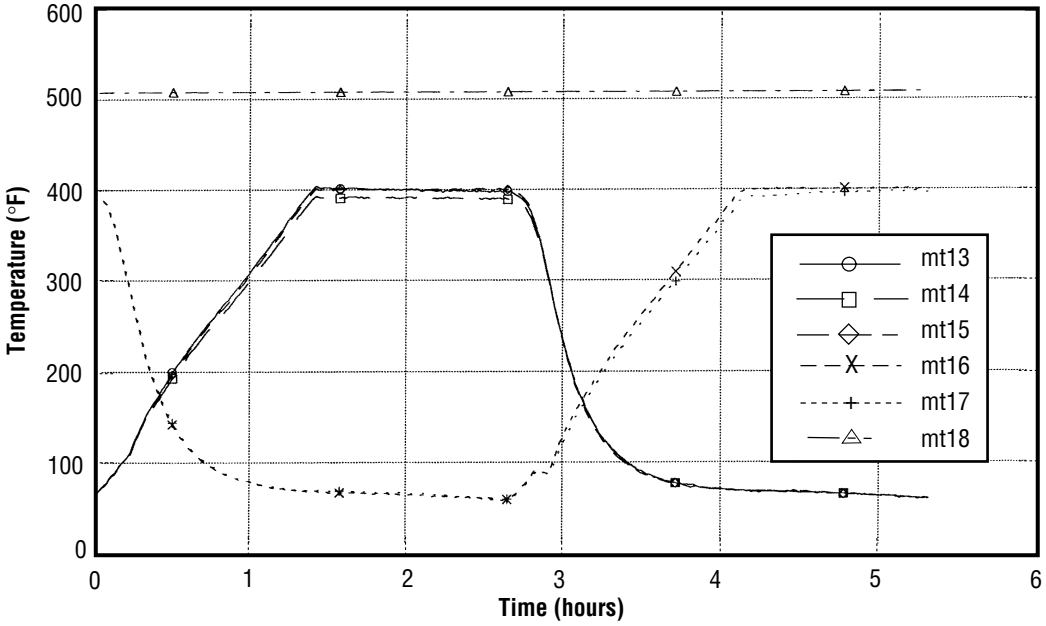

FIGURE A–4.—Plot 4: 5A sorbent bed temperatures 4BMS baseline 1 testing—day/night mode, continuous day elapsed time from 2–11–96, 01:40:00.

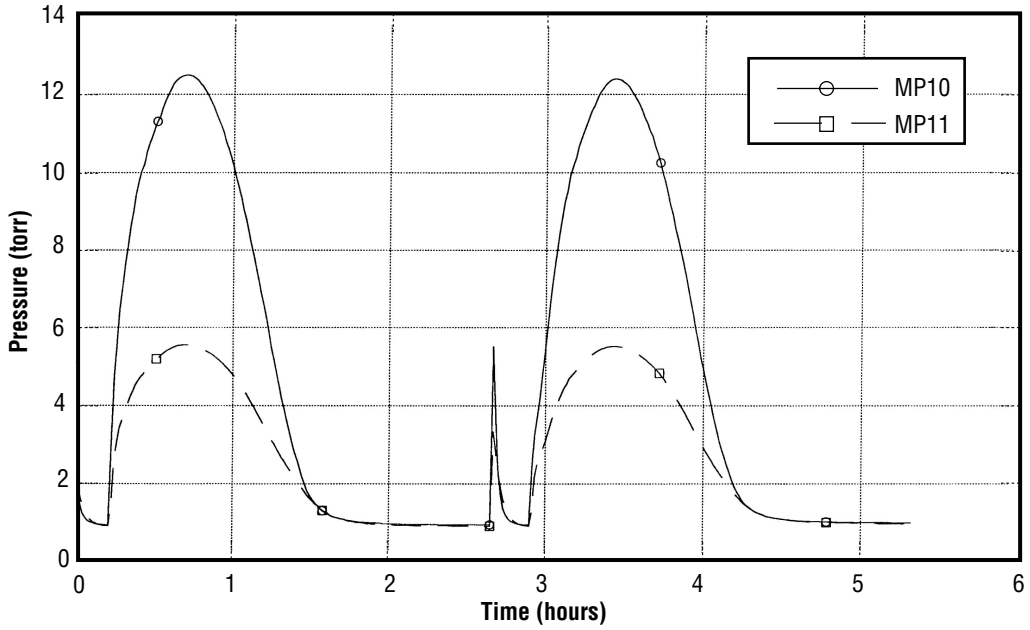

FIGURE A–5.—Plot 5: Vacuum line pressures 4BMS baseline 1 testing—day/night mode, continuous day elapsed time from 2–11–96, 01:40:00.

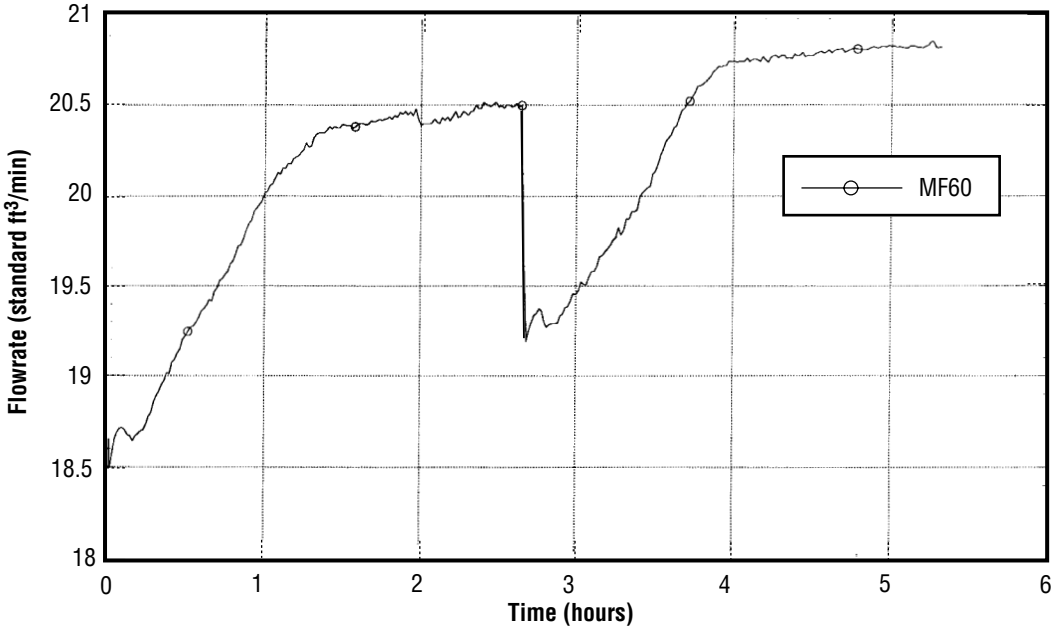

FIGURE A–6.—Plot 6: Flowrate 4BMS baseline 1 testing—day/night mode, continuous day elapsed time from 2–11–96, 01:40:00.

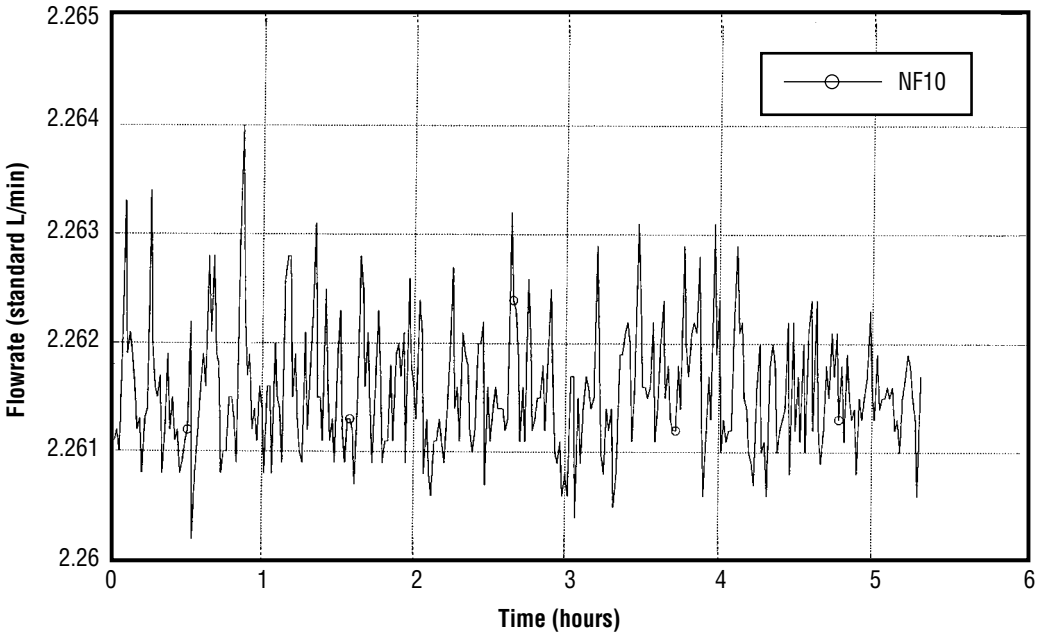

FIGURE A–7.—Plot 7: CO_2 injection flowrate 4BMS baseline 1 testing—day/night mode, continuous day elapsed time from 2–11–96, 01:40:00.

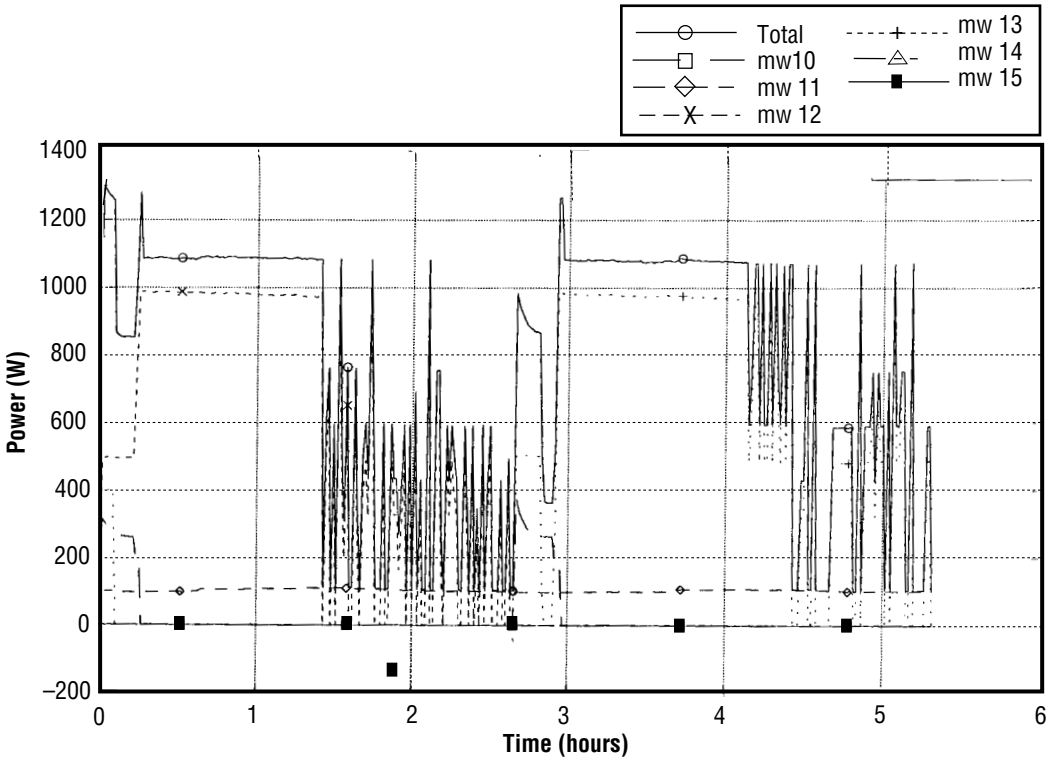

FIGURE A–8.—Plot 8: Power consumption 4BMS baseline 1 testing—day/night mode, continuous day elapsed time from 2–11–96, 01:40:00.

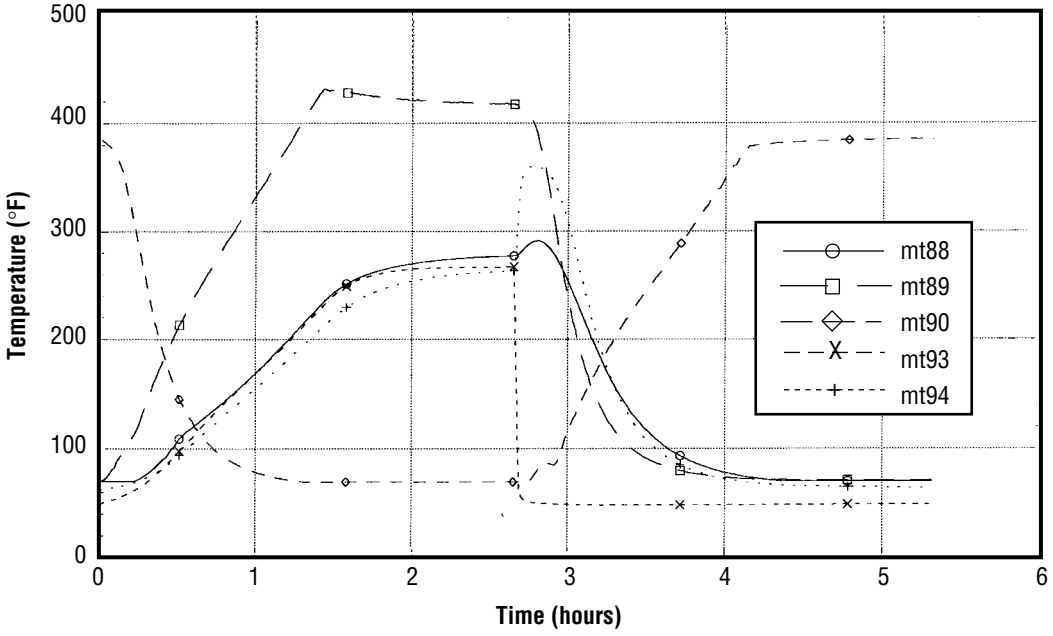

FIGURE A–9.—Plot 9: 5A sorbent bed 309 temperatures 4BMS baseline 1 testing—day/night mode, continuous day elapsed time from 2–11–96, 01:40:00.

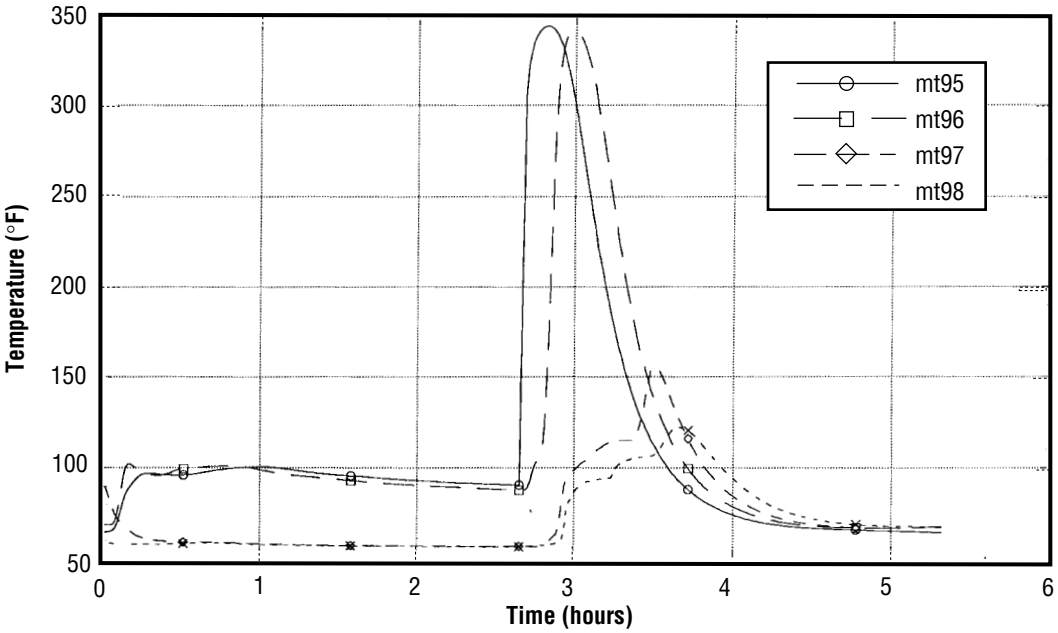

FIGURE A–10.—Plot 10: Dessicant bed temperatures 4BMS baseline 1 testing—day/night mode, continuous day elapsed time from 2–11–96, 01:40:00.

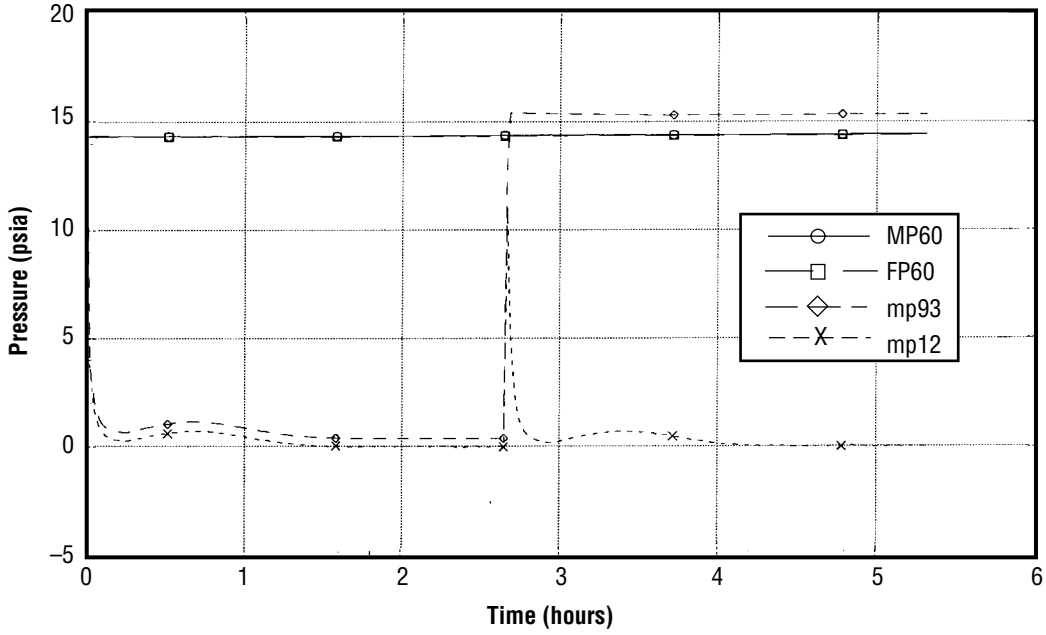

FIGURE A–11.—Plot 11: Inlet/module/bed 309 pressures 4BMS baseline 1 testing—day/night mode, continuous day elapsed time from 2–11–96, 01:40:00.

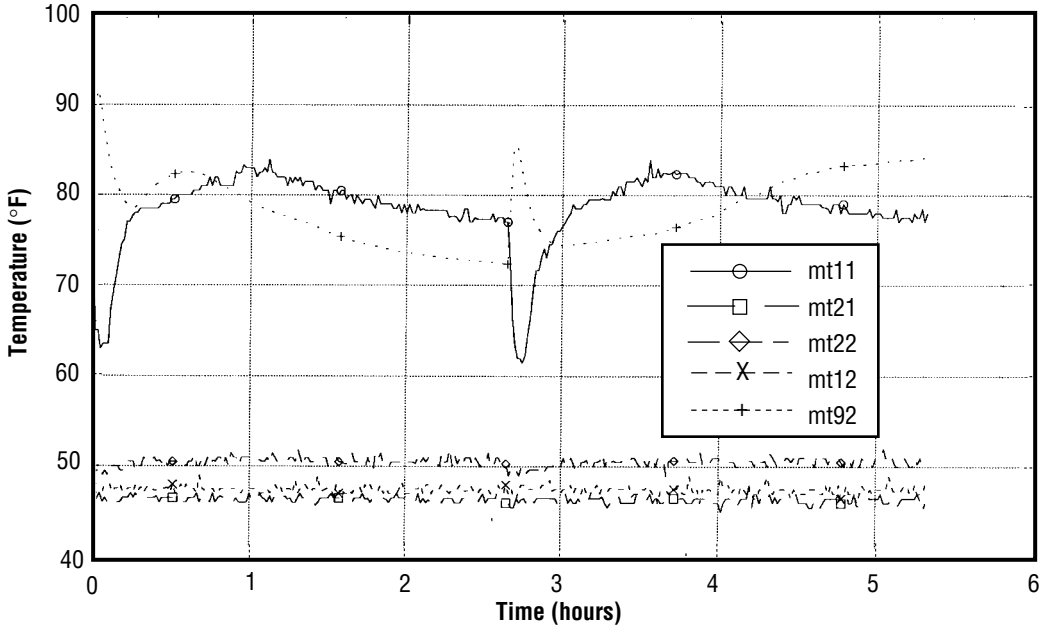

FIGURE A–12.—Plot 12: Process temperatures 4BMS baseline 1 testing—day/night mode, continuous day elapsed time from 2–11–96, 01:40:00.

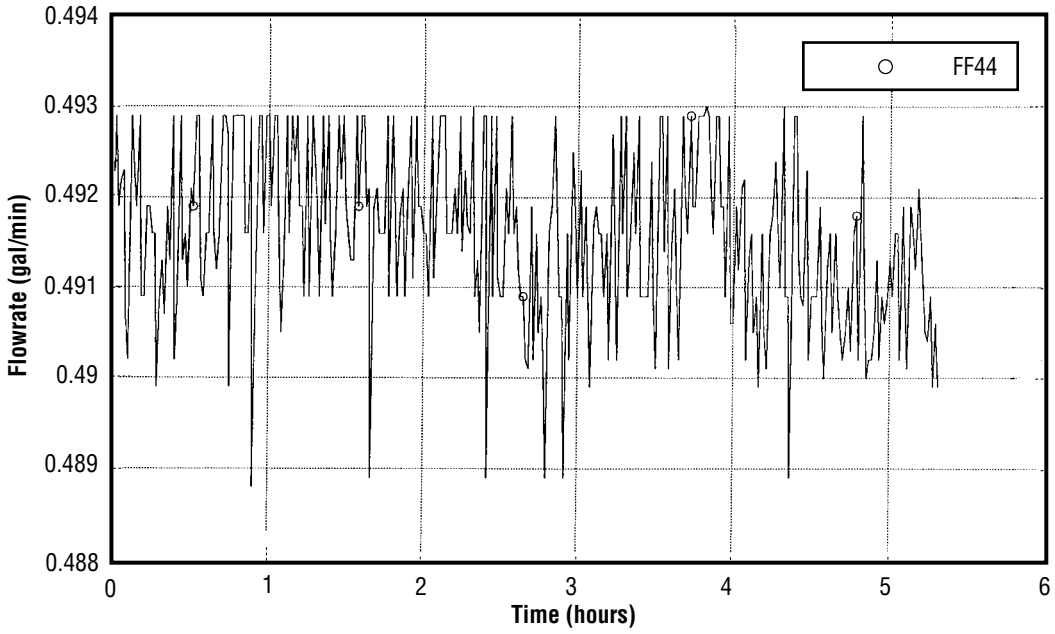

FIGURE A–13.—Plot 13: Precooler coolant flowrate 4BMS baseline 1 testing—day/night mode, continuous day elapsed time from 2–11–96, 01:40:00.

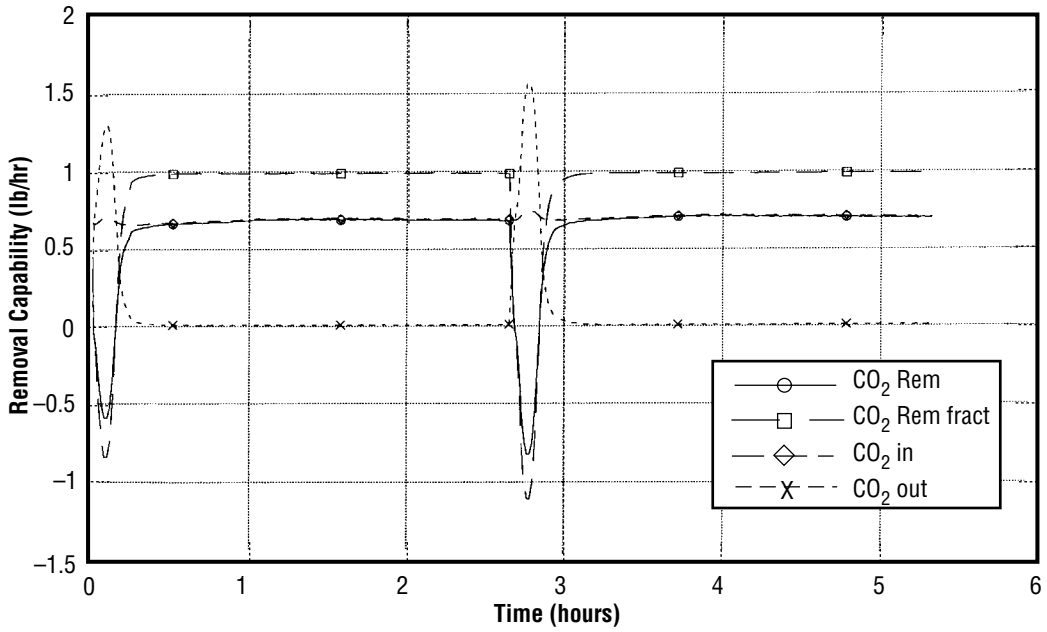

FIGURE A–14.—Plot 14: CO_2 removal capability 4BMS baseline 1 testing—day/night mode, continuous day elapsed time from 2–11–96, 01:40:00.

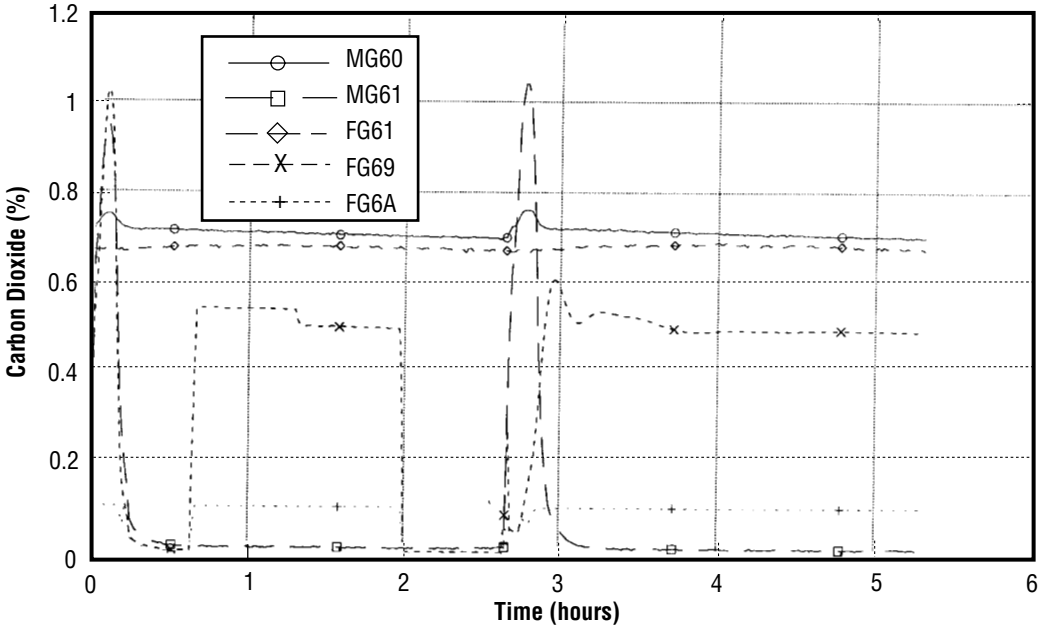

FIGURE A–15.—Plot 15: Percent carbon dioxide 4BMS baseline 1 testing—day/night mode, continuous day elapsed time from 2–11–96, 01:40:00.

Pretest Baseline 2—Day/Night Operations
(160-min half cycle, 204 °C regeneration temperature)

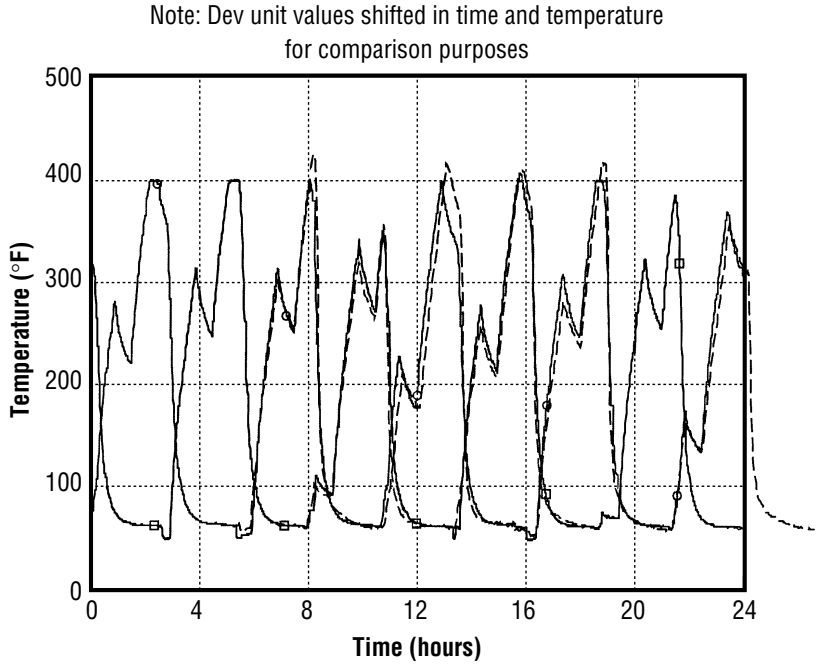

FIGURE A–16.—Sorbent bed temperature comparison: POST CDRA (solid lines) versus dev unit (dashed lines) elapsed time from 2–23–96, 17:00:00 POST heaters set at 96/500 W.

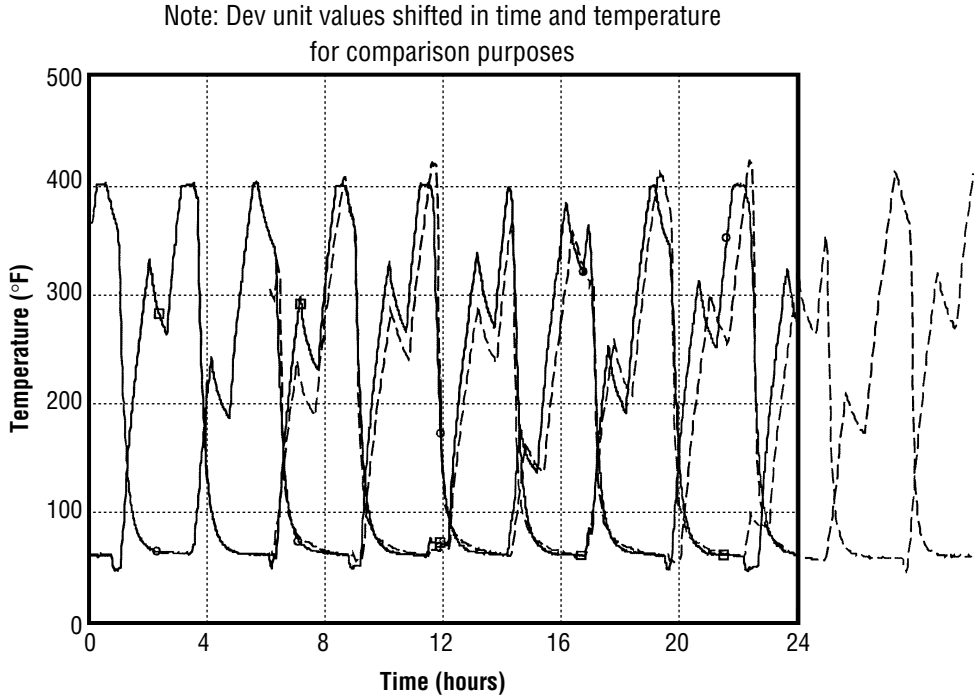

FIGURE A–17.—Sorbent bed temperature comparison: POST CDRA (solid lines) versus dev unit (dashed lines) elapsed time from 2–22–96, 10:40:00 POST heaters set at 1,000/500 W.

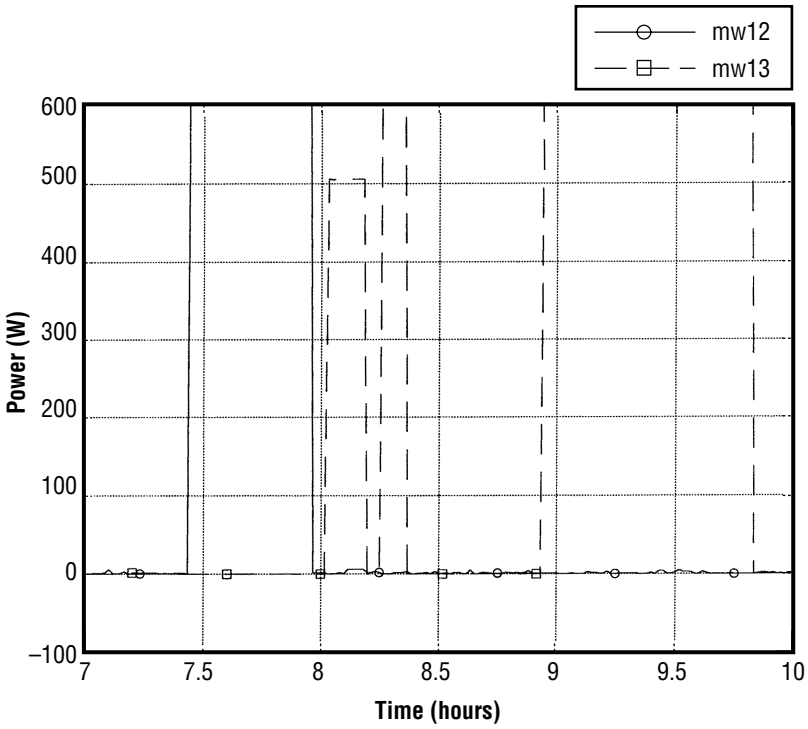

FIGURE A–18.—Power dropout at B1–B2 cycle change.

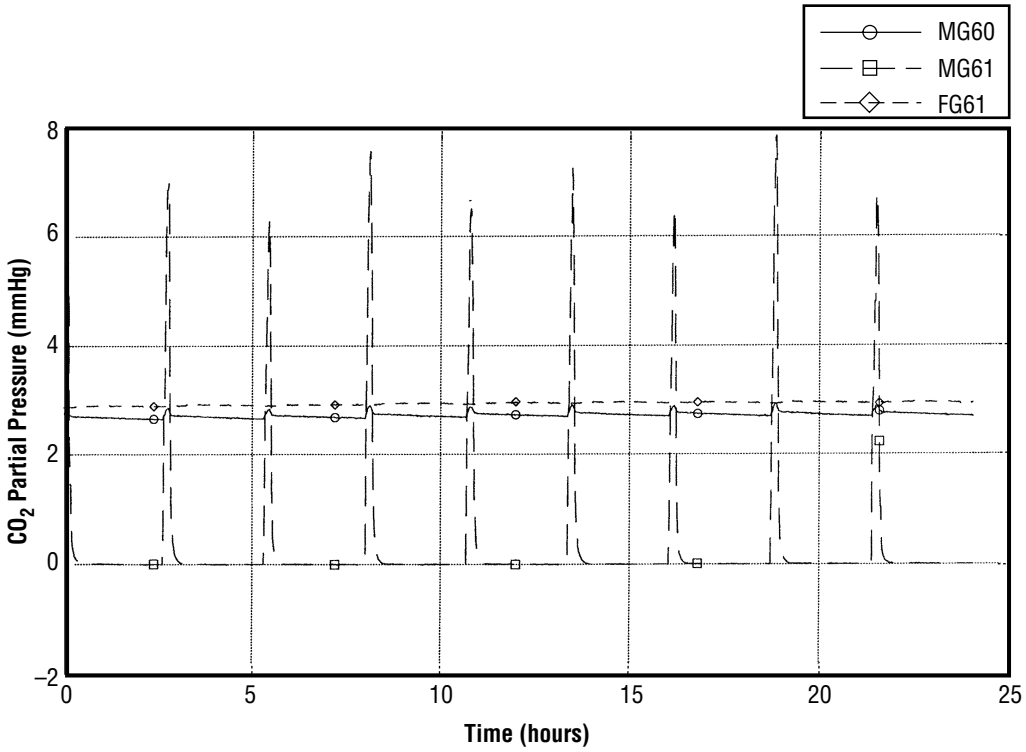

FIGURE A–19.—Plot 1: Carbon dioxide partial pressure 4BMS baseline 2 testing—day/night mode, elapsed time from 2–23–96, 17:00:00.

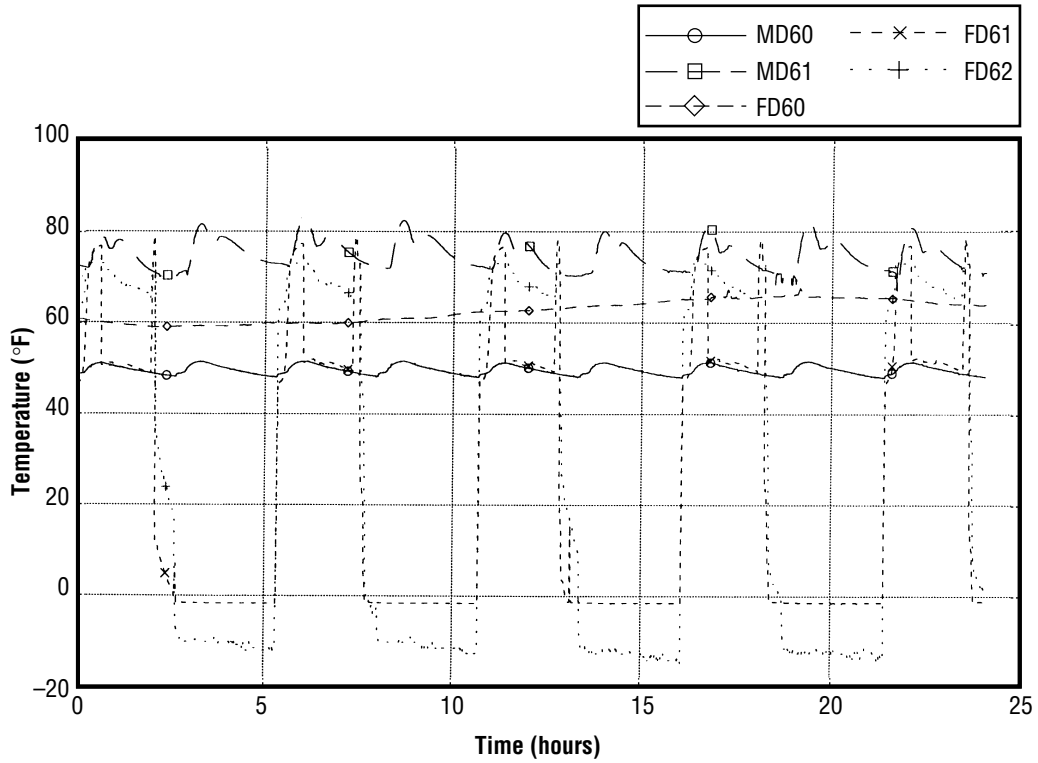

FIGURE A–20.—Plot 2: Dewpoint temperatures 4BMS baseline 2 testing—day/night mode elapsed time from 2–23–96, 17:00:00.

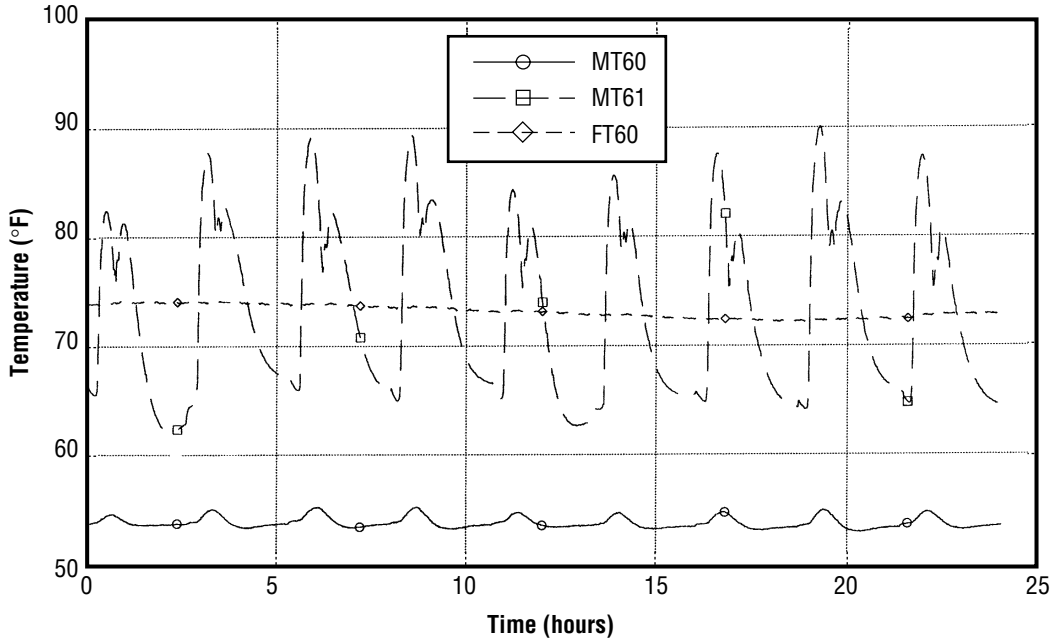

FIGURE A–21—Plot 3: Inlet/outlet/module temperatures 4BMS baseline 2 testing—day/night mode elapsed time from 2–23–96, 17:00:00.

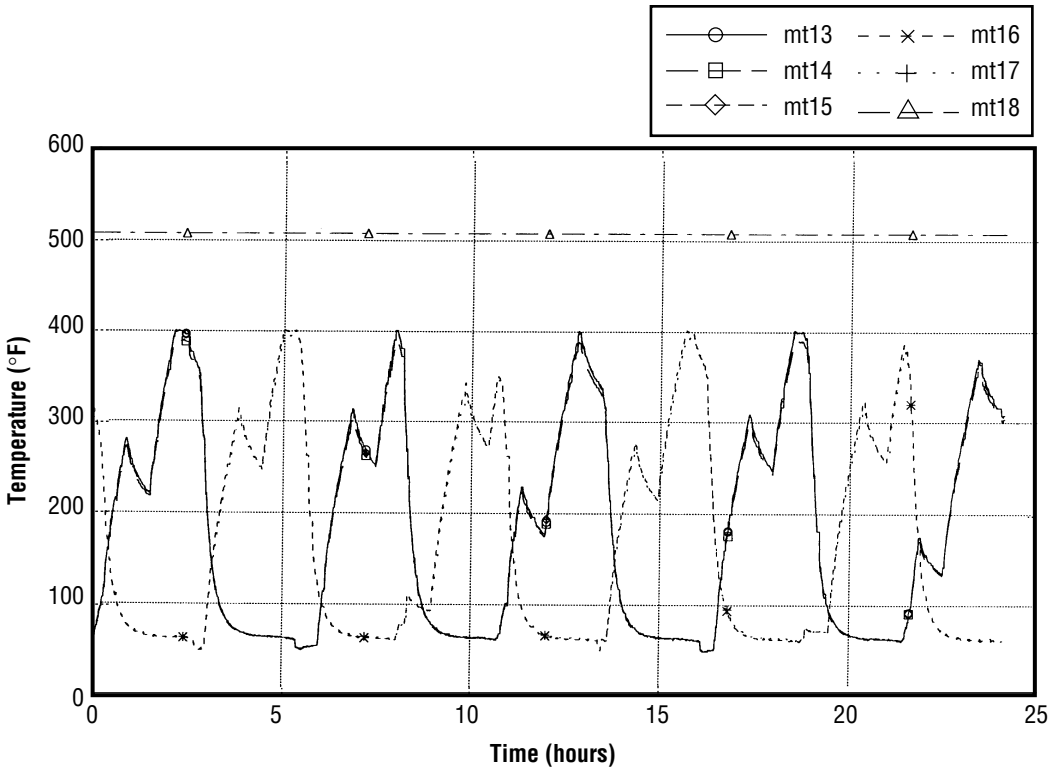

FIGURE A–22.—Plot 4: 5A sorbent bed temperatures 4BMS baseline 2 testing—day/night mode elapsed time from 2–23–96, 17:00:00.

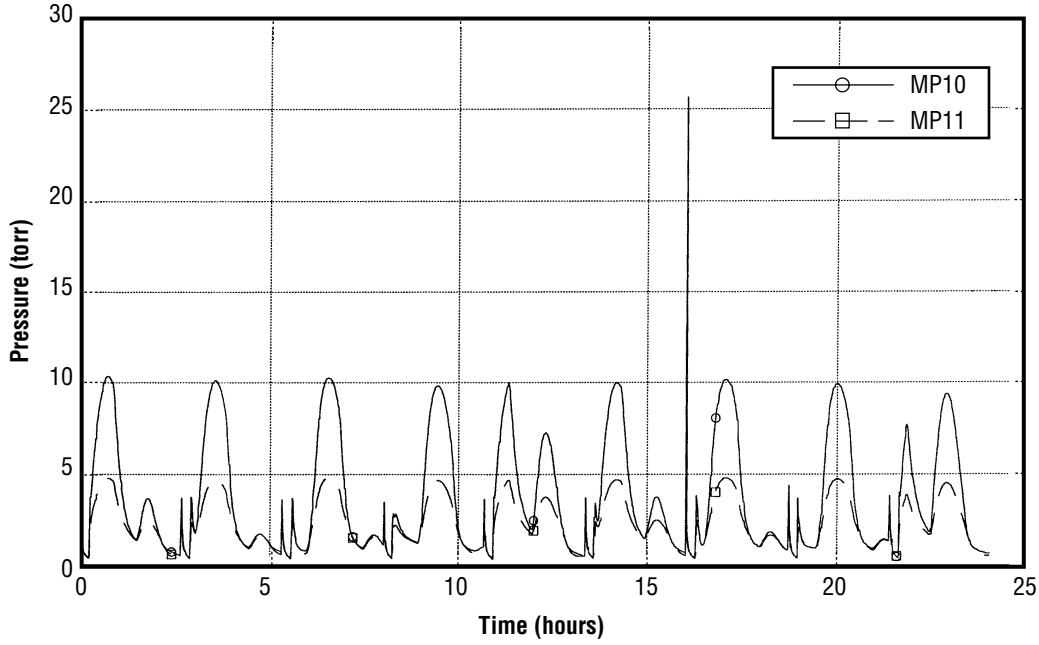

FIGURE A–23.—Plot 5: Vacuum line pressures 4BMS baseline 2 testing—day/night mode elapsed time from 2–23–96, 17:00:00.

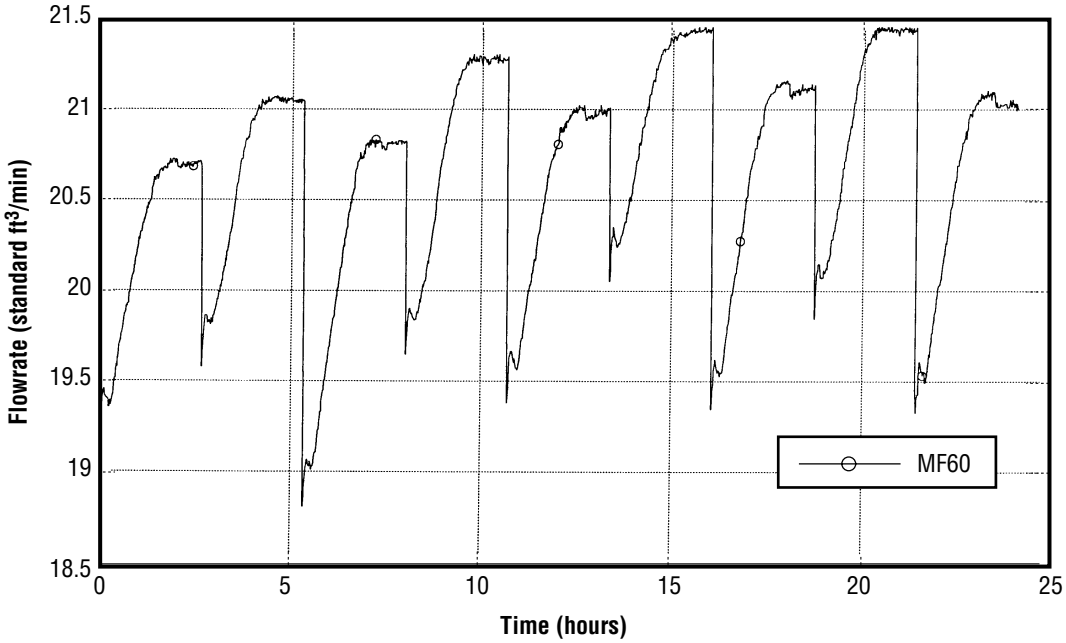

FIGURE A–24.—Plot 6: Flowrate 4BMS baseline 2 testing—day/night mode elapsed time from 2–23–96, 17:00:00.

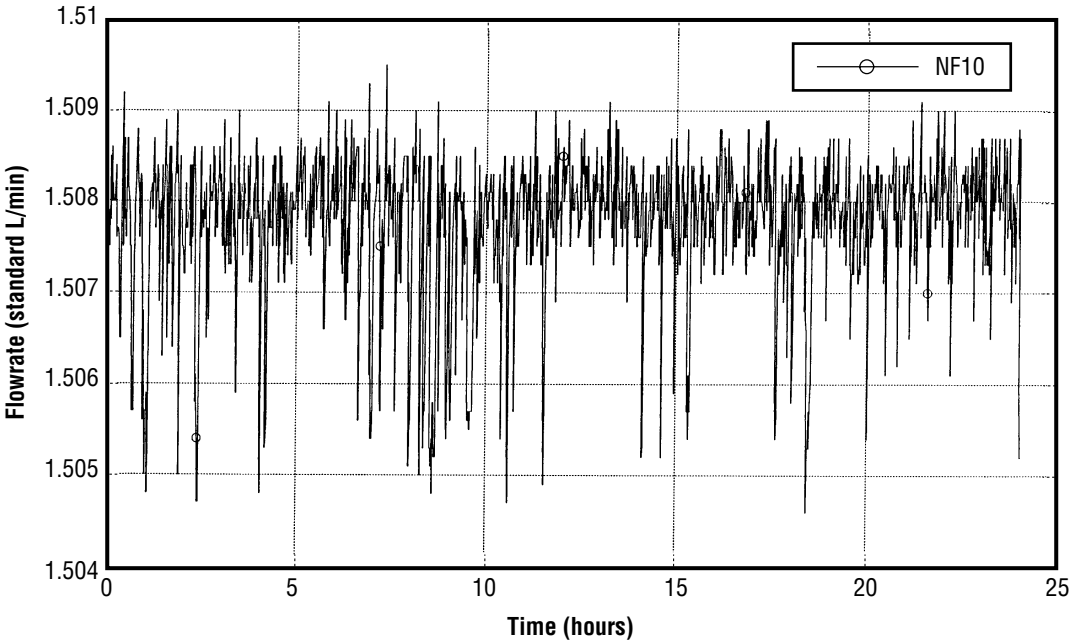

FIGURE A–25.—Plot 7: CO_2 injection flowrate 4BMS baseline 2 testing—day/night mode elapsed time from 2–23–96, 17:00:00.

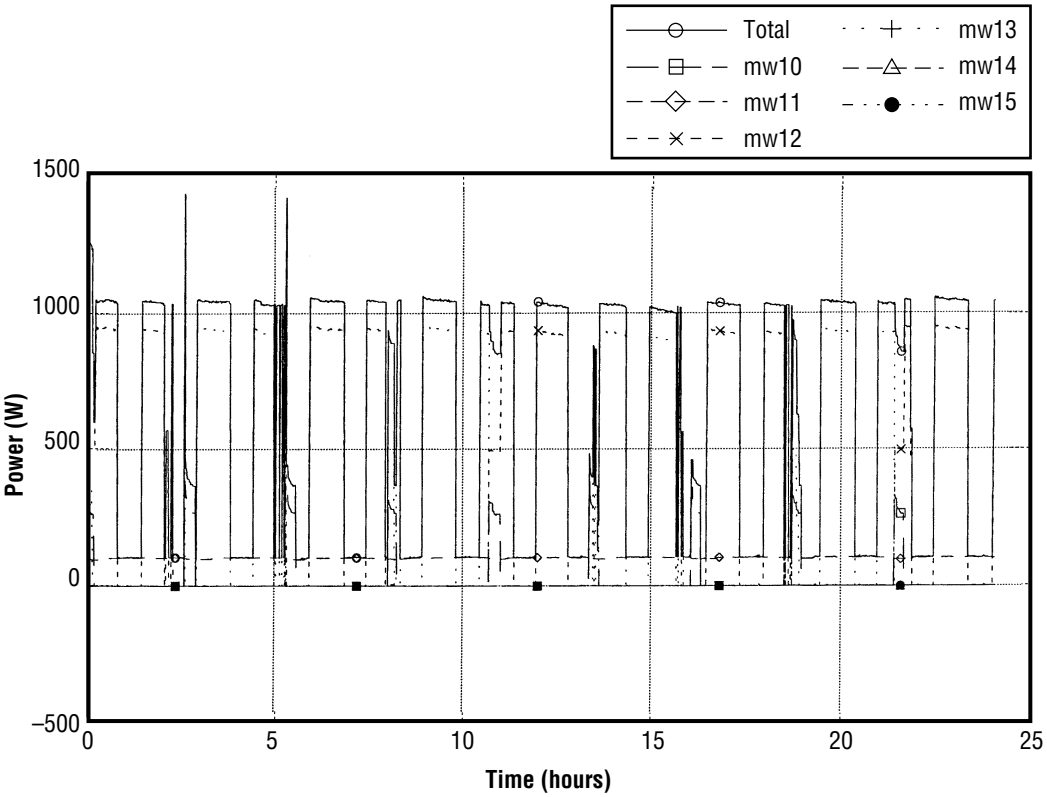

FIGURE A–26.—Plot 8: Power consumption 4BMS baseline 2 testing—day/night mode elapsed time from 2–23–96, 17:00:00.

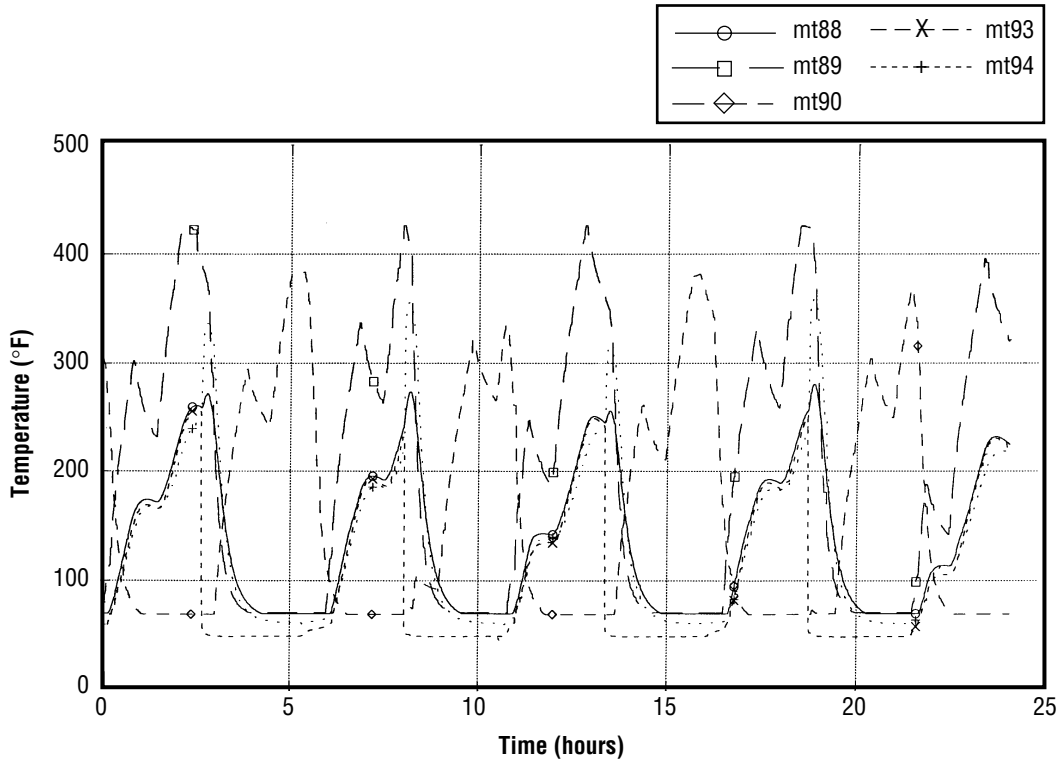

FIGURE A–27.—Plot 9: 5A sorbent bed 309 temperatures 4BMS baseline 2 testing—day/night mode elapsed time from 2–23–96, 17:00:00.

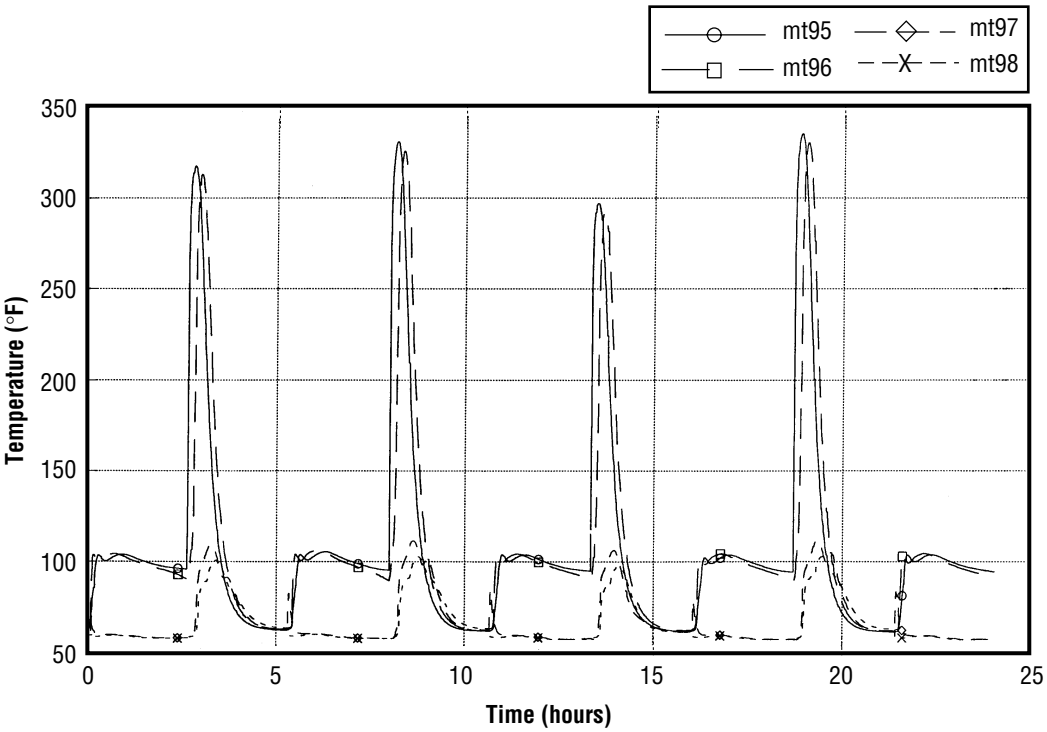

FIGURE A–28.—Plot 10: Dessicant bed temperatures 4BMS baseline 2 testing—day/night mode elapsed time from 2–23–96, 17:00:00.

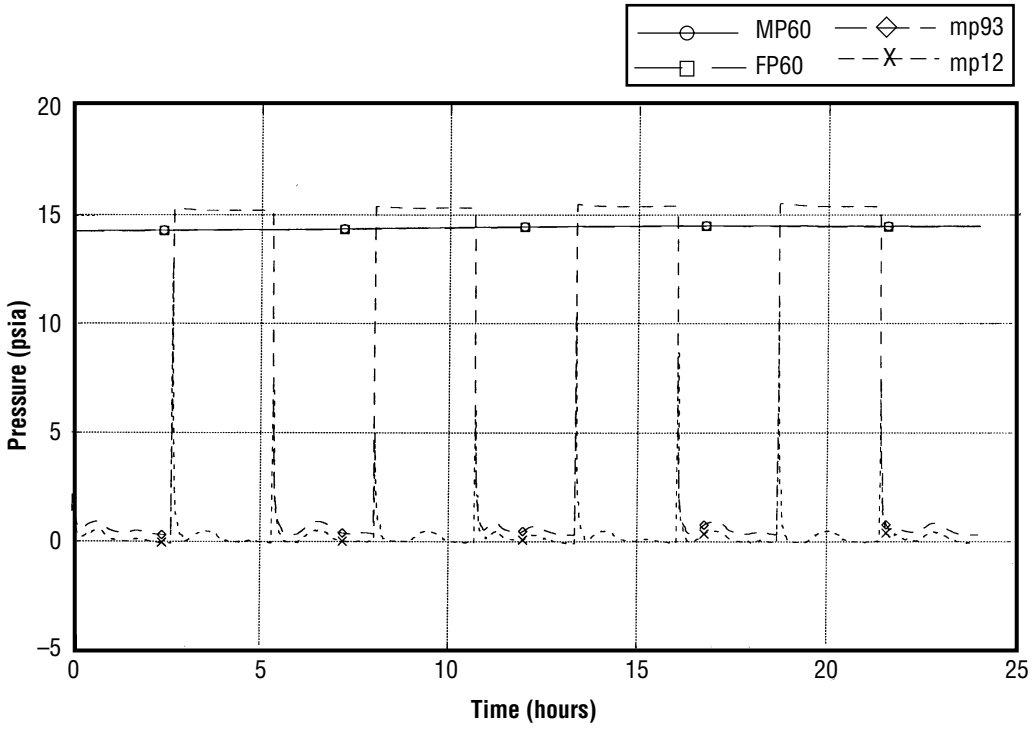

FIGURE A–29.—Plot 11: Inlet/module/bed 309 pressures 4BMS baseline 2 testing—day/night mode elapsed time from 2–23–96, 17:00:00.

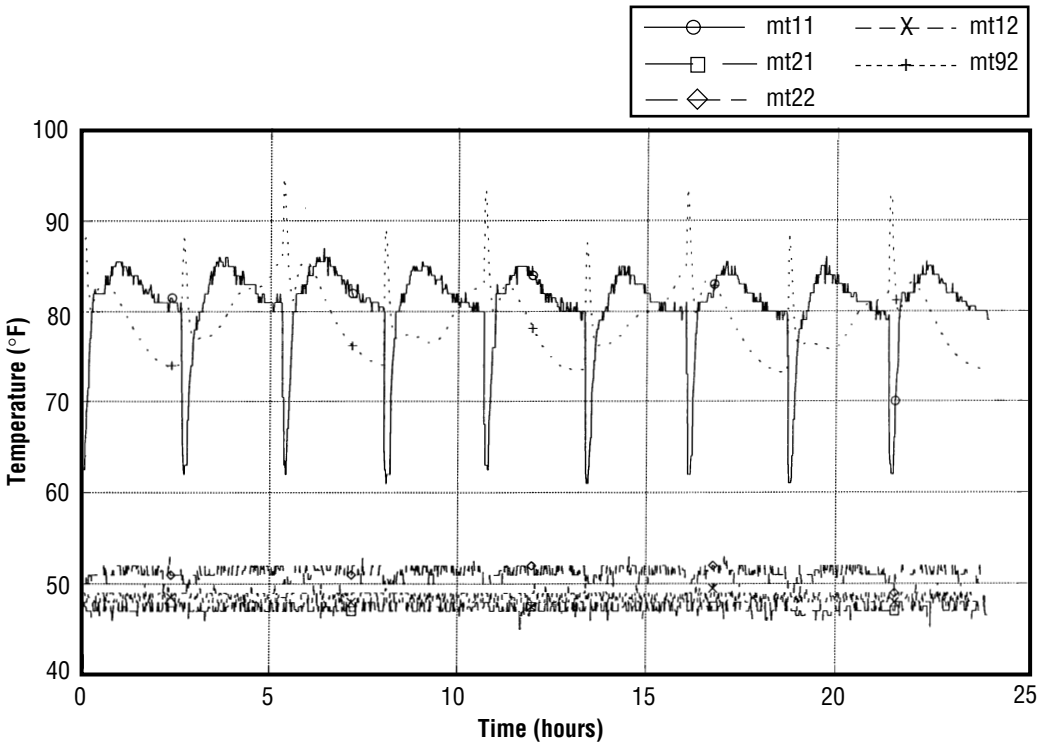

FIGURE A–30.—Plot 12: Process temperatures 4BMS baseline 2 testing—day/night mode elapsed time from 2–23–96, 17:00:00.

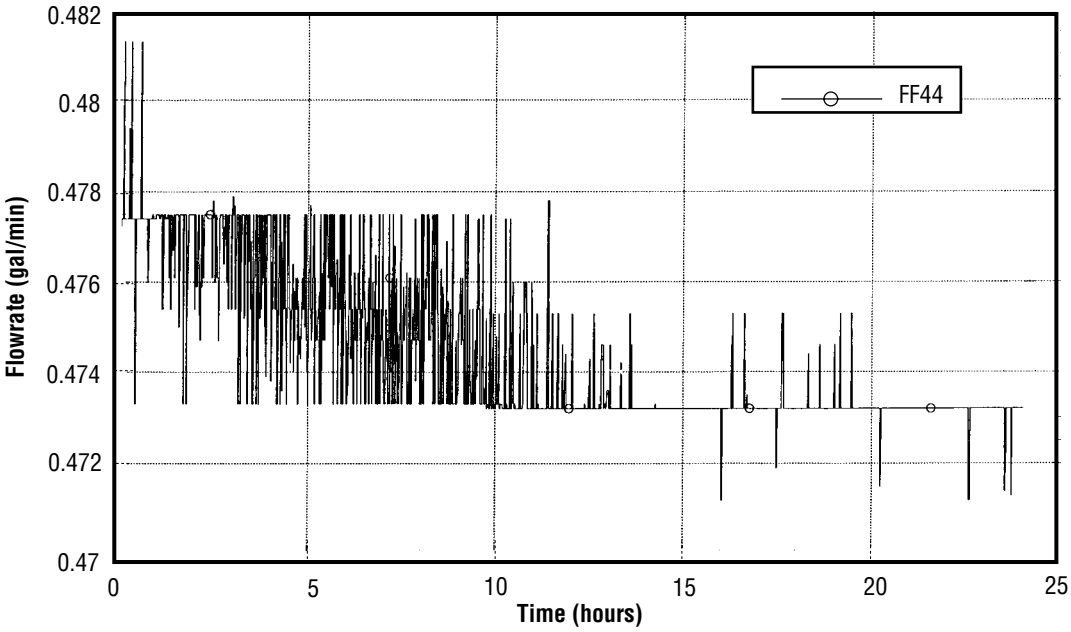

FIGURE A–31.—Plot 13: Precooler coolant flowrate 4BMS baseline 2 testing—day/night mode elapsed time from 2–23–96, 17:00:00.

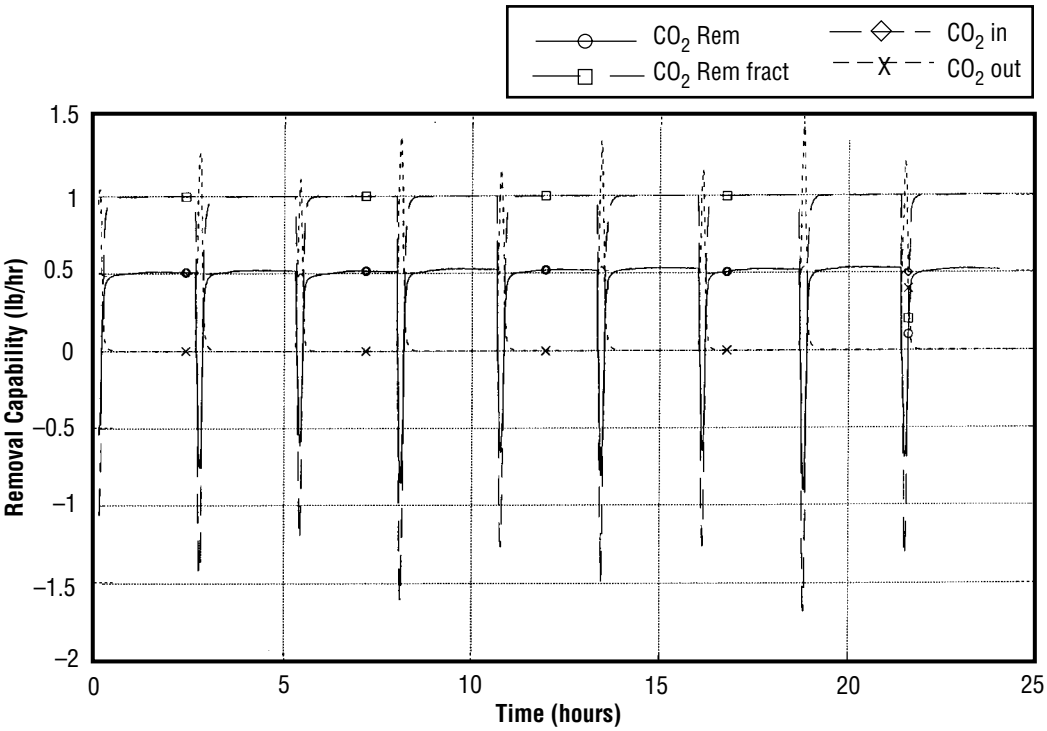

FIGURE A–32.—Plot 14: CO_2 removal capability 4BMS baseline 2 testing—day/night mode elapsed time from 2–23–96, 17:00:00.

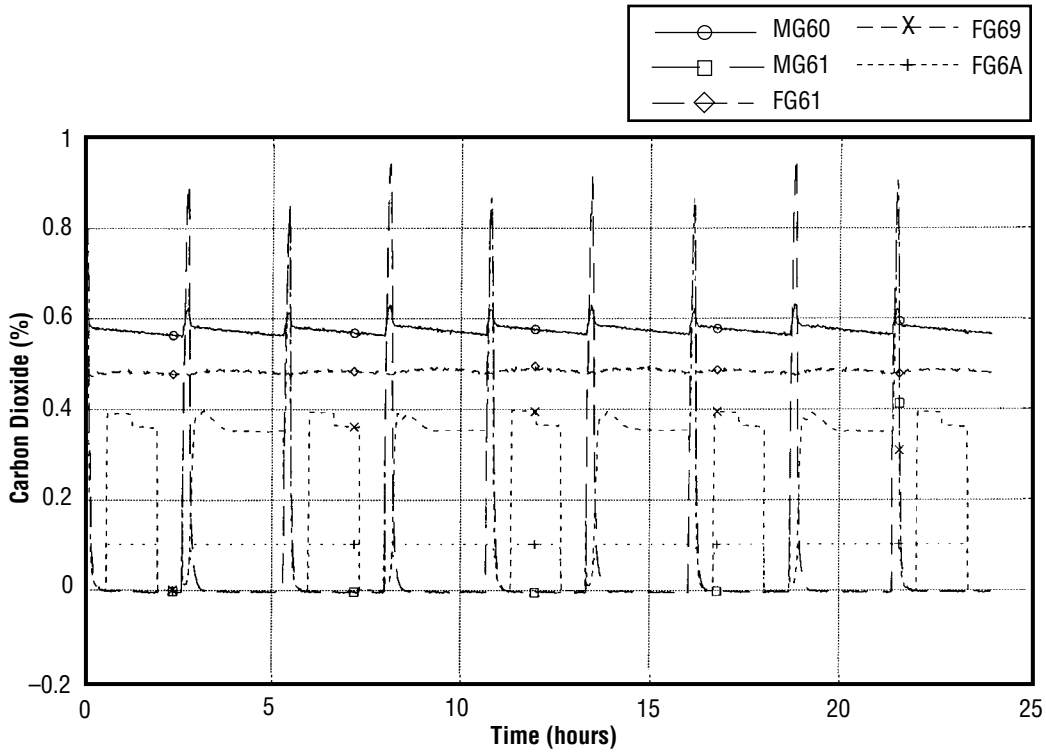

FIGURE A–33.—Plot 15: Percent carbon dioxide 4BMS baseline 2 testing—day/night mode elapsed time from 2–23–96, 17:00:00.

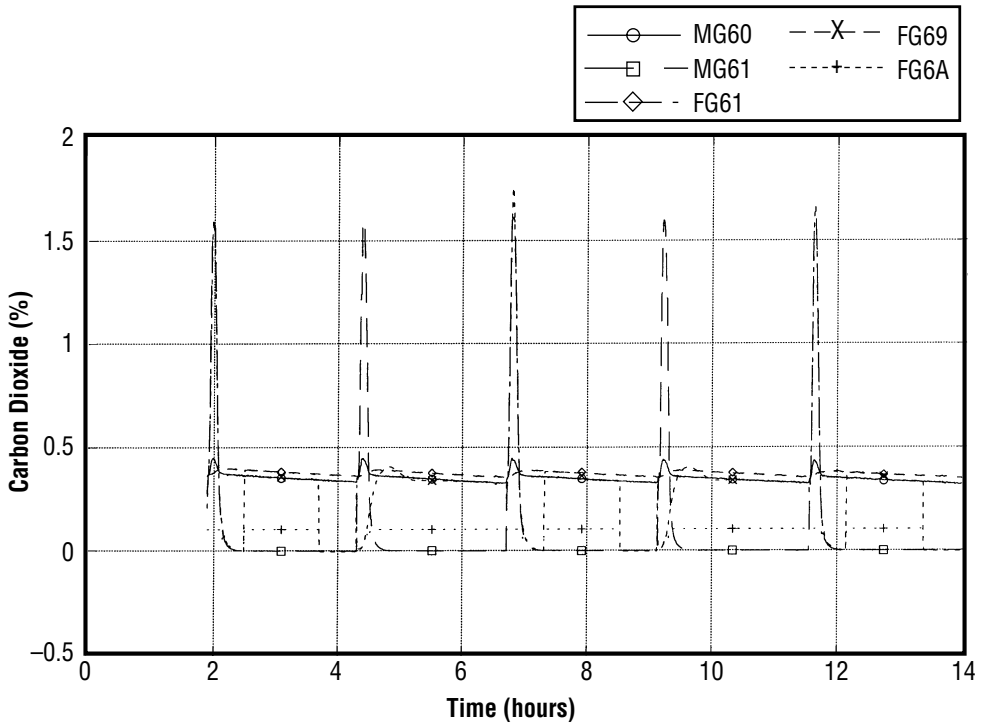

FIGURE A–34.—Plot 1: Percent carbon dioxide 4BMS baseline 3A testing—day/night mode elapsed time from 3–2–96, 00:00:00.

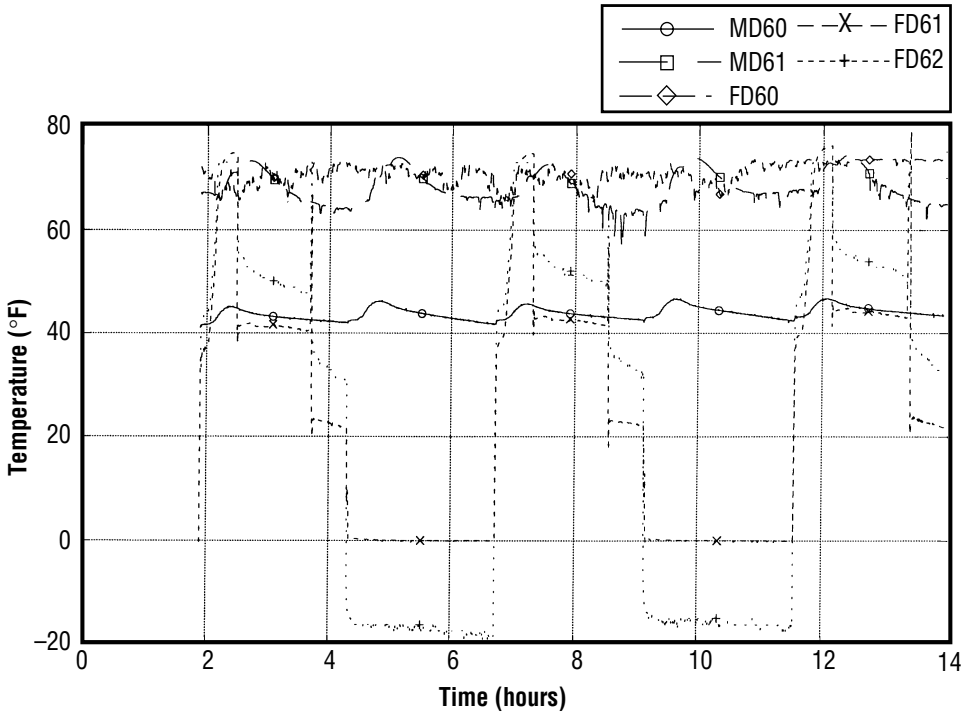

FIGURE A–35.—Plot 2: Dewpoint temperatures 4BMS baseline 3A testing—day/night mode elapsed time from 3–2–96, 00:00:00.

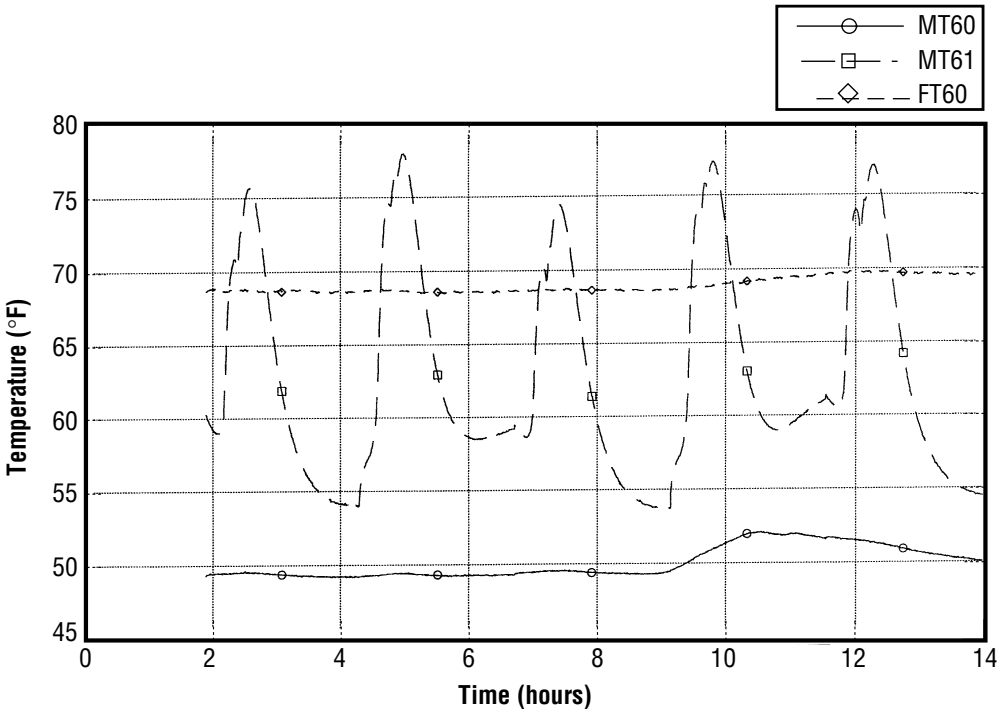

FIGURE A–36.—Plot 3: Inlet/outlet/module temperatures 4BMS baseline 3A testing—day/night mode elapsed time from 3–2–96, 00:00:00.

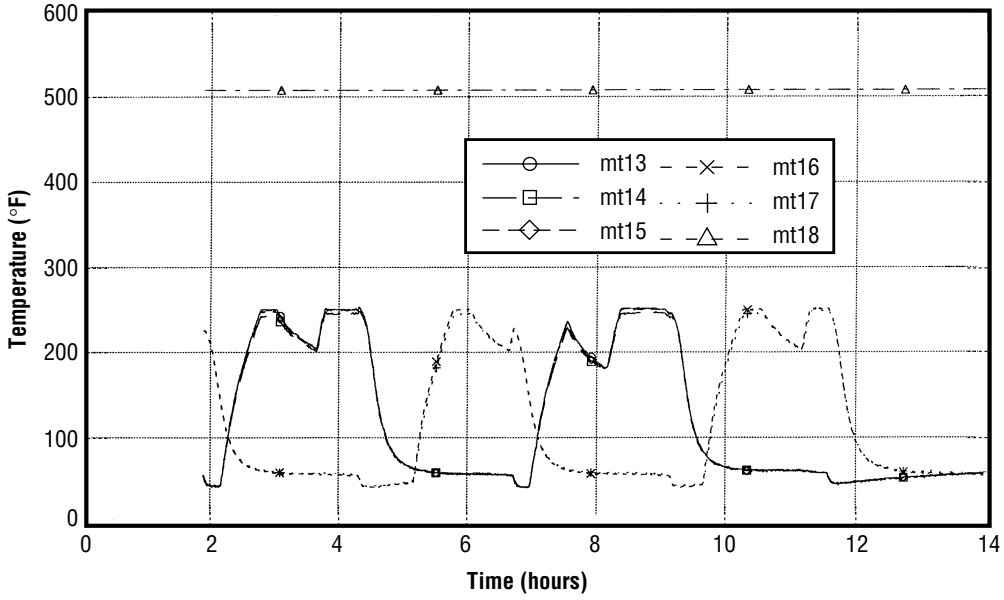

FIGURE A–37.—Plot 4: 5A sorbent bed temperatures 4BMS baseline 3A testing—day/night mode elapsed time from 3–2–96, 00:00:00.

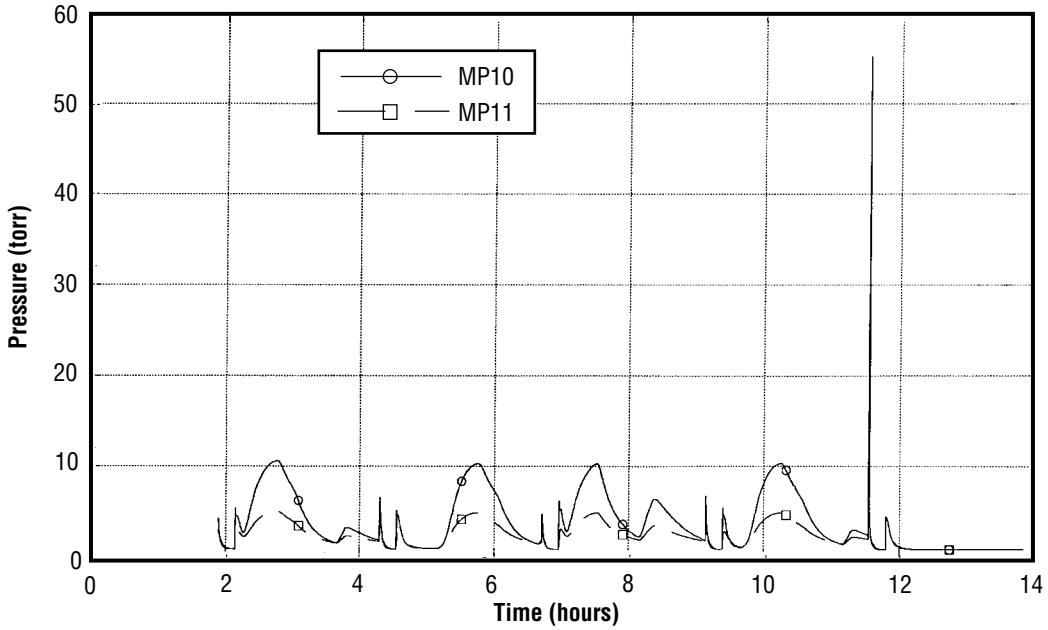

FIGURE A–38.—Plot 5: Vacuum line pressures 4BMS baseline 3A testing—day/night mode elapsed time from 3–2–96, 00:00:00.

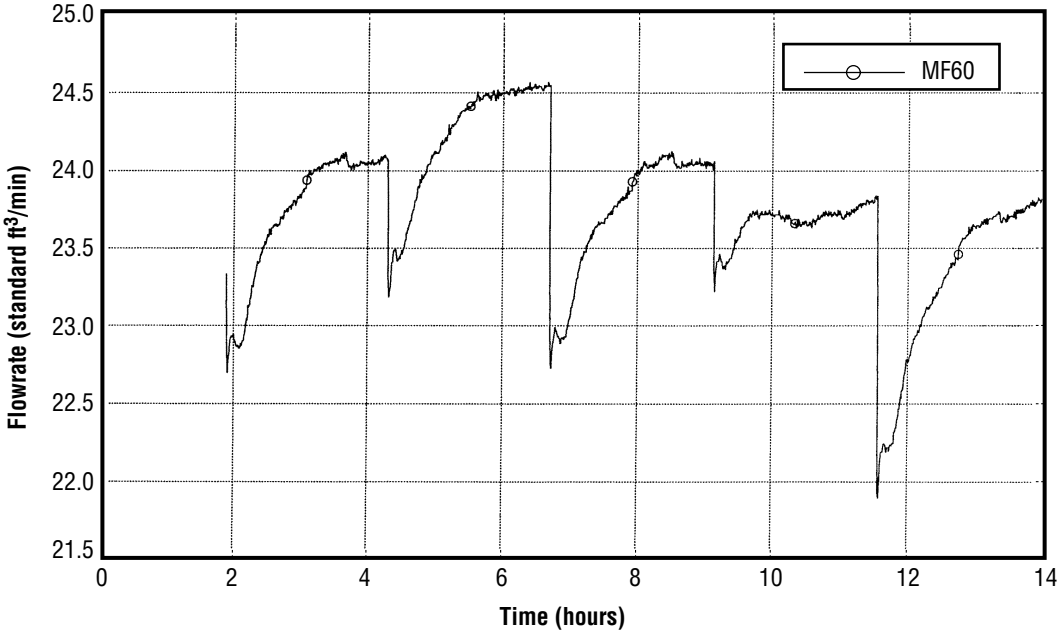

FIGURE A–39.—Plot 6: Flowrate 4BMS baseline 3A testing—day/night mode elapsed time from 3–2–96, 00:00:00.

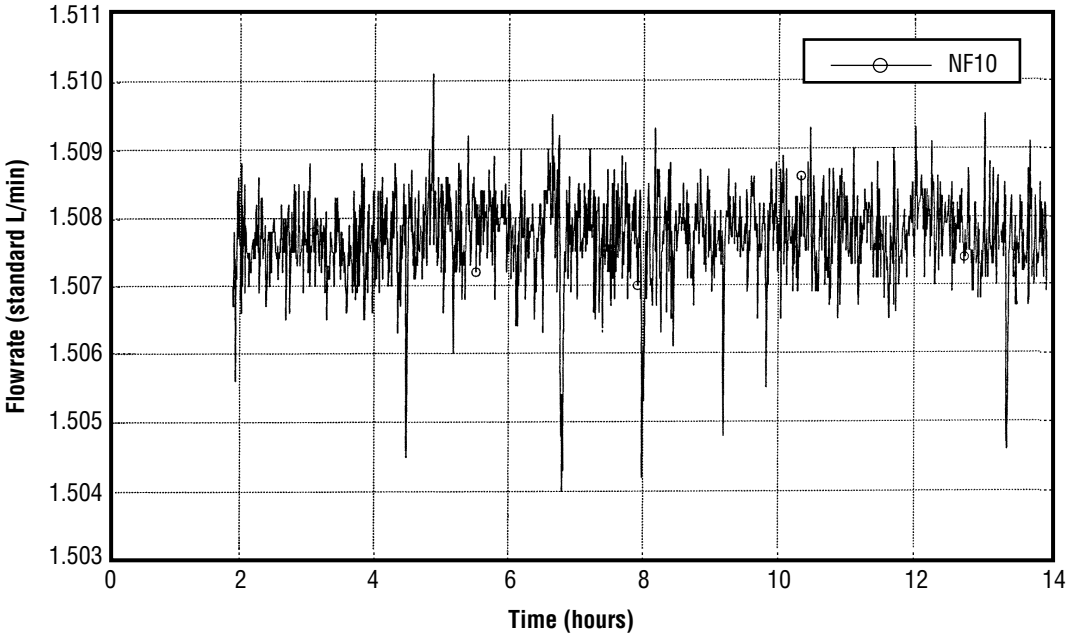

FIGURE A–40.—Plot 7: CO_2 injection flowrate 4BMS baseline 3A testing—day/night mode elapsed time from 3–2–96, 00:00:00.

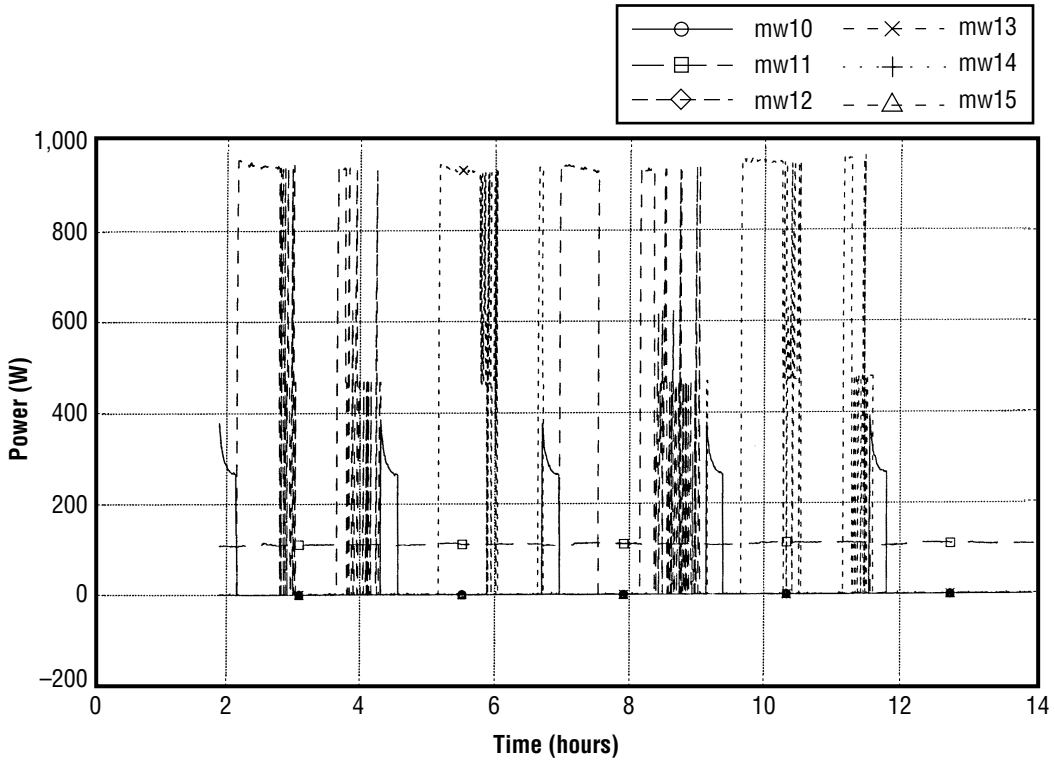

FIGURE A–41.—Plot 8: Power consumption 4BMS baseline 3A testing—day/night mode elapsed time from 3–2–96, 00:00:00.

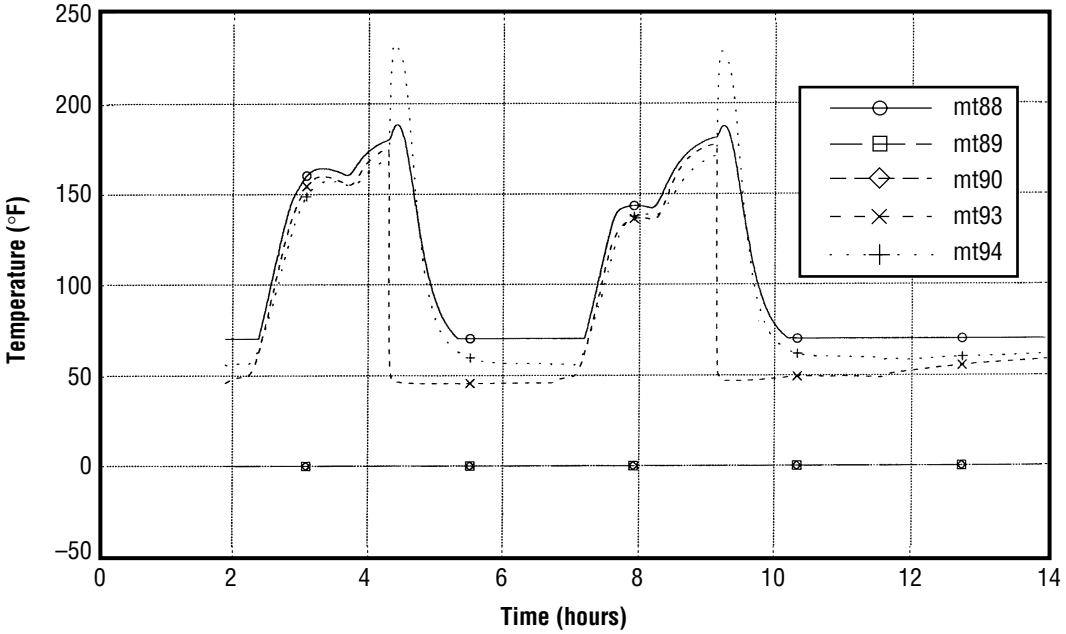

FIGURE A–42.—Plot 9: 5A sorbent bed 308 temperatures 4BMS baseline 3A testing—day/night mode elapsed time from 3–2–96, 00:00:00.

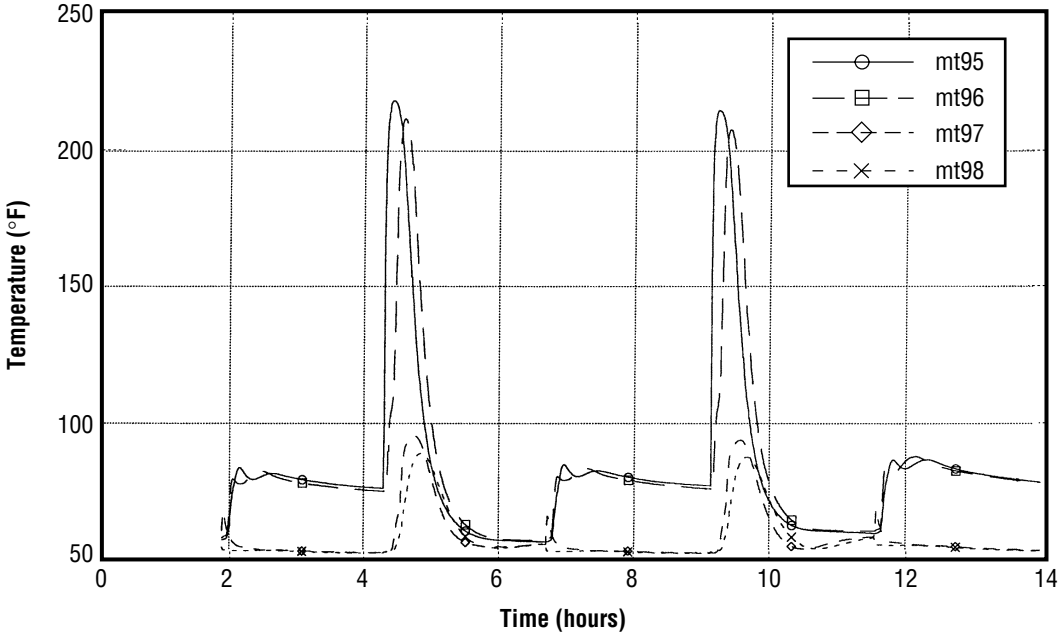

FIGURE A–43.—Plot 10: Dessicant bed 308 temperatures 4BMS baseline 3A testing—day/night mode elapsed time from 3–2–96, 00:00:00.

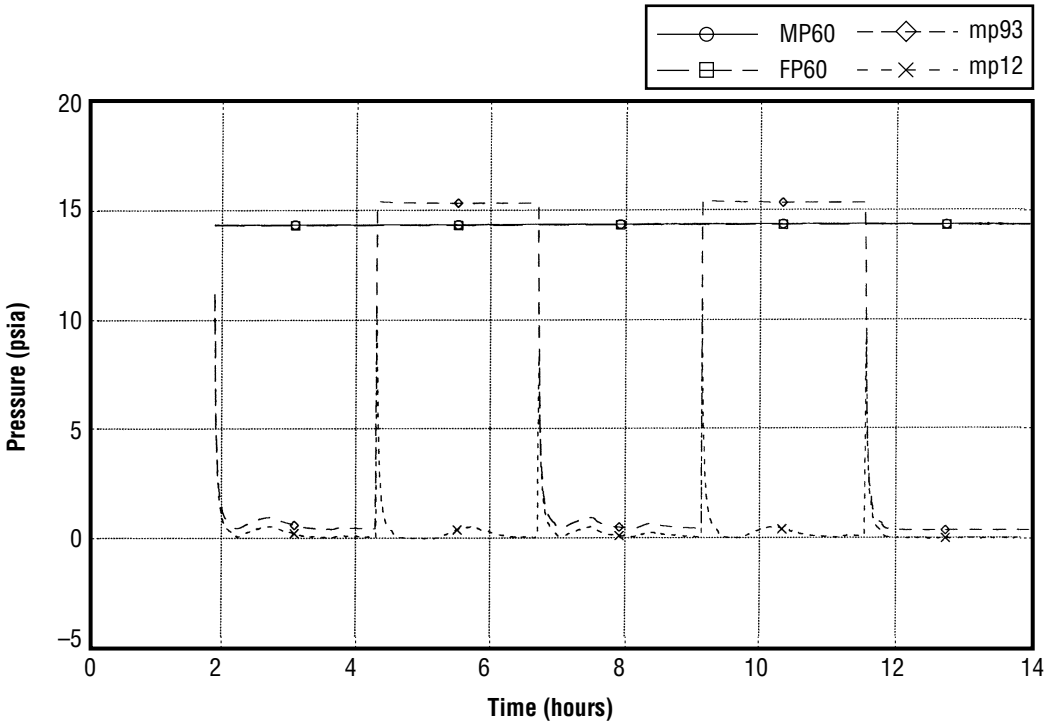

FIGURE A–44.—Plot 11: Inlet/module/bed 309 pressures 4BMS baseline 3A testing—day/night mode elapsed time from 3–2–96, 00:00:00.

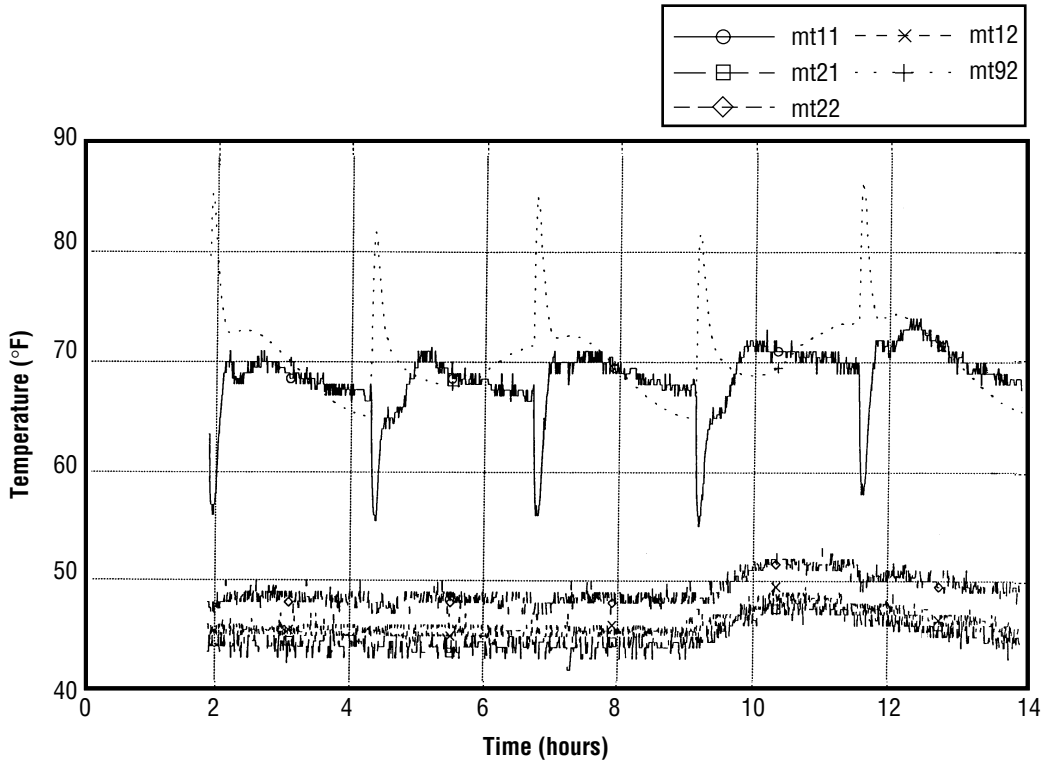

FIGURE A–45.—Plot 12: Process temperatures 4BMS baseline 3A testing—day/night mode elapsed time from 3–2–96, 00:00:00.

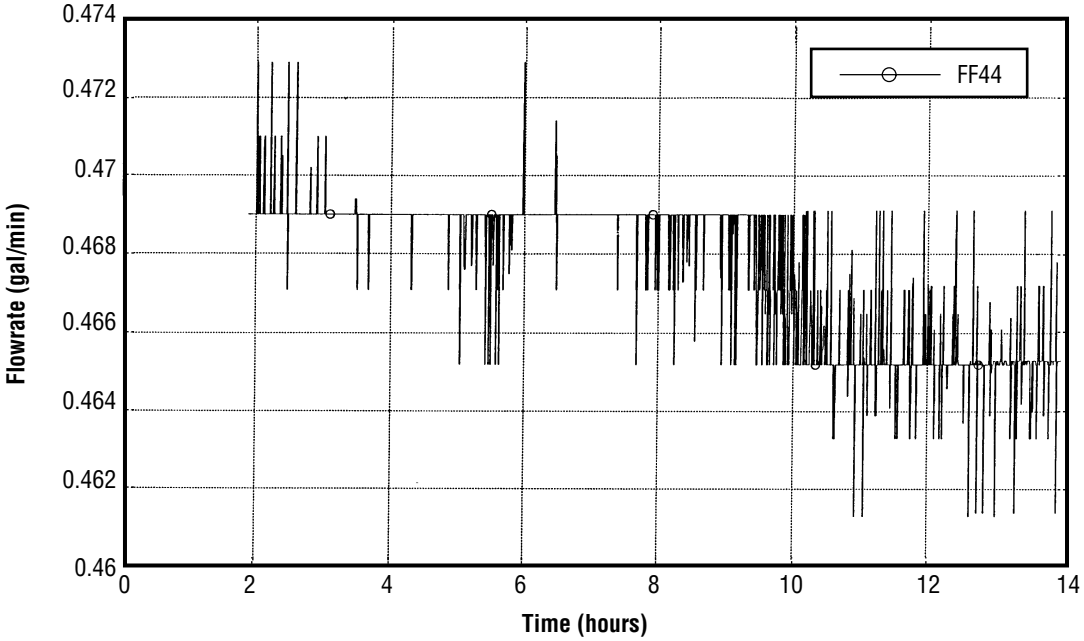

FIGURE A–46.—Plot 13: Precooler coolant flowrate 4BMS baseline 3A testing—day/night mode, elapsed time from 3–2–96, 00:00:00.

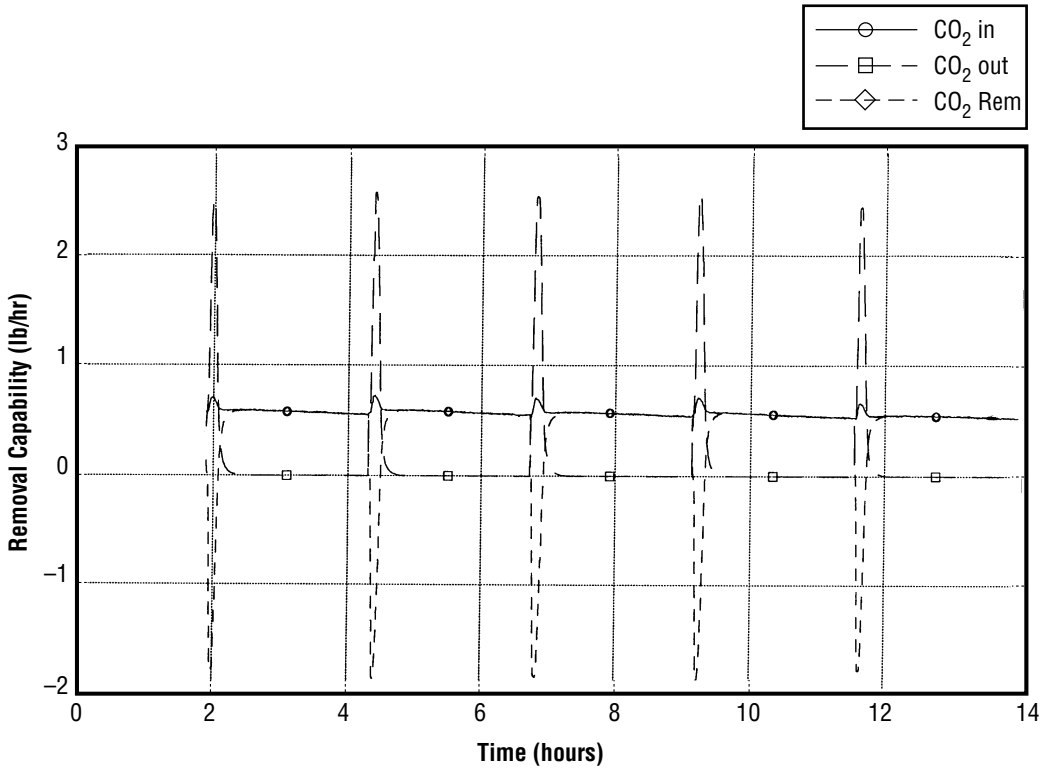

FIGURE A–47.—Plot 14: CO_2 removal capability 4BMS baseline 3A testing—day/night mode, elapsed time from 3–2–96, 00:00:00.

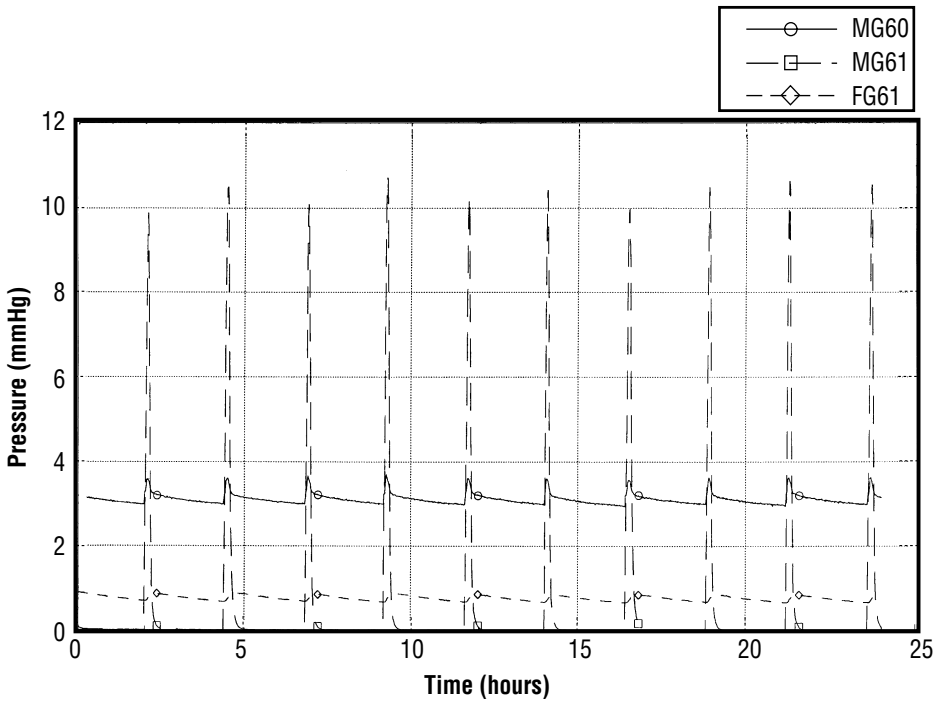

FIGURE A–48.—Plot 1: Carbon dioxide partial pressure 4BMS baseline 3B testing—day/night mode, elapsed time from 3–10–96, 00:00:00.

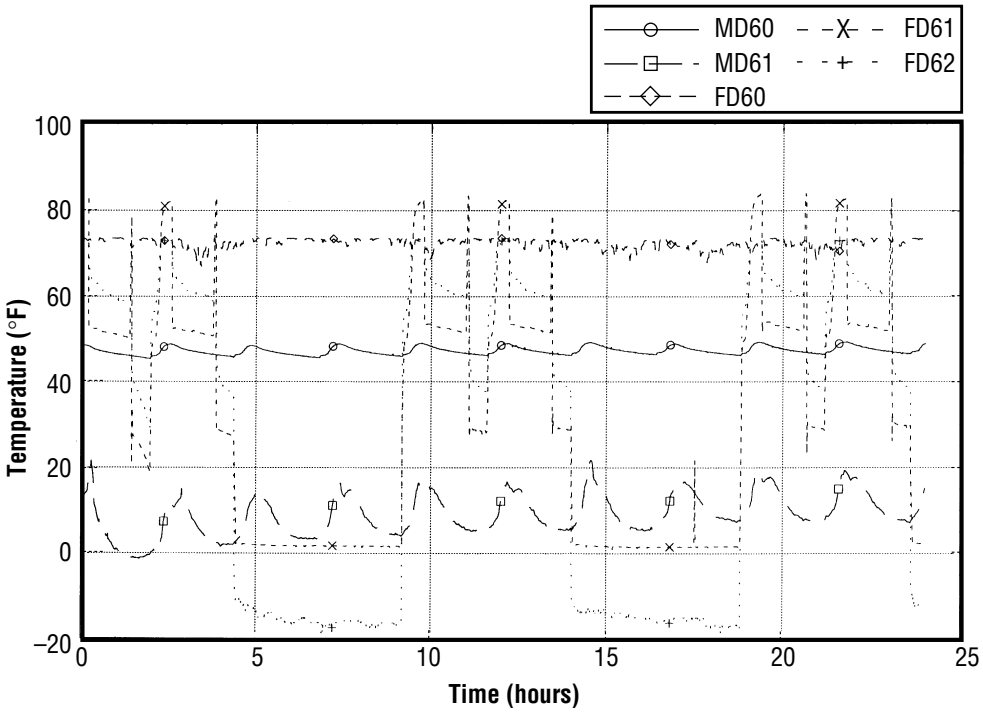

FIGURE A–49.—Plot 2: Dewpoint temperatures 4BMS baseline 3B testing—day/night mode, elapsed time from 3–10–96, 00:00:00.

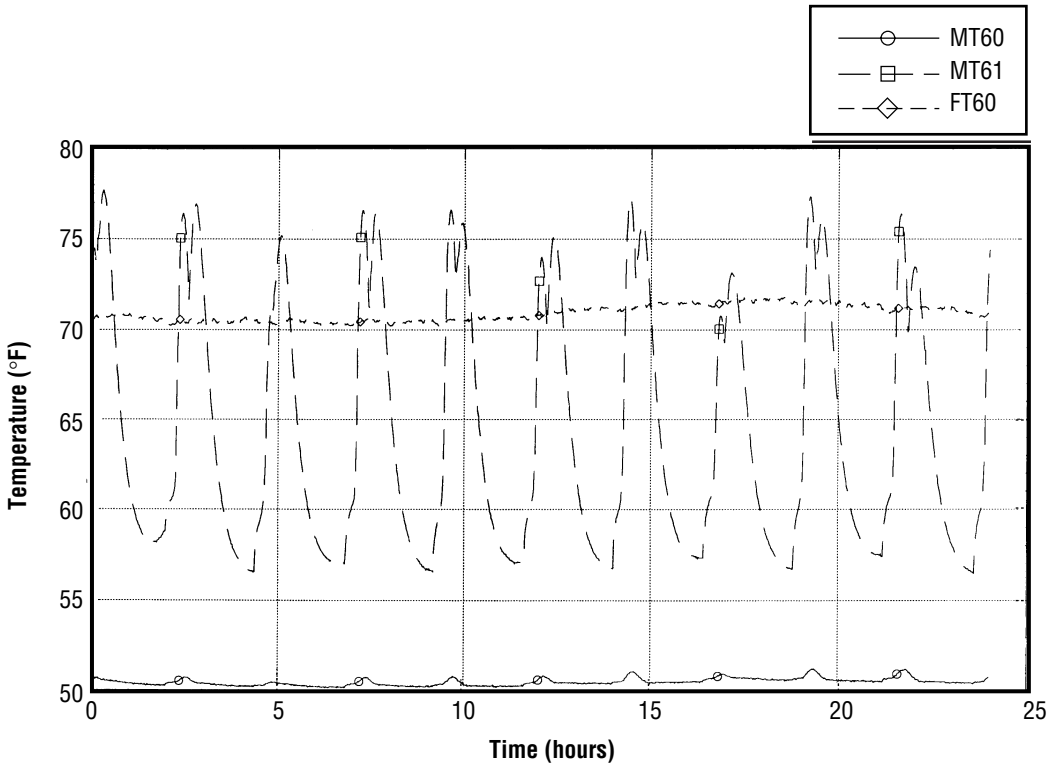

FIGURE A–50.—Plot 3: Inlet/outlet module temperatures 4BMS baseline 3B testing—day/night mode, elapsed time from 3–10–96, 00:00:00.

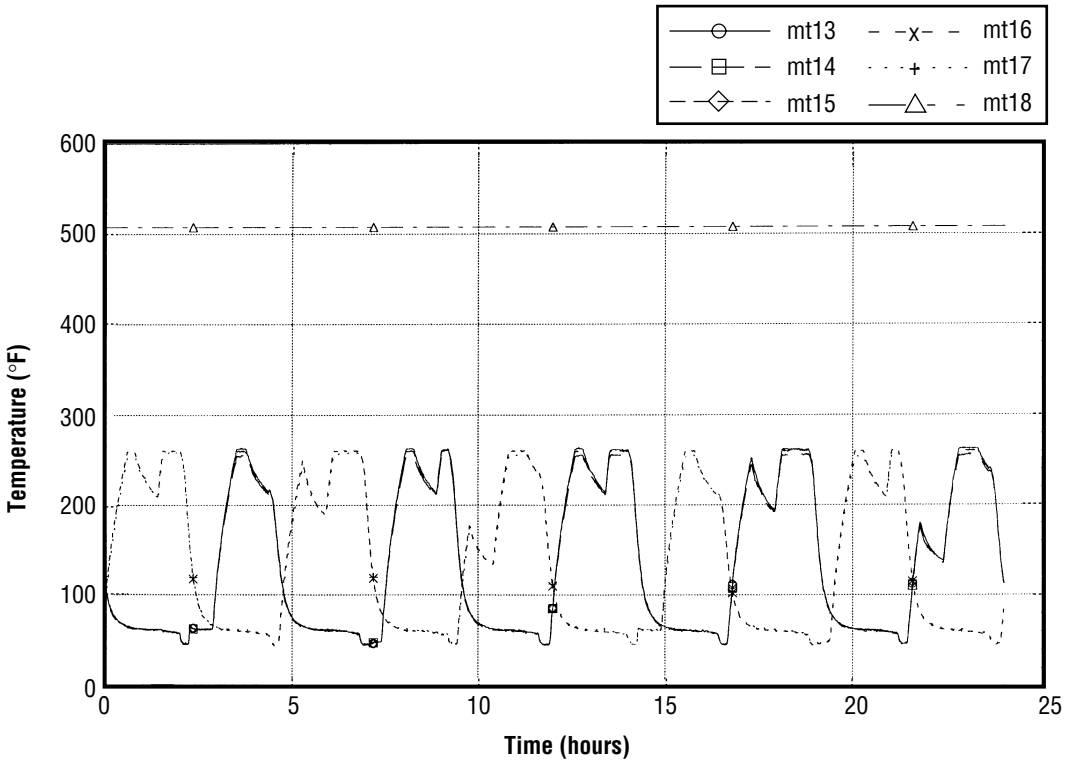

FIGURE A–51.—Plot 4: 5A sorbent bed temperatures 4BMS baseline 3B testing—day/night mode, elapsed time from 3–10–96, 00:00:00.

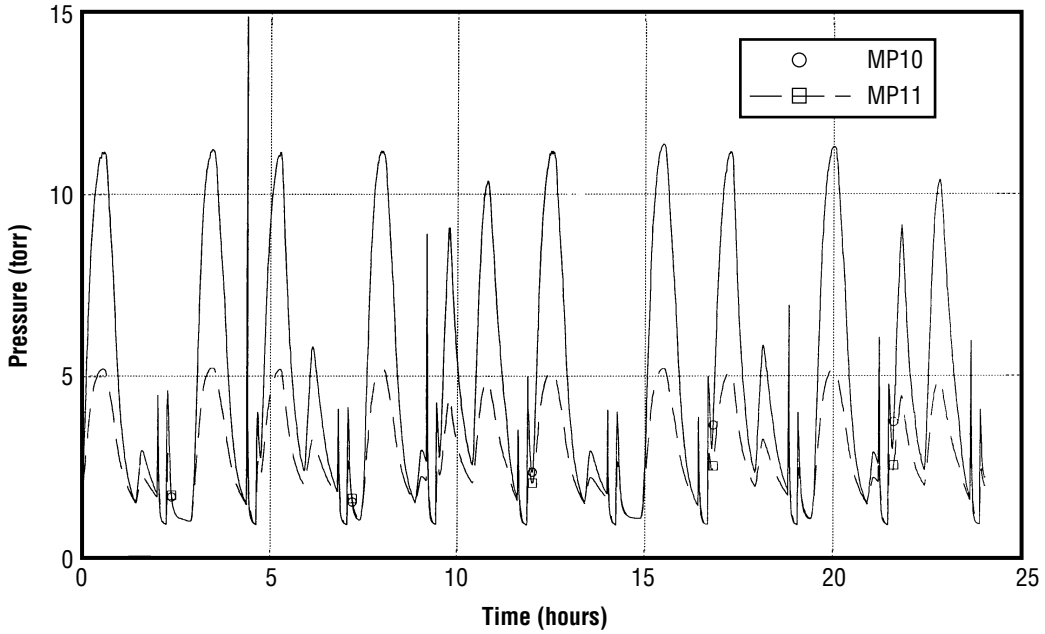

FIGURE A–52.—Plot 5: Vacuum line pressures 4BMS baseline 3B testing—day/night mode, elapsed time from 3–10–96, 00:00:00.

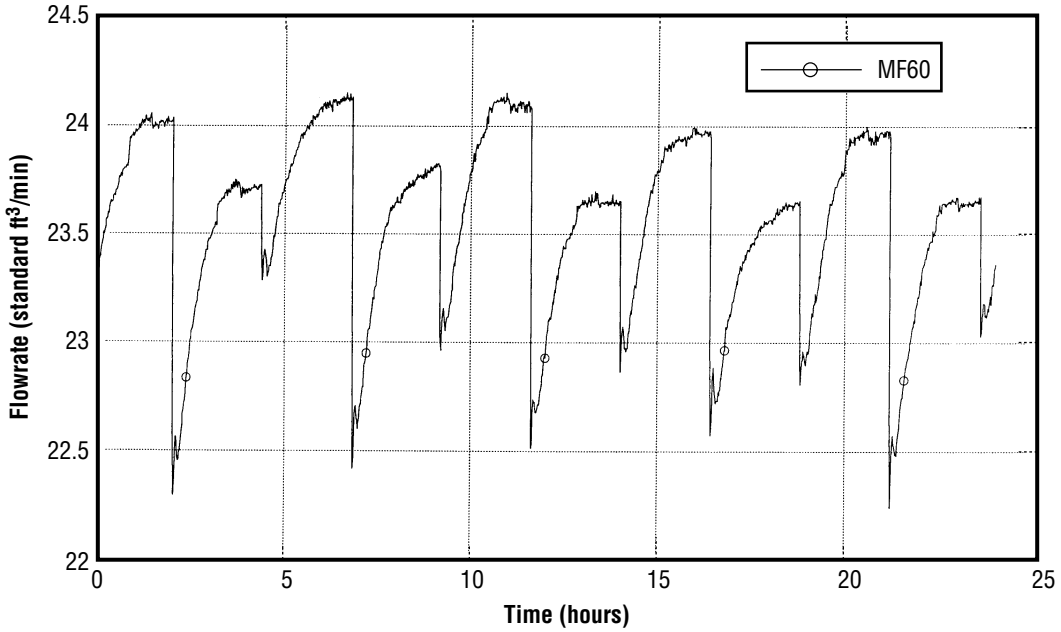

FIGURE A–53.—Plot 6: Flowrate 4BMS baseline 3B testing—day/night mode, elapsed time from 3–10–96, 00:00:00.

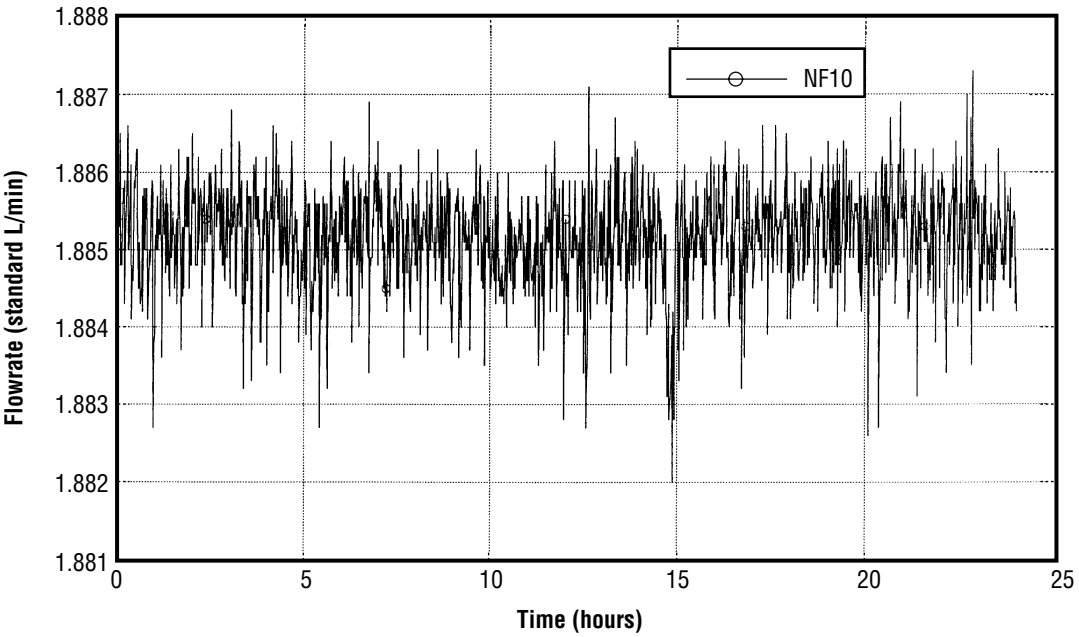

FIGURE A–54.—Plot 7: CO_2 injection flowrate 4BMS baseline 3B testing—day/night mode, elapsed time from 3–10–96, 00:00:00.

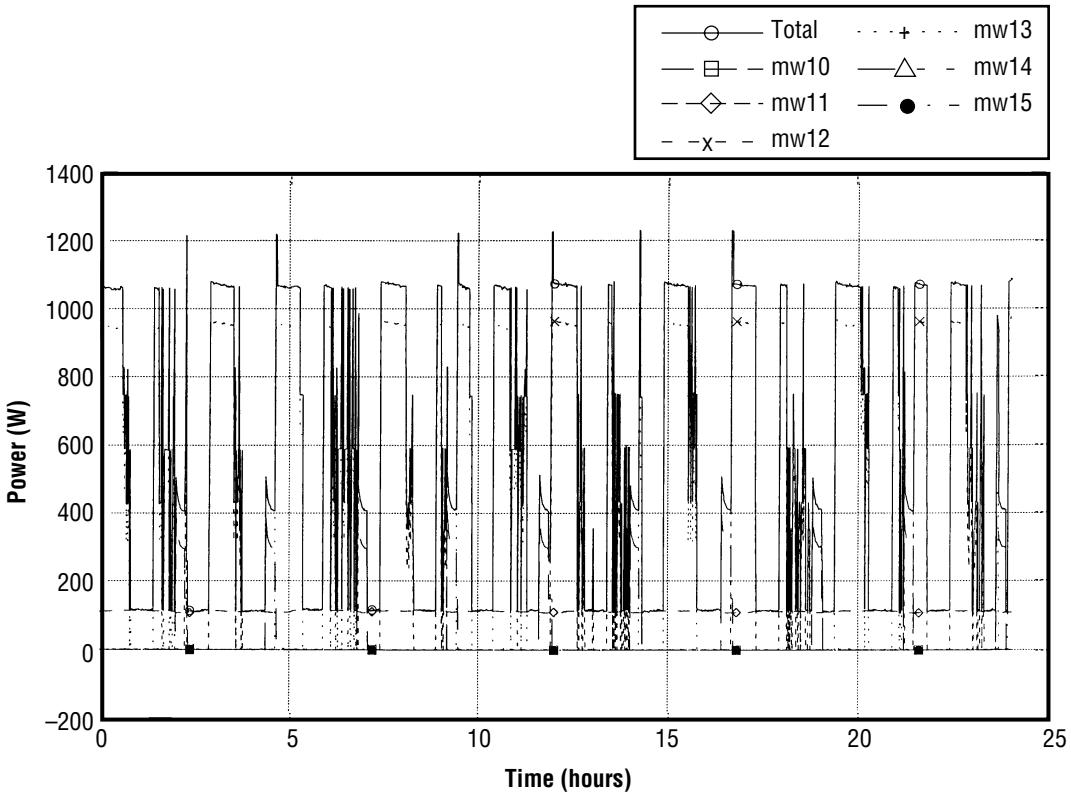

FIGURE A–55.—Plot 8: Power consumption 4BMS baseline 3B testing—day/night mode, elapsed time from 3–10–96, 00:00:00.

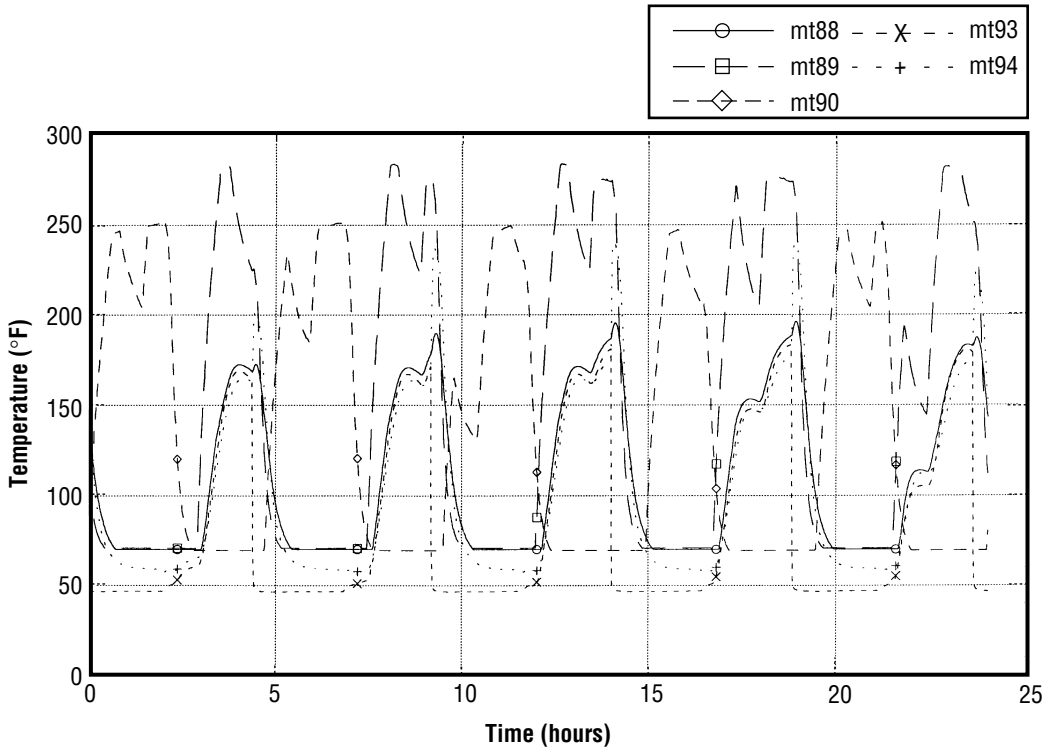

FIGURE A–56.—Plot 9: 5A sorbent bed 308 temperatures 4BMS baseline 3B testing—day/night mode, elapsed time from 3–10–96, 00:00:00.

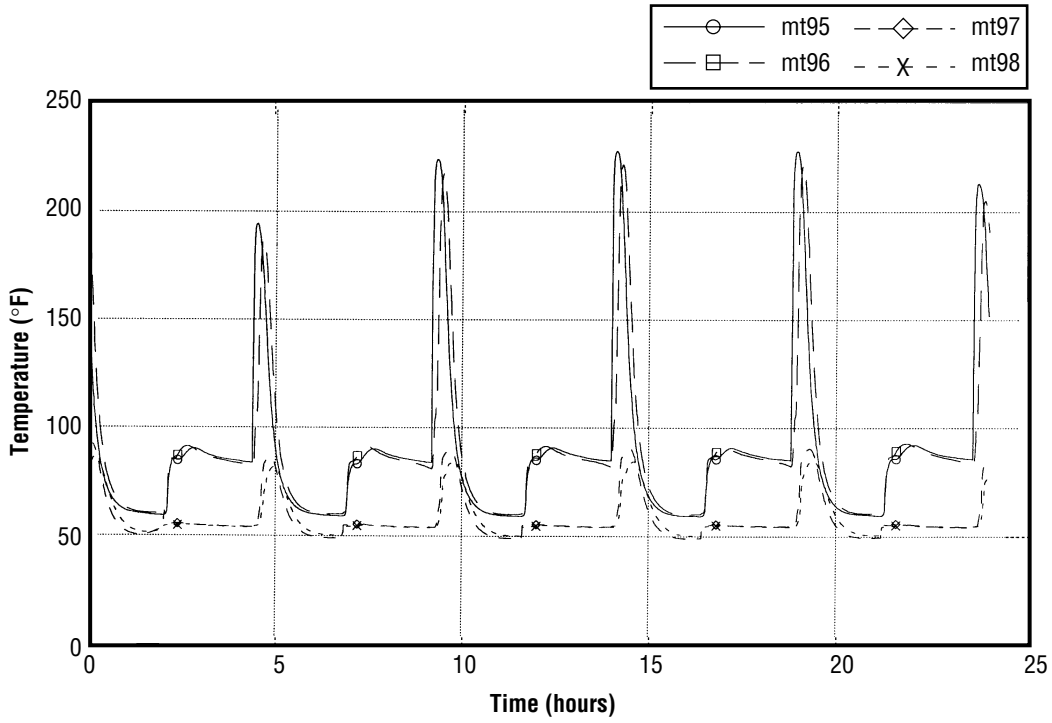

FIGURE A–57.—Plot 10: Dessicant bed temperatures 4BMS baseline 3B testing—day/night mode, elapsed time from 3–10–96, 00:00:00.

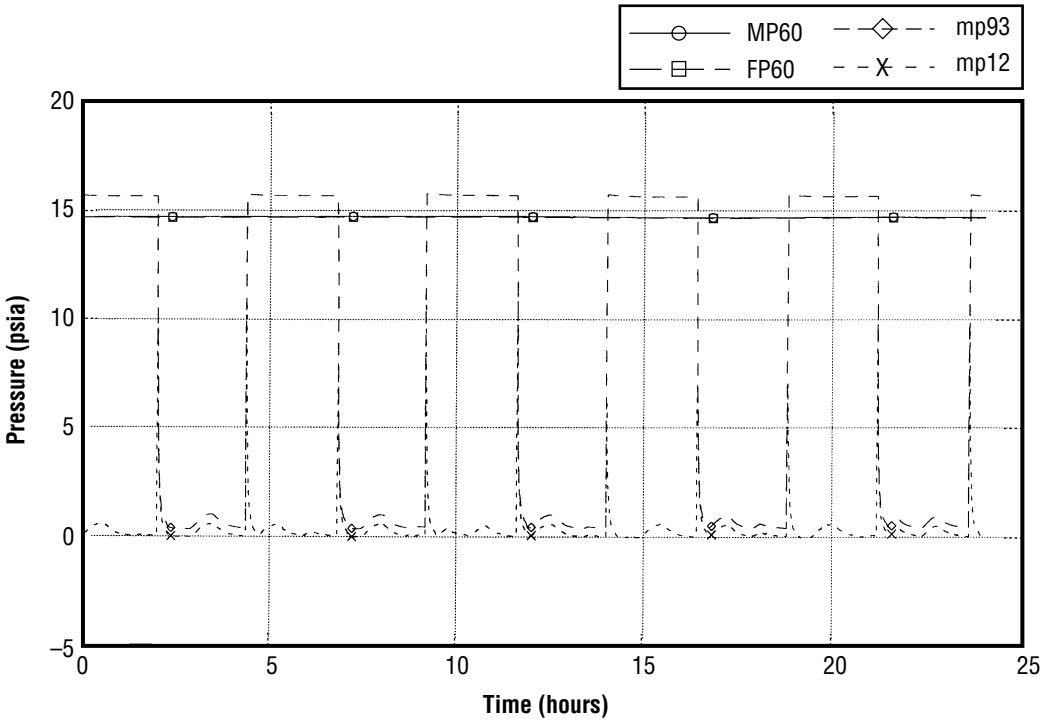

FIGURE A–58.—Plot 11: Inlet/module/bed 309 pressures 4BMS baseline 3B testing—day/night mode, elapsed time from 3–10–96, 00:00:00.

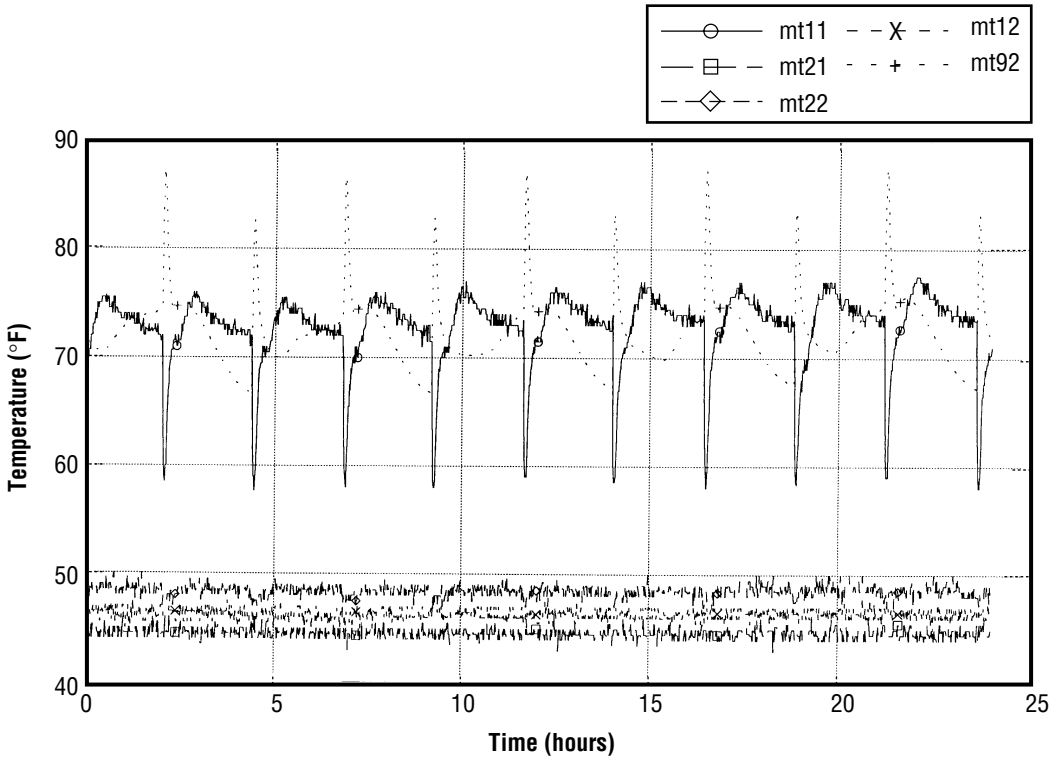

FIGURE A–59.—Plot 12: Process temperatures 4BMS baseline 3B testing day/night mode, elapsed time from 3–10–96, 00:00:00.

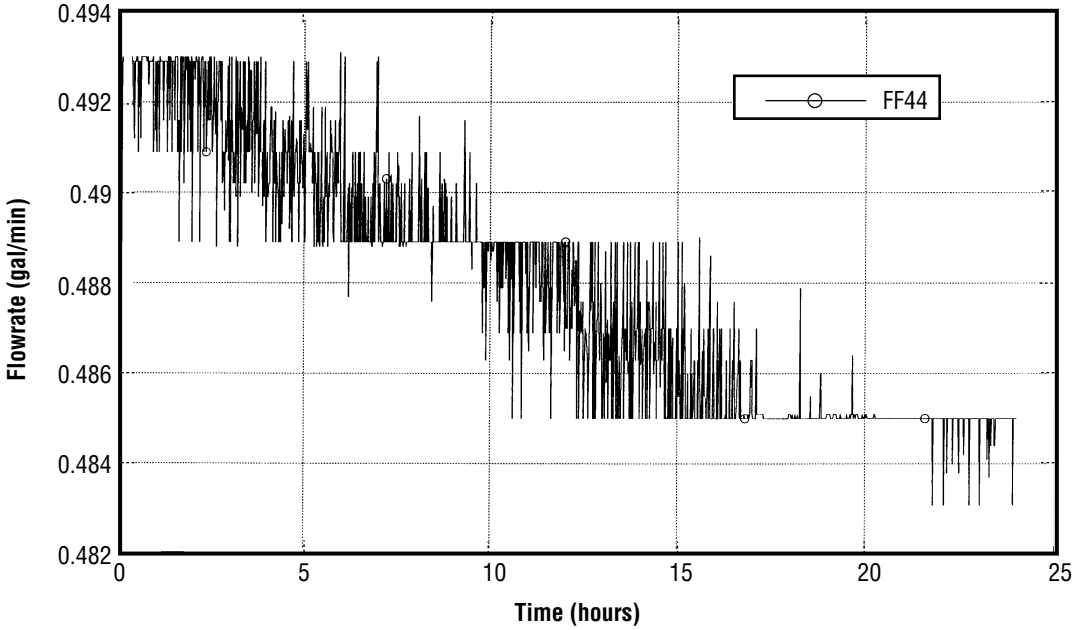

FIGURE A–60.—Plot 13: Precooler coolant flowrate 4BMS baseline 3B testing—day/night mode, elapsed time from 3–10–96, 00:00:00.

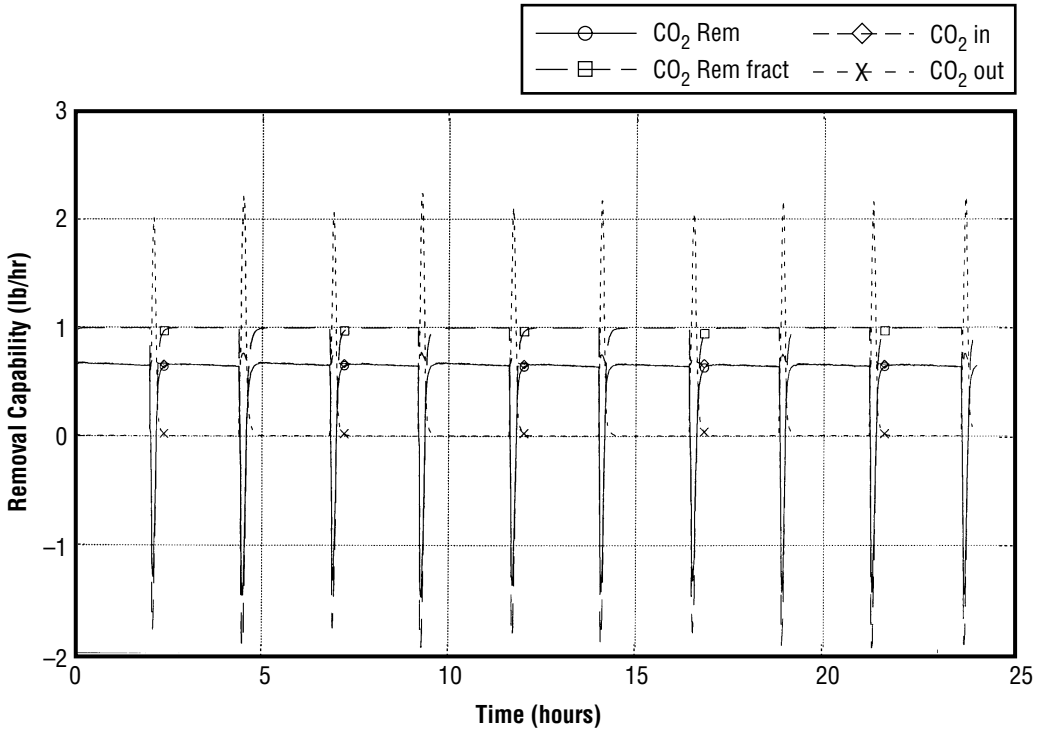

FIGURE A–61.—Plot 14: CO_2 removal capability 4BMS baseline 3B testing—day/night mode, elapsed time from 3–10–96, 00:00:00.

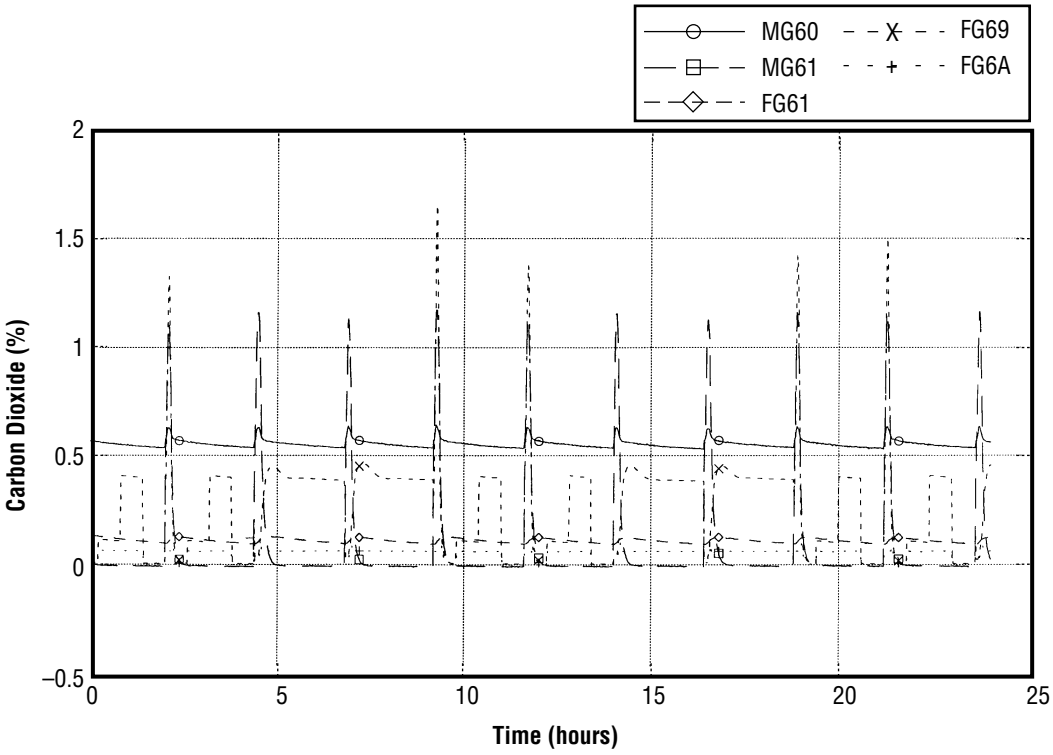

FIGURE A–62.—Plot 15: Percent carbon dioxide 4BMS baseline 3B testing—day/night mode, elapsed time from 3–10–96, 00:00:00.

APPENDIX B—
CMS TEMPERATURE AND PRESSURE DATA PLOTS

Test chamber temperature and pressure were maintained within the specified ranges during all periods of uninterrupted operations between March 22 and April 12, 1996. A severe valley in the pressure data was observed on April 8. This was caused by switching data acquisition files to accommodate the time change to daylight savings time.

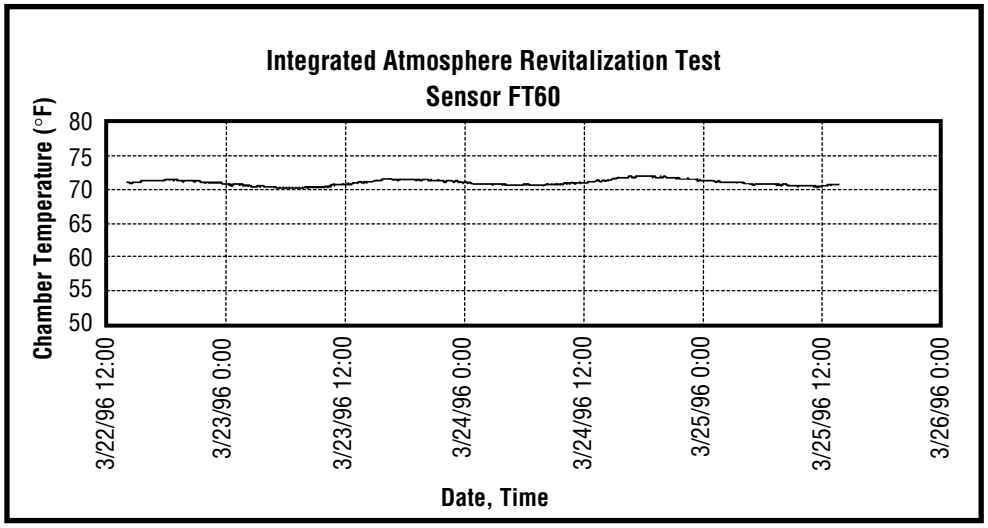
Integrated Atmosphere Revitalization Test
Sensor FT60
Chamber Temperature (°F)
80
75
70
65
60
55
50
3/22/96 12:00
3/23/96 0:00
3/23/96 12:00
3/24/96 0:00
3/24/96 12:00
3/25/96 0:00
3/25/96 12:00
3/26/96 0:00
Date, Time

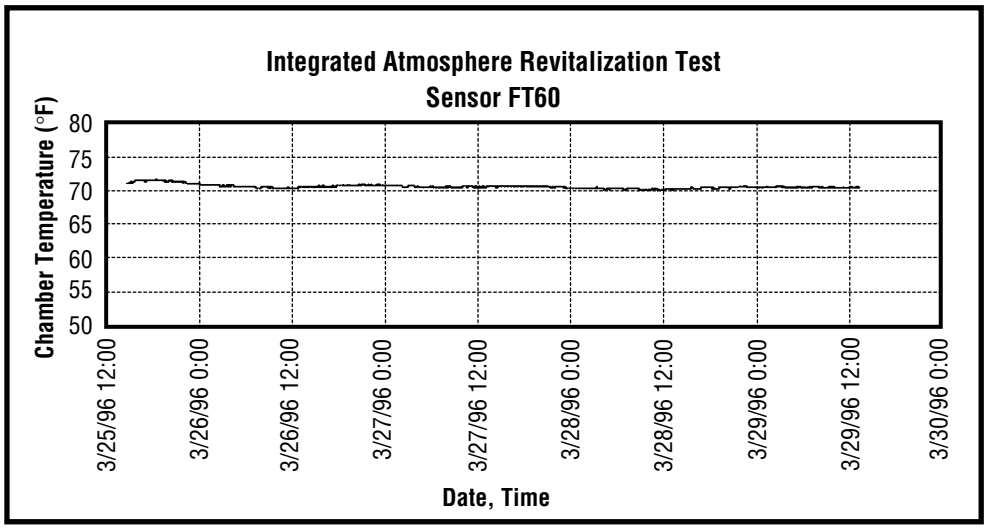
Integrated Atmosphere Revitalization Test
Sensor FT60
Chamber Temperature (°F)
80
75
70
65
60
55
50
3/25/96 12:00
3/26/96 0:00
3/26/96 12:00
3/27/96 0:00
3/27/96 12:00
3/28/96 0:00
3/28/96 12:00
3/29/96 0:00
3/29/96 12:00
3/30/96 0:00
Date, Time

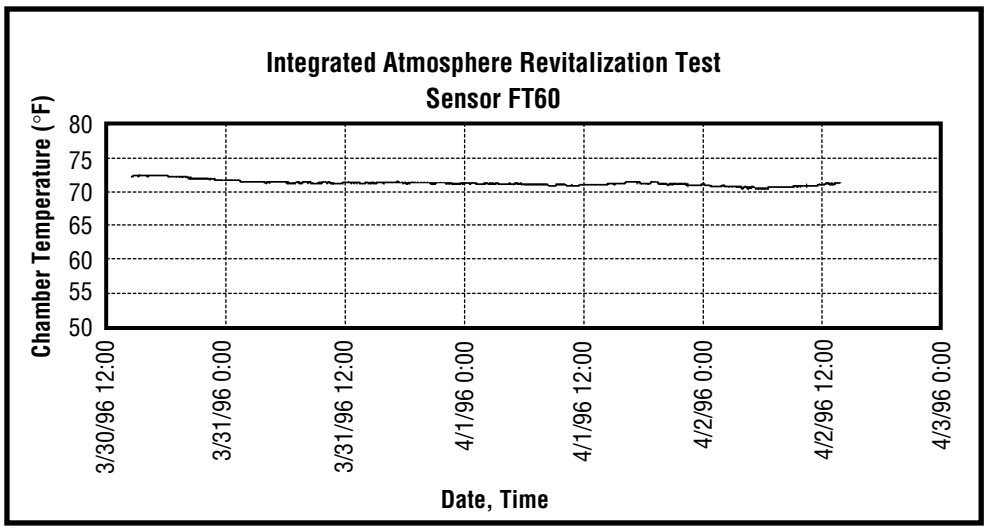
Integrated Atmosphere Revitalization Test
Sensor FT60
Chamber Temperature (°F)
80
75
70
65
60
55
50
3/30/96 12:00
3/31/96 0:00
3/31/96 12:00
4/1/96 0:00
4/1/96 12:00
4/2/96 0:00
4/2/96 12:00
4/3/96 0:00
Date, Time

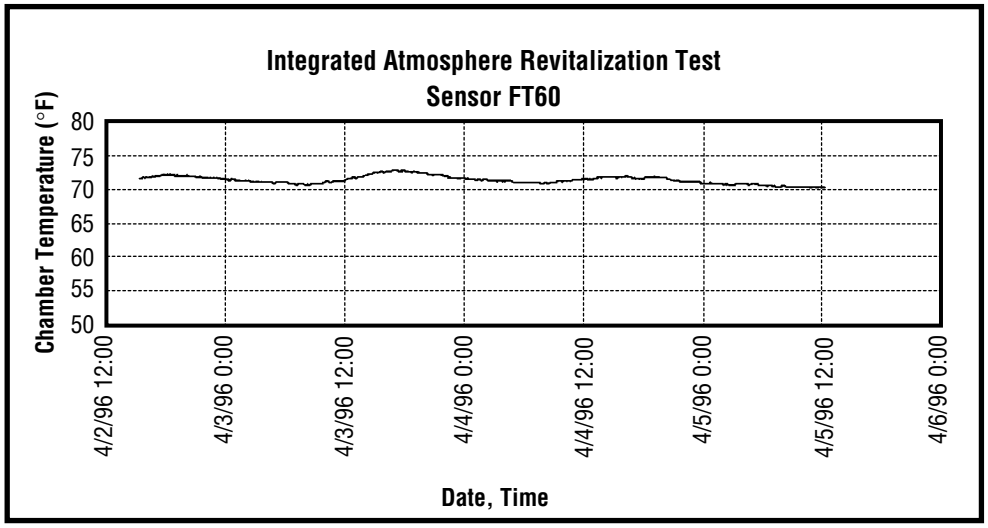
Integrated Atmosphere Revitalization Test
Sensor FT60
Chamber Temperature (°F)
80
75
70
65
60
55
50
4/2/96 12:00
4/3/96 0:00
4/3/96 12:00
4/4/96 0:00
4/4/96 12:00
4/5/96 0:00
4/5/96 12:00
4/6/96 0:00
Date, Time

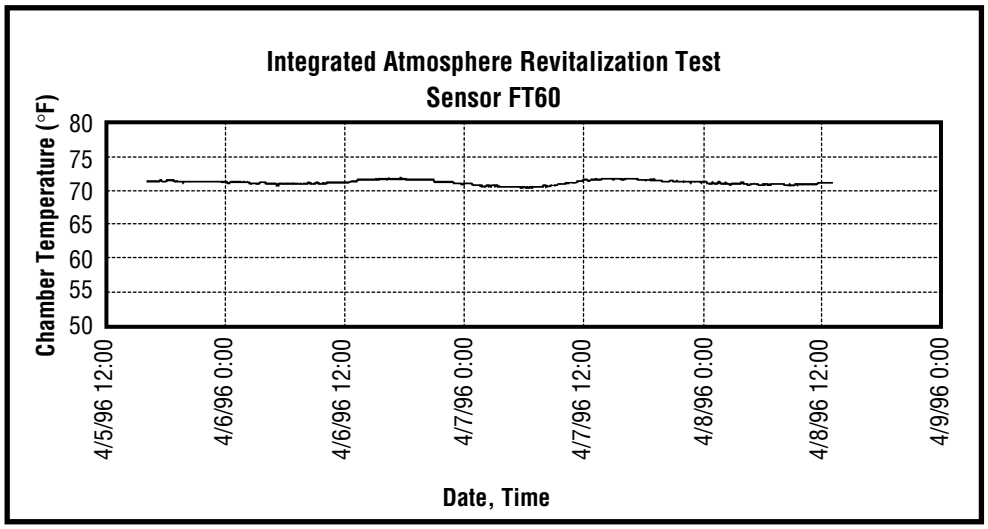
Integrated Atmosphere Revitalization Test
Sensor FT60
Chamber Temperature (°F)
80
75
70
65
60
55
50
4/5/96 12:00
4/6/96 0:00
4/6/96 12:00
4/7/96 0:00
4/7/96 12:00
4/8/96 0:00
4/8/96 12:00
4/9/96 0:00
Date, Time

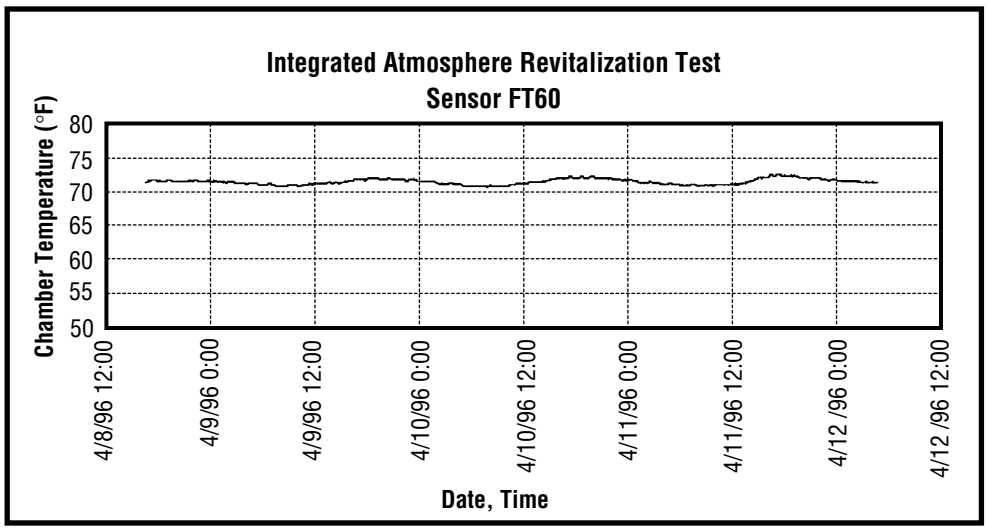
Integrated Atmosphere Revitalization Test
Sensor FT60
Chamber Temperature (°F)
80
75
70
65
60
55
50
4/8/96 12:00
4/9/96 0:00
4/9/96 12:00
4/10/96 0:00
4/10/96 12:00
4/11/96 0:00
4/11/96 12:00
4/12 /96 0:00
4/12 /96 12:00
Date, Time

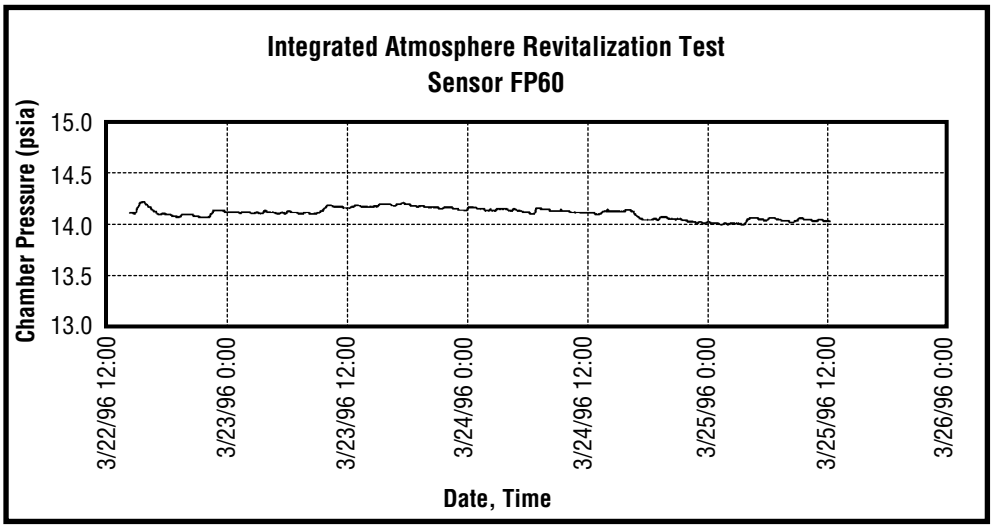
Integrated Atmosphere Revitalization Test
Sensor FP60
Chamber Pressure (psia)
15.0
14.5
14.0
13.5
13.0
3/22/96 12:00
3/23/96 0:00
3/23/96 12:00
3/24/96 0:00
3/24/96 12:00
3/25/96 0:00
3/25/96 12:00
3/26/96 0:00
Date, Time

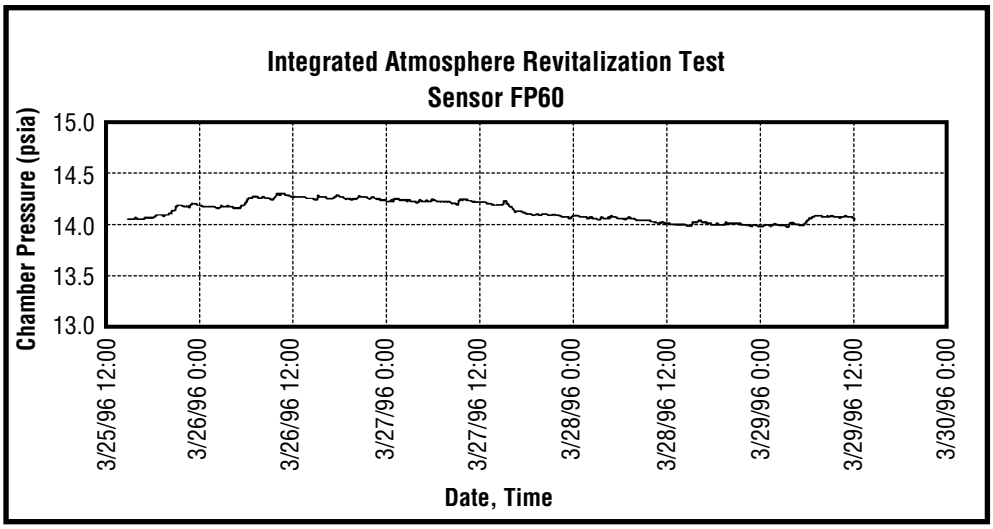
Integrated Atmosphere Revitalization Test
Sensor FP60
Chamber Pressure (psia)
15.0
14.5
14.0
13.5
13.0
3/25/96 12:00
3/26/96 0:00
3/26/96 12:00
3/27/96 0:00
3/27/96 12:00
3/28/96 0:00
3/28/96 12:00
3/29/96 0:00
3/29/96 12:00
3/30/96 0:00
Date, Time

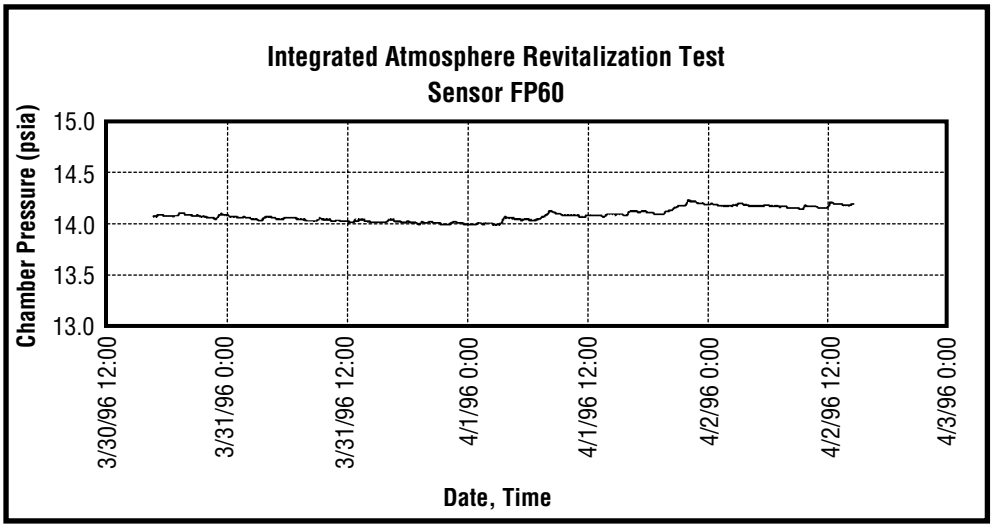
Integrated Atmosphere Revitalization Test
Sensor FP60
Chamber Pressure (psia)
15.0
14.5
14.0
13.5
13.0
3/30/96 12:00
3/31/96 0:00
3/31/96 12:00
4/1/96 0:00
4/1/96 12:00
4/2/96 0:00
4/2/96 12:00
4/3/96 0:00
Date, Time

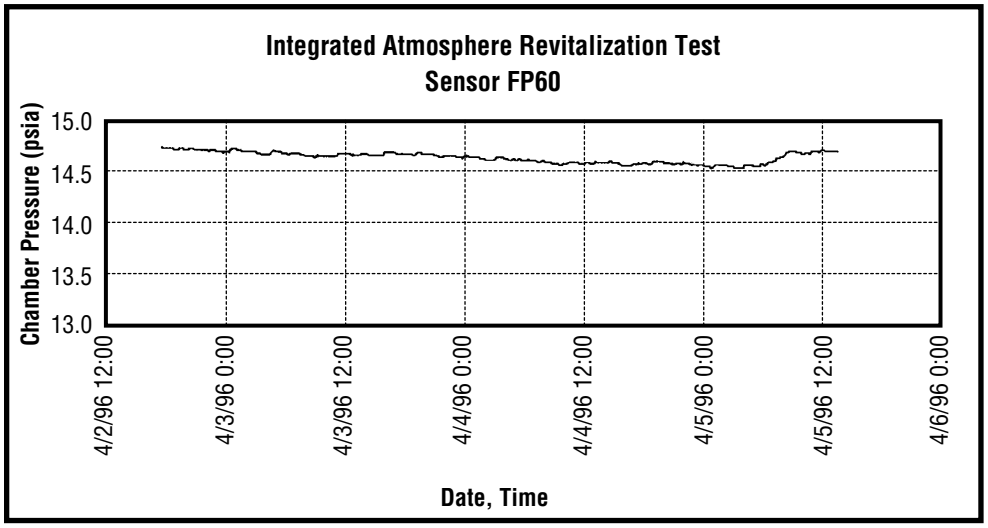
Integrated Atmosphere Revitalization Test
Sensor FP60
Chamber Pressure (psia)
15.0
14.5
14.0
13.5
13.0
4/2/96 12:00
4/3/96 0:00
4/3/96 12:00
4/4/96 0:00
4/4/96 12:00
4/5/96 0:00
4/5/96 12:00
4/6/96 0:00
Date, Time

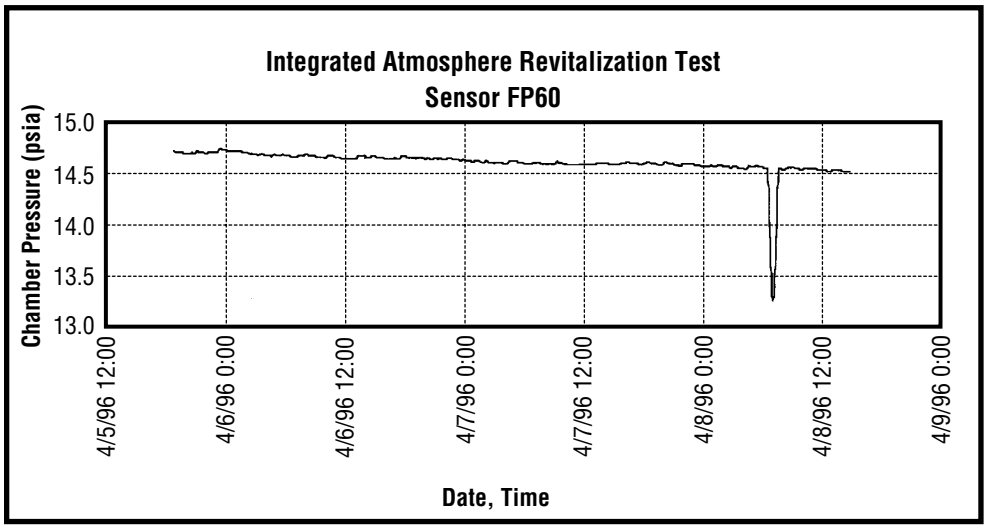
Integrated Atmosphere Revitalization Test
Sensor FP60
Chamber Pressure (psia)
15.0
14.5
14.0
13.5
13.0
4/5/96 12:00
4/6/96 0:00
4/6/96 12:00
4/7/96 0:00
4/7/96 12:00
4/8/96 0:00
4/8/96 12:00
4/9/96 0:00
Date, Time

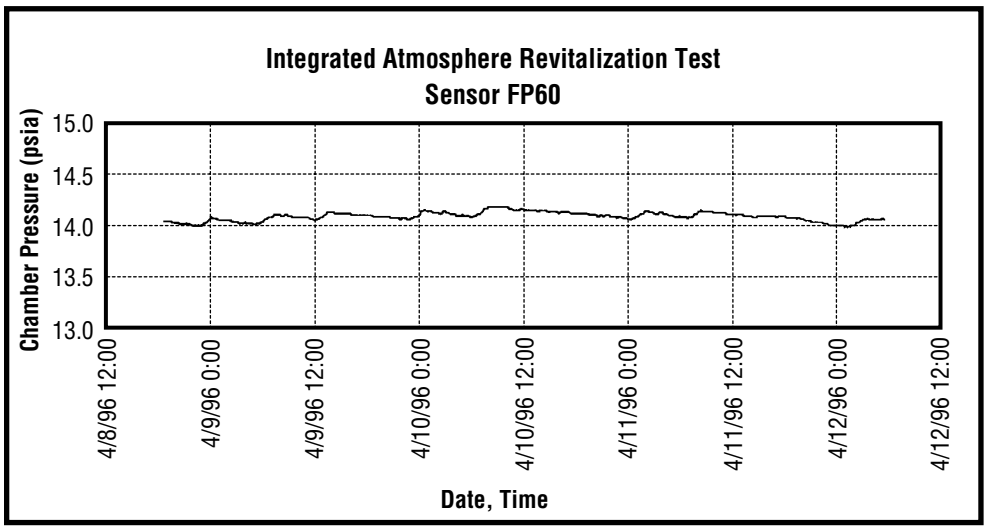
Integrated Atmosphere Revitalization Test
Sensor FP60
Chamber Pressure (psia)
15.0
14.5
14.0
13.5
13.0
4/8/96 12:00
4/9/96 0:00
4/9/96 12:00
4/10/96 0:00
4/10/96 12:00
4/11/96 0:00
4/11/96 12:00
4/12/96 0:00
4/12/96 12:00
Date, Time

APPENDIX C—
SUMMARY OF CMS ATMOSPHERIC SAMPLES

The following tables provide a summary of the test chamber atmospheric composition as determined by several sampling and analysis techniques. Results for the major atmospheric constituents, N_2, O_2, CO_2, and H_2O, are provided. Good agreement was obtained for measurements made by the various methods.

Test Day	Oxygen (Percentage by Volume)			
	Grab	MCA	GC	CMS
1	20.6	20.2	21.4	20.0
2	19.5	19.7	21.7	19.5
3	19.5	20.3	21.7	20.2
6	19.8	20.1	NR	20.3
7	ND	20.7	21.9	20.6
8	20.4	20.5	21.8	20.7
9	20.5	20.9	22.0	20.7
10	20.1	20.3	20.9	20.7
13	19.5	20.3	21.4	20.9
14	20.5	20.5	21.6	20.9
15	20.4	20.8	21.9	21.1
16	19.7	20.2	21.3	20.6
17	20.6	20.4	21.1	20.6
20	19.7	20.4	21.1	20.7
21	20.0	20.5	21.3	21.0
22	19.9	20.2	21.2	20.7
23	19.5	20.6	NR	20.9
24	21.0	20.8	20.4	20.8
27	20.3	20.7	21.4	20.6
28	20.4	20.4	21.0	20.8
29	20.8	20.3	21.1	20.8
30	20.2	20.6	21.2	20.8

Test Day	Nitrogen (Percentage by Volume)		
	Grab	MCA	GC
1	87.2	77.9	82.1
2	78.6	79.1	80.8
3	75.7	78.1	80.8
6	76.3	77.4	NR
7	ND	77.8	80.1
8	77.8	77.3	80.2
9	78.0	77.8	80.3
10	79.5	78.0	82.0
13	74.3	77.0	79.0
14	79.7	77.7	80.8
15	78.5	77.8	81.1
16	76.5	77.6	79.7
17	80.3	78.2	80.2
20	76.8	77.7	79.7
21	77.5	77.9	80.1
22	77.8	77.9	80.3
23	76.6	78.5	NR
24	78.4	78.2	77.7
27	76.2	78.2	79.8
28	76.5	77.9	79.3
29	79.9	77.9	80.2
30	77.3	78.0	80.4

ND Not Detected
NR Not Reported

Test Day	Carbon Dioxide (Percentage by Volume)				
	Grab	MCA	GC	CMS IR	Ext. IR
1	0.44	0.39	NR	0.47	0.42
2	0.37	0.34	0.41	0.42	0.37
3	0.38	0.34	0.40	0.42	0.36
6	0.34	0.33	NR	0.44	0.36
7	ND	0.35	0.37	0.42	0.38
8	0.35	0.29	0.35	0.38	0.35
9	0.34	0.33	0.37	0.38	0.36
10	0.36	0.33	0.44	0.40	0.37
13	0.31	0.35	0.36	0.39	0.35
14	0.38	0.37	0.38	0.43	NR
15	0.34	0.33	0.36	0.37	NR
16	0.34	0.33	0.38	0.40	0.35
17	0.37	0.32	0.36	0.41	0.38
20	0.34	0.33	0.36	0.39	0.38
21	0.35	0.34	0.36	0.40	0.34
22	0.39	0.37	0.40	0.44	0.42
23	0.35	0.32	NR	0.40	0.35
24	0.33	0.33	0.34	0.38	0.36
27	0.33	0.36	0.38	0.41	NR
28	0.33	0.33	0.37	0.4	0.36
29	0.32	0.33	0.37	0.41	0.36
30	0.36	0.40	0.41	0.41	0.35

Test Day	Water Vapor (Percentage by Volume)	
	MCA	GC
1	1.09	1.20
2	1.20	1.30
3	1.20	1.30
6	1.20	NR
7	1.20	1.40
8	1.30	1.30
9	1.30	1.30
10	1.10	1.40
13	1.00	1.30
14	1.10	1.40
15	1.10	1.40
16	1.00	1.40
17	1.30	1.40
20	1.30	1.20
21	1.20	1.20
22	1.30	1.30
23	1.30	NR
24	1.30	0.24
27	1.30	1.30
28	1.30	1.40
29	1.30	1.30
30	1.40	1.40

ND Not Detected
NR Not Reported

APPENDIX D—
CMS ATMOSPHERIC GRAB SAMPLE RESULTS

Given below is a summary of CMS atmospheric grab samples collected during the IART. According to these samples, the CMS averaged 78 percent nitrogen, 21.1 percent oxygen, and 0.35 percent carbon dioxide.

Test Day	Analyte (Percentage by Volume)					
	Nitrogen	Oxygen	Carbon Dioxide	Hydrogen	Methane	Carbon Monoxide
1	87.2	20.6	0.44	NR	<0.0003	<0.0005
2	78.6	19.5	0.37	NR	<0.0003	<0.0005
3	75.7	19.5	0.38	NR	<0.0003	<0.0005
6	76.3	19.8	0.34	NR	<0.0003	<0.0005
7	ND	ND	ND	ND	ND	ND
8	77.8	20.4	0.35	NR	<0.0003	<0.0005
9	78.0	20.5	0.34	NR	<0.0003	<0.0005
10	79.5	20.0	0.36	NR	<0.0003	<0.0005
13	74.3	19.5	0.31	NR	<0.0003	<0.0005
14	79.2	20.5	0.38	NR	<0.0003	<0.0005
15	78.5	20.4	0.34	NR	<0.0003	<0.0005
16	76.5	19.7	0.34	NR	<0.0003	<0.0005
17	80.3	20.6	0.37	NR	<0.0003	<0.0005
20	76.8	19.7	0.34	NR	<0.0003	<0.0005
21	77.5	20.0	0.35	NR	<0.0003	<0.0005
22	77.8	19.9	0.39	NR	<0.0003	<0.0005
23	76.6	19.5	0.35	NR	<0.0003	<0.0005
24	78.4	21.0	0.33	NR	<0.0003	<0.0005
27	76.2	20.3	0.33	NR	<0.0003	<0.0005
28	76.5	20.4	0.33	NR	<0.0003	<0.0005
29	79.9	20.8	0.32	NR	<0.0003	<0.0005
30	77.3	20.2	0.36	NR	<0.0003	<0.0005

ND Not Detected
NR Not Reported

APPENDIX E—
CMS ATMOSPHERIC GRAB SAMPLE RESULTS FOR OZONE AND NITROGEN DIOXIDE

These results demonstrate that the TCCS does not produce nitrogen oxides from the nitrogen in the air during normal operations. Also, ozone is not produced by the operation of electric motors and electronic equipment.

Test Day	Sample Location	Analyte	Concentration (ppm)
16	CMS	Nitrogen Dioxide	<0.05
17	CMS	Ozone	<0.05
17	High Bay	Ozone	<0.05
28	CMS	Ozone	<0.05
28	High Bay	Ozone	<0.05
30	CMS	Ozone	<0.05
30	High Bay	Ozone	<0.05
30	Outdoors	Ozone	0.05

FIGURE E–1.—CMS atmospheric sample results for nitrogen dioxide and ozone.

APPENDIX F—
CDRA INTEGRATED TESTING SUPPORTING DATA

Performance of the CDRA is documented by the following data plots obtained from early in the integrated test (3–14–96), mid-test (3–27–96), and late in the test (4–11–96).

1. Early Test Phase

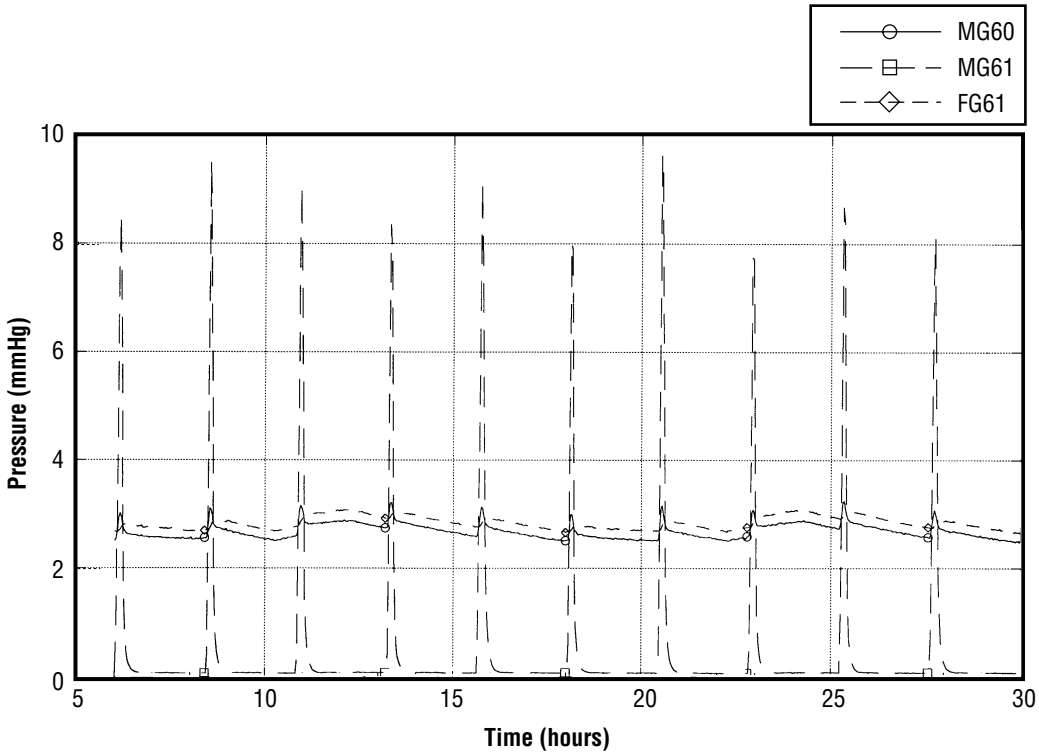

FIGURE F–1.—Plot 1: Carbon dioxide partial pressure 4BMS integrated air revitalization testing elapsed time from 3–14–96, 00:00:00.

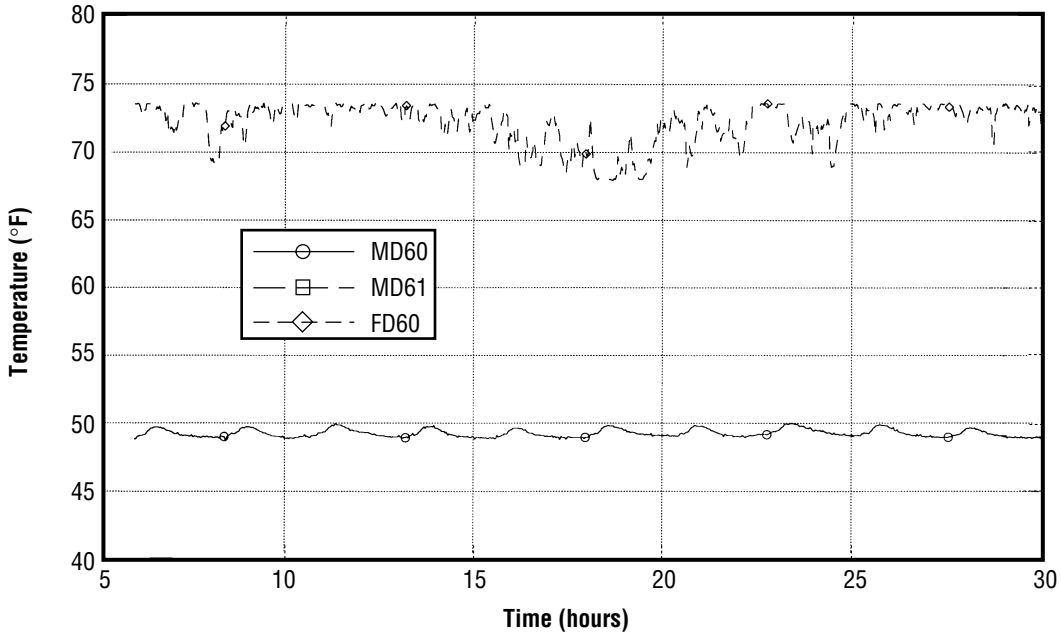

FIGURE F–2.—Plot 2: Dewpoint temperatures 4BMS integrated air revitalization testing—elapsed time from 3–14–96, 00:00:00.

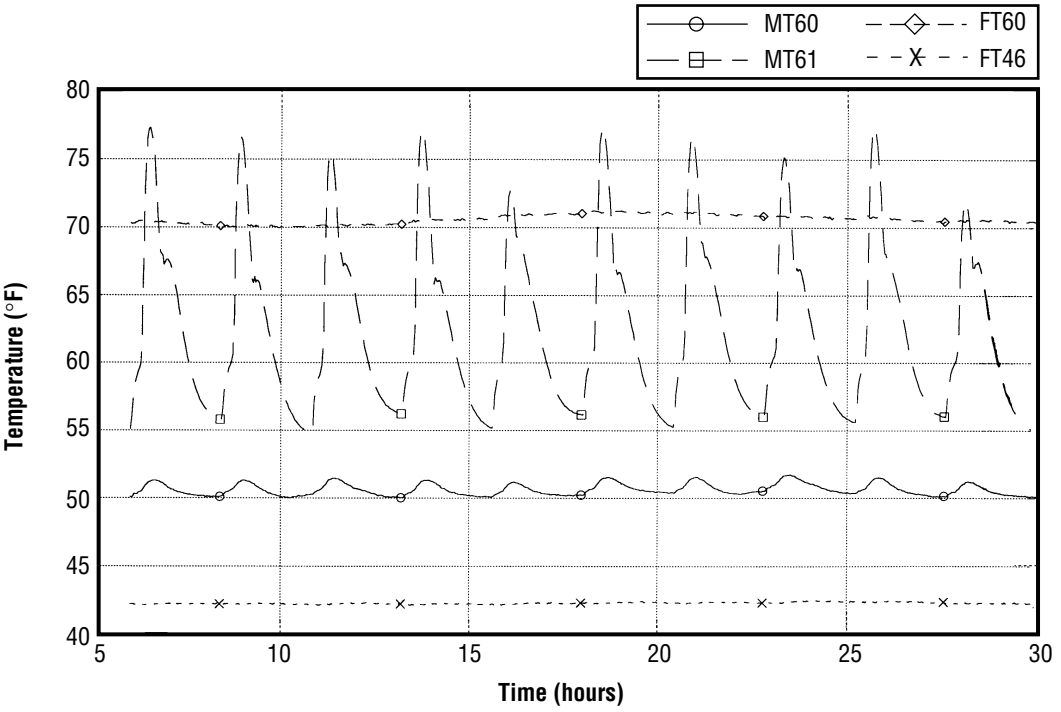

FIGURE F–3.—Plot 3: Inlet/outlet/module/coolant temperatures 4BMS integrated air revitalization testing—elapsed time from 3–14–96, 00:00:00.

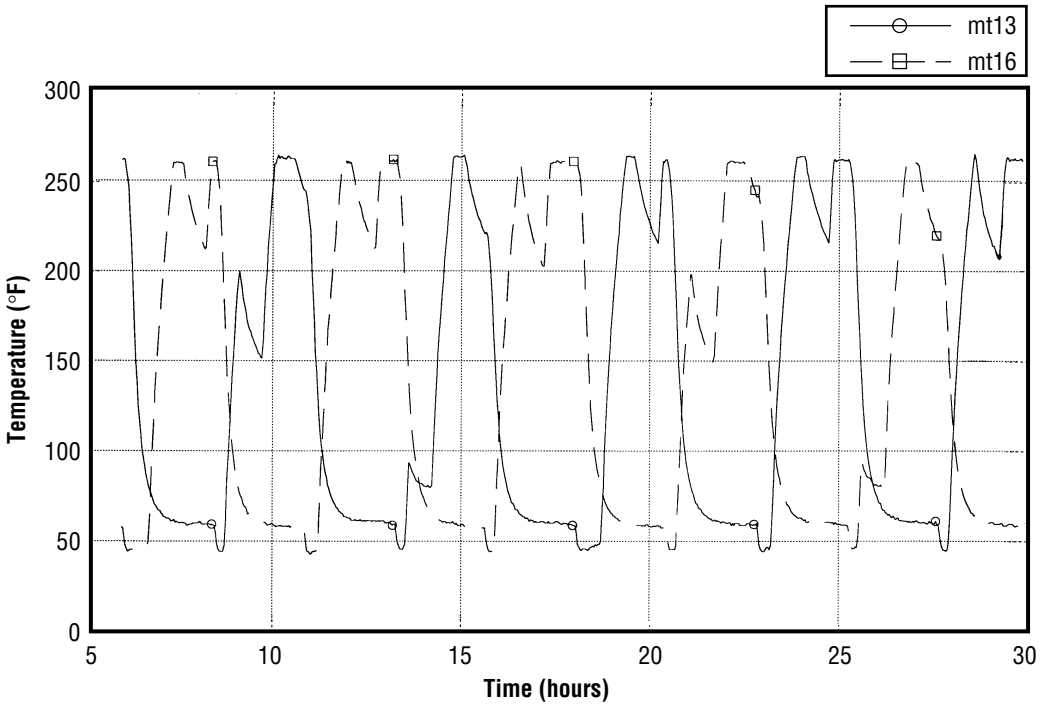

FIGURE F–4.—Plot 4: 5A sorbent bed temperatures 4BMS integrated air revitalization testing—elapsed time from 3–14–96, 00:00:00.

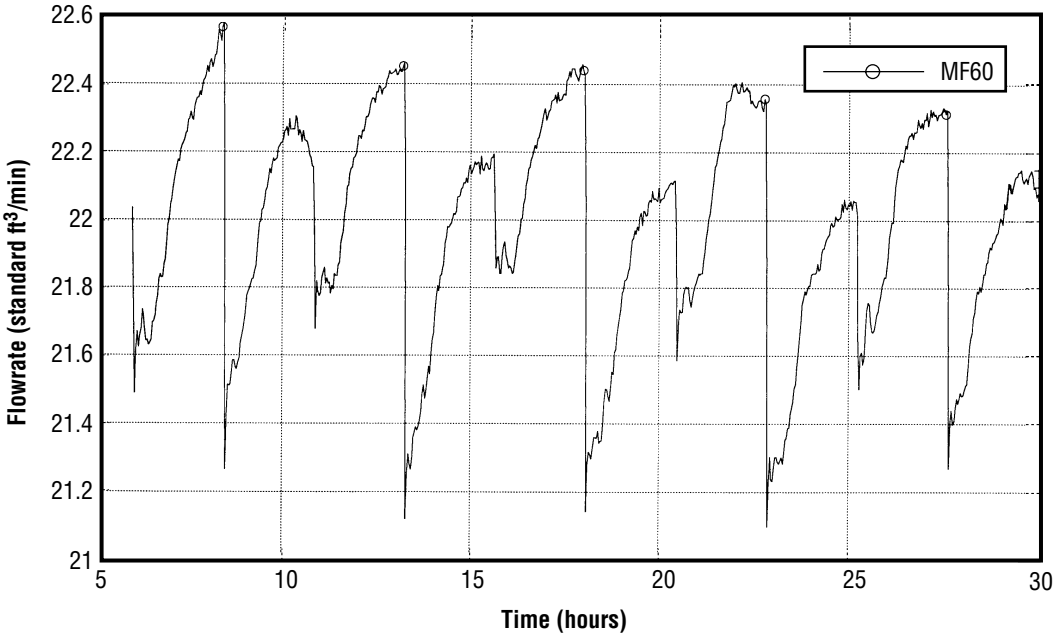

FIGURE F–5.—Plot 5: Flowrate 4BMS integrated air revitalization testing—elapsed time from 3–14–96, 00:00:00.

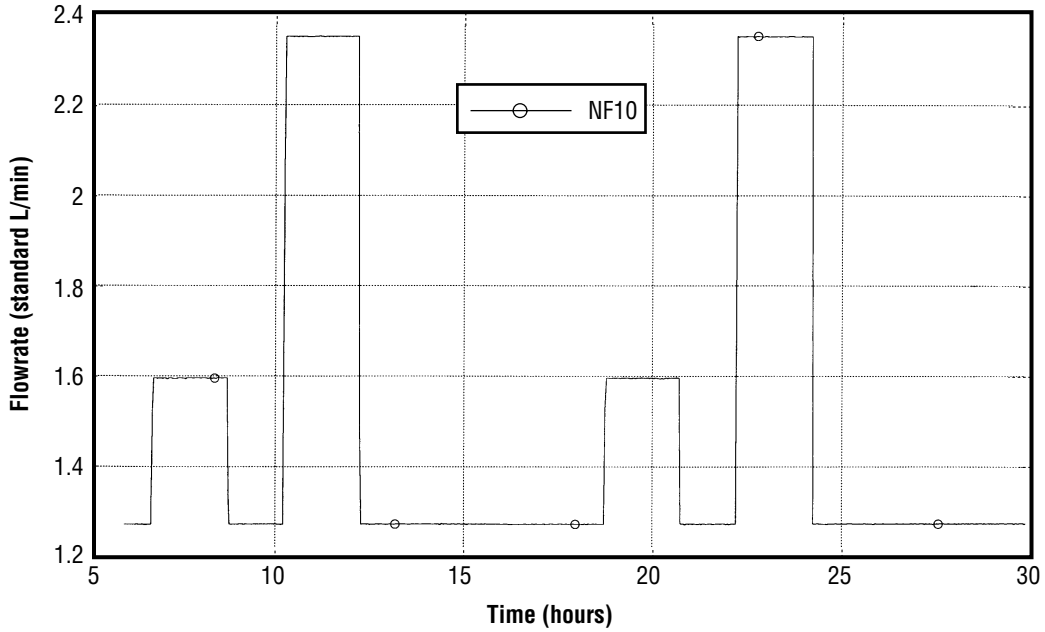

FIGURE F–6.—Plot 6: CO_2 injection flowrate 4BMS integrated air revitalization testing—elapsed time from 3–14–96, 00:00:00.

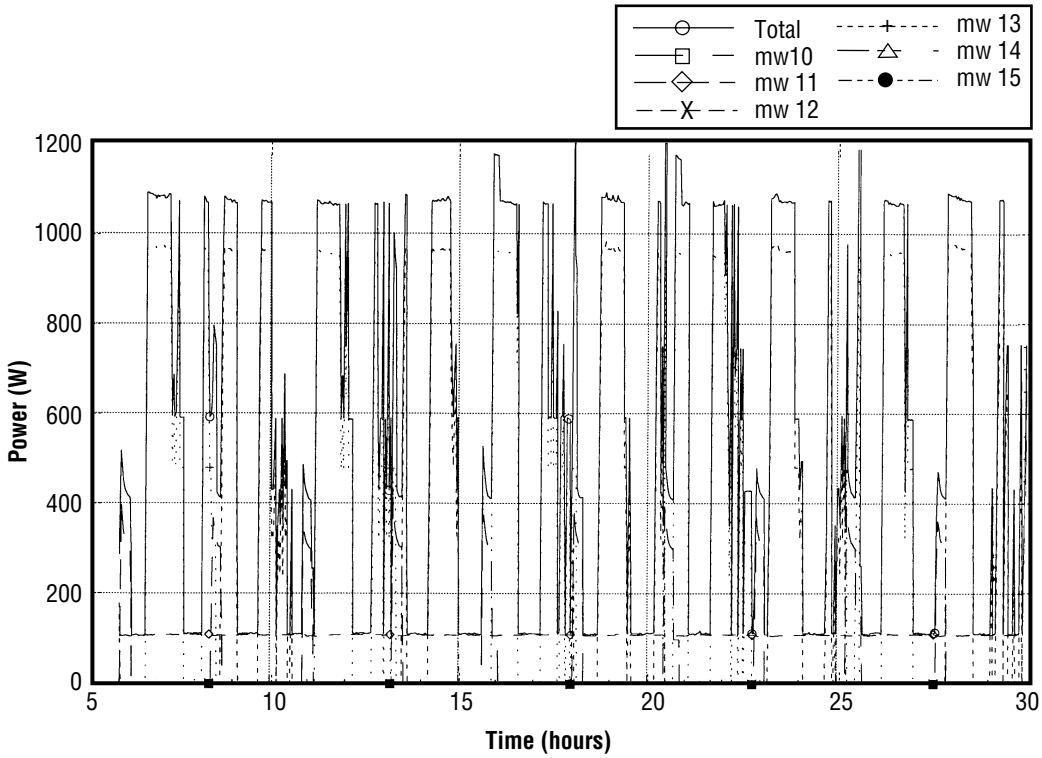

FIGURE F–7.—Plot 7: Power consumption 4BMS integrated air revitalization testing—elapsed time from 3–14–96, 00:00:00.

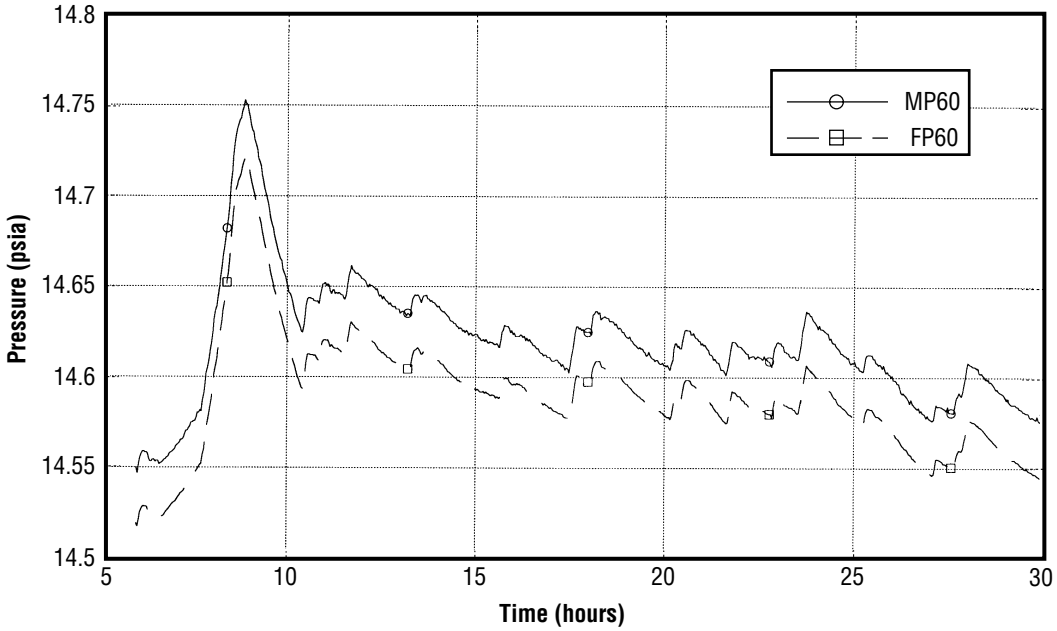

FIGURE F–8.—Plot 8: Inlet/module pressures 4BMS integrated air revitalization testing— elapsed time from 3–14–96, 00:00:00.

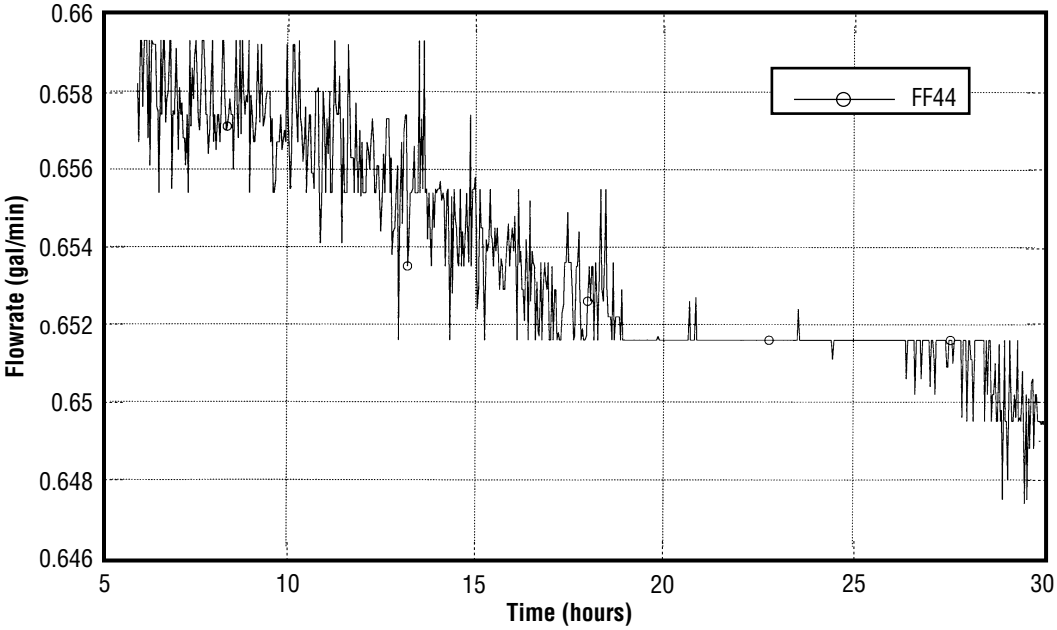

FIGURE F–9.—Plot 9: Precooler coolant flowrate 4BMS integrated air revitalization testing— elapsed time from 3–14–96, 00:00:00.

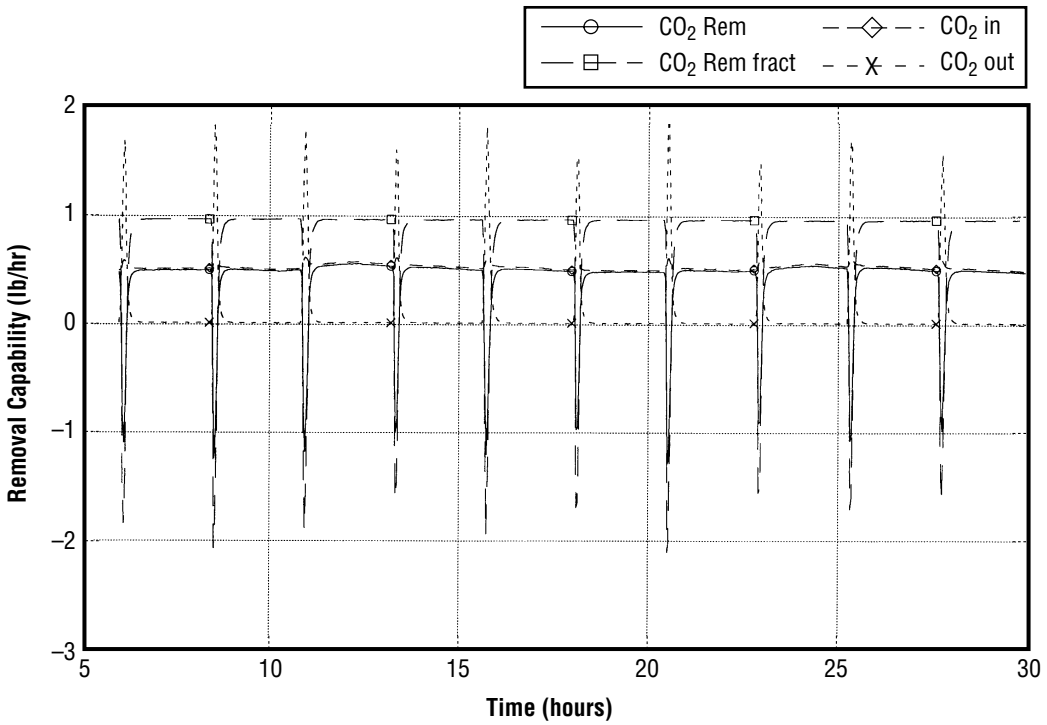

FIGURE F–10.—Plot 10: CO_2 removal capability 4BMS integrated air revitalization testing—elapsed time from 3–14–96, 00:00:00.

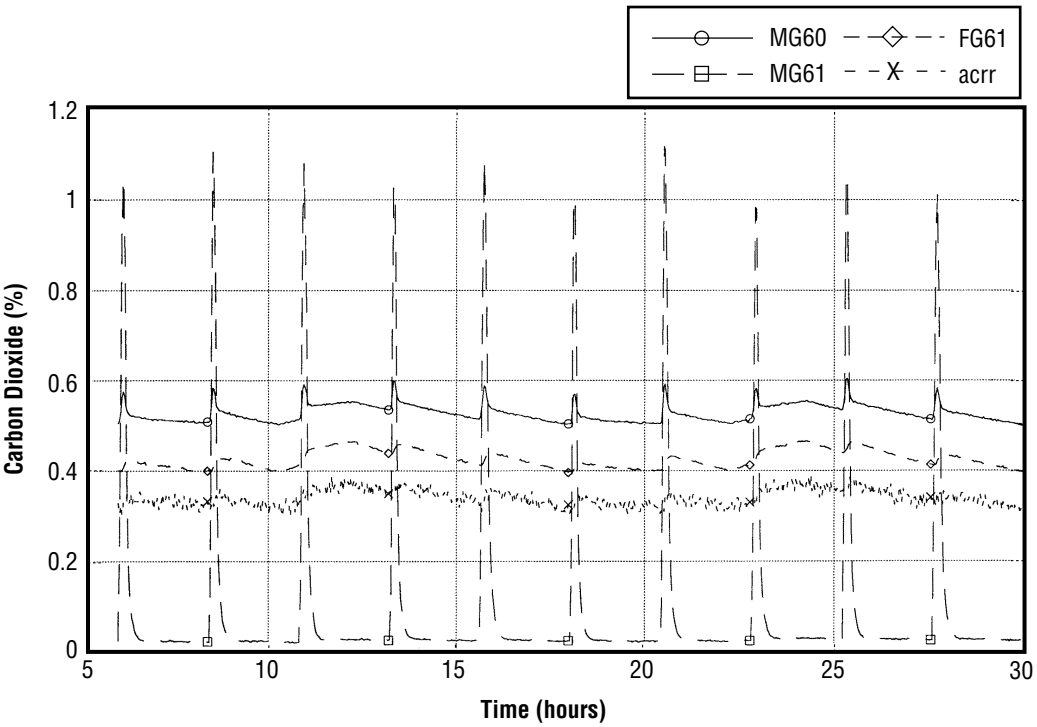

FIGURE F–11.—Plot 11: Percent carbon dioxide 4BMS integrated air revitalization testing—elapsed time from 3–14–96, 00:00:00.

2. Mid-Test Phase

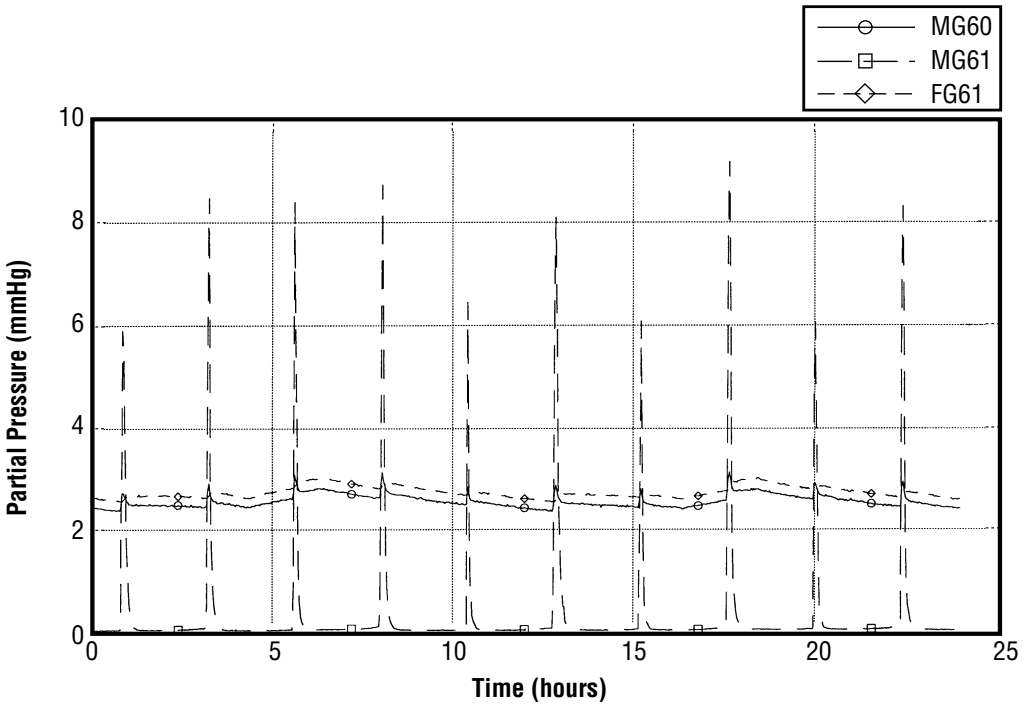

FIGURE F–12.—Plot 1: Carbon dioxide partial pressure 4BMS integrated air revitalization testing—elapsed time from 3–27–96, 00:00:00.

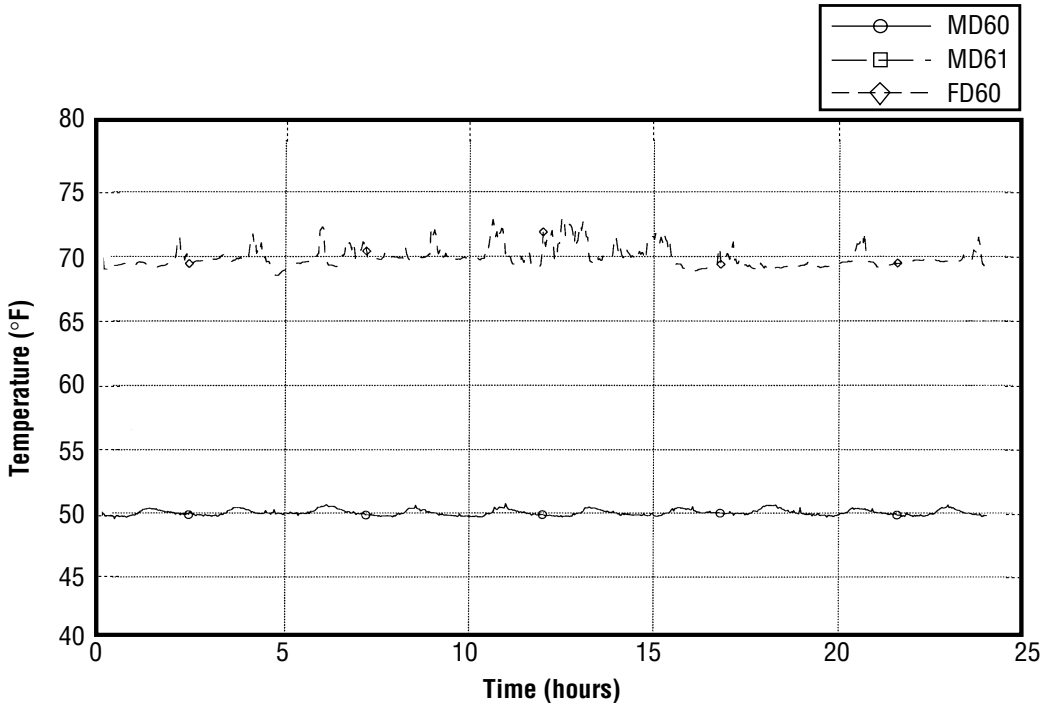

FIGURE F–13.—Plot 2: Dewpoint temperatures 4BMS integrated air revitalization testing—elapsed time from 3–27–96, 00:00:00.

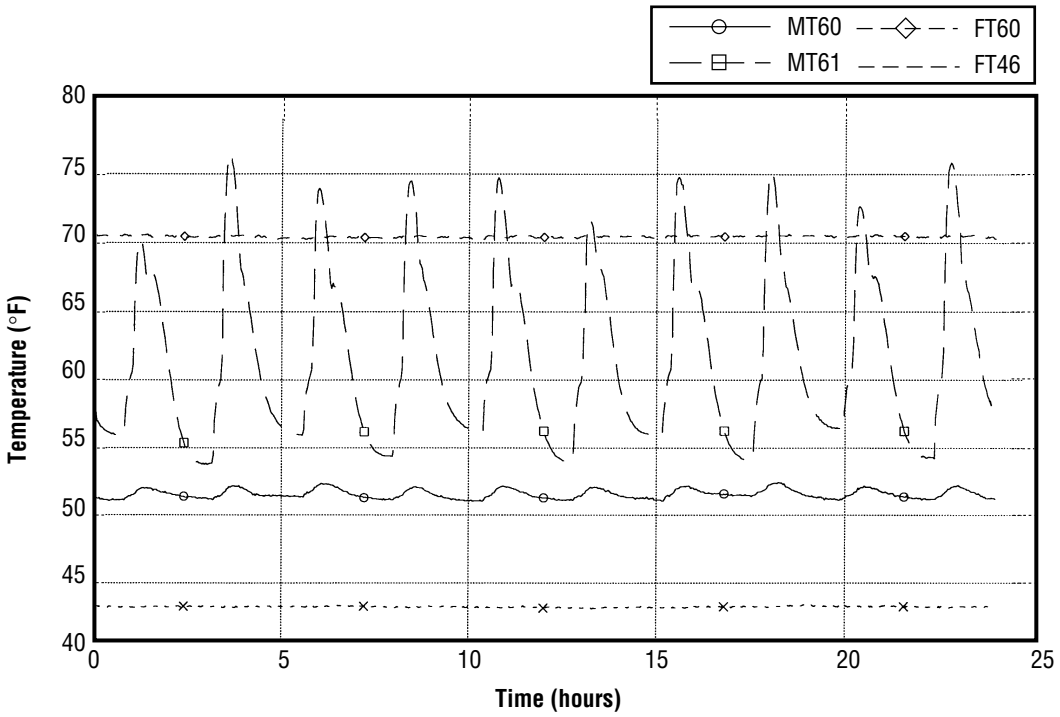

FIGURE F–14.—Plot 3: Inlet/outlet/module/coolant temperatures 4BMS integrated air revitalization testing—elapsed time from 3–27–96, 00:00:00.

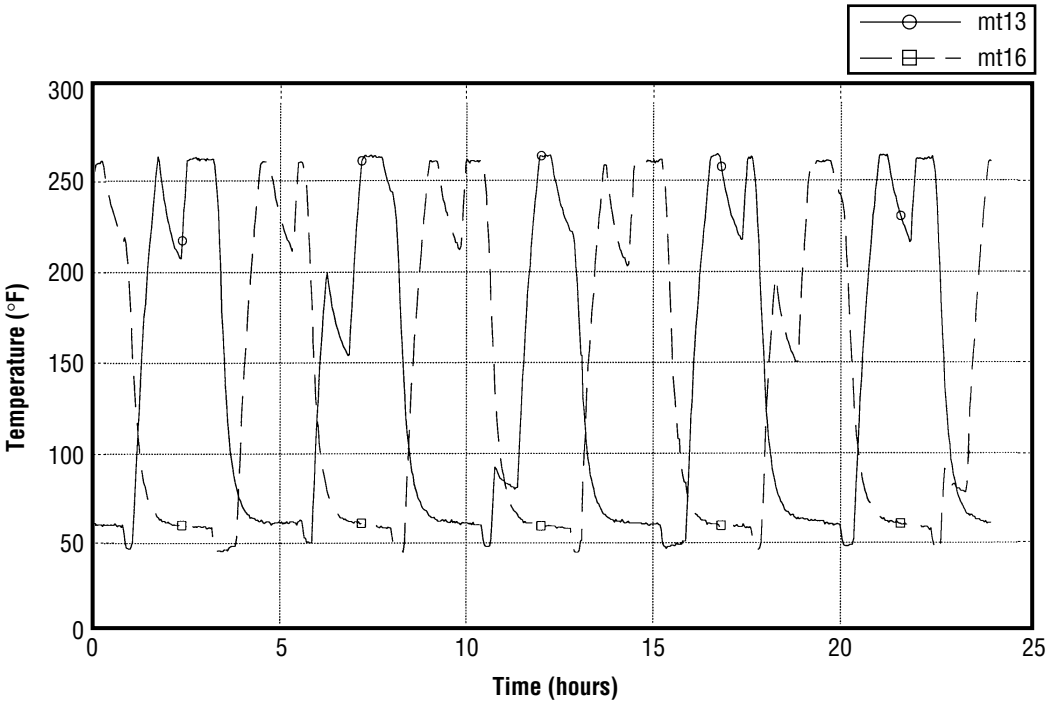

FIGURE F–15.—Plot 4: 5A sorbent bed temperatures 4BMS integrated air revitalization testing—elapsed time from 3–27–96, 00:00:00.

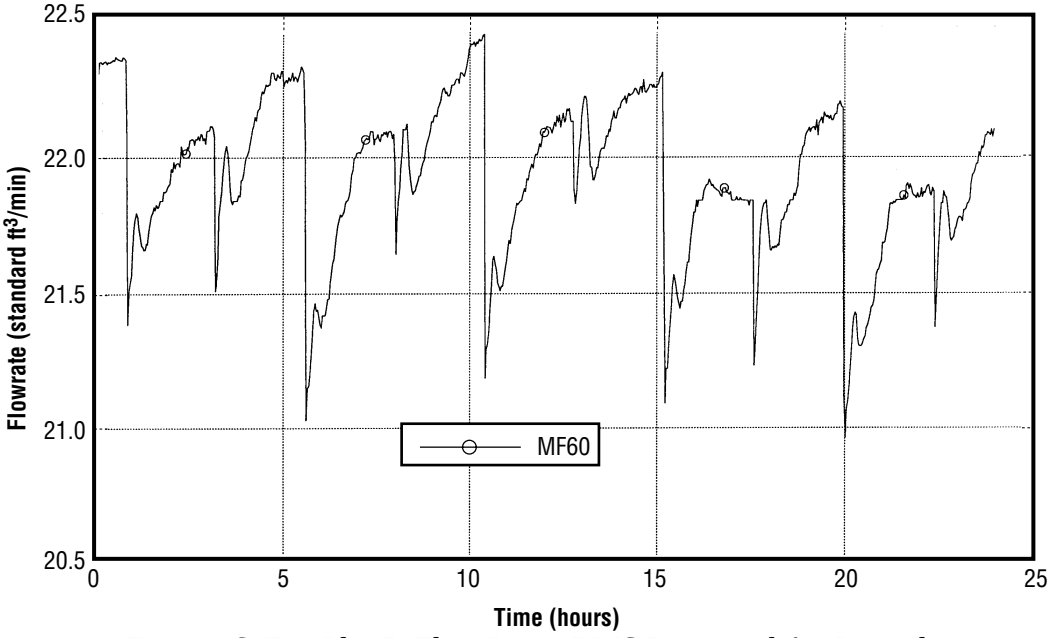

FIGURE F–16.—Plot 5: Flowrate 4BMSintegrated air revitalization testing—elapsed time from 3–27–96, 00:00:00.

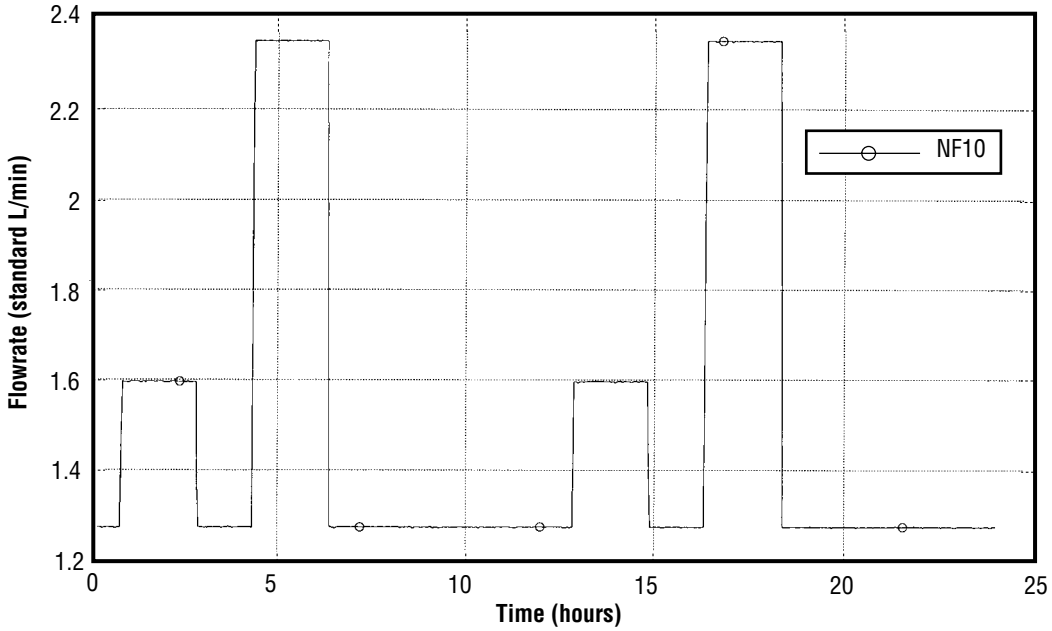

FIGURE F–17.—Plot 6: CO_2 injection flowrate 4BMS integrated air revitalization testing—elapsed time from 3–27–96, 00:00:00.

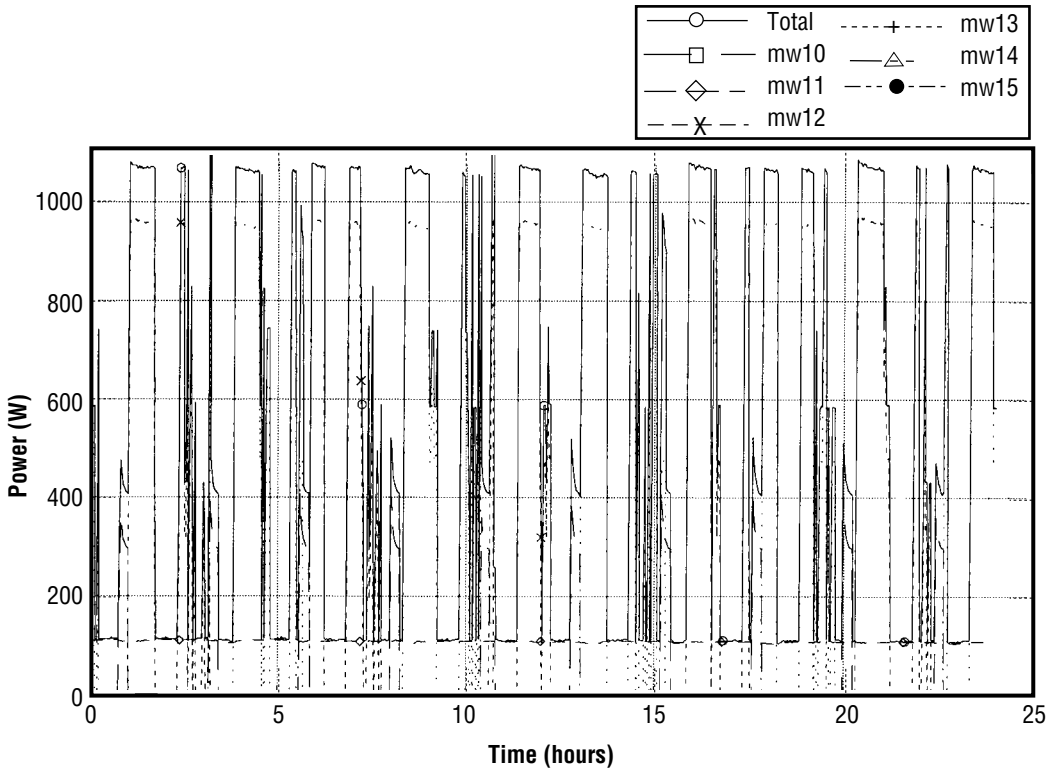

FIGURE F–18.—Plot 7: Power consumption 4BMS integrated air revitalization testing—elapsed time from 3–27–96, 00:00:00.

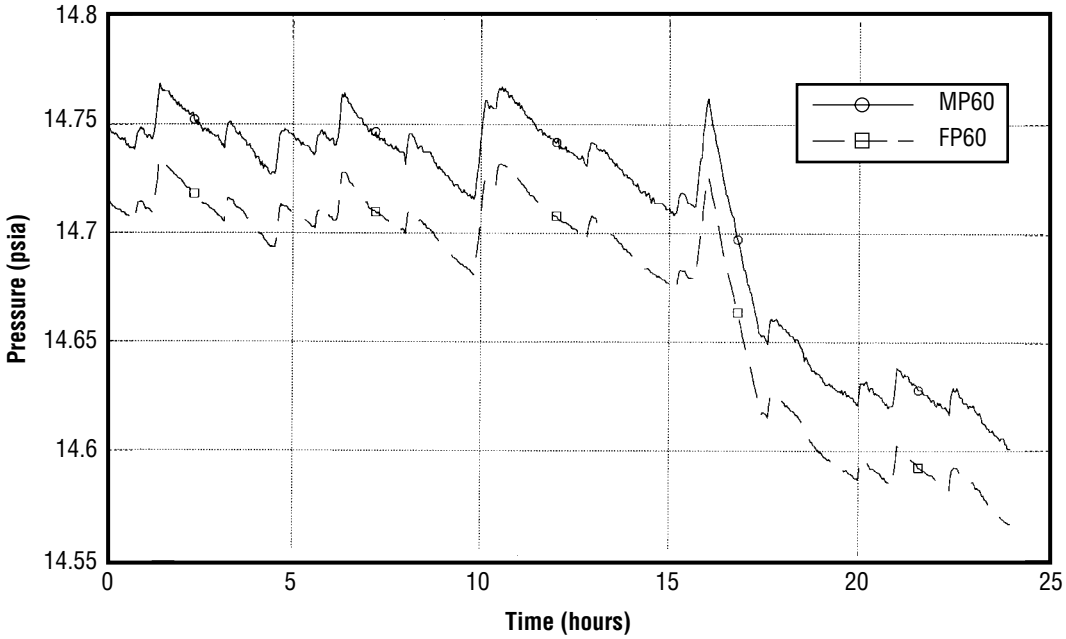

FIGURE F–19.—Plot 8: Inlet/module pressures 4BMS integrated air revitalization testing—elapsed time from 3–27–96, 00:00:00.

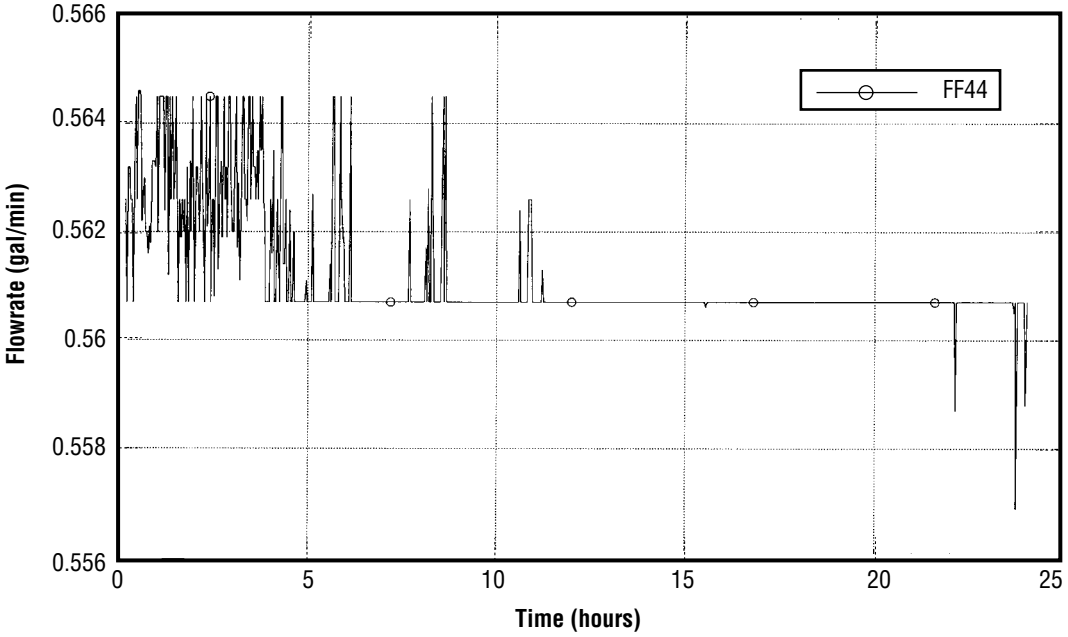

FIGURE F–20.—Plot 9: Precoolant flowrate 4BMS integrated air revitalization testing—elapsed time from 3–27–96, 00:00:00.

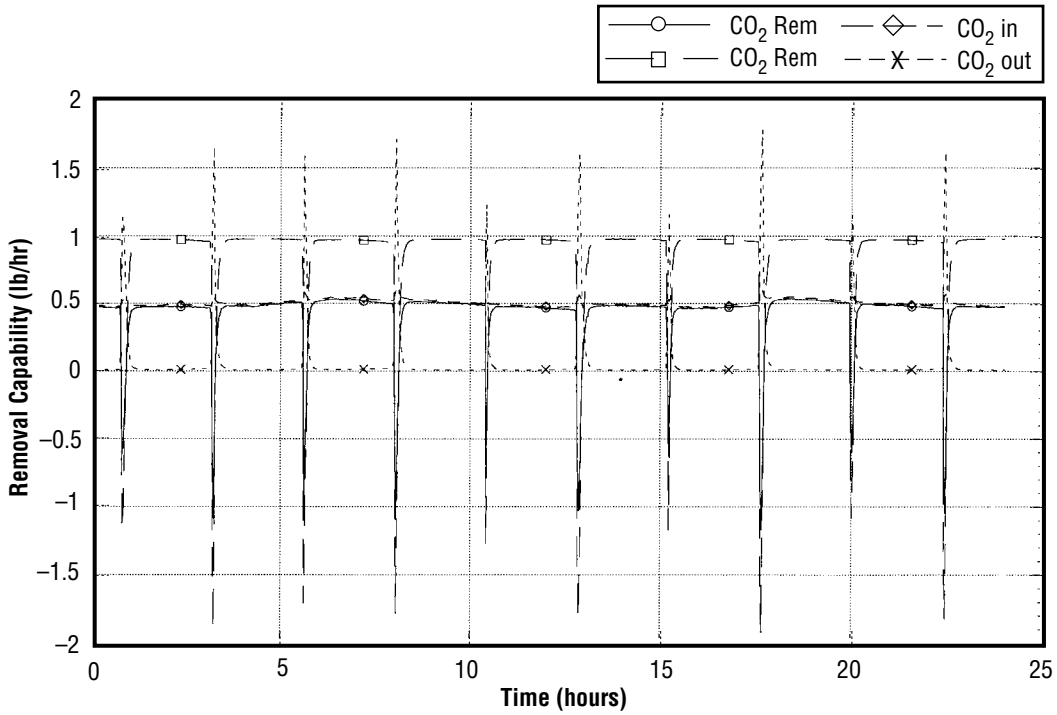

FIGURE F–21.—Plot 10: CO_2 removal capability 4BMS integrated air revitalization testing—elapsed time from 3–27–96, 00:00:00.

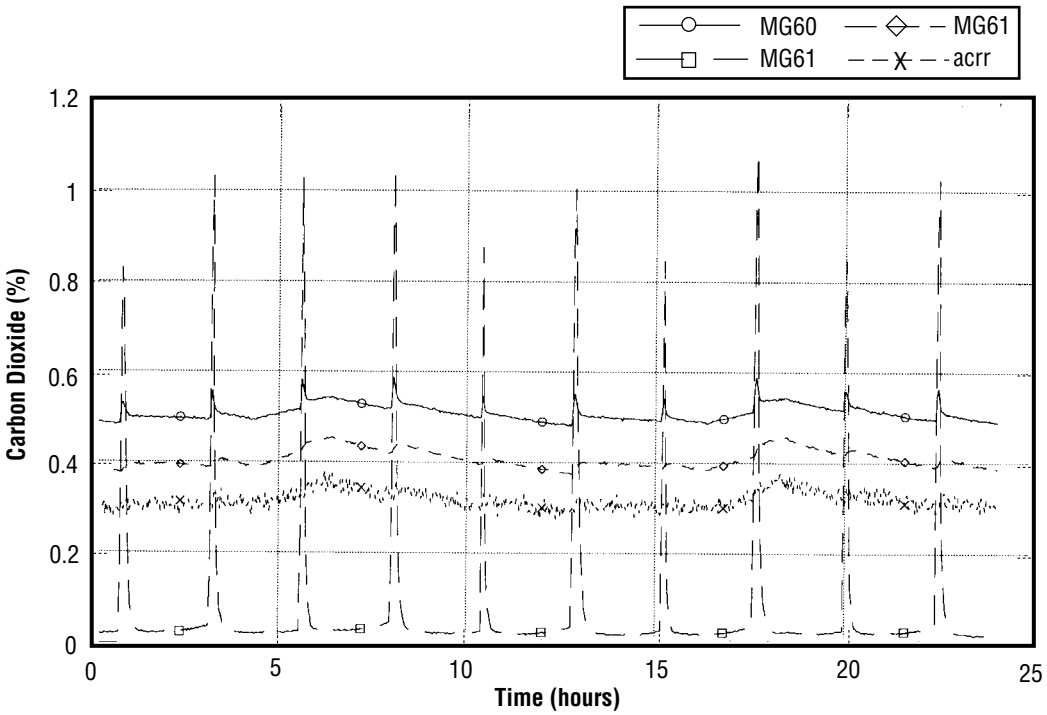

FIGURE F–22.—Plot 11: Percent carbon dioxide 4BMS integrated air revitalization testing—elapsed time from 3–27–96, 00:00:00.

3. Late Test Phase

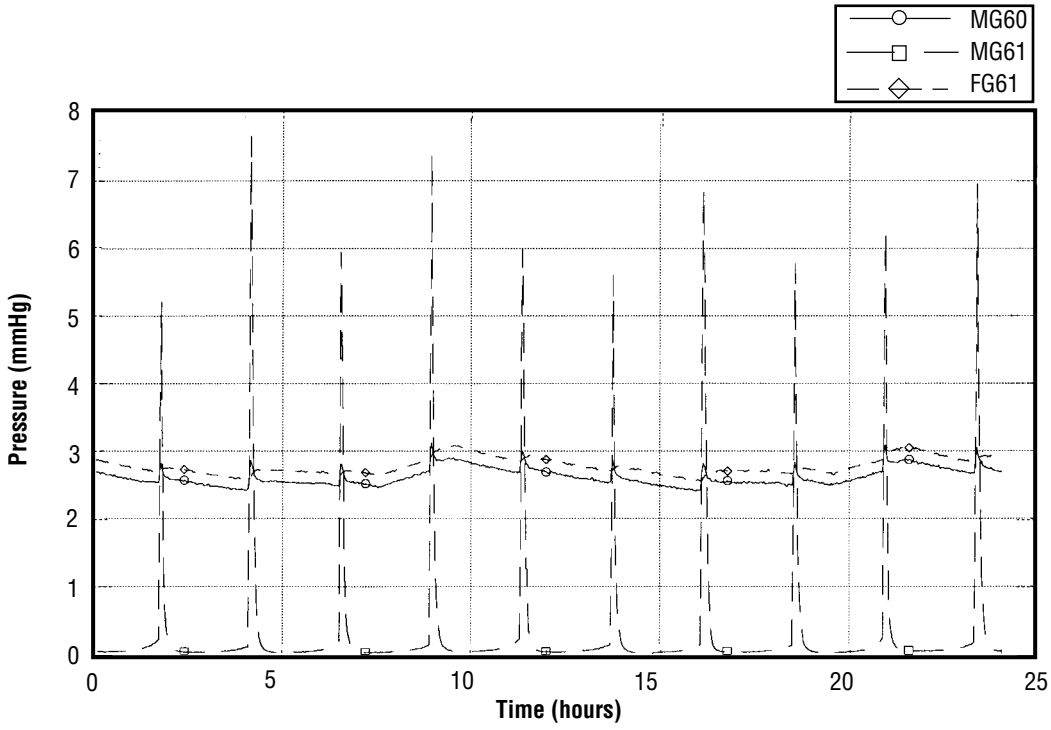

FIGURE F–23.—Plot 1. Carbon dioxide partial pressure 4BMS integrated air revitalization testing—elapsed time from 4–11–96, 00:00:00.

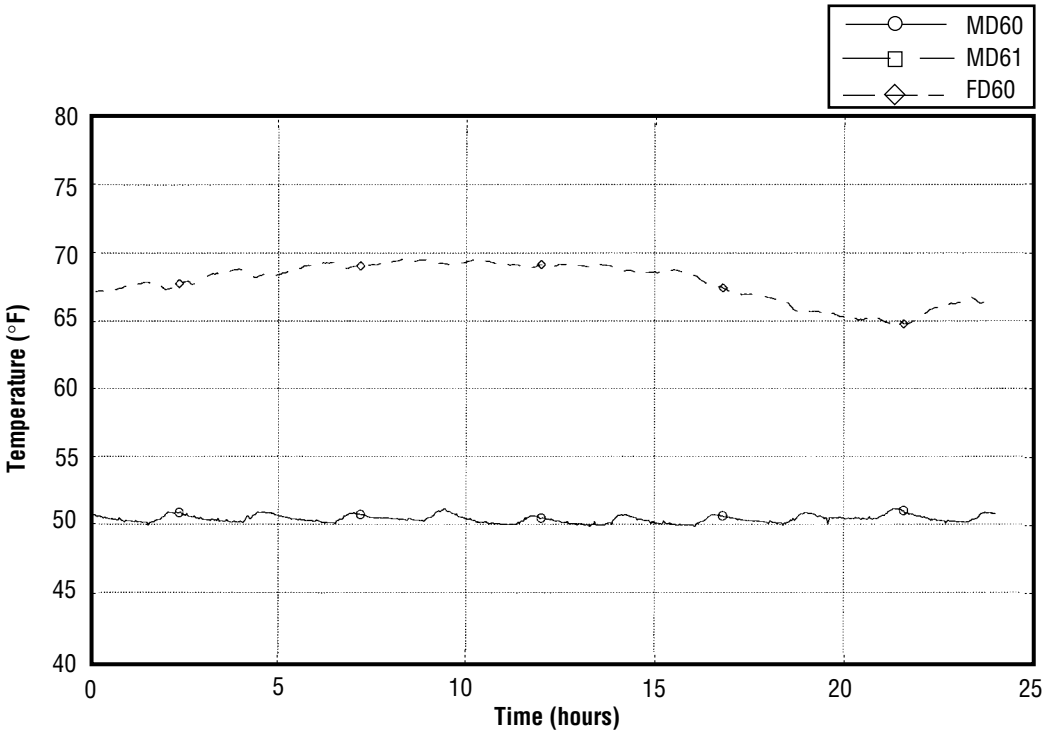

FIGURE F–24.—Plot 2: Dewpoint temperatures 4BMS integrated air revitalization testing—elapsed time from 4–11–96, 00:00:00.

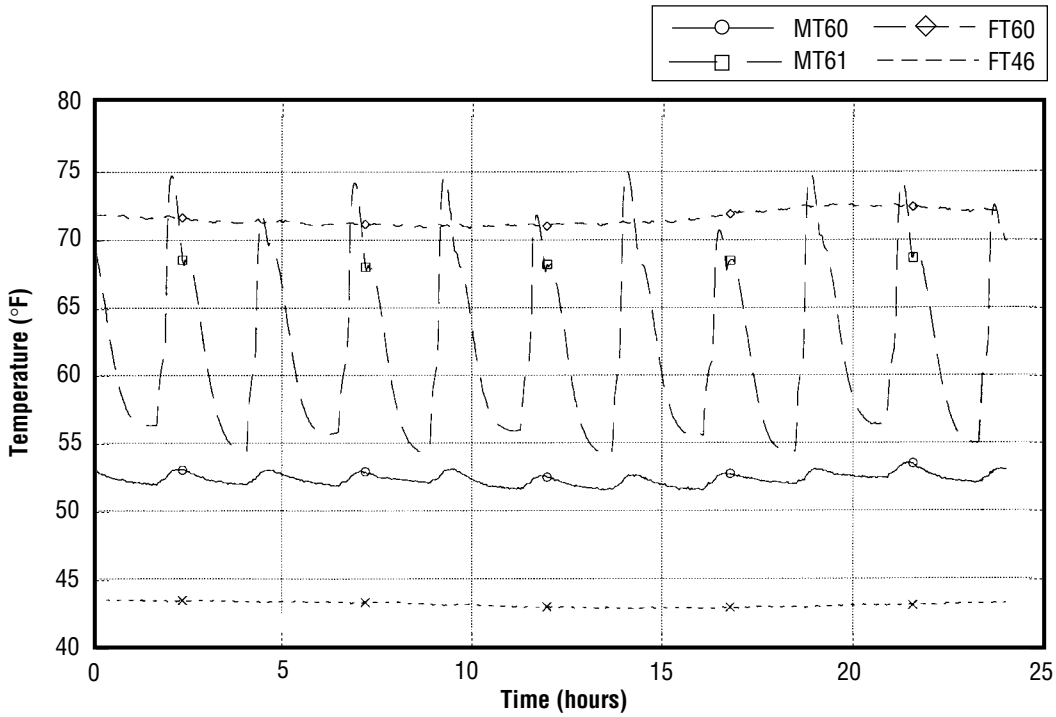

FIGURE F–25.—Plot 3: Inlet/outlet/module/coolant temperatures 4BMS integrated air revitalization testing—elapsed time from 4–11–96, 00:00:00.

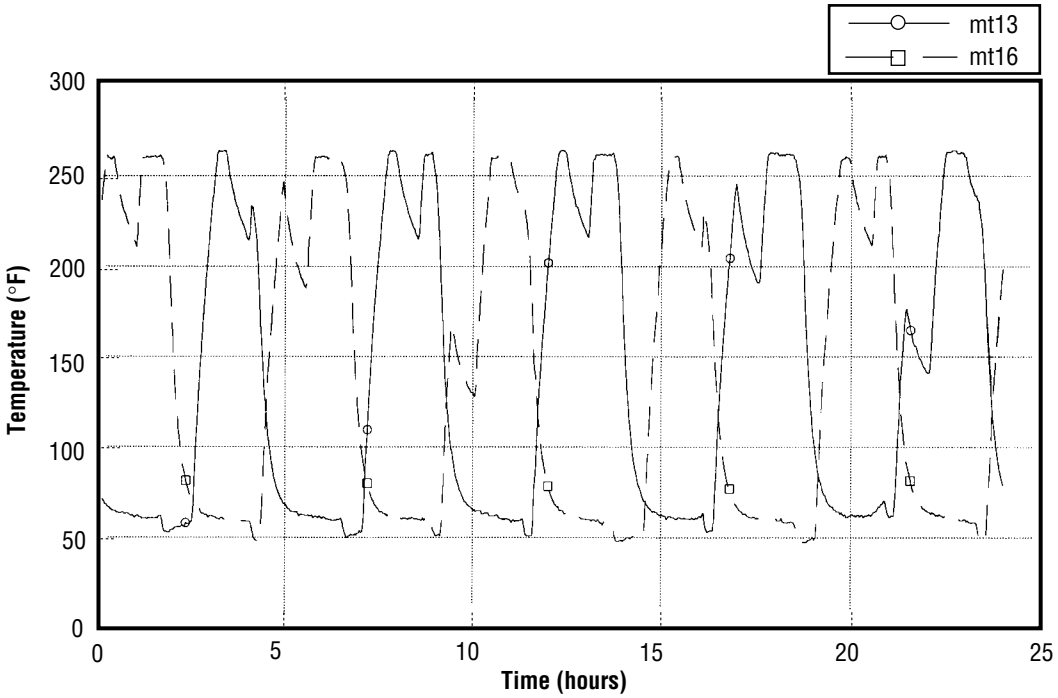

FIGURE F–26.—Plot 4: 5A sorbent bed temperatures 4BMS integrated air revitalization testing—elapsed time from 4–11–96, 00:00:00.

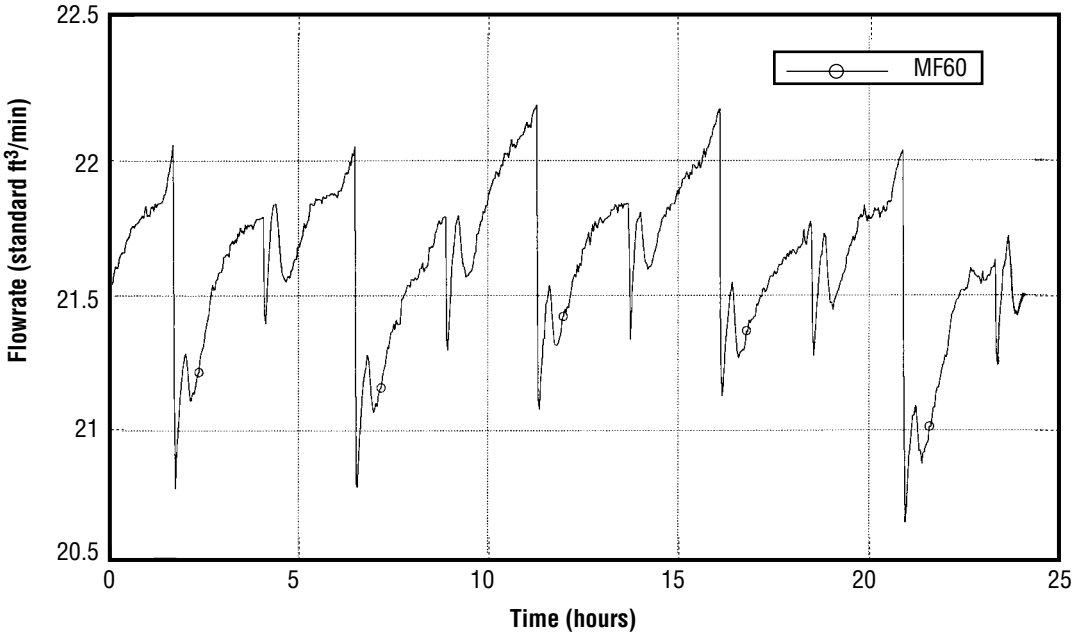

FIGURE F–27.—Plot 5: Flowrate 4BMS integrated air revitalization testing—elapsed time from 4–11–96, 00:00:00.

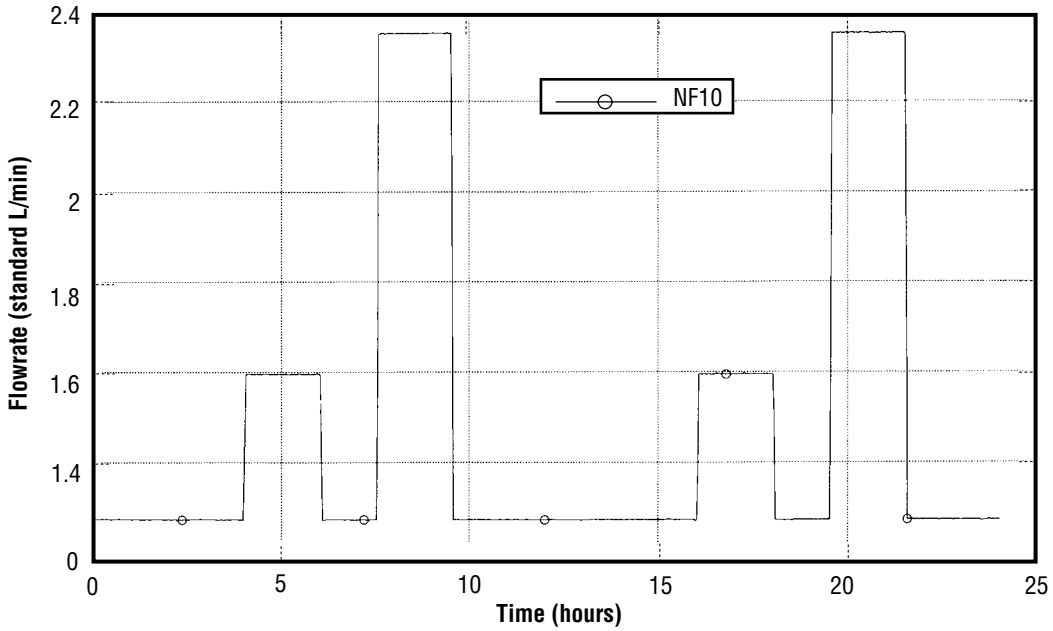

FIGURE F–28.—Plot 6: CO_2 injection flowrate 4BMS integrated air revitalization testing—elapsed time from 4–11–96, 00:00:00.

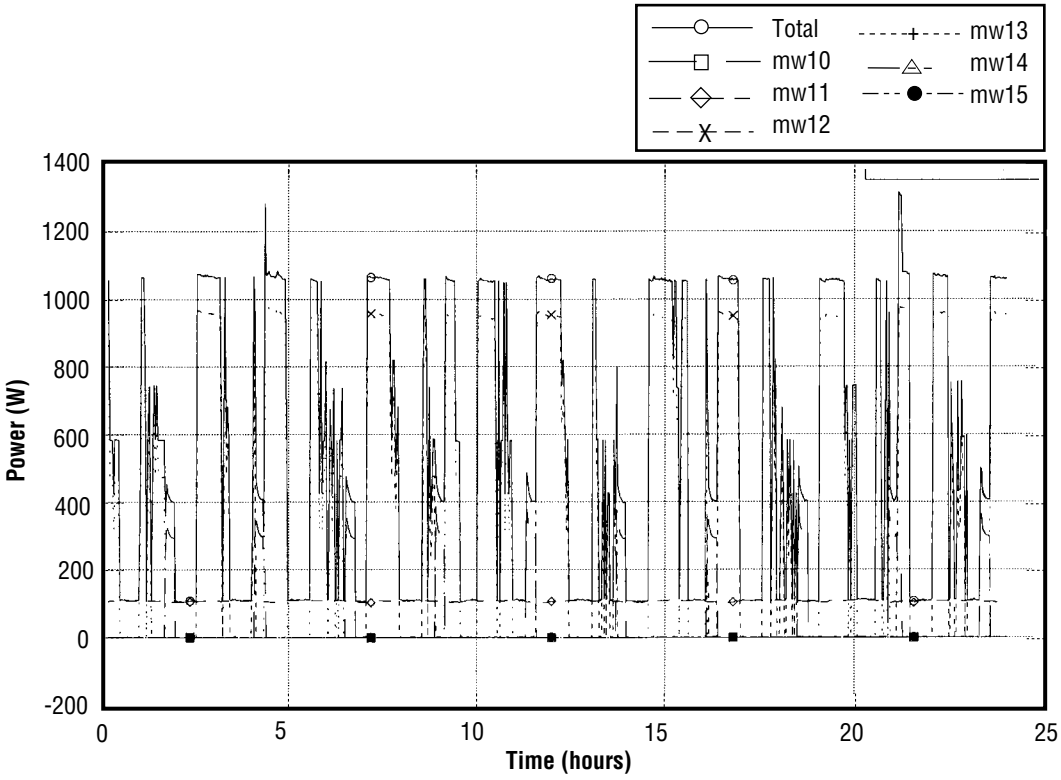

FIGURE F–29.—Plot 7: Power consumption 4BMS integrated air revitalization testing—elapsed time from 4–11–96, 00:00:00.

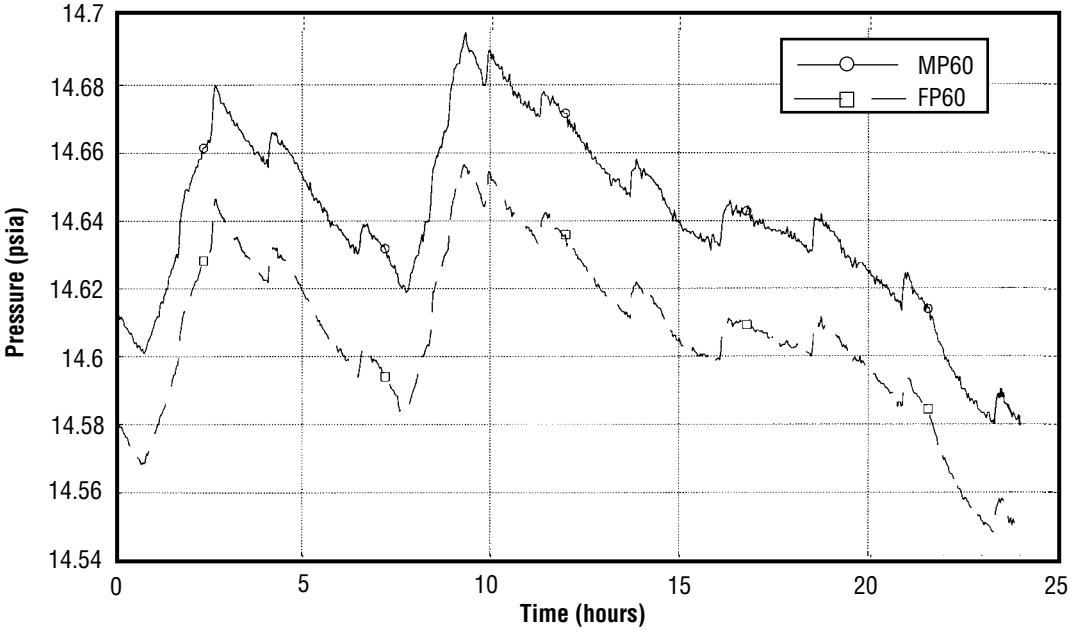

FIGURE F–30.—Plot 8: Inlet/module pressures 4BMS integrated air revitalization testing—elapsed time from 4–11–96, 00:00:00.

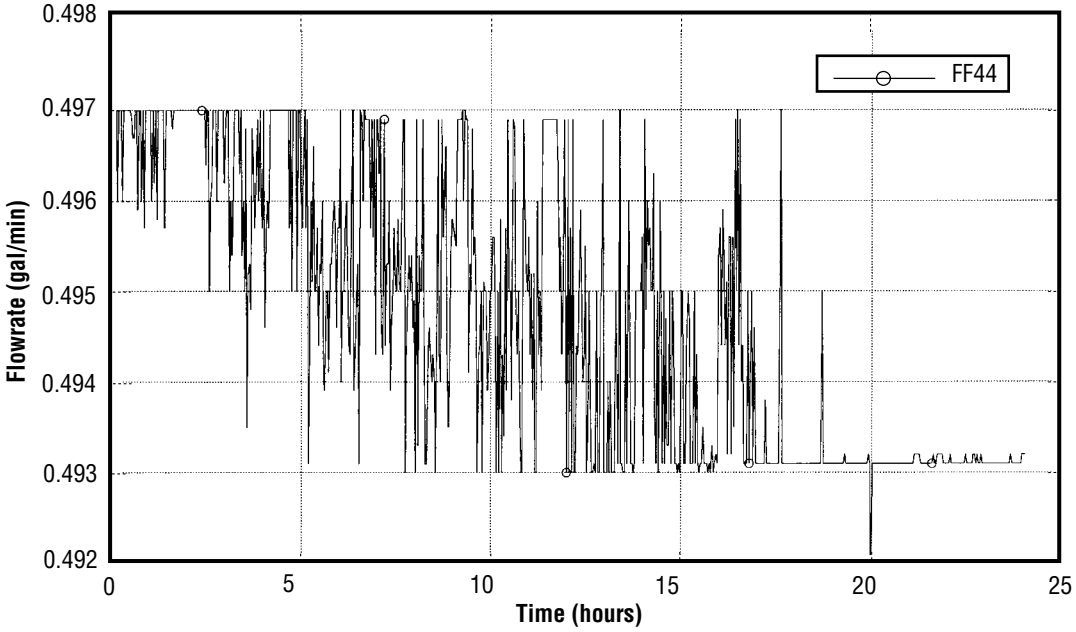

FIGURE F–31.—Plot 9: Precooler coolant flowrate 4BMS integrated air revitalization testing—elapsed time from 4–11–96, 00:00:00.

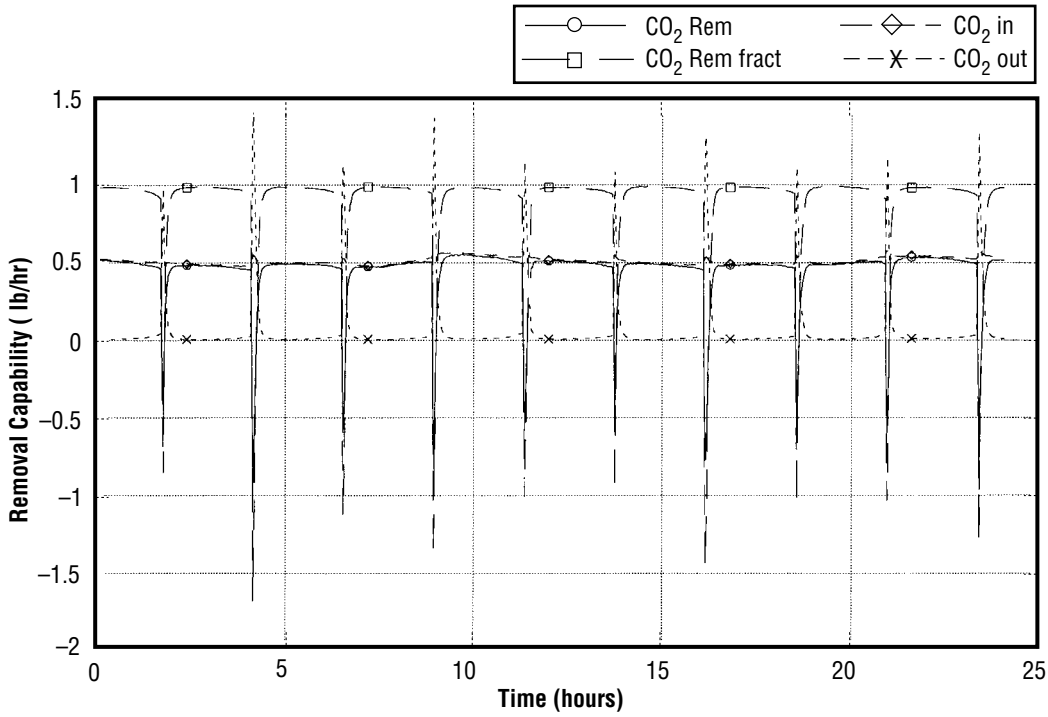

FIGURE F–32.—Plot 10: CO_2 removal capability 4BMS integrated air revitalization testing—elapsed time from 4–11–96, 00:00:00.

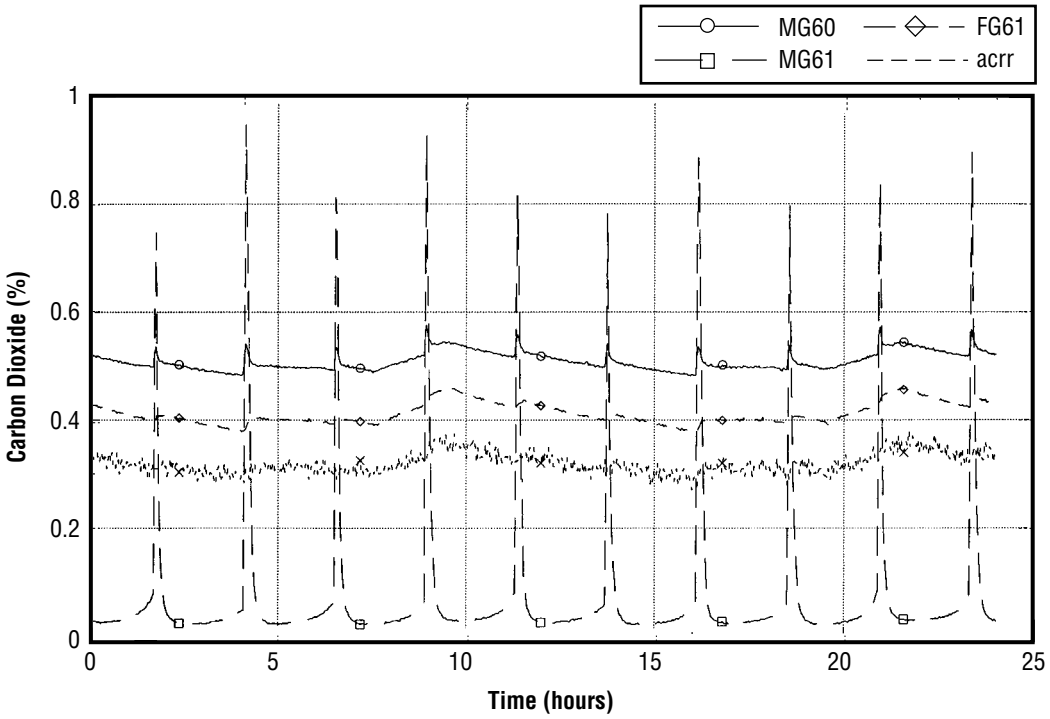

FIGURE F–33.—Plot 11: Percent carbon dioxide 4BMS integrated air revitalization testing—elapsed time from 4–11–96, 00:00:00.

APPENDIX G—
CMS OXYGEN PARTIAL PRESSURE RESPONSE

The following data plots show the test chamber oxygen partial pressure and the effects of various perturbations on it. Oxygen injection had the major effect, while the removal rate to simulate metabolic activity had a secondary effect.

Significant breaks in the data were caused by lost data when the host control computer shut down on March 29, 1996. Approximately 10 min of data were lost during this time; however, all ARS subassemblies continued to operate normally. This shutdown caused the metabolic simulation setpoints to be lost and oxygen was not injected as needed from 13:50 on March 29 to 14:15 on March 30. During this time, nitrogen was injected to maintain the chamber total pressure. This problem was corrected on March 29 by resetting the metabolic simulation setpoints.

A second loss of data was experienced on April 4, 1996. Again, the ARS subassemblies continued operating normally. The host computer was restarted, the metablic simulation setpoints reset, and the test continued without incident.

The last loss of data occurred on April 8, 1996, when a new data acquisition file was started to transition the control and data acquisition computers to daylight savings time.

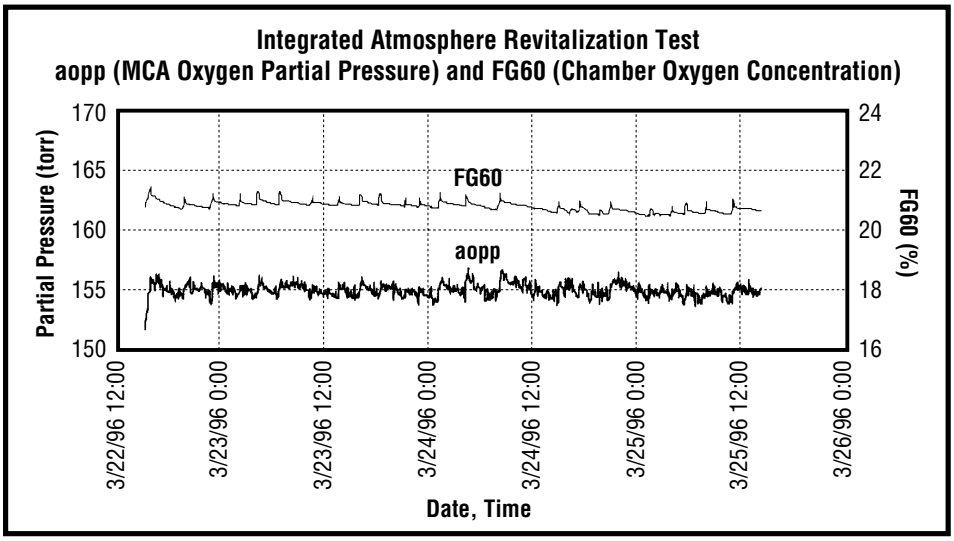
Integrated Atmosphere Revitalization Test
aopp (MCA Oxygen Partial Pressure) and FG60 (Chamber Oxygen Concentration)
Partial Pressure (torr)
FG60 (%)
FG60
aopp
170
165
160
155
150
24
22
20
18
16
3/22/96 12:00
3/23/96 0:00
3/23/96 12:00
3/24/96 0:00
3/24/96 12:00
3/25/96 0:00
3/25/96 12:00
3/26/96 0:00
Date, Time

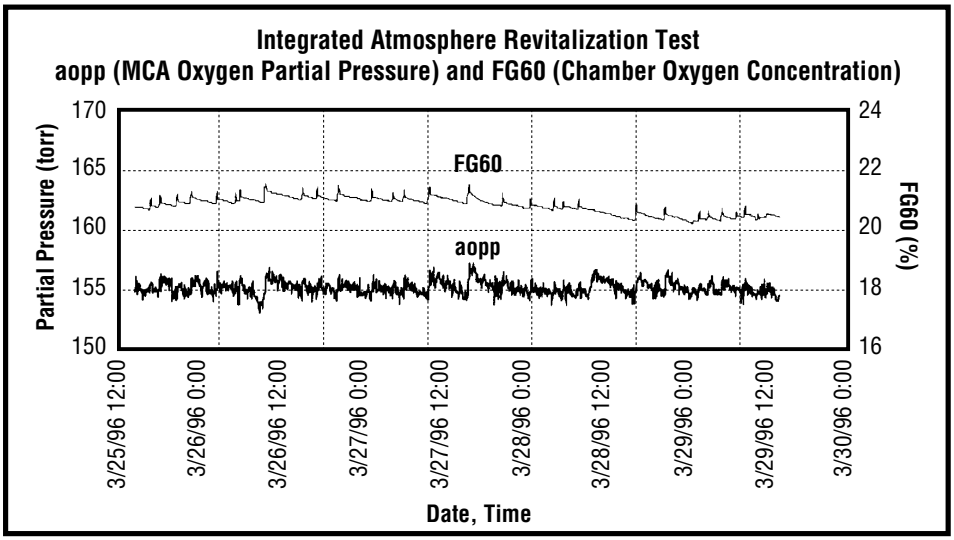
Integrated Atmosphere Revitalization Test
aopp (MCA Oxygen Partial Pressure) and FG60 (Chamber Oxygen Concentration)
Partial Pressure (torr)
FG60 (%)
FG60
aopp
170
165
160
155
150
24
22
20
18
16
3/25/96 12:00
3/26/96 0:00
3/26/96 12:00
3/27/96 0:00
3/27/96 12:00
3/28/96 0:00
3/28/96 12:00
3/29/96 0:00
3/29/96 12:00
3/30/96 0:00
Date, Time

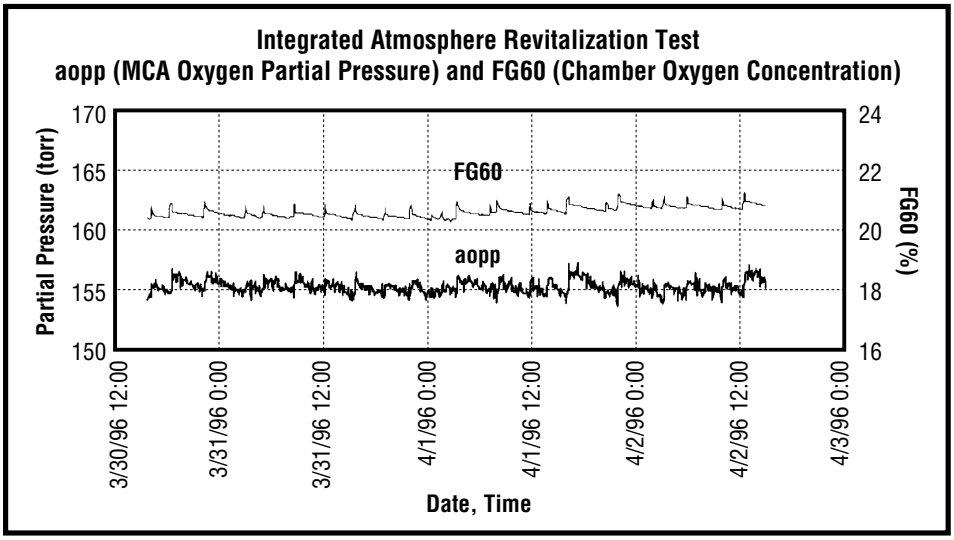
Integrated Atmosphere Revitalization Test
aopp (MCA Oxygen Partial Pressure) and FG60 (Chamber Oxygen Concentration)
Partial Pressure (torr)
FG60 (%)
FG60
aopp
170
165
160
155
150
24
22
20
18
16
3/30/96 12:00
3/31/96 0:00
3/31/96 12:00
4/1/96 0:00
4/1/96 12:00
4/2/96 0:00
4/2/96 12:00
4/3/96 0:00
Date, Time

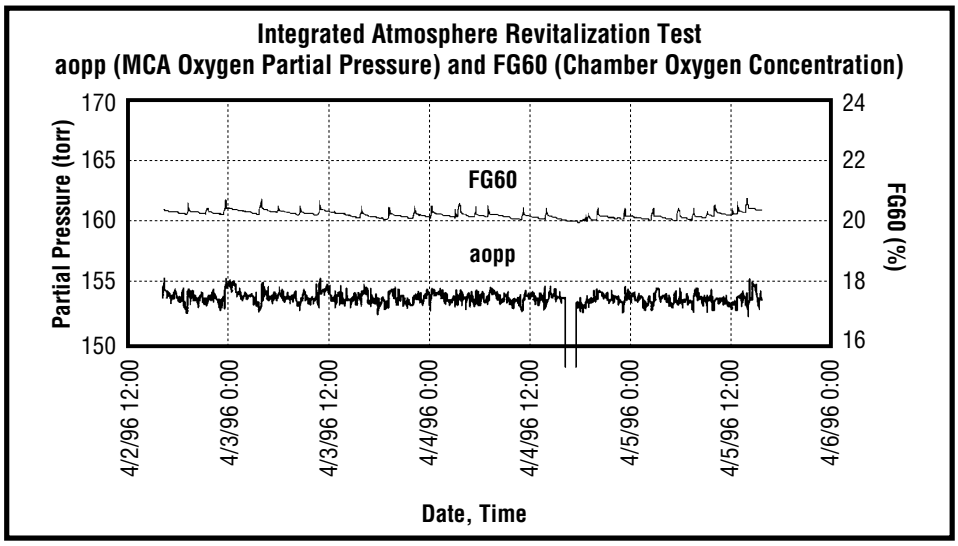
Integrated Atmosphere Revitalization Test
aopp (MCA Oxygen Partial Pressure) and FG60 (Chamber Oxygen Concentration)
Partial Pressure (torr)
FG60 (%)
FG60
aopp
170
165
160
155
150
24
22
20
18
16
4/2/96 12:00
4/3/96 0:00
4/3/96 12:00
4/4/96 0:00
4/4/96 12:00
4/5/96 0:00
4/5/96 12:00
4/6/96 0:00
Date, Time

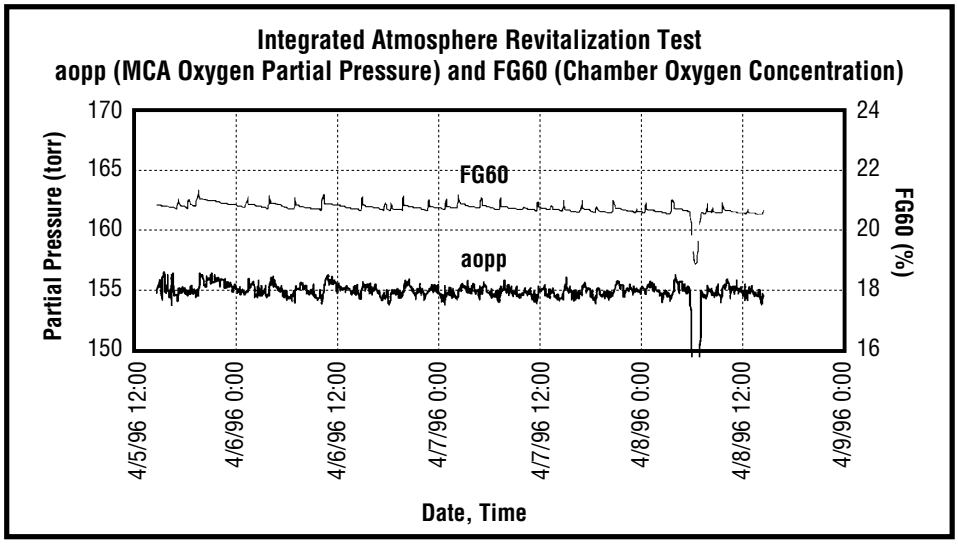
Integrated Atmosphere Revitalization Test
aopp (MCA Oxygen Partial Pressure) and FG60 (Chamber Oxygen Concentration)
Partial Pressure (torr)
FG60 (%)
FG60
aopp
170
165
160
155
150
24
22
20
18
16
4/5/96 12:00
4/6/96 0:00
4/6/96 12:00
4/7/96 0:00
4/7/96 12:00
4/8/96 0:00
4/8/96 12:00
4/9/96 0:00
Date, Time

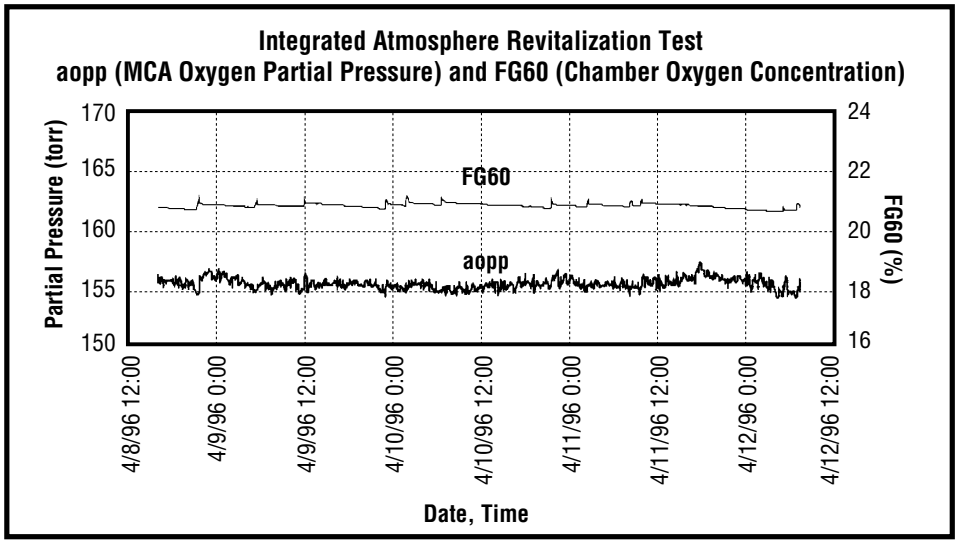
Integrated Atmosphere Revitalization Test
aopp (MCA Oxygen Partial Pressure) and FG60 (Chamber Oxygen Concentration)
Partial Pressure (torr)
FG60 (%)
FG60
aopp
170
165
160
155
150
24
22
20
18
16
4/8/96 12:00
4/9/96 0:00
4/9/96 12:00
4/10/96 0:00
4/10/96 12:00
4/11/96 0:00
4/11/96 12:00
4/12/96 0:00
4/12/96 12:00
Date, Time

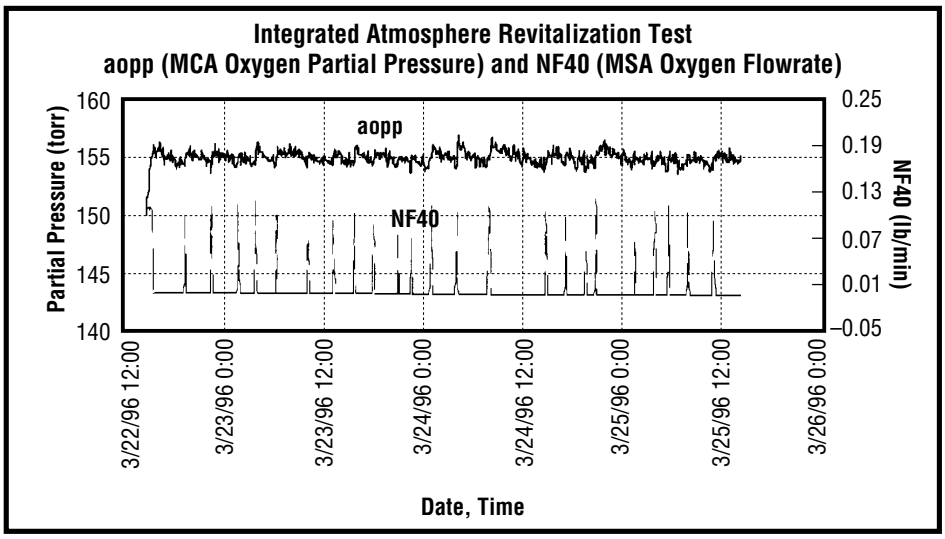
Integrated Atmosphere Revitalization Test
aopp (MCA Oxygen Partial Pressure) and NF40 (MSA Oxygen Flowrate)
Partial Pressure (torr)
160
155
150
145
140
aopp
NF40
0.25
0.19
0.13
0.07
0.01
–0.05
NF40 (lb/min)
3/22/96 12:00
3/23/96 0:00
3/23/96 12:00
3/24/96 0:00
3/24/96 12:00
3/25/96 0:00
3/25/96 12:00
3/26/96 0:00
Date, Time

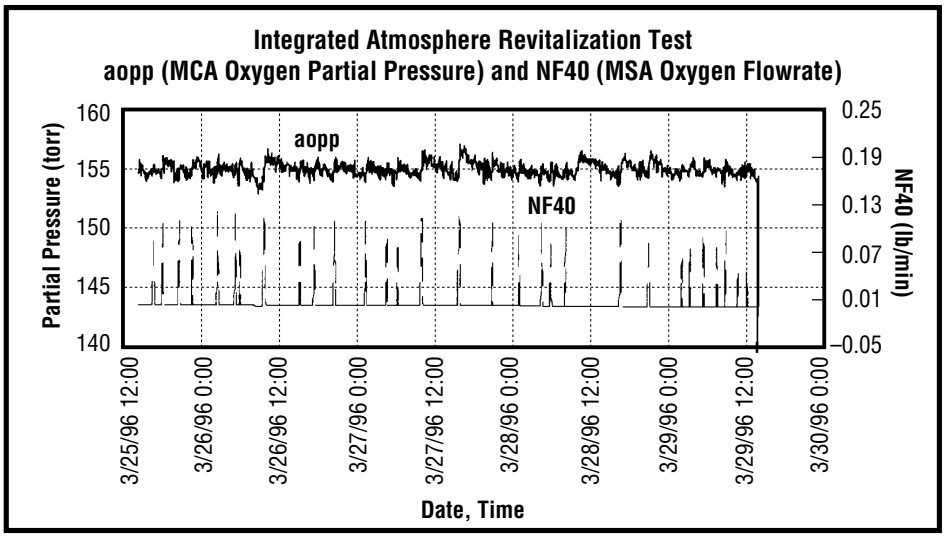
Integrated Atmosphere Revitalization Test
aopp (MCA Oxygen Partial Pressure) and NF40 (MSA Oxygen Flowrate)
Partial Pressure (torr)
160
155
150
145
140
aopp
NF40
0.25
0.19
0.13
0.07
0.01
–0.05
NF40 (lb/min)
3/25/96 12:00
3/26/96 0:00
3/26/96 12:00
3/27/96 0:00
3/27/96 12:00
3/28/96 0:00
3/28/96 12:00
3/29/96 0:00
3/29/96 12:00
3/30/96 0:00
Date, Time

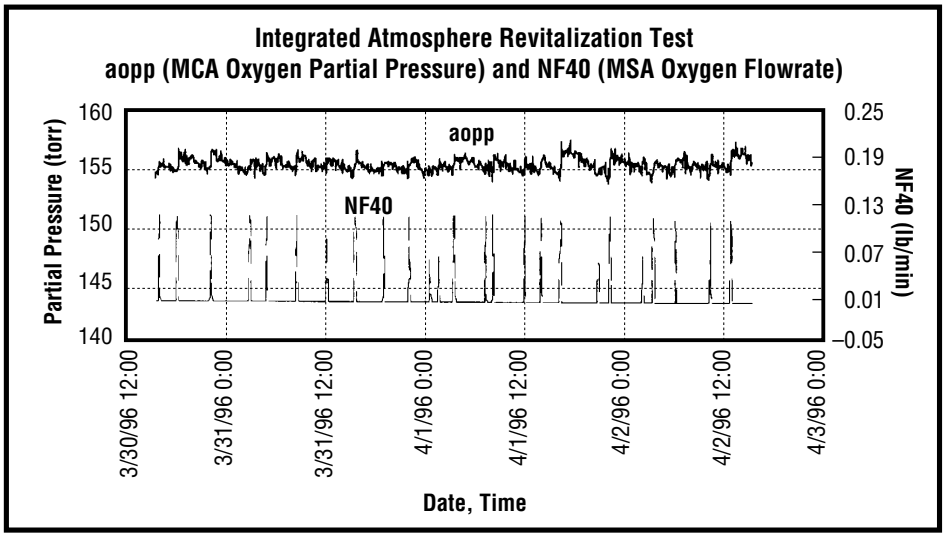
Integrated Atmosphere Revitalization Test
aopp (MCA Oxygen Partial Pressure) and NF40 (MSA Oxygen Flowrate)
Partial Pressure (torr)
160
155
150
145
140
aopp
NF40
0.25
0.19
0.13
0.07
0.01
–0.05
NF40 (lb/min)
3/30/96 12:00
3/31/96 0:00
3/31/96 12:00
4/1/96 0:00
4/1/96 12:00
4/2/96 0:00
4/2/96 12:00
4/3/96 0:00
Date, Time

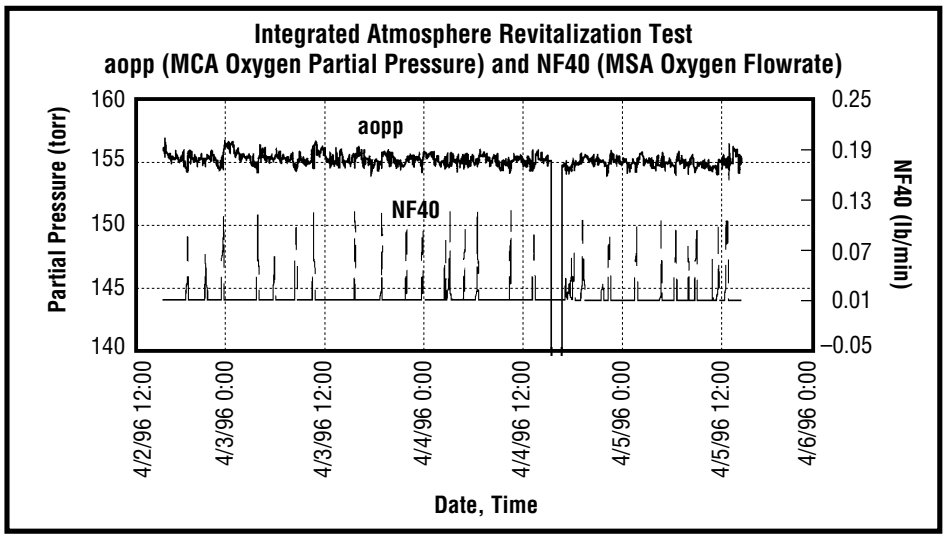
Integrated Atmosphere Revitalization Test
aopp (MCA Oxygen Partial Pressure) and NF40 (MSA Oxygen Flowrate)
Partial Pressure (torr)
NF40 (lb/min)
aopp
NF40
160
155
150
145
140
0.25
0.19
0.13
0.07
0.01
–0.05
4/2/96 12:00
4/3/96 0:00
4/3/96 12:00
4/4/96 0:00
4/4/96 12:00
4/5/96 0:00
4/5/96 12:00
4/6/96 0:00
Date, Time

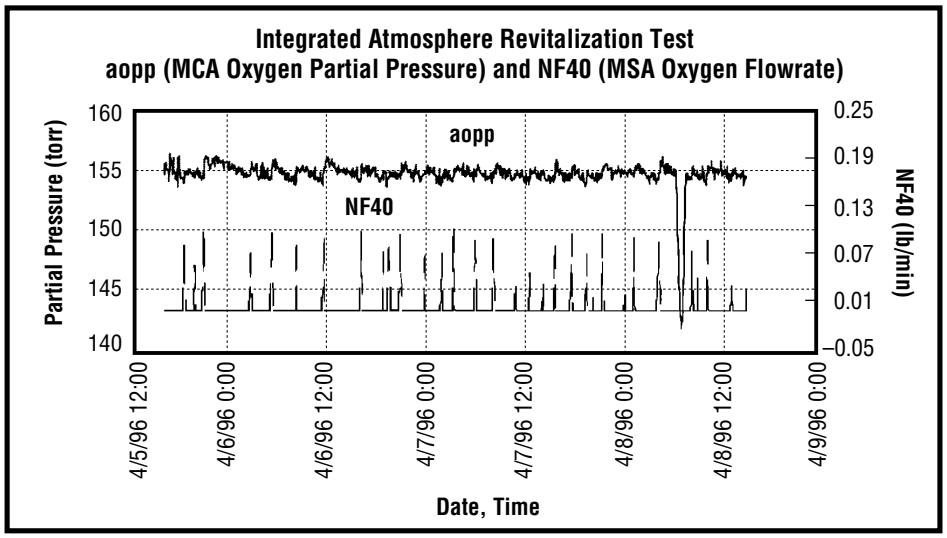
Integrated Atmosphere Revitalization Test
aopp (MCA Oxygen Partial Pressure) and NF40 (MSA Oxygen Flowrate)
Partial Pressure (torr)
NF40 (lb/min)
aopp
NF40
160
155
150
145
140
0.25
0.19
0.13
0.07
0.01
–0.05
4/5/96 12:00
4/6/96 0:00
4/6/96 12:00
4/7/96 0:00
4/7/96 12:00
4/8/96 0:00
4/8/96 12:00
4/9/96 0:00
Date, Time

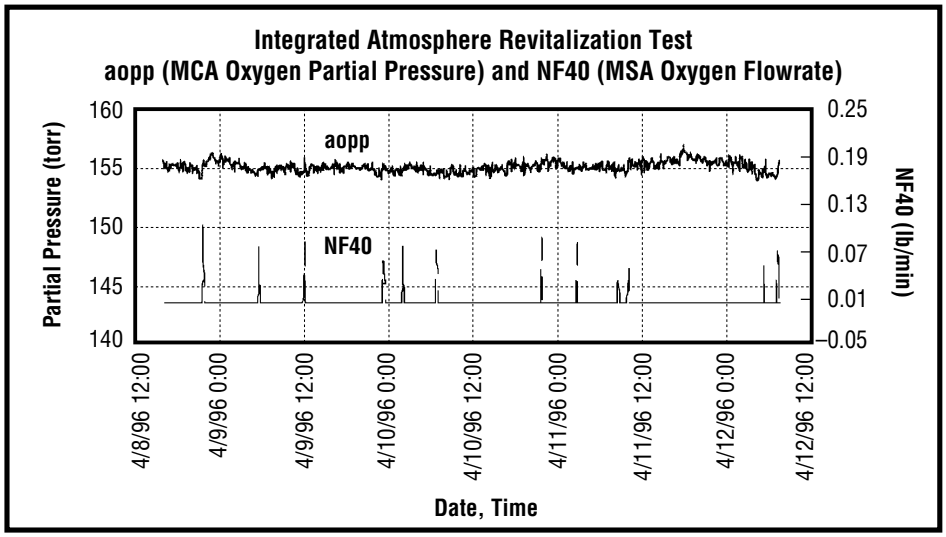
Integrated Atmosphere Revitalization Test
aopp (MCA Oxygen Partial Pressure) and NF40 (MSA Oxygen Flowrate)
Partial Pressure (torr)
NF40 (lb/min)
aopp
NF40
160
155
150
145
140
0.25
0.19
0.13
0.07
0.01
–0.05
4/8/96 12:00
4/9/96 0:00
4/9/96 12:00
4/10/96 0:00
4/10/96 12:00
4/11/96 0:00
4/11/96 12:00
4/12/96 0:00
4/12/96 12:00
Date, Time

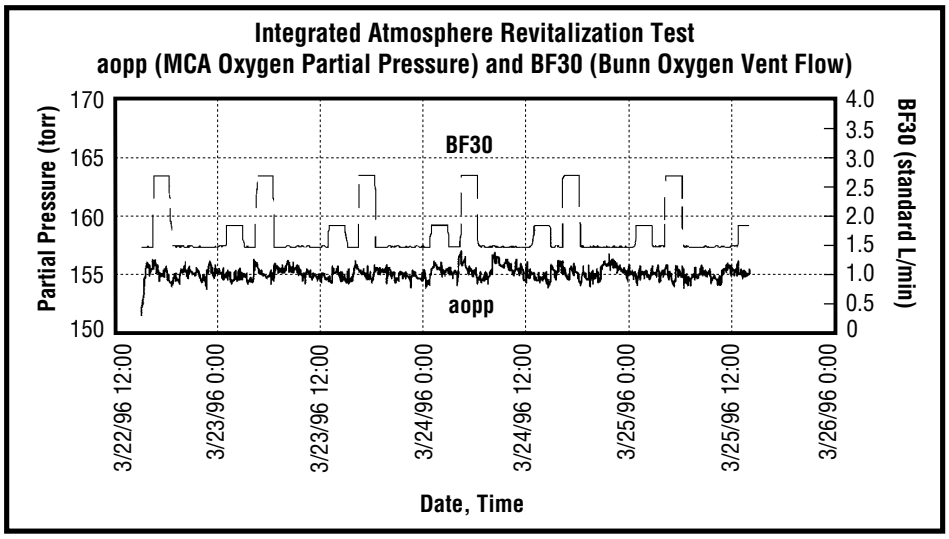
Integrated Atmosphere Revitalization Test
aopp (MCA Oxygen Partial Pressure) and BF30 (Bunn Oxygen Vent Flow)
Partial Pressure (torr)
BF30 (standard L/min)
BF30
aopp
170
165
160
155
150
4.0
3.5
3.0
2.5
2.0
1.5
1.0
0.5
0
3/22/96 12:00
3/23/96 0:00
3/23/96 12:00
3/24/96 0:00
3/24/96 12:00
3/25/96 0:00
3/25/96 12:00
3/26/96 0:00
Date, Time

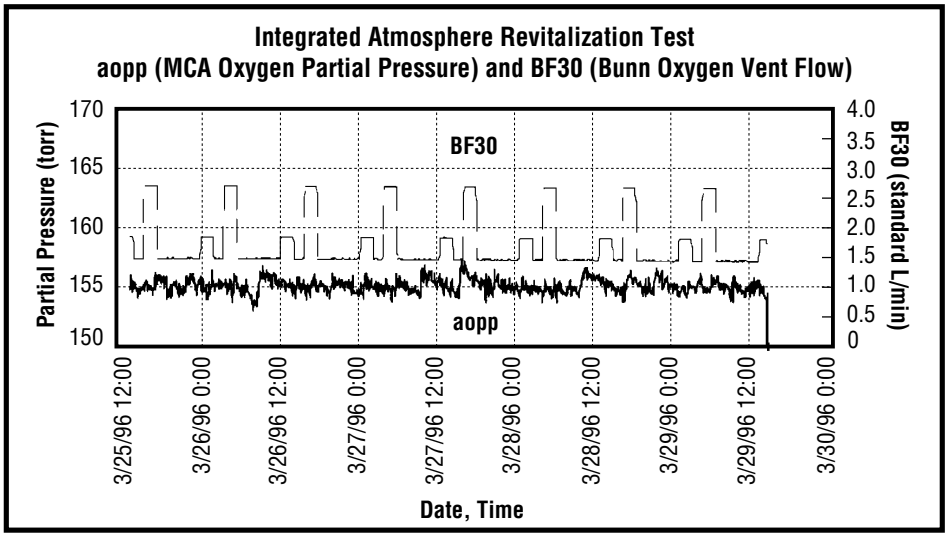
Integrated Atmosphere Revitalization Test
aopp (MCA Oxygen Partial Pressure) and BF30 (Bunn Oxygen Vent Flow)
Partial Pressure (torr)
BF30 (standard L/min)
BF30
aopp
170
165
160
155
150
4.0
3.5
3.0
2.5
2.0
1.5
1.0
0.5
0
3/25/96 12:00
3/26/96 0:00
3/26/96 12:00
3/27/96 0:00
3/27/96 12:00
3/28/96 0:00
3/28/96 12:00
3/29/96 0:00
3/29/96 12:00
3/30/96 0:00
Date, Time

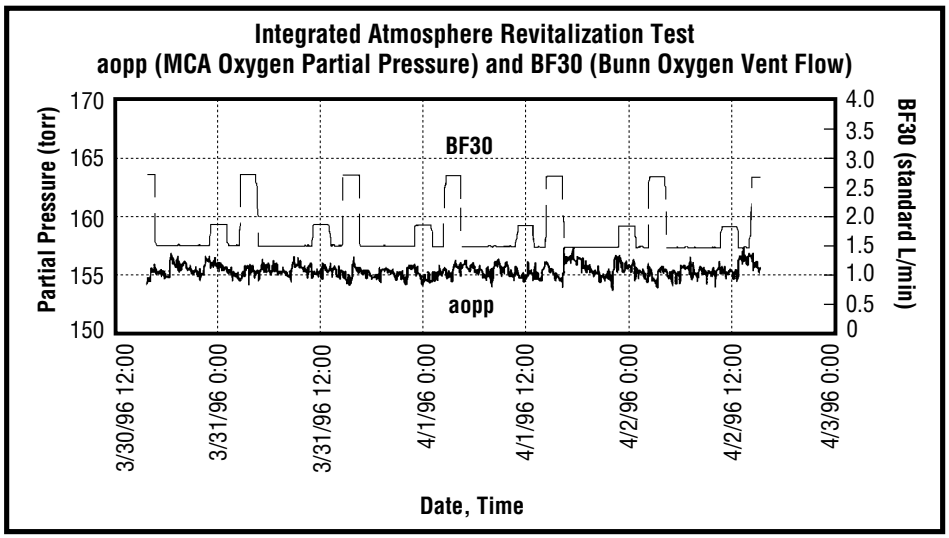
Integrated Atmosphere Revitalization Test
aopp (MCA Oxygen Partial Pressure) and BF30 (Bunn Oxygen Vent Flow)
Partial Pressure (torr)
BF30 (standard L/min)
BF30
aopp
170
165
160
155
150
4.0
3.5
3.0
2.5
2.0
1.5
1.0
0.5
0
3/30/96 12:00
3/31/96 0:00
3/31/96 12:00
4/1/96 0:00
4/1/96 12:00
4/2/96 0:00
4/2/96 12:00
4/3/96 0:00
Date, Time

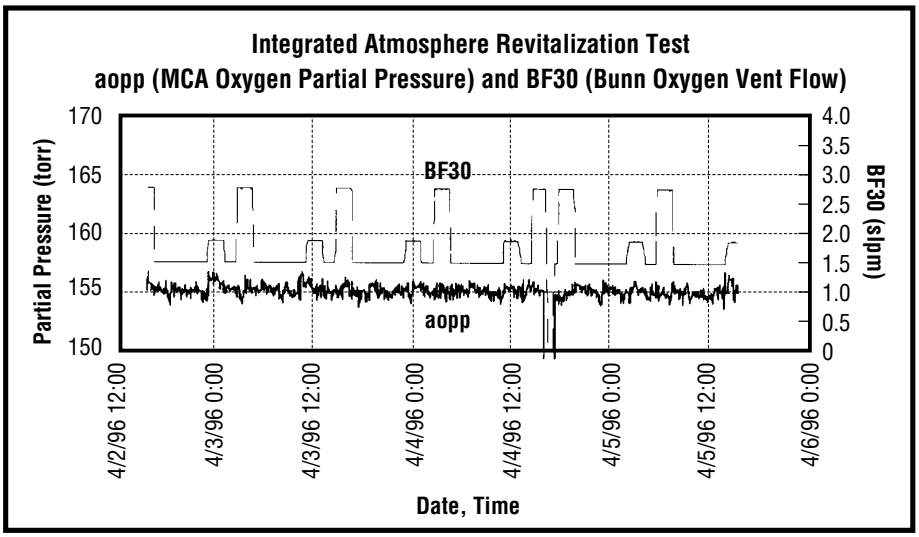
Integrated Atmosphere Revitalization Test
aopp (MCA Oxygen Partial Pressure) and BF30 (Bunn Oxygen Vent Flow)
Partial Pressure (torr)
BF30 (slpm)
BF30
aopp
170
165
160
155
150
4.0
3.5
3.0
2.5
2.0
1.5
1.0
0.5
0
4/2/96 12:00
4/3/96 0:00
4/3/96 12:00
4/4/96 0:00
4/4/96 12:00
4/5/96 0:00
4/5/96 12:00
4/6/96 0:00
Date, Time

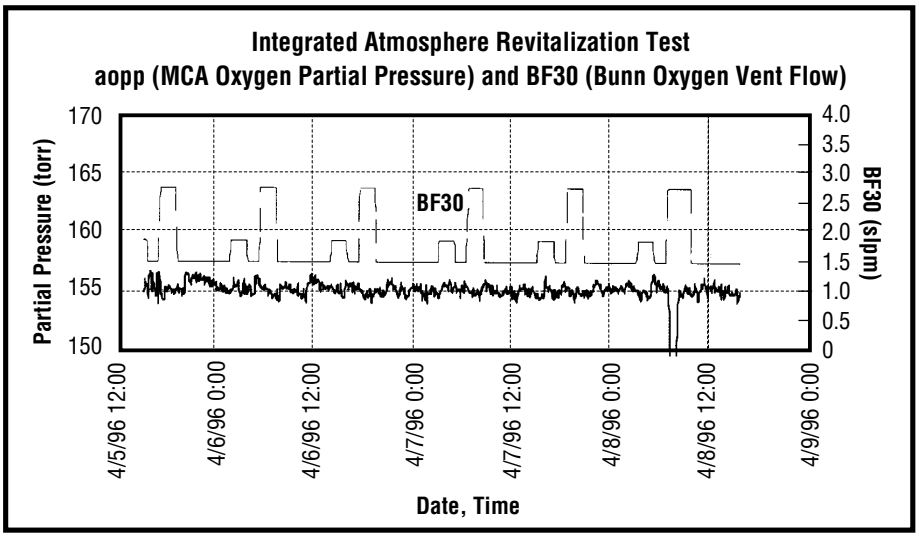
Integrated Atmosphere Revitalization Test
aopp (MCA Oxygen Partial Pressure) and BF30 (Bunn Oxygen Vent Flow)
Partial Pressure (torr)
BF30 (slpm)
BF30
170
165
160
155
150
4.0
3.5
3.0
2.5
2.0
1.5
1.0
0.5
0
4/5/96 12:00
4/6/96 0:00
4/6/96 12:00
4/7/96 0:00
4/7/96 12:00
4/8/96 0:00
4/8/96 12:00
4/9/96 0:00
Date, Time

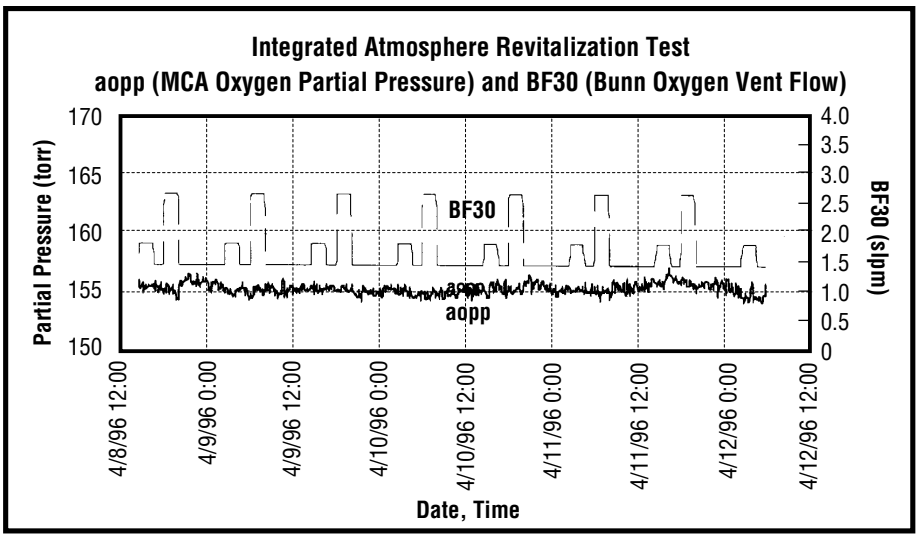
Integrated Atmosphere Revitalization Test
aopp (MCA Oxygen Partial Pressure) and BF30 (Bunn Oxygen Vent Flow)
Partial Pressure (torr)
BF30 (slpm)
BF30
aopp
aopp
170
165
160
155
150
4.0
3.5
3.0
2.5
2.0
1.5
1.0
0.5
0
4/8/96 12:00
4/9/96 0:00
4/9/96 12:00
4/10/96 0:00
4/10/96 12:00
4/11/96 0:00
4/11/96 12:00
4/12/96 0:00
4/12/96 12:00
Date, Time

APPENDIX H—
CMS RESPONSE TO NITROGEN INJECTION

The following data plots show the test chamber nitrogen partial pressure and the effect of nitrogen injection on it. Makeup of nitrogen via injection had the only measurable effect on the chamber's nitrogen partial pressure.

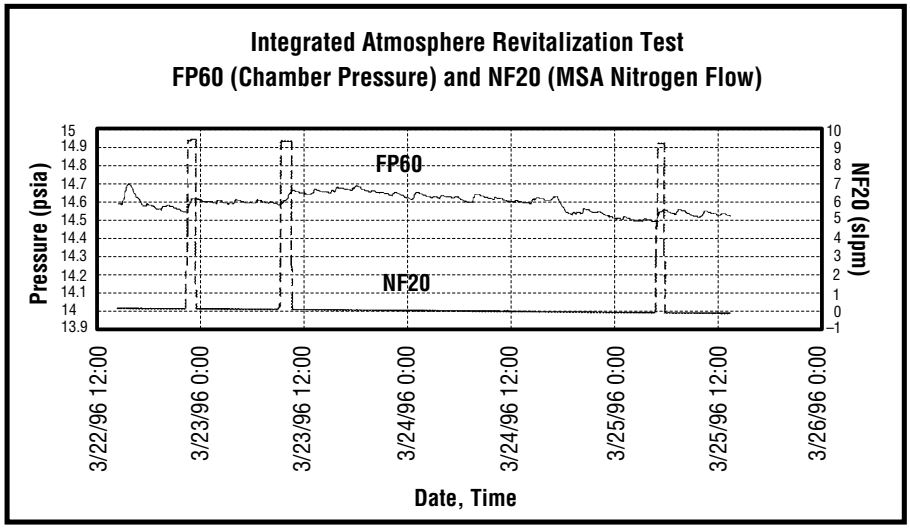
Integrated Atmosphere Revitalization Test
FP60 (Chamber Pressure) and NF20 (MSA Nitrogen Flow)
Pressure (psia)
NF20 (slpm)
FP60
NF20
15
14.9
14.8
14.7
14.6
14.5
14.4
14.3
14.2
14.1
14
13.9
10
9
8
7
6
5
4
3
2
1
0
–1
3/22/96 12:00
3/23/96 0:00
3/23/96 12:00
3/24/96 0:00
3/24/96 12:00
3/25/96 0:00
3/25/96 12:00
3/26/96 0:00
Date, Time

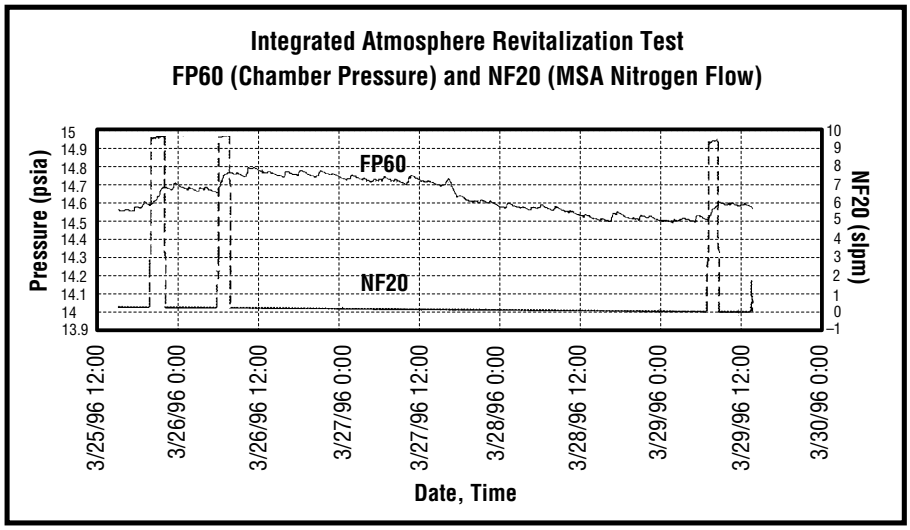
Integrated Atmosphere Revitalization Test
FP60 (Chamber Pressure) and NF20 (MSA Nitrogen Flow)
Pressure (psia)
NF20 (slpm)
FP60
NF20
15
14.9
14.8
14.7
14.6
14.5
14.4
14.3
14.2
14.1
14
13.9
10
9
8
7
6
5
4
3
2
1
0
–1
3/25/96 12:00
3/26/96 0:00
3/26/96 12:00
3/27/96 0:00
3/27/96 12:00
3/28/96 0:00
3/28/96 12:00
3/29/96 0:00
3/29/96 12:00
3/30/96 0:00
Date, Time

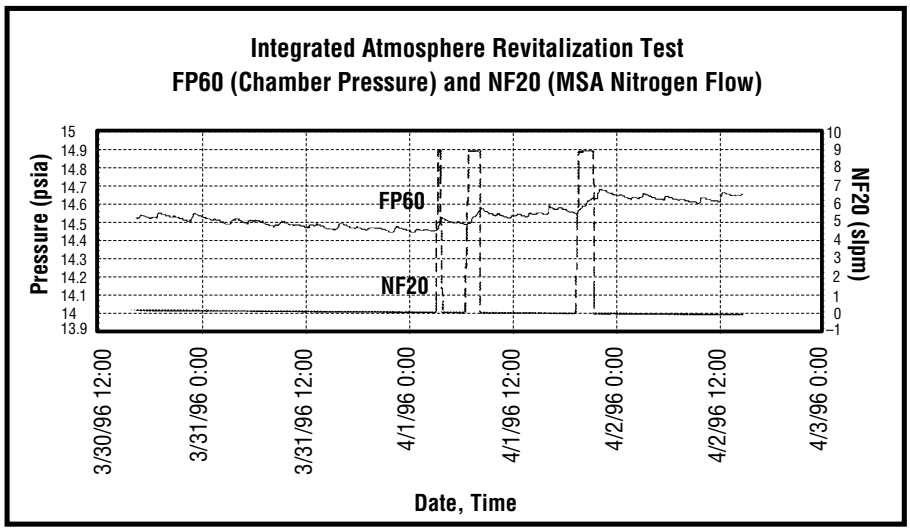
Integrated Atmosphere Revitalization Test
FP60 (Chamber Pressure) and NF20 (MSA Nitrogen Flow)
Pressure (psia)
NF20 (slpm)
FP60
NF20
15
14.9
14.8
14.7
14.6
14.5
14.4
14.3
14.2
14.1
14
13.9
10
9
8
7
6
5
4
3
2
1
0
–1
3/30/96 12:00
3/31/96 0:00
3/31/96 12:00
4/1/96 0:00
4/1/96 12:00
4/2/96 0:00
4/2/96 12:00
4/3/96 0:00
Date, Time

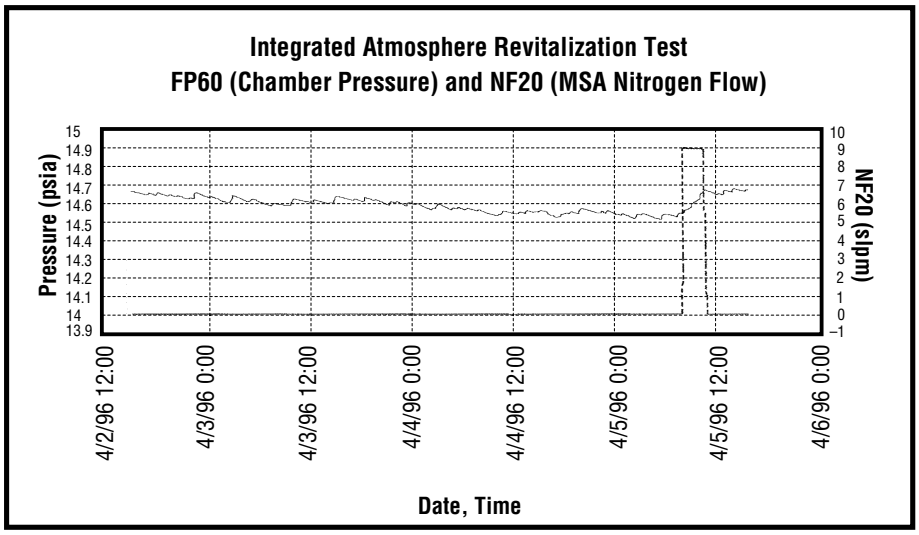
Integrated Atmosphere Revitalization Test
FP60 (Chamber Pressure) and NF20 (MSA Nitrogen Flow)
Pressure (psia)
NF20 (slpm)
15
14.9
14.8
14.7
14.6
14.5
14.4
14.3
14.2
14.1
14
13.9
10
9
8
7
6
5
4
3
2
1
0
–1
4/2/96 12:00
4/3/96 0:00
4/3/96 12:00
4/4/96 0:00
4/4/96 12:00
4/5/96 0:00
4/5/96 12:00
4/6/96 0:00
Date, Time

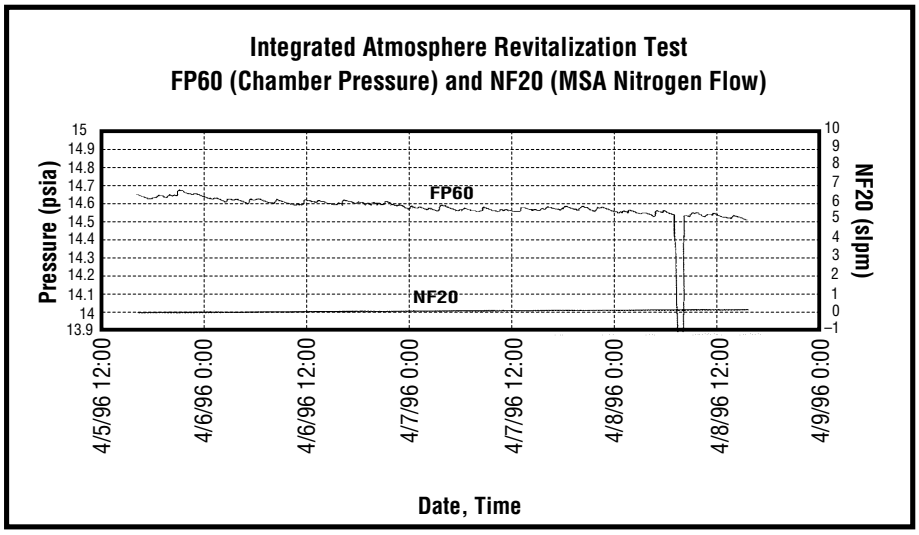
Integrated Atmosphere Revitalization Test
FP60 (Chamber Pressure) and NF20 (MSA Nitrogen Flow)
Pressure (psia)
NF20 (slpm)
FP60
NF20
15
14.9
14.8
14.7
14.6
14.5
14.4
14.3
14.2
14.1
14
13.9
10
9
8
7
6
5
4
3
2
1
0
–1
4/5/96 12:00
4/6/96 0:00
4/6/96 12:00
4/7/96 0:00
4/7/96 12:00
4/8/96 0:00
4/8/96 12:00
4/9/96 0:00
Date, Time

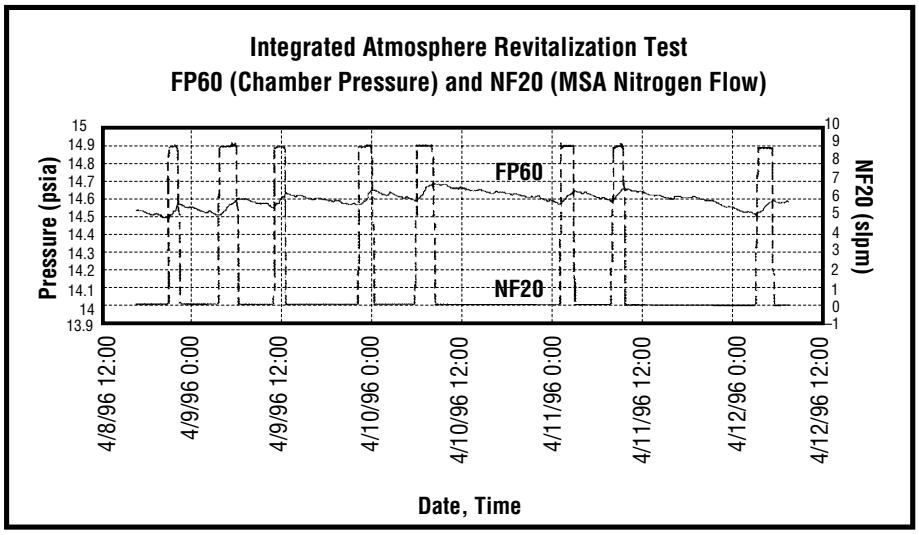
Integrated Atmosphere Revitalization Test
FP60 (Chamber Pressure) and NF20 (MSA Nitrogen Flow)
Pressure (psia)
NF20 (slpm)
FP60
NF20
15
14.9
14.8
14.7
14.6
14.5
14.4
14.3
14.2
14.1
14
13.9
10
9
8
7
6
5
4
3
2
1
0
–1
4/8/96 12:00
4/9/96 0:00
4/9/96 12:00
4/10/96 0:00
4/10/96 12:00
4/11/96 0:00
4/11/96 12:00
4/12/96 0:00
4/12/96 12:00
Date, Time

APPENDIX I—
CMS CARBON DIOXIDE PARTIAL PRESSURE RESPONSE

The following data plots show the test chamber carbon dioxide partial pressure during the uninterrupted portions of the test. Periods of lost data were observed on March 29, April 4, and April 8, 1996, as a result of a host computer shutdown, a second host computer shutdown, and data acquisition system transition to daylight savings time, respectively.

The primary factor that influenced the carbon dioxide partial pressure, other than CDRA operation, was the metabolic injection. This can be seen by the carbon dioxide partial pressure response relative to the metabolic simulation injection rate.

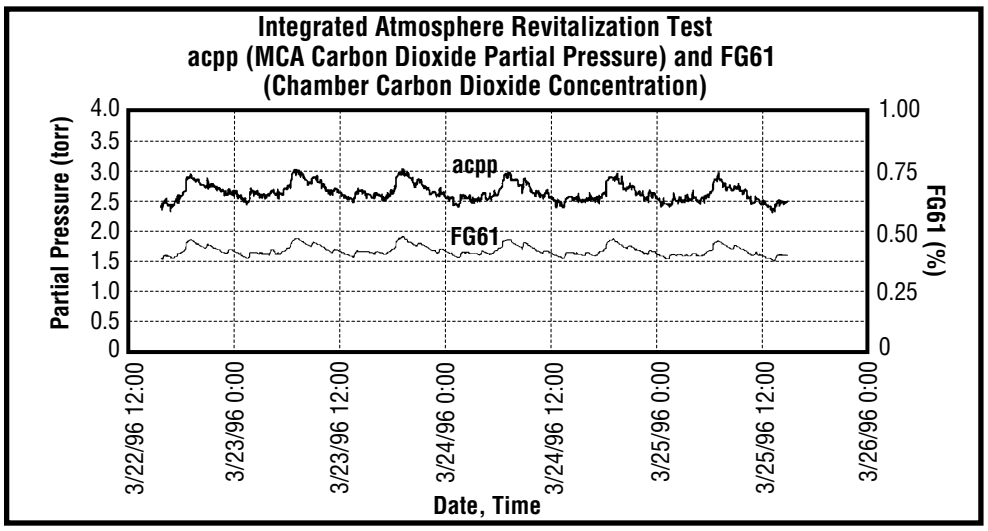
Integrated Atmosphere Revitalization Test
acpp (MCA Carbon Dioxide Partial Pressure) and FG61
(Chamber Carbon Dioxide Concentration)
Partial Pressure (torr)
FG61 (%)
acpp
FG61
4.0
3.5
3.0
2.5
2.0
1.5
1.0
0.5
0
1.00
0.75
0.50
0.25
0
3/22/96 12:00
3/23/96 0:00
3/23/96 12:00
3/24/96 0:00
3/24/96 12:00
3/25/96 0:00
3/25/96 12:00
3/26/96 0:00
Date, Time

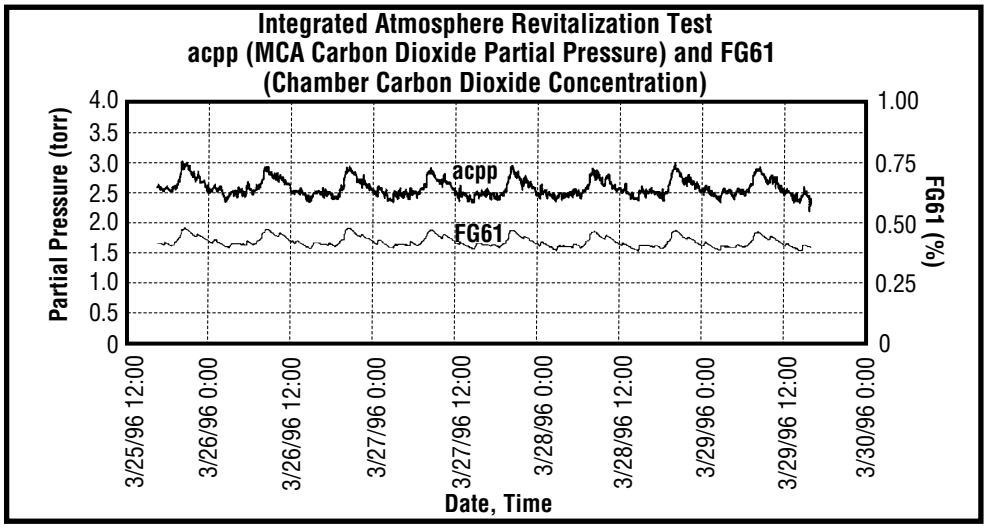
Integrated Atmosphere Revitalization Test
acpp (MCA Carbon Dioxide Partial Pressure) and FG61
(Chamber Carbon Dioxide Concentration)
Partial Pressure (torr)
FG61 (%)
acpp
FG61
4.0
3.5
3.0
2.5
2.0
1.5
1.0
0.5
0
1.00
0.75
0.50
0.25
0
3/25/96 12:00
3/26/96 0:00
3/26/96 12:00
3/27/96 0:00
3/27/96 12:00
3/28/96 0:00
3/28/96 12:00
3/29/96 0:00
3/29/96 12:00
3/30/96 0:00
Date, Time

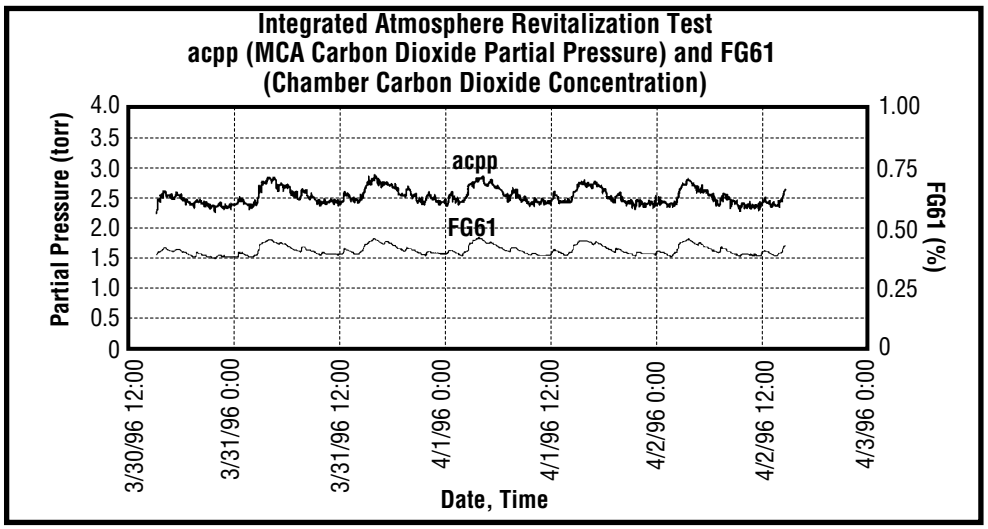
Integrated Atmosphere Revitalization Test
acpp (MCA Carbon Dioxide Partial Pressure) and FG61
(Chamber Carbon Dioxide Concentration)
Partial Pressure (torr)
FG61 (%)
acpp
FG61
4.0
3.5
3.0
2.5
2.0
1.5
1.0
0.5
0
1.00
0.75
0.50
0.25
0
3/30/96 12:00
3/31/96 0:00
3/31/96 12:00
4/1/96 0:00
4/1/96 12:00
4/2/96 0:00
4/2/96 12:00
4/3/96 0:00
Date, Time

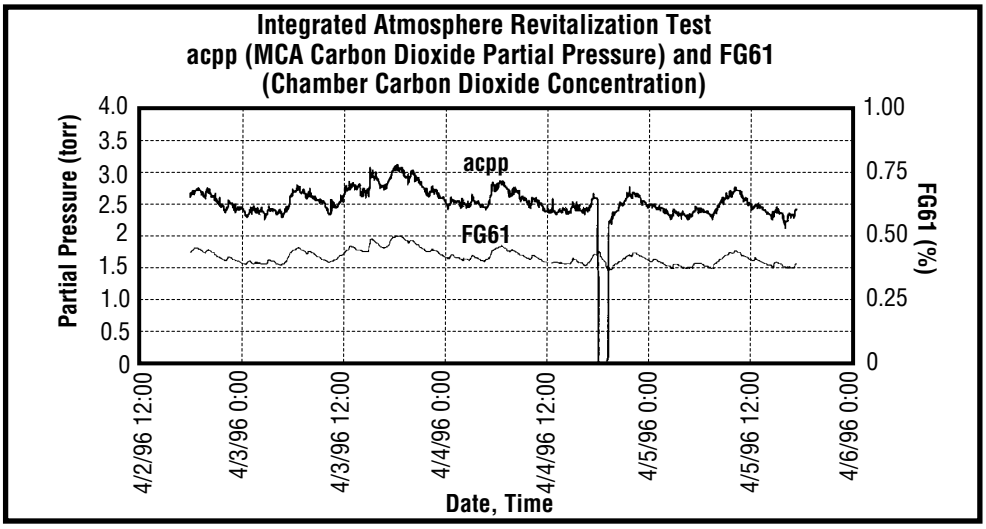
Integrated Atmosphere Revitalization Test
acpp (MCA Carbon Dioxide Partial Pressure) and FG61
(Chamber Carbon Dioxide Concentration)
Partial Pressure (torr)
FG61 (%)
acpp
FG61
4.0
3.5
3.0
2.5
2.0
1.5
1.0
0.5
0
1.00
0.75
0.50
0.25
0
4/2/96 12:00
4/3/96 0:00
4/3/96 12:00
4/4/96 0:00
4/4/96 12:00
4/5/96 0:00
4/5/96 12:00
4/6/96 0:00
Date, Time

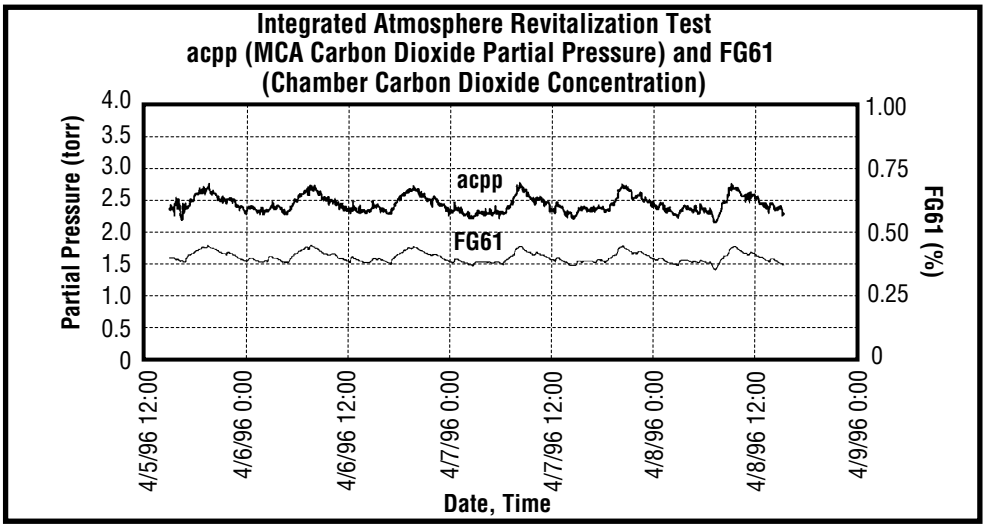
Integrated Atmosphere Revitalization Test
acpp (MCA Carbon Dioxide Partial Pressure) and FG61
(Chamber Carbon Dioxide Concentration)
Partial Pressure (torr)
FG61 (%)
acpp
FG61
4.0
3.5
3.0
2.5
2.0
1.5
1.0
0.5
0
1.00
0.75
0.50
0.25
0
4/5/96 12:00
4/6/96 0:00
4/6/96 12:00
4/7/96 0:00
4/7/96 12:00
4/8/96 0:00
4/8/96 12:00
4/9/96 0:00
Date, Time

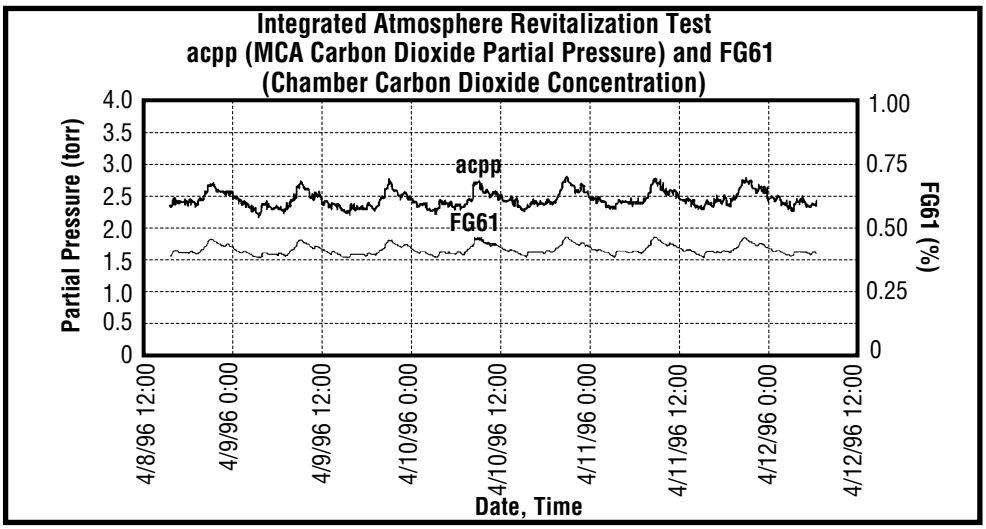
Integrated Atmosphere Revitalization Test
acpp (MCA Carbon Dioxide Partial Pressure) and FG61
(Chamber Carbon Dioxide Concentration)
Partial Pressure (torr)
FG61 (%)
acpp
FG61
4.0
3.5
3.0
2.5
2.0
1.5
1.0
0.5
0
1.00
0.75
0.50
0.25
0
4/8/96 12:00
4/9/96 0:00
4/9/96 12:00
4/10/96 0:00
4/10/96 12:00
4/11/96 0:00
4/11/96 12:00
4/12/96 0:00
4/12/96 12:00
Date, Time

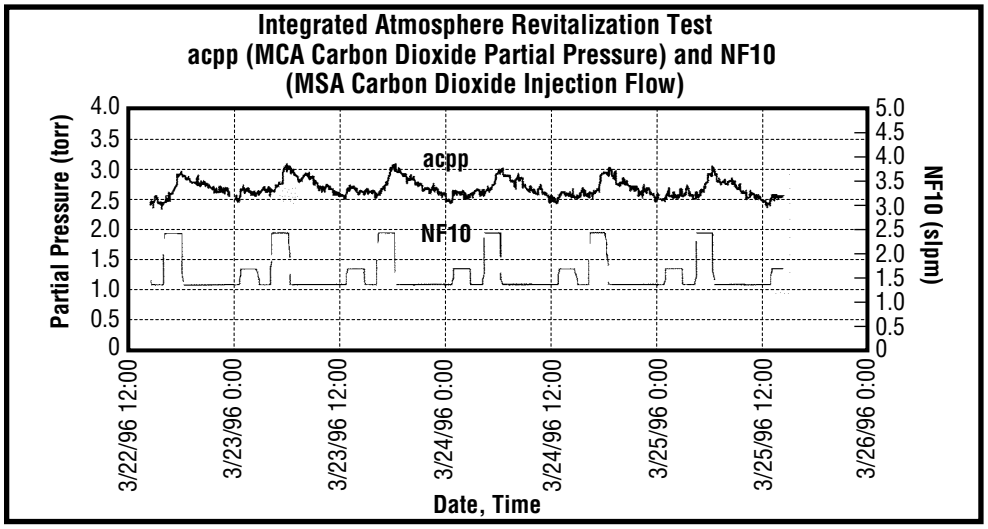
Integrated Atmosphere Revitalization Test
acpp (MCA Carbon Dioxide Partial Pressure) and NF10
(MSA Carbon Dioxide Injection Flow)
Partial Pressure (torr)
NF10 (slpm)
acpp
NF10
4.0
3.5
3.0
2.5
2.0
1.5
1.0
0.5
0
5.0
4.5
4.0
3.5
3.0
2.5
2.0
1.5
1.0
0.5
0
3/22/96 12:00
3/23/96 0:00
3/23/96 12:00
3/24/96 0:00
3/24/96 12:00
3/25/96 0:00
3/25/96 12:00
3/26/96 0:00
Date, Time

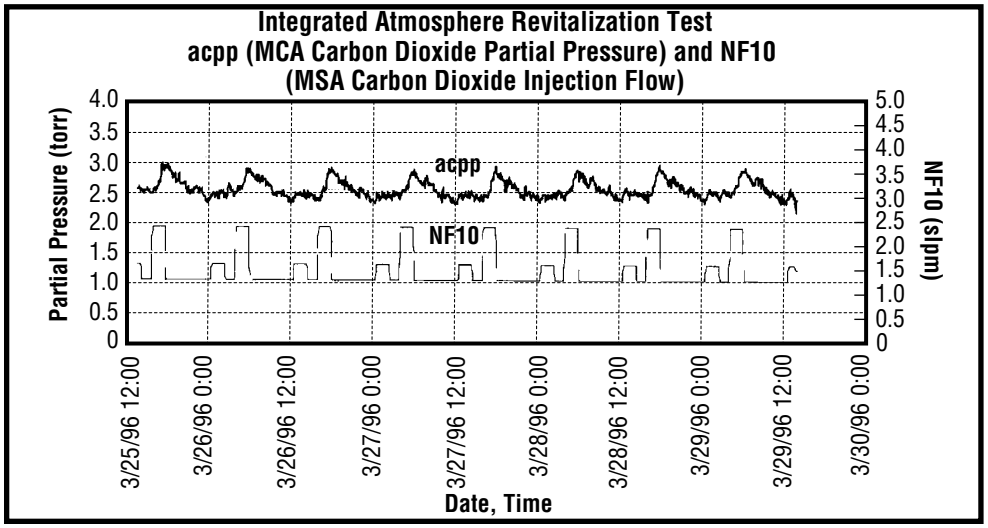
Integrated Atmosphere Revitalization Test
acpp (MCA Carbon Dioxide Partial Pressure) and NF10
(MSA Carbon Dioxide Injection Flow)
Partial Pressure (torr)
NF10 (slpm)
acpp
NF10
4.0
3.5
3.0
2.5
2.0
1.5
1.0
0.5
0
5.0
4.5
4.0
3.5
3.0
2.5
2.0
1.5
1.0
0.5
0
3/25/96 12:00
3/26/96 0:00
3/26/96 12:00
3/27/96 0:00
3/27/96 12:00
3/28/96 0:00
3/28/96 12:00
3/29/96 0:00
3/29/96 12:00
3/30/96 0:00
Date, Time

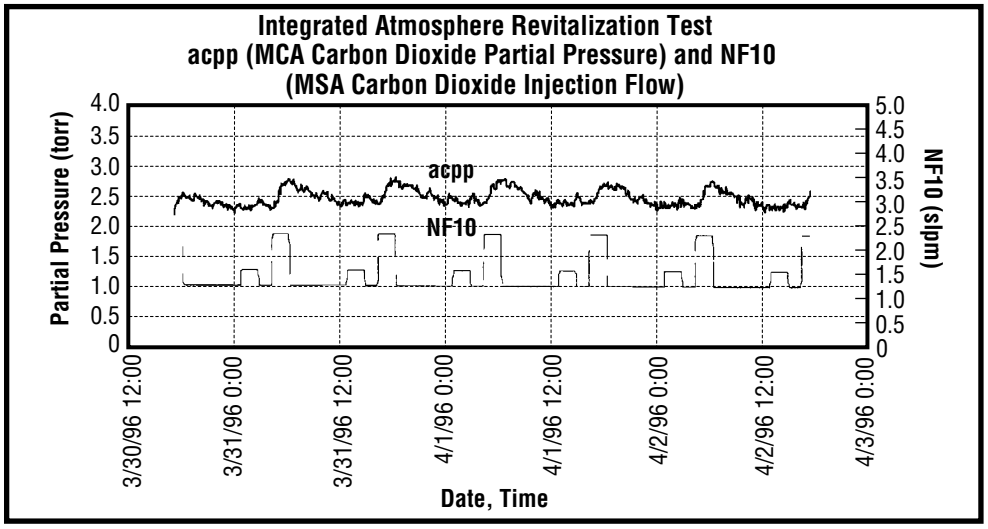
Integrated Atmosphere Revitalization Test
acpp (MCA Carbon Dioxide Partial Pressure) and NF10
(MSA Carbon Dioxide Injection Flow)
Partial Pressure (torr)
NF10 (slpm)
acpp
NF10
4.0
3.5
3.0
2.5
2.0
1.5
1.0
0.5
0
5.0
4.5
4.0
3.5
3.0
2.5
2.0
1.5
1.0
0.5
0
3/30/96 12:00
3/31/96 0:00
3/31/96 12:00
4/1/96 0:00
4/1/96 12:00
4/2/96 0:00
4/2/96 12:00
4/3/96 0:00
Date, Time

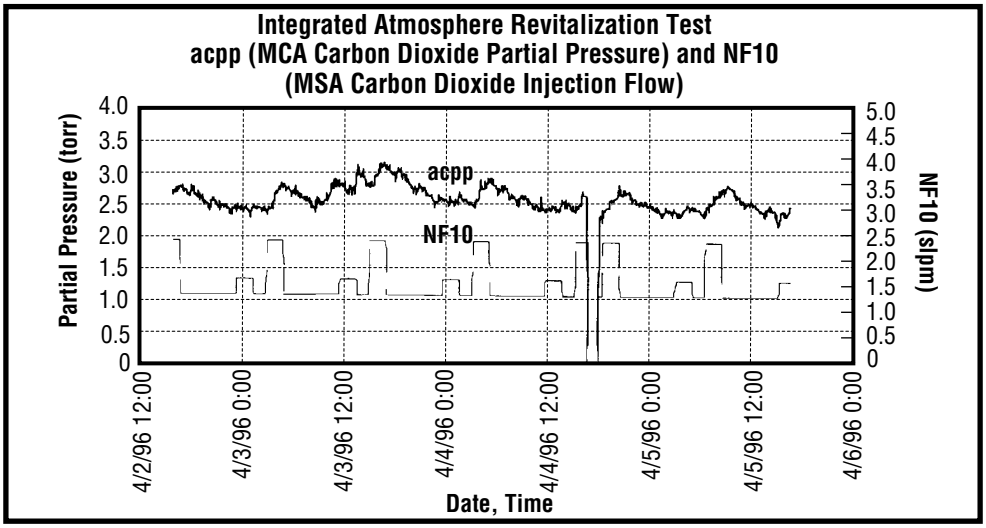
Integrated Atmosphere Revitalization Test
acpp (MCA Carbon Dioxide Partial Pressure) and NF10
(MSA Carbon Dioxide Injection Flow)
Partial Pressure (torr)
NF10 (slpm)
acpp
NF10
4.0
3.5
3.0
2.5
2.0
1.5
1.0
0.5
0
5.0
4.5
4.0
3.5
3.0
2.5
2.0
1.5
1.0
0.5
0
4/2/96 12:00
4/3/96 0:00
4/3/96 12:00
4/4/96 0:00
4/4/96 12:00
4/5/96 0:00
4/5/96 12:00
4/6/96 0:00
Date, Time

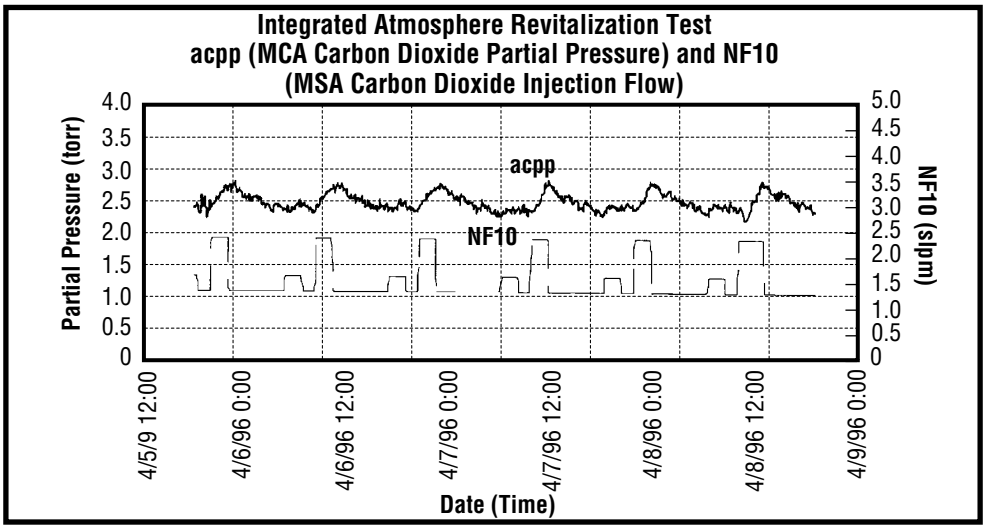
Integrated Atmosphere Revitalization Test
acpp (MCA Carbon Dioxide Partial Pressure) and NF10
(MSA Carbon Dioxide Injection Flow)
Partial Pressure (torr)
NF10 (slpm)
acpp
NF10
4.0
3.5
3.0
2.5
2.0
1.5
1.0
0.5
0
5.0
4.5
4.0
3.5
3.0
2.5
2.0
1.5
1.0
0.5
0
4/5/9 12:00
4/6/96 0:00
4/6/96 12:00
4/7/96 0:00
4/7/96 12:00
4/8/96 0:00
4/8/96 12:00
4/9/96 0:00
Date (Time)

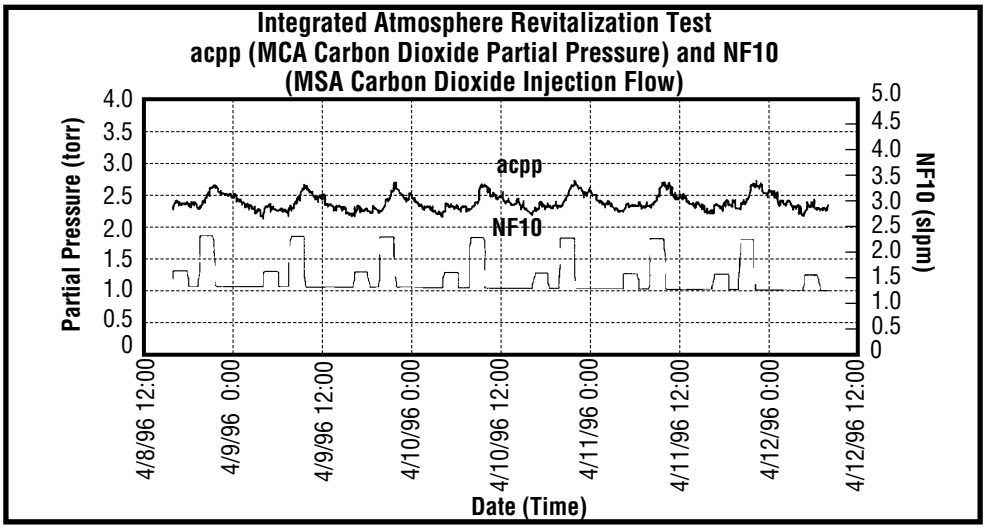
Integrated Atmosphere Revitalization Test
acpp (MCA Carbon Dioxide Partial Pressure) and NF10
(MSA Carbon Dioxide Injection Flow)
Partial Pressure (torr)
NF10 (slpm)
acpp
NF10
4.0
3.5
3.0
2.5
2.0
1.5
1.0
0.5
0
5.0
4.5
4.0
3.5
3.0
2.5
2.0
1.5
1.0
0.5
0
4/8/96 12:00
4/9/96 0:00
4/9/96 12:00
4/10/96 0:00
4/10/96 12:00
4/11/96 0:00
4/11/96 12:00
4/12/96 0:00
4/12/96 12:00
Date (Time)

APPENDIX J—
CMS DEWPOINT RESPONSE

The following data plots show the test chamber response for water vapor during the uninterrupted periods of the test. These data are shown as dewpoint and are compared to the metabolic simulation water injection flowrate. As can be seen, the chamber dewpoint fluctuated as a directly with the injection rate. Water injection was the strongest influence on the chamber atmopsheric water content. The data are consistent throughout the test, with one exception. On March 28, 1996, the dewpoint increases by approximately 2.5 °C. This increase was the result of recalibrating the MCA after its verification cycle indicated that the water reading was running very close to its lower boundary of acceptability. This was the only calibration made during the entire test. Gaps in data are shown on March 29, April 4, and April 8, 1996. The gaps on March 29 and April 4 were caused by host computer shutdowns, while the gap on April 8 resulted from transitioning the data acquisition computer clock to daylight savings time. In all cases, the ARS subassemblies continued to operate normally.

During the test, samples were collected by the MCA using various sample line lengths. Samples were collected initially from the 30.5 m (100 ft) sample line length. A transition occurred on March 29 at 14:42 to the 15.2 m (50 ft) sample line length. When this occurred, the dewpoint sensor reading at 15.2 m quickly rose to the level previously reported by the sensor located at the 30.5 m sample port. This further demonstrated the effects of pressure drop in the sample line on dewpoint readings. Following sampling at 15.2 m, the sample line length was changed to 22.9 m (75 ft) at 13:51 on April 3. On April 4 at 16:16, the host computer shutdown caused the sample line length to be reset at 15.2 m. This was discovered on April 8 at 08:00 when the sample line length was changed to 7.6 m (25 ft). Since only about 24 hr of sampling had occurred at the 22.9-m length, a second transition to this length was made at 12:00 on April 10, 1996. Sampling continued using this sample line length until 08:03 on April 12, 1996, when the integrated test ended.

As can be seen by the data plots, no changes in the MCA water vapor response resulted from changes in the sample line length. This result strongly indicates that the MCA water vapor readings are not sensitive to sample line length, and adsorption of water vapor on the sample line internal walls does not occur at a level significant enough to have a noticeable effect on the readings.

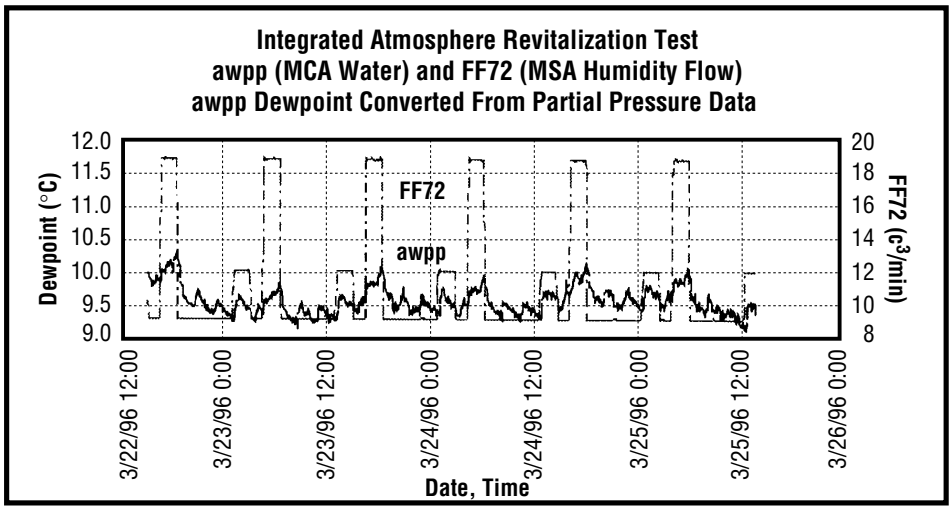
Integrated Atmosphere Revitalization Test
awpp (MCA Water) and FF72 (MSA Humidity Flow)
awpp Dewpoint Converted From Partial Pressure Data
Dewpoint (°C)
FF72 (c3/min)
FF72
awpp
12.0
11.5
11.0
10.5
10.0
9.5
9.0
20
18
16
14
12
10
8
3/22/96 12:00
3/23/96 0:00
3/23/96 12:00
3/24/96 0:00
3/24/96 12:00
3/25/96 0:00
3/25/96 12:00
3/26/96 0:00
Date, Time

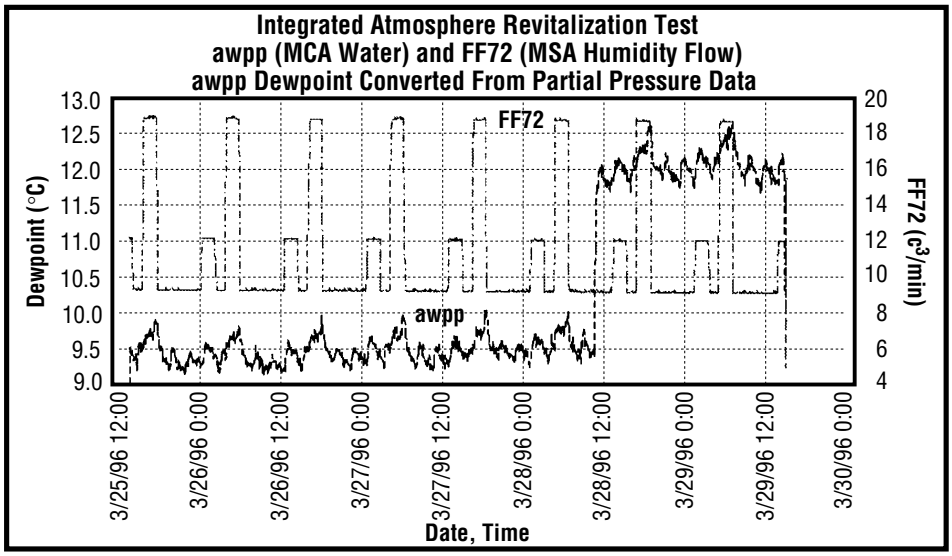
Integrated Atmosphere Revitalization Test
awpp (MCA Water) and FF72 (MSA Humidity Flow)
awpp Dewpoint Converted From Partial Pressure Data
Dewpoint (°C)
FF72 (c3/min)
FF72
awpp
13.0
12.5
12.0
11.5
11.0
10.5
10.0
9.5
9.0
20
18
16
14
12
10
8
6
4
3/25/96 12:00
3/26/96 0:00
3/26/96 12:00
3/27/96 0:00
3/27/96 12:00
3/28/96 0:00
3/28/96 12:00
3/29/96 0:00
3/29/96 12:00
3/30/96 0:00
Date, Time

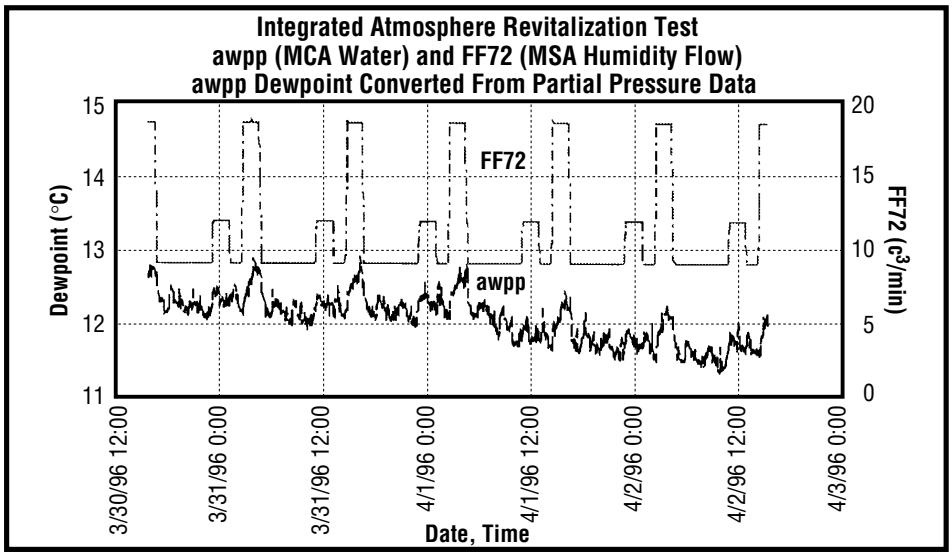
Integrated Atmosphere Revitalization Test
awpp (MCA Water) and FF72 (MSA Humidity Flow)
awpp Dewpoint Converted From Partial Pressure Data
Dewpoint (°C)
FF72 (c3/min)
FF72
awpp
15
14
13
12
11
20
15
10
5
0
3/30/96 12:00
3/31/96 0:00
3/31/96 12:00
4/1/96 0:00
4/1/96 12:00
4/2/96 0:00
4/2/96 12:00
4/3/96 0:00
Date, Time

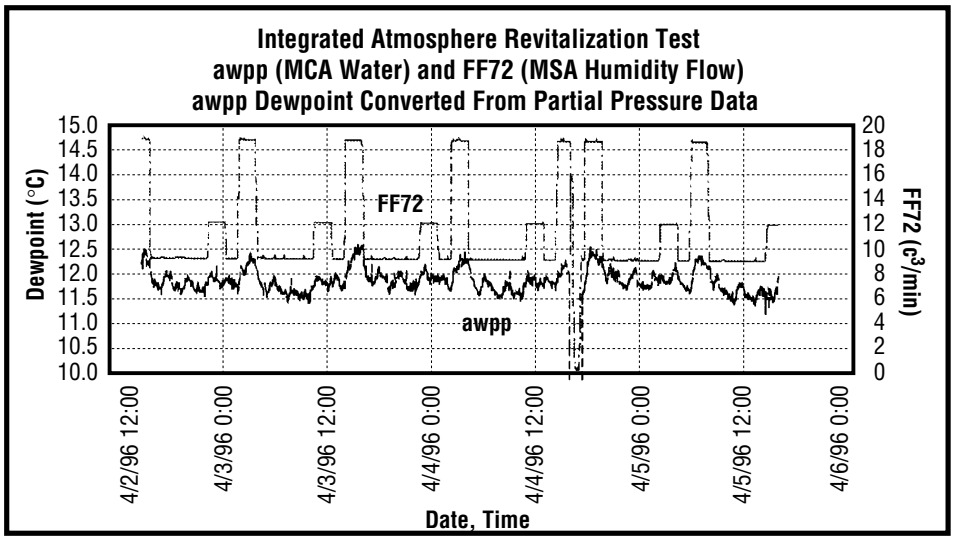
Integrated Atmosphere Revitalization Test
awpp (MCA Water) and FF72 (MSA Humidity Flow)
awpp Dewpoint Converted From Partial Pressure Data
Dewpoint (°C)
FF72 (c³/min)
FF72
awpp
Date, Time
4/2/96 12:00
4/3/96 0:00
4/3/96 12:00
4/4/96 0:00
4/4/96 12:00
4/5/96 0:00
4/5/96 12:00
4/6/96 0:00

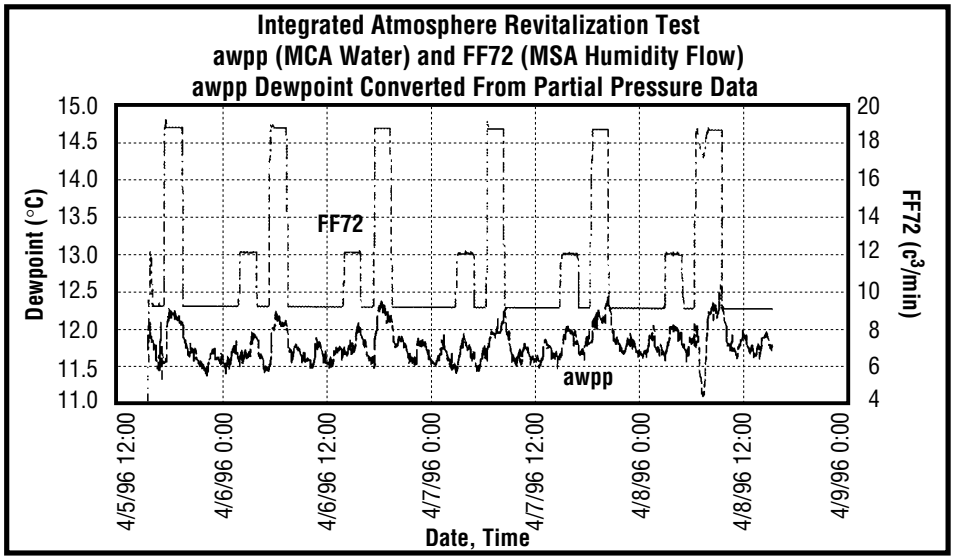
Integrated Atmosphere Revitalization Test
awpp (MCA Water) and FF72 (MSA Humidity Flow)
awpp Dewpoint Converted From Partial Pressure Data
Dewpoint (°C)
FF72 (c³/min)
FF72
awpp
Date, Time
4/5/96 12:00
4/6/96 0:00
4/6/96 12:00
4/7/96 0:00
4/7/96 12:00
4/8/96 0:00
4/8/96 12:00
4/9/96 0:00

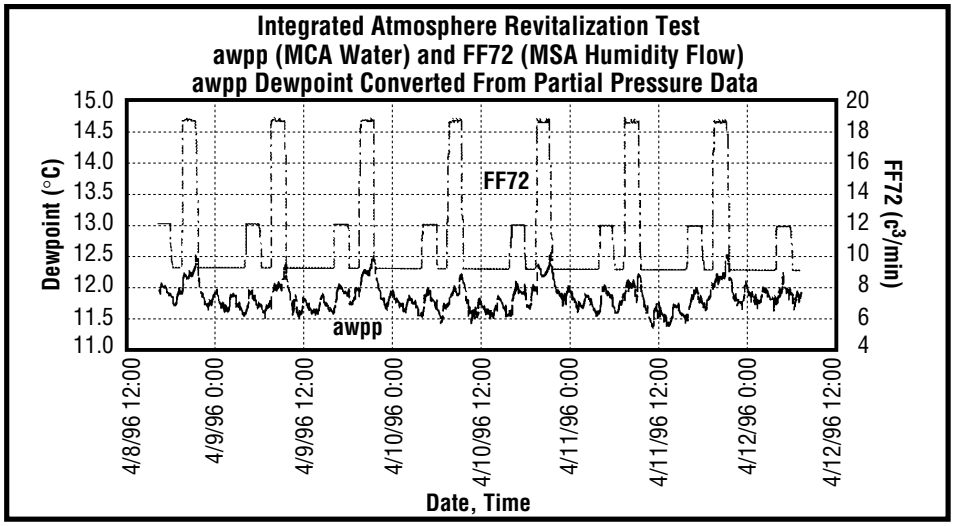
Integrated Atmosphere Revitalization Test
awpp (MCA Water) and FF72 (MSA Humidity Flow)
awpp Dewpoint Converted From Partial Pressure Data
Dewpoint (°C)
FF72 (c³/min)
FF72
awpp
Date, Time
4/8/96 12:00
4/9/96 0:00
4/9/96 12:00
4/10/96 0:00
4/10/96 12:00
4/11/96 0:00
4/11/96 12:00
4/12/96 0:00
4/12/96 12:00

APPENDIX K—
MCA RESPONSE TO HUMIDITY CYCLING

The following data plots show the MCA's response to humidity swings in the test chamber atmosphere. The relative humidity in the chamber was varied between approximately 47 percent and 80 percent by temporarily disabling the condensing heat exchanger coolant flowrate.

During this testing, the samples were collected for analysis by the MCA at four different sample line lengths. At least two complete cycles between the upper and lower relative humidity limits were conducted while collecting samples at the four sample line lengths. Samples were collected using the 30.5 m (100 ft) sample line length initially and then transitioned to shorter lengths. Two humidity cycles were completed and the sample line length changed to 15.2 m (50 ft) on April 16, 1996, at 11:00. Following two additional humidity cycles, the sample line length was changed to 22.9 m (75 ft) at 15:35 on April 16. On April 17 at 12:07, the sample line length was changed to 7.6 m (25 ft) for the final two cycles. These transitions can be seen in the data plots.

As an example, when the sample line length changed from 30.5 m to 15.2 m, the dewpoint reading at 15.2 m (AD62) rose to the level previously seen by the sensor located at 30.5 m (AD60). While the reading at 30.5 m continued to track the chamber humidity level, its response was sluggish because it did not have active flow. Similar responses were observed as the sample line length changed.

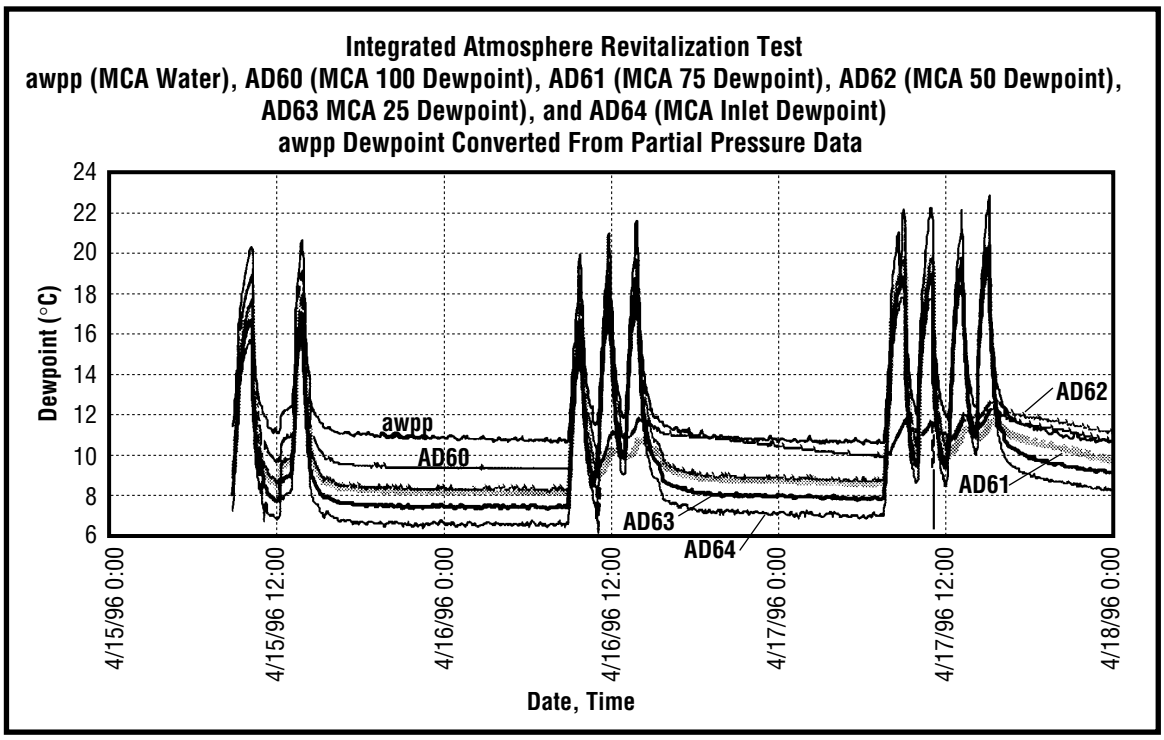
Integrated Atmosphere Revitalization Test
awpp (MCA Water), AD60 (MCA 100 Dewpoint), AD61 (MCA 75 Dewpoint), AD62 (MCA 50 Dewpoint),
AD63 MCA 25 Dewpoint), and AD64 (MCA Inlet Dewpoint)
awpp Dewpoint Converted From Partial Pressure Data
Dewpoint (°C)
24
22
20
18
16
14
12
10
8
6
awpp
AD60
AD62
AD61
AD63
AD64
4/15/96 0:00
4/15/96 12:00
4/16/96 0:00
4/16/96 12:00
4/17/96 0:00
4/17/96 12:00
4/18/96 0:00
Date, Time

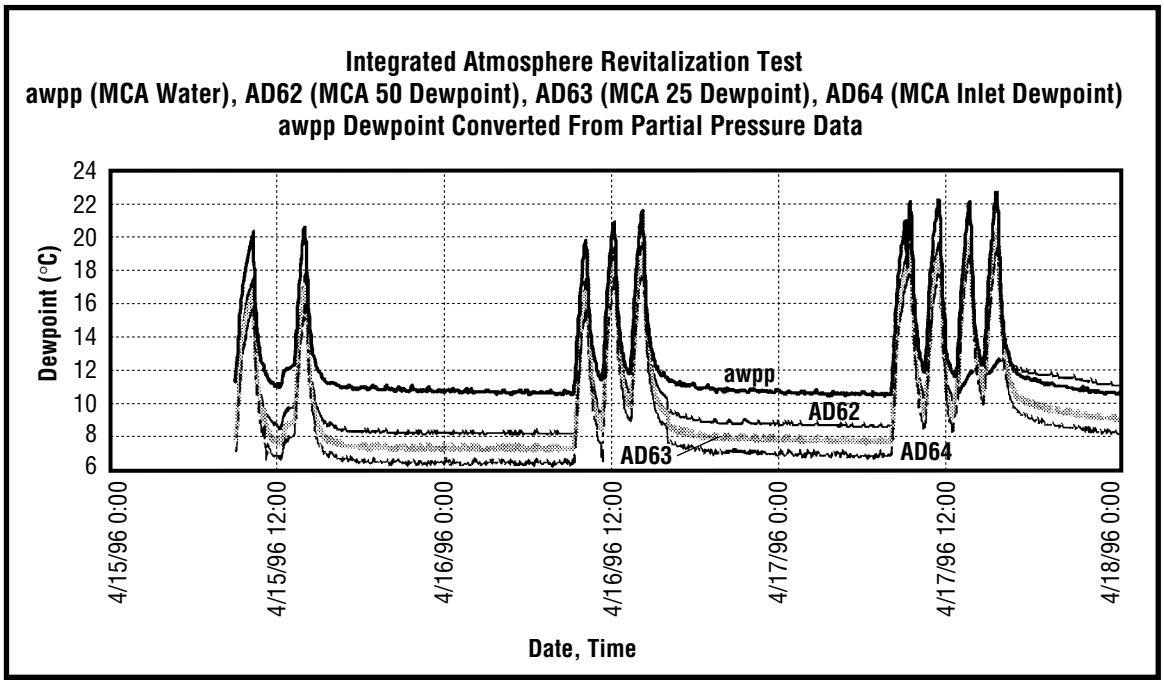
Integrated Atmosphere Revitalization Test
awpp (MCA Water), AD62 (MCA 50 Dewpoint), AD63 (MCA 25 Dewpoint), AD64 (MCA Inlet Dewpoint)
awpp Dewpoint Converted From Partial Pressure Data
Dewpoint (°C)
24
22
20
18
16
14
12
10
8
6
awpp
AD62
AD63
AD64
4/15/96 0:00
4/15/96 12:00
4/16/96 0:00
4/16/96 12:00
4/17/96 0:00
4/17/96 12:00
4/18/96 0:00
Date, Time

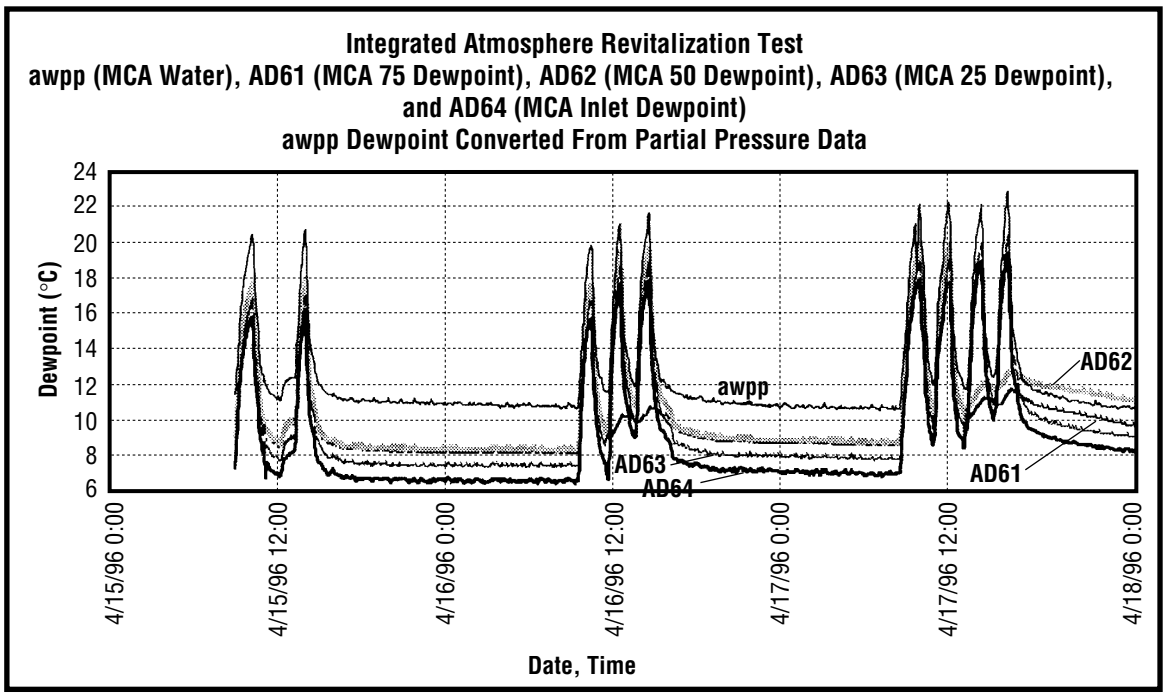
Integrated Atmosphere Revitalization Test
awpp (MCA Water), AD61 (MCA 75 Dewpoint), AD62 (MCA 50 Dewpoint), AD63 (MCA 25 Dewpoint), and AD64 (MCA Inlet Dewpoint)
awpp Dewpoint Converted From Partial Pressure Data
Dewpoint (°C)
24
22
20
18
16
14
12
10
8
6
awpp
AD62
AD63
AD64
AD61
4/15/96 0:00
4/15/96 12:00
4/16/96 0:00
4/16/96 12:00
4/17/96 0:00
4/17/96 12:00
4/18/96 0:00
Date, Time

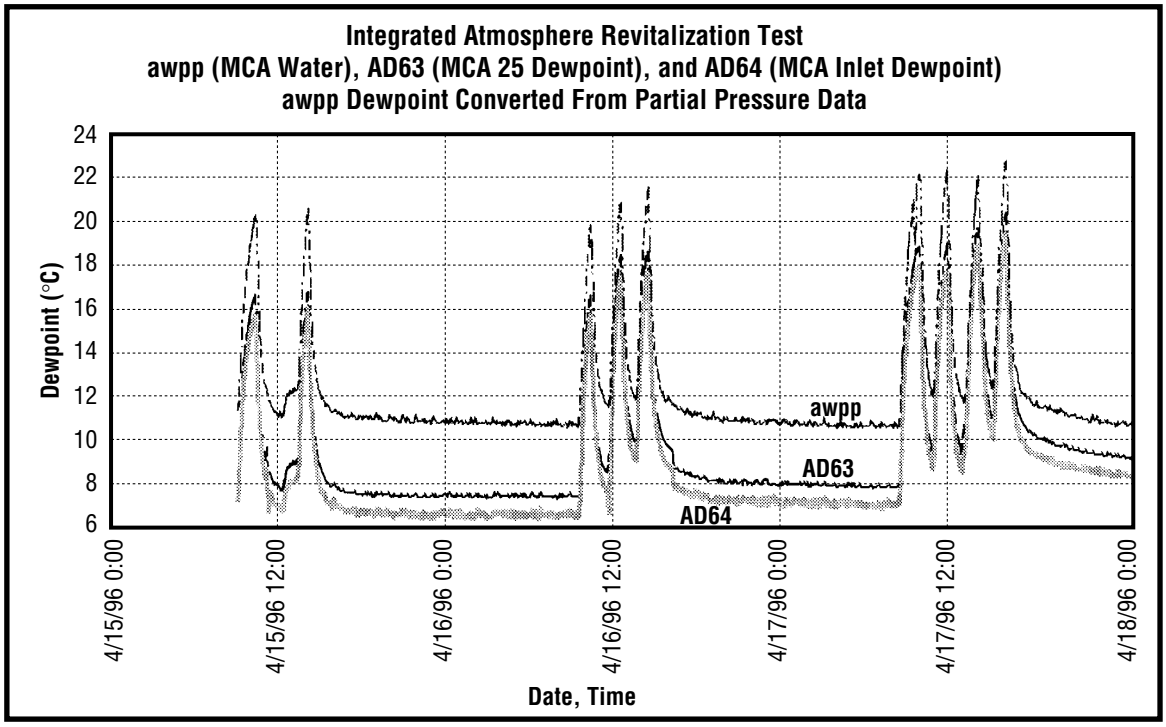
Integrated Atmosphere Revitalization Test
awpp (MCA Water), AD63 (MCA 25 Dewpoint), and AD64 (MCA Inlet Dewpoint)
awpp Dewpoint Converted From Partial Pressure Data
Dewpoint (°C)
24
22
20
18
16
14
12
10
8
6
awpp
AD63
AD64
4/15/96 0:00
4/15/96 12:00
4/16/96 0:00
4/16/96 12:00
4/17/96 0:00
4/17/96 12:00
4/18/96 0:00
Date, Time

APPENDIX L—
TCCS ENERGY BALANCE CALCULATIONS

Energy Balance With Methane Injection

Hypothesis:

Temperature rise in the high-temperature oxidizer can be influenced by the presence of methane. The heat of reaction liberated by oxidizing methane may be sufficient to cause a noticeable temperature rise in the reactor.

Assumptions:

- Temperature rise in the reactor is caused by methane oxidation only
- Constant heater power input
- Neglect temperature changes since flowrates are reported at standard conditions
- Air composition is 79 percent by volume nitrogen and 21 percent by volume oxygen
- Nitrogen is inert and its molar flowrate is unchanged through the reactor.

Conditions:

- 3.38 mole/min or 2.72 standard cubic feet per minute (scfm) airflow at approximately 60 °C (140 °F) at the reactor assembly outlet
- 0.0105 mole/min or 14 standard cubic inches per minute (scim) of 3 percent by volume methane in air 22.2 °C (72 °F) is injected into the air stream before entering the reactor assembly
- Total combined flowrate entering the catalytic reactor assembly is 3.37 mole/min (difference between outlet molar flowrate and bleed flowrate)
- Inlet temperature to the catalyst bed is 360 °C (680 °F).

Species	Feed	Produced	Reacted	Exhausted
Nitrogen	2.63	0	0	2.63
100-Percent Oxidation				
Methane	0.000314	0	0.000314	0
Oxygen	0.740256	0	0.000628	0.7396280
Carbon Dioxide	0.001339	0.0003138	0	0.0016530
Water	0	0.0006276	0	0.0006276
75-Percent Oxidation				
Methane	0.000314	0	0.000235	0.000078
Oxygen	0.740256	0	0.000471	0.739785
Carbon Dioxide	0.001339	0.000235	0	0.001574
Water	0	0.000471	0	0.000471
50-Percent Oxidation				
Methane	0.000314	0	0.000157	0.0001570
Oxygen	0.740256	0	0.000314	0.7399420
Carbon Dioxide	0.001339	0.000157	0	0.0015745
Water	0	0.000314	0	0.0003140
25-Percent Oxidation				
Methane	0.000314	0	0.000078	0.0002350
Oxygen	0.740256	0	0.000157	0.7400990
Carbon Dioxide	0.001339	0.000078	0	0.0014176
Water	0	0.000157	0	0.0001570
Zero-Percent Oxidation				
Methane	0.000314	0	0	0.000314
Oxygen	0.740256	0	0	0.740256
Carbon Dioxide	0.001339	0	0	0.001339
Water	0	0	0	0

FIGURE L–1.—Molar flowrates as a function of methane oxidation efficiency (mole/min).

Determine reactor energy losses:

From week 85 data of the TCCS life test (ref. NASA TM–108488)

- Catalyst bed inlet temperature of 654.07 K (715.85 °F)
- Catalyst bed midpoint temperature of 671.21 K (748.51 °F)
- Catalyst bed outlet temperature of 672.80 K (751.37 °F)
- Measured methane oxidation efficiency of 98.5 percent.

Molar flowrates are shown in figure L—2.

Species	Feed	Produced	Reacted	Exhausted
Nitrogen	2.63	0	0	2.63
Methane	0.000314	0	0.000309	0.000004
Oxygen	0.740256	0	0.000628	0.739637
Carbon Dioxide	0.001339	0.000309	0	0.001648
Water	0.033124	0.000619	0	0.033742

FIGURE L–2.—Molar flowrates (mole/min).

Using the following definitions of enthalpy (J/mole-K), the enthalpies:

Nitrogen	$8.27 + 0.00100T$
Methane	$5.34 + 0.0114T$
Oxygen	$8.27 + 0.000258T$
Carbon dioxide	$10.34 + 0.00274T$
Water	$8.22 + 0.00015T$

Enthalpy at the catalyst bed inlet	36,934.21 J/min
Enthalpy at the catalyst bed outlet	39,030.25 J/min
Energy input from heater	9411.60 J/min
Heat of reaction (moles methane × –802,319 J/min)	–248.22 J/min

$$H_{inlet} - \Delta H_{rxn} + q_{in} = H_{outlet} + q_{lost}$$

Solving for q_{lost} results in a calculated energy loss of 7,563.78 J/min if the reactor outlet temperature is the basis. An energy loss of 7,732.49 J/min is calculated if the reactor midpoint temperature is used as the basis.

Applying the equations for enthalpy for each species to the different methane oxidation cases and calculating the heat of reaction for methane for each case result tin the following equation for the energy balance around the catalytic reactor bed:

100 percent methane oxidation	$0.0059240T^2 + 98.3862T - 68878.97 = 0$
75 percent methane oxidation	$0.0059255T^2 + 98.3846T - 68815.68 = 0$
50 percent methane oxidation	$0.0059269T^2 + 98.3828T - 68752.38 = 0$
25 percent methane oxidation	$0.0059284T^2 + 98.3817T - 68689.10 = 0$
0 percent methane oxidation	$0.0059299T^2 + 98.3798T - 68625.81 = 0$

Solving the energy balance equations for T provides a prediction for the outlet catalytic bed temperature shown in figure L–3.

Efficiency	Kelvin	Celsius	Fahrenheit
100	672.83	399.68	751.42
75	672.24	399.09	750.36
50	671.65	398.50	749.30
25	671.05	397.90	748.22
0	670.46	397.31	747.16

FIGURE L–3.—Prediction for the outlet catalytic bed temperatures.

Likewise, using the energy losses calculated by setting the catalyst bed midpoint temperature as the basis results in the following energy balance equations and predicted catalyst bed midpoint temperatures:

100 percent methane oxidation	$0.0059240T^2 + 98.3862T - 68710.26 = 0$
75 percent methane oxidation	$0.0059255T^2 + 98.3846T - 68646.97 = 0$
50 percent methane oxidation	$0.0059269T^2 + 98.3828T - 68583.67 = 0$
25 percent methane oxidation	$0.0059284T^2 + 98.3817T - 68520.39 = 0$
0 percent methane oxidation	$0.0059299T^2 + 98.3798T - 68457.10 = 0$

Solving the energy balance equations for T provides a prediction for the outlet catalytic bed temperature shown in figure L–4. Figure L–5 gives the TCCS high-temperature catalytic oxidizer temperatures.

Efficiency	Kelvin	Celsius	Fahrenheit
100	671.24	398.09	748.56
75	670.65	397.50	747.50
50	670.06	396.91	746.44
25	669.47	396.32	745.38
0	668.88	395.73	744.31

FIGURE L–4.—Prediction for the outlet catalytic bed temperatures.

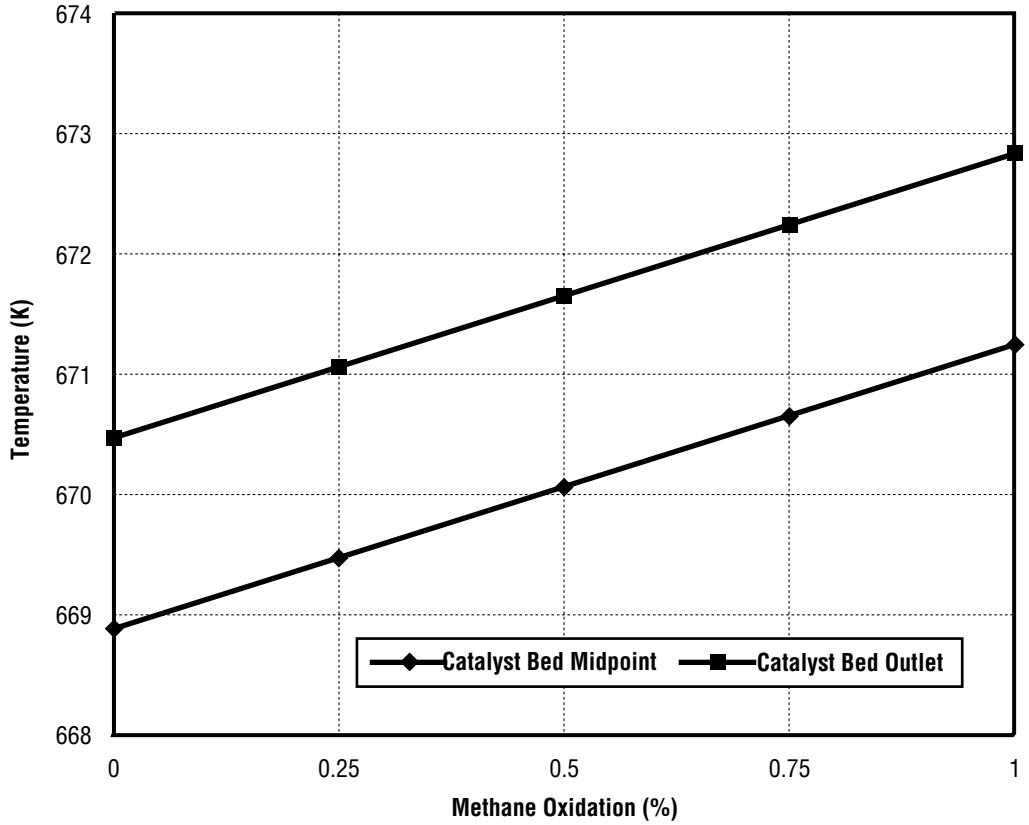

FIGURE L–5.—TCCS high-temperature catalytic oxidizer temperatures.

Energy Balance Without Methane Injection

TCCS Catalytic Oxidizer Energy Balance

Using the conditions experienced during the IART, a cooler condition was experienced because the heater energy input was held constant. This resulted in an overall downward shift in reactor temperature profile. This shift also resulted in changes in the overall energy losses. The energy balance calculations conducted earlier were adjusted for this case.

- Catalytic bed inlet temperature 648.15 K (707 °F)
- Catalytic bed outlet temperature 667.59 K (742 °F)
- Inlet enthalpy 36,407.27 J/min
- Outlet enthalpy 38,472.72 J/min
- Heat of reaction 0 (no methane injected)
- Heater energy input 9,411.60 J/min

Applying the energy balance lead to a predicted energy loss of 7,346.15 J/min.

Using the individual species definitions for enthalpy, the overall energy balance is found to be:

$$0.0059223T^2 + 98.37278T - 68313.74 = 0$$

Solving for temperature, T, results in a temperature of 667.61 K. This result checks with the observed catalytic bed outlet temperature. As a result, the correlation of the temperature at the catalytic bed outlet to methane oxidation efficiency must be adjusted. The resulting correlation is shown in figure L–6.

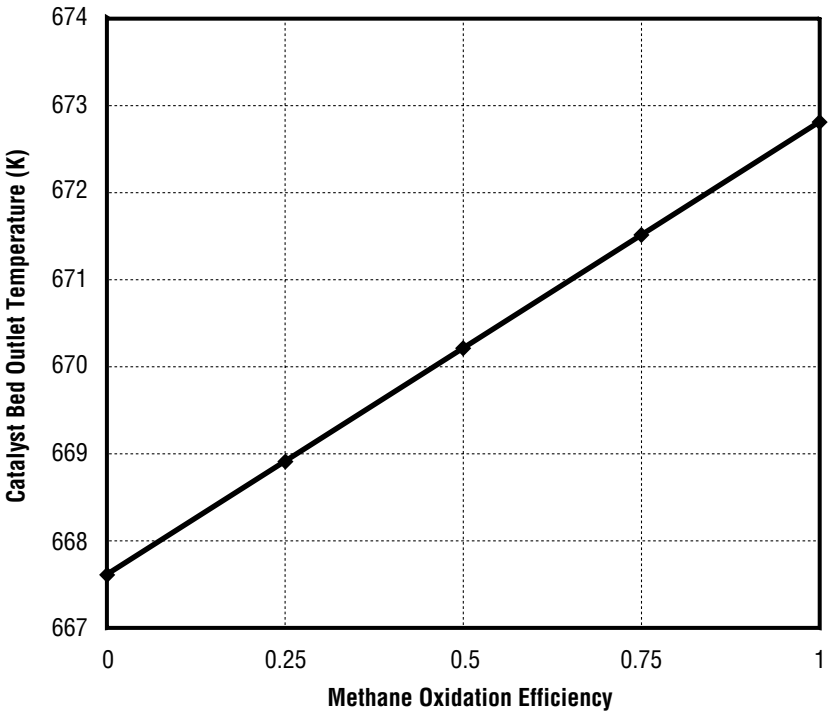

FIGURE L–6.—Effects of methane oxidation efficiency on catalyst bed outlet temperature.

REPORT DOCUMENTATION PAGE

Form Approved
OMB No. 0704-0188

1. AGENCY USE ONLY *(Leave Blank)*	2. REPORT DATE	3. REPORT TYPE AND DATES COVERED
	August 1997	Technical Memorandum

4. TITLE AND SUBTITLE

International Space Station Program Phase III Integrated Atmosphere Revitalization Subsystem Test Final Report

5. FUNDING NUMBERS

6. AUTHORS

J.L. Perry, G.D. Franks, and J.C. Knox

7. PERFORMING ORGANIZATION NAMES(S) AND ADDRESS(ES)

George C. Marshall Space Flight Center
Marshall Space Flight Center, Alabama 35812

8. PERFORMING ORGANIZATION REPORT NUMBER

9. SPONSORING/MONITORING AGENCY NAME(S) AND ADDRESS(ES)

National Aeronautics and Space Administration
Washington, DC 20546–0001

10. SPONSORING/MONITORING AGENCY REPORT NUMBER

NASA TM–108541

11. SUPPLEMENTARY NOTES

Prepared by Structures and Dynamics Laboratory, Science and Engineering Directorate

12a. DISTRIBUTION/AVAILABILITY STATEMENT

Unclassified–Unlimited

12b. DISTRIBUTION CODE

13. ABSTRACT *(Maximum 200 words)*

Testing of the *International Space Station* (*ISS*) U.S. Segment baseline configuration of the Atmosphere Revitalization Subsystem (ARS) by NASA's Marshall Space Flight Center (MSFC) was conducted as part of the Environmental Control and Life Support System (ECLSS) design and development program. This testing was designed to answer specific questions regarding the control and performance of the baseline ARS subassemblies in the *ISS* U.S. Segment configuration. These questions resulted from the continued maturation of the *ISS* ECLSS configuration and design requirement changes since 1992.

The test used pressurized oxygen injection, a mass spectrometric major constituent analyzer, a Four-Bed Molecular Sieve Carbon Dioxide Removal Assembly, and a Trace Contaminant Control Subassembly to maintain the atmospheric composition in a sealed chamber at *ISS* specifications for 30 days. Human metabolic processes for a crew of four were simulated according to projected *ISS* mission time lines. The performance of a static feed water electrolysis Oxygen Generator Assembly was investigated during the test preparation phases; however, technical difficulties prevented its use during the integrated test.

The Integrated ARS Test (IART) program built upon previous closed-door and open-door integrated testing conducted at MSFC between 1987 and 1992. It is the most advanced test of an integrated ARS conducted by NASA to demonstrate its end-to-end control and overall performance. IART test objectives, facility design, pretest analyses, test and control requirements, and test results are presented.

14. SUBJECT TERMS

environmental control, life support, atmosphere, spacecraft, carbon dioxide, oxygen, space station

15. NUMBER OF PAGES

172

16. PRICE CODE

NTIS

17. SECURITY CLASSIFICATION OF REPORT	18. SECURITY CLASSIFICATION OF THIS PAGE	19. SECURITY CLASSIFICATION OF ABSTRACT	20. LIMITATION OF ABSTRACT
Unclassified	Unclassified	Unclassified	Unlimited